I N A U G U R A L – D I S S E R T A T I O N

zur

Erlangung der Doktorwürde

der

Naturwissenschaftlich–Mathematischen Gesamtfakultät

der

R U P R E C H T – K A R L S – U N I V E R S I T Ä T

H E I D E L B E R G

vorgelegt von

M.Sc. Lilli Bergner

aus Dresden

Tag der mündlichen Prüfung

.....

Fast numerical methods for robust nonlinear optimal control under uncertainty

Betreuer

Professor Dr. Christian Kirches

Professor Dr. Dr. h.c.mult. Hans Georg Bock

Zusammenfassung

Diese Arbeit behandelt verschiedene Aspekte der Klasse der nichtlinearen Optimalsteuerungsprobleme unter Unsicherheit. Dabei handelt es sich um Optimierungsprobleme, die die Optimierung eines durch einen dynamischen Prozess bestimmten Systems mit der Problematik unsicherer Parameter, die durch eine Wahrscheinlichkeitsverteilung modelliert werden, verbinden.
Wir geben einen ausführlichen Überblick über verschiedene Verfahren zur Propagierung der Unsicherheiten durch das dynamische System und zur Robustifizierung der optimalen Lösung. Zur Umwandlung der unsicheren Optimalsteuerungsprobleme im Wahrscheinlichkeitsraum in deterministische, sogenannte Surrogate-Modelle verwenden wir die Polynomial Chaos Transformation, eine in den Ingenieurwissenschaften weit verbreitete Methode zur Unsicherheitsquantifizierung. Aufgrund ihrer Grösse und Komplexität sind die entstehenden Surrogate-Optimalsteuerungsprobleme für herkömmliche Optimalsteuerungssoftware nur schwer lösbar. Diese Problematik wird erschwert, wenn das Ausgangssproblem, wie in der hier betrachteten Problemklasse, stark nichtlinear ist. In diesem Fall wird eine hohe Expansionsordnung benötigt um die nichtlineare Unsicherheitsfortpflanzung abbilden zu können.
Wir entwickeln zwei algorithmische Verfahren, die zur effizienten Lösung der unsicheren Optimalsteuerungsproblemen beitragen. Dazu leiten wir einen adaptiven Algorithmus her, der die Eigenschaft ausnutzt, dass die unterschiedlichen Zustandsvariablen in unterschiedlicher Stärke von den unsicheren Eingangsparametern abhängen. Mithilfe von Fehlerschätzern bestimmt der Algorithmus für jede Zustandsvariable adaptiv die optimale Expansionsordnung. Dies hat zwei Vorteile: die Laufzeit, die benötigt wird um eine Lösung des unsicheren Problemes mit ausreichender Genauigkeit zu finden, wird verringert und wir erhalten zusätzliche Mechanismen zur Verifizierung der Lösung.
Als zweite algorithmische Verbesserung schlagen wir ein strukturausnutzendes Verfahren zur effizienten Ableitungsberechnung in Optimalsteuerungsproblemen vor. Der Algorithmus verwendet die spezielle Struktur, die durch die spektrale Projektion in der Polynomial Chaos Methode entsteht. So können Modellinformationen wiederverwendet und die häufig vorkommende Dünnbesetztheit der Jacobi-Matritzen ausgenutzt werden. Dies führt zu beträchtlichen Einsparungen Newton-artiger Verfahren für die Lösung des hochdimensionalen Surrogate-Problems.
Ergänzend zu den zwei algorithmischen Beiträgen zeigen wir in einem Konvergenzbeweis, dass die Lösungen der Surrogate-Optimalsteuerungsprobleme nach Anwendung der Polynomial Chaos Methode für steigende Expansionsordnungen zu der korrekten Lösung des unsicheren Problems konvergieren.

Eine weitere anspruchsvolle Problemstellung dieser Arbeit ist die Lösung von unsicheren Optimalsteuerungsproblemen mit Zufallsbeschränkungen, sogenannten Chance Constraints. Dabei handelt es sich um eine probabilistische Robustifizierung des Problems im Wahrscheinlichkeitsraum, die weder zu konservativ ist noch das Risiko unterschätzt, dass die Beschränkung für bestimmte Zufallsrealisierungen zu verletzen. Wir entwickleln dazu eine effiziente, auf der Polynomial Chaos Expansion aufbauende Methode um die sogenannten Erreichbarkeitsmengen der unsicheren Zustandsvariablen zu berechnen. Es wird gezeigt, wie Zufallsbeschränkungen durch diese Erreichbarkeitsmengen mit einer garantierten Güte approximiert werden können.

Alle in dieser Arbeit entwickelten Verfahren sind der Implementierung in direkte Methoden der Optimalsteuerung zugänglich. Ihre Effizienz und Eignung für nichtlineare Optimalsteuerungsprobleme zeigen wir in numerischen Experimenten anhand von zwei prototypischen Anwendungen. Für die Veranschaulichung der Auswirkungen der Unsicherheitsfortpflanzung verwenden wir dabei ausführliche Monte-Carlo-Simulationen. Als industrielles Anwendungsproblem betrachten wir das komplexe Optimalsteuerungsproblem einer Adsoptionkälteanlage unter Unsicherheit, das in Zusammenarbeit mit dem Lehrstuhl für Technische Thermodynamik der RWTH Aachen entstanden ist.

Abstract

This thesis treats different aspects of nonlinear optimal control problems under uncertainty in which the uncertain parameters are modeled probabilistically. We apply the polynomial chaos expansion, a well known method for uncertainty quantification, to obtain deterministic surrogate optimal control problems. Their size and complexity pose a computational challenge for traditional optimal control methods. For nonlinear optimal control, this difficulty is increased because a high polynomial expansion order is necessary to derive meaningful statements about the nonlinear and asymmetric uncertainty propagation. To this end, we develop an adaptive optimization strategy which refines the approximation quality separately for each state variable using suitable error estimates. The benefits are twofold: we obtain additional means for solution verification and reduce the computational effort for finding an approximate solution with increased precision. The algorithmic contribution is complemented by a convergence proof showing that the solutions of the optimal control problem after application of the polynomial chaos method approach the correct solution for increasing expansion orders.

To obtain a further speed-up in solution time, we develop a structure-exploiting algorithm for the fast derivative generation. The algorithm makes use of the special structure induced by the spectral projection to reuse model derivatives and exploit sparsity information leading to a fast automatic sensitivity generation. This greatly reduces the computational effort of Newton-type methods for the solution of the resulting high-dimensional surrogate problem.

Another challenging topic of this thesis are optimal control problems with chance constraints, which form a probabilistic robustification of the solution that is neither too conservative nor underestimates the risk. We develop an efficient method based on the polynomial chaos expansion to compute nonlinear propagations of the reachable sets of all uncertain states and show how it can be used to approximate individual and joint chance constraints. The strength of the obtained estimator in guaranteeing a satisfaction level is supported by providing an a-priori error estimate with exponential convergence in case of sufficiently smooth solutions.

All methods developed in this thesis are readily implemented in state-of-the-art direct methods to optimal control. Their performance and suitability for optimal control problems is evaluated in a numerical case study on two nonlinear real-world problems using Monte Carlo simulations to illustrate the effects of the propagated uncertainty on the optimal control solution. As an industrial application, we solve a challenging optimal control problem modeling an adsorption refrigeration system under uncertainty.

Acknowledgments

I would like to express my deepest graditude to my advisor Christian Kirches for his continued encouragement, trust and his patience and guidance during the research and writing process of my PhD thesis at the Faculty of Mathematics and Computer Science at Heidelberg University. I have been lucky to have a supervisor who responded to my questions and queries so promptly. My sincere thanks go equally to my second advisor Georg Bock and to Johannes Schlöder for providing the stimulating and open environment of the group *Simulation and Optimization* at the Interdisciplinary Center for Scientific Computing (IWR).

For many fruitful discussions, insightful comments and, last but not least, for many enjoyable extra-curricular activities, I would like to thank all my colleagues at Heidelberg University. It was a great experience to spend three years in this group. The group's optimal control software MUSCOD-II has been extensively used to obtain the numerical results of this thesis. Moreover, I would like to thank Thomas Klöpfer for his help in technical problems that came up during my work.
For their kind welcome, I would like to thank my colleagues of my fourth year of my PhD thesis at the Institute for Mathematical Optimization at the Technische Universität Braunschweig. In particular, I appreciate the help of Paul Manns for his deep insight into a wide range of mathematical topics and his contribution to my research.
For the fruitful collaboration, I would like to thank Uwe Bau from the Chair of Technical Thermodynamics LTT of the RWTH Aachen University. Without his patience and his helpful explanations, I would not have been able to understand the physics behind adsorption chillers and heat pumps.

Participating in the Heidelberg Graduate School MathComp played an important role during my PhD. Not only am I grateful for their financial help for attending conferences and workshops but also for the opportunity to take part in the Graduate School speaker's committee and to organize conferences myself.

Completing this thesis would have been more difficult without the continuous exchange with my Heidelberg friends. I would like to thank my family for their moral support, and my wonderful boyfriend Gianluca for the very exciting last years.

Contents

Introduction

The recent growth of computational power and the progress of the research in theory and algorithms open up the possibility to solve more and more complex optimal control problems. Often the knowledge of the physical systems is not complete or suffers from insufficient data or assumptions taken to simplify the complex properties. In other cases even inherently random model quantities are present, e.g. consider the turbulent fluctuations of a flow field around an airplane wing. The neglection of this uncertainty however leads to inaccurate results that do not reflect the physical reality.
In optimal control under uncertainty, the uncertainty within the model is treated in a systematic way by taking into account that the behavior of the complex system varies from one realization of the uncertain quantity to another. Predictions need to be made not only for one single fixed realization, but for all possible outcomes. The aim is to produce solutions with concrete, quantifiable measures of uncertainty thanks to which we know how good the predictions are.

Problem description and challenges

Based on the assumption that structural information about a-priori uncertainty is at hand, e.g. in form of probability distributions or moment information, uncertain parameters or initial conditions can be modeled probabilistically. In this case, the random variables act as carrier of the uncertainty. This approach can be regarded as a general way to include all knowledge about the uncertainty into the model.
Techniques to deal with uncertainty within mathematical problems originate from a number of different fields – statistics and probability theory, but also control theory, optimization, dynamical systems, and many fields of engineering and computational science. Notably mechanics, fluid dynamics and aerodynamics have contributed to a wealth of advanced methods useful for the quantification of uncertainty.

In this thesis, we study the mathematical problem class of nonlinear optimal control problems, that is, time-dependent optimization problems containing ordinary differential equations in their dynamics. After an appropriate discretization and parametrization of the continuous problem, finding a solution amounts to solving a large-scale structured nonlinear program (NLP). Every iteration of an NLP algorithm requires a large number of forward solves of the uncertain dynamical system. This quickly becomes incompatible with the wide-spread Monte Carlo sampling (MCS) method which typically requires a huge number of samples to yield meaningful results. Addressing this issue, we use the polynomial chaos (PC) method, another well-known uncertainty quantification method, to construct deterministic surrogates, which can be solved in place of the original uncertain optimal control problems. The benefits of the polynomial chaos method are the broad applicability to nonlinear problems with possibly large variance and different types of probability distributions, as well as guaranteed mean-square convergence for sufficiently smooth forward problems with a means for error control by increasing the expansion order. One challenge of this thesis is to prove that this fast spectral convergence also applies to optimal control problems that may result in different control policies for different expansion orders.

The practical use of the PC method presents some major difficulties: the computational cost becomes prohibitive when (i) the dimension of the parameters modeling the uncertainty is even moderately large ("curse of dimensionality") or (ii) the uncertainty evolves in a very nonlinear fashion or even suffers from stochastic discontinuities or long-term integration. In optimal control problems, we are mainly faced with the difficulty of a strong nonlinear dependence on the random input, requiring a large PC order and consequently a very complex surrogate problem to solve. Accurate results are possible but additional structure exploitation and numerical procedures are indispensable to prevent a convergence breakdown and an explosion of the problem size.

Another important challenge in the field of optimal control under uncertainty is the robustification of the optimal solution against variations of the uncertain inputs. The notions of optimality and robustness of the objective function as well as constraint satisfaction under uncertainty must be properly treated regarding specific application-dependent demands by appropriate measures of robustness. A valuable solution should not only be able to make precise statements about the uncertainty propagation within the dynamical system but use the obtained information to take robustification decisions. The aim is to ensure that the solution remains feasible and near optimal even when the data changes. As a useful side effect and second benefit, robustification often involves the decrease of the deviation of the uncertainty, thus controlling to some extent the aforementioned high nonlinear parameter dependence of the solution.
The different robustification methods can be distinguished by their numerical computation procedure as well as the resulting tradeoff between optimality and robustness, also called the price of robustness. Common approaches are a worst-case robustification against all possible outcomes, or the use of a safety margin based on the variance. The first approach is an example resulting in a very high price of robustness, that is, the solutions are often found to be overly conservative or the problem might even become infeasible. In contrast, the second approach generally does not allow for reliable statements about the obtained level of robustness. A preferred approach to this end is to make use of chance constraints, probabilistic formulations that require constraint satisfaction with a selectable probability level while excluding a well-defined number of extreme outcomes, leading to decisions that are neither too conservative nor too risk-seeking. The immediate computation of chance constraints by determining the propagated density is not tractable for most nonlinear real-world instances and their efficient computation within optimal control problem is an open problem.

Contributions of the thesis

The aims of this thesis are two-fold: (i) to develop computationally tractable formulations together with efficient numerical algorithms and a convergence analysis for optimal control problems under uncertainty, and (ii) to develop reformulations of general chance constraints with a robustness guarantee applicable to nonlinear optimal control problems.

Theoretical convergence analysis for uncertain optimal control

We contribute a convergence proof of the polynomial chaos method for a general class of nonlinear optimal control problems with parametric uncertainties. To this end we show that the solutions of the polynomial chaos surrogates corresponding to the uncertain optimal control problem approach the correct solution for increasing expansion orders. This convergence study addresses the issue that optimal control problems may lead to different control policies for

different polynomial chaos expansion orders. Consequently the spectral convergence property of the polynomial chaos method does not directly apply to this class of problems.

Fast solution methods for uncertain optimal control

To deal with the high polynomial order – and consequently high computational effort – that is necessary to capture the nonlinear uncertainty propagation, we develop fast structure-exploiting polynomial chaos methods suitable for nonlinear optimal control. Based on the preceding convergence analysis, we propose an adaptive optimization strategy suitable for direct methods for optimal control to identify the optimal expansion order for each state variable making use of appropriate error estimates. The main idea is the exploitation of an adaptive strategy for the state basis order selection. The benefit of the adaptive algorithm is a substantial reduction of the computational effort for finding reliable results with a precision that can be verified by the derived error estimates. Moreover, the algorithm returns an "optimal" expansion order, which is useful for repeated solution, e.g., in a feedback loop. A challenging numerical case study demonstrates that the proposed adaptive strategy leads to a significant performance gain without loss of accuracy.

As a second advancement, we propose a derivative projection aiming to compute efficiently the derivatives required for the solution of the surrogate optimal control problems. The special structure induced by the spectral projection is exploited in order to reuse model derivatives and take advantage of sparsity structure information. The consequence is a fast automatic sensitivity generation which greatly reduces the computational effort of Newton-type methods for the solution of the resulting high-dimensional surrogate problem. The results are complemented by a complexity comparison with a standard finite difference approach. In a numerical case study, we demonstrate that the practical performance speed-up agrees with the theoretically predicted gain, which is proportional to the sparsity factor of the Jacobian matrix.

Chance-constrained optimal control

Another major topic of this thesis is chance-constrained optimal control. Our first contribution is the development of an algorithmic strategy to compute reachable sets in state space of stochastic optimal control problems based on extreme realizations of the polynomial chaos surrogate states. The algorithm is implemented in a differentiability preserving way into direct methods for optimal control. Second, we apply the developed reachable set formulation to the reformulation of chance constraints in a very general form. To support the strength of the proposed estimation, we contribute a proof of convergence with an a-priori error estimate depending on the regularity of the solution in the parametric space.
In a numerical case study, we illustrate the tradeoff between low cost objective, chance constraint satisfaction and variance minimization. The main intention is to demonstrate the suitability of the proposed robustification technique for nonlinear optimal control problems under uncertainty.

Case Studies

The two new algorithms for the fast numerical solution of optimal control problems under uncertainty and the new chance constraint robustification method are tested in detail on two very different nonlinear optimal control problems that are inspired by real-world processes.
Moreover, as an industrial application, we solve a challenging nonlinear optimal control problem modeling an adsorption refrigeration system – which for the first time is considered under

uncertainty. The system was developed in collaboration with the Chair of Technical Thermodynamics LTT of the RWTH Aachen University. The dynamic DAE process is provided as a blackbox in form of a dynamic Modelica model and connected to the optimization algorithm via the standardized Functional Mock-up Interface (FMI). The focus of this third example is a first feasibility study of a real industrial application.

Previous work

Our contributions concern the theoretical foundation of the use of polynomial chaos methods for optimal control problems under uncertainty, the development of fast numerical solution methods and a new robustification approach for chance constrained optimal control problems using polynomial chaos methods. In the following, we describe previous studies that are relevant to these research topics. For an overview of existing works on risk measures, general uncertainty quantification and robustification methods for optimal control under uncertainty and past and current research in polynomial chaos methods, we refer to the sections 2.2, 2.3 and 3.3, respectively.

Theoretical aspects of polynomial chaos methods for optimal control problems

The theoretical aspects of polynomial chaos based approximation algorithms for uncertain optimal control problems, e.g. the rate or quality of the approximation of state trajectories or the objective value, have not been subject to systematic investigation in many scientific works. Relevant to the research topics of this thesis are the following: Anitescu [6] derives an approximation method based on polynomial chaos for constrained parametric finite-dimensional optimization problems and proves that, given a parametric/uncertain constrained optimization problem, solving the PC approximation of the Karush–Kuhn–Tucker (KKT) system is equivalent to solving directly the polynomial chaos approximation of the original problem, which is advantageous in some situations. His focus is on the existence of solutions of the finite-dimensional constrained optimization problem and in our main proof in Section 3.5 we will make use of some of his results. Ruths et al. [130] show convergence of the pseudospectral sampling method for optimal ensemble control, a simpler variant of the problem considered here. Phelps et al. [119, 120] consider the question of consistent approximations restricted to the class of optimal control problems in which only the objective function involves an integration over the stochastic space. After discretizing the uncertain objective functional by numerical quadrature in form of a sample average approximation scheme, they show convergence of the sequence of stationary points for the approximate problem to a stationary point of the original problem.

Fast numerical solution methods for polynomial chaos optimal control problems

Well known iterative or adaptive implementations of polynomial chaos methods include the recomputation of the polynomial basis over time based on probabilistic moment information of the evolving distribution, cf. [115, 56, 99], and local basis methods such as multi-element generalized polynomial chaos (ME-gPC), cf. [148], which decompose the underlying probability space using the relative error in variance as error control. These works address in particular the setting of high-dimensional stochastic spaces, discontinuities in the parametric space, long-time integration and evolution equations with stochastic forcing. Their goal is to enable the use of low-order polynomial chaos methods while retaining a sufficient level of accuracy, e.g., by scaling down the local degree of perturbation. The developed adaptive algorithm in this

thesis is based on a basis order selection strategy for optimal control problems. For the uncertainty quantification in forward problems, problem-dependent basis order selection strategies have already been addressed in [77, 116, 102].

Chance constrained optimal control

The approximation of chance constraints in optimal control problems under uncertainty is an active research topic. In the following short survey, we focus on approaches applicable to the polynomial chaos method. Several works address the approximation of chance constraints using only the mean and the variance, e.g., by using a Gaussian fit on the propagated state variables [111, 80], or by applying the Cantelli-Chebyshev inequality [53, 104]. Such approximation techniques generally result in a convexified approximation, but do not lead to guaranteed bounds for chance constraints for general nonlinear systems. Besides linearization, other simplifying assumptions on the information prior can be incorporated into the problem formulation e.g. via maximum likelihood methods.
Monte Carlo sampling methods have been combined with the polynomial chaos approach for the approximation of chance constraints in optimal control problems, e.g. [100]. A related approach is scenario-based sampling that has been applied to optimal control by Calafiore et al. [30, 31]. The authors also provide a satisfaction guarantee with a reasonable bound on the number of samples. This bound is significantly better than the crude bound of MCS but only applicable to problems with a convex dependence on the uncertainty.
A combination of polynomial chaos methods and interval analysis in control theory has been studies by Terejanu in, e.g. [146]. The author applies a transformation from Legendre to Bernstein polynomials whose coefficients have favorable range enclosure properties. Smith, Ponci et al. and Monti, Ponci et al. [139, 140, 108] use the deterministic surrogate resulting from the polynomial chaos method to obtain the worst-case, expected and best-case output for a low-pass filter and for robust stability of a closed-loop system.

Thesis structure

The remainer of this thesis consists of six major chapters.
Chapter 1 gives an overview about (deterministic) optimal control theory and algorithms. We first introduce the problem class in Section 1.1 and derive the necessary optimality conditions based on Pontryagin's minimum principle in Section 1.2. After a brief overview of solution methods in Section 1.3, we give a detailed description of the direct multiple shooting method for optimal control in Section 1.4.

In Chapter 2, we describe the main problem of optimal control under uncertainty in an informal manner. We start by introducing the uncertain optimal control problem as an extension of parametric optimal control in Section 2.1 and proceed with an overview of risk measures in Section 2.2. The chapter closes with a detailed survey of existing techniques for uncertainty propagation in dynamical systems and optimal control problems in Section 2.3.

The main new contributions of this thesis are in the chapters 3 to 5.
Chapter 3 contains a thorough analysis of the uncertain optimal control problem. In Section 3.1, we set-up first properties of this problem class. We proceed in Section 3.2 with a summary of the most important definitions and results of spectral projections with orthogonal polynomials, which also form the foundation of the polynomial chaos method described thereafter in Section 3.3. The topic of Section 3.4 is the application of the polynomial chaos method to the uncertain optimal control problem with the derivation of the polynomial chaos surrogate problem. Similar to the deterministic problem version in Section 1.2, we discuss

well-posedness and necessary optimality conditions. The major contribution is the proof of convergence of the polynomial chaos surrogates in Section 3.5.

Chapter 4 contains the algorithmic counterpart of the preceding theoretical chapter, containing as a major contribution the adaptive algorithm for the fast solution of the uncertain optimal control problem in Section 4.1. As another algorithmic improvement, we present the fast structure-exploiting derivative generation in Section 4.2.

The topic of Chapter 5 is the robustification of the optimal control problem under uncertainty. In Section 5.1, we develop a method for the approximation of reachable sets for state trajectories based on the polynomial chaos method. We give two algorithms for the implementation in direct methods for optimal control. An important contribution is the resulting chance constraint approximation derived in Section 5.2.

Numerical results for the two new algorithms for the fast numerical solution of optimal control problems under uncertainty as well as the new chance constraint robustification method are summarized in Chapter 6, Sections 6.1 and 6.2, using two nonlinear optimal control problems based on real-world processes. In Section 6.3, we present results for the industrial application study of an adsorption refrigeration system.

A conclusion in Chapter 7 summarizes the results of this thesis and raises further research questions.

Two appendices close this thesis. Appendix A contains the most important definitions and lemmas of probability theory that are needed throughout this thesis. Useful results of perturbation analysis for initial value problems and for nonlinear programming problems are collected in Appendix B.

1 Optimal control theory and algorithms

We give an overview of optimal control theory and algorithms. First we introduce the problem class and derive the necessary optimality conditions in terms of the Pontryagin's minimum principle. After a short overview of solution methods, we give a detailed description of the direct multiple shooting method for optimal control problems.
This chapter is based on the dissertation [82] and the textbook [35].

1.1 Problem definition

The origins of optimal control theory lie in Bernoulli's Brachistochrone problem from 1696 which asks to determine the curve along which a body travels from one fixed point to another in the shortest time taking into account the gravitational force. Solutions were found by Leibniz, Newton, Bernoulli himself and l'Hôpital. Particularly Leibniz and Newton's subsequent works on the field of variational analysis contributed to the early growth of optimal control theory. The main developments in this field started in the 1950th with the works of Pontryagin and collaborators and since then, a large research effort has been put into this problem class.
A continuous optimal control problem is described in terms of states which evolve in time from a given initial state according to certain laws of dynamics ranging from ordinary differential equations (ODEs), partial differential equations (PDEs), stochastic differential equations and discrete difference equations. We consider the dynamical system to be in the form of an ODE system. The evolution of the states is influenced according to some performance criterion by a control function taken from a set of admissible controls. Together with some constraints on the control and the state functions, the problem becomes a constrained nonlinear, infinite-dimensional optimization problem with the goal to determine the optimal control function and state trajectories.

Definition 1.1.1 *A* continuous optimal control problem *is a constrained infinite–dimensional optimization problem of the form*

$$\min_{\boldsymbol{x},\boldsymbol{u}} \quad J[\boldsymbol{x},\boldsymbol{u}] := \int_{t_0}^{t_\mathrm{f}} l(\boldsymbol{x}(t),\boldsymbol{u}(t),\boldsymbol{p})\,\mathrm{d}t + m(\boldsymbol{x}(t_\mathrm{f}),\boldsymbol{p}) \tag{OCP}$$

$$\text{s.t.} \quad \dot{\boldsymbol{x}}(t) = \boldsymbol{f}(\boldsymbol{x}(t),\boldsymbol{u}(t),\boldsymbol{p}) \qquad t \in [t_0,t_\mathrm{f}]\ a.e. \tag{1.1a}$$

$$\boldsymbol{x}(t_0) = \boldsymbol{x}_0(\boldsymbol{p}) \tag{1.1b}$$

$$\boldsymbol{u}(t) \in U(t) \qquad t \in [t_0,t_\mathrm{f}]\ a.e. \tag{1.1c}$$

$$\boldsymbol{0} \geqslant \boldsymbol{c}(\boldsymbol{x}(t),\boldsymbol{u}(t),\boldsymbol{p}) \qquad t \in [t_0,t_\mathrm{f}]\ a.e. \tag{1.1d}$$

$$\boldsymbol{0} \geqslant \boldsymbol{r}_\mathrm{in}(\boldsymbol{x}(t_\mathrm{f}),\boldsymbol{p}) \tag{1.1e}$$

$$\boldsymbol{0} = \boldsymbol{r}_\mathrm{eq}(\boldsymbol{x}(t_\mathrm{f}),\boldsymbol{p}) \tag{1.1f}$$

in which we determine a dynamic process, called state trajectory,

$$\boldsymbol{x} : [t_0,t_\mathrm{f}] \to \mathbb{R}^n$$

on a time horizon $[t_0, t_f] \subset \mathbb{R}$*, described by a system of ODEs with right hand side*

$$\boldsymbol{f} : \mathbb{R}^n \times \mathbb{R}^{n_u} \times \mathbb{R}^{n_p} \to \mathbb{R}^n,$$

and initial conditions

$$\boldsymbol{x}(t_0) = \boldsymbol{x}_0(\boldsymbol{p})$$

affected by a control

$$\boldsymbol{u} : [t_0, t_f] \to \mathbb{R}^{n_u}$$

taking values in a control set

$$U(t) \subseteq \mathbb{R}^{n_u}$$

that may or may not be dependent on time. The goal is to minimize a performance index

$$J : \mathbb{R}^n \times \mathbb{R}^{n_u} \to \mathbb{R}$$

composed out of the Lagrange *term* $l(\boldsymbol{x}(t), \boldsymbol{u}(t), \boldsymbol{p})$ *and the* Mayer *term* $m(\boldsymbol{x}(t_f), \boldsymbol{p})$ *formulated as a final state penalty. The set of admissible state and control trajectories can be restricted by the introduction of path constraints, formulated either as mixed state-control, pure state or pure control constraints on the whole time horizon* $[t_0, t_f]$*,*

$$\boldsymbol{c} : \mathbb{R}^n \times \mathbb{R}^{n_u} \times \mathbb{R}^{n_p} \to \mathbb{R}^{n_c}$$

and end point constraints, formulated as equality or inequality constraints,

$$\boldsymbol{r}_{\text{eq}} : \mathbb{R}^n \times \mathbb{R}^{n_p} \to \mathbb{R}^{n_{r_{\text{eq}}}} \text{ and } \boldsymbol{r}_{\text{in}} : \mathbb{R}^n \times \mathbb{R}^{n_p} \to \mathbb{R}^{n_{r_{\text{in}}}}.$$

All equations may or may not depend on time-independent model parameters $\boldsymbol{p} \in \mathbb{R}^{n_p}$ *describing global properties of the dynamic process and its environment.*

The *admissible control set*

$$\mathcal{U} := \{u(t) \in L^\infty([t_0, t_f], \mathbb{R}^{n_u}) \mid u(t) \in U(t),\ t \in [t_0, t_f] \text{ a.e.}\}$$

is defined to be the set of all measurable and essentially bounded control functions contained in the control set. The variable $\boldsymbol{x}(t)$ describes the system state of the process at any time $t \in [t_0, t_f]$.

$$\mathcal{X} := W^{1,\infty}([t_0, t_f], \mathbb{R}^n)$$

denotes the set of all measurable and essentially bounded state trajectories with measurable and essentially bounded derivatives.
For a given admissible control, existence and uniqueness of the solution to the initial value problem (IVP) (1.1a) and (1.1b) follows from the Picard-Lindelöf threorem if $\boldsymbol{f}$ is assumed to be piecewise Lipschitz continuous. A summary of these results is provided in the Appendix B.1. We assume further that all other functions are continuously differentiable.

Given the generality of the constraints (1.1a)–(1.1f) under consideration, we must assume that they are compatible, that is, that there is at least one admissible pair $(\boldsymbol{x}, \boldsymbol{u})$.

Definition 1.1.2 *A trajectory* $(\boldsymbol{x}, \boldsymbol{u})$ *is said to be* admissible *if* $\boldsymbol{x} \in \mathcal{X}$ *and* $\boldsymbol{u} \in \mathcal{U}$ *and they satisfy the constraints* (1.1a) – (1.1f).

Denoting by

$$\partial_{\boldsymbol{x}} \boldsymbol{r}_{\text{eq}} := \frac{\partial \boldsymbol{r}_{\text{eq}}}{\partial \boldsymbol{x}}, \ \partial_{\boldsymbol{x}} \boldsymbol{r}_{\text{in}} := \frac{\partial \boldsymbol{r}_{\text{in}}}{\partial \boldsymbol{x}}$$

the Jacobian matrices of the end point constraints, which are of dimension $n_{\text{r}_{\text{eq}}} \times n$, $n_{\text{r}_{\text{in}}} \times n$, respectively, a constraint qualification for the end point constraints at $\boldsymbol{x}(t_{\text{f}})$ can be formulated as

$$\text{rank} = \begin{pmatrix} \partial_{\boldsymbol{x}} \boldsymbol{r}_{\text{eq}}(\boldsymbol{x}(t_{\text{f}}), \boldsymbol{p}) & \boldsymbol{0} \\ \partial_{\boldsymbol{x}} \boldsymbol{r}_{\text{in}}(\boldsymbol{x}(t_{\text{f}}), \boldsymbol{p}) & \text{diag}\big(\boldsymbol{r}_{\text{in}}(\boldsymbol{x}(t_{\text{f}}), \boldsymbol{p})\big) \end{pmatrix} = n_{\text{r}_{\text{eq}}} + n_{\text{r}_{\text{in}}}.$$

Definition 1.1.3 *A trajectory* $(\boldsymbol{x}^\star, \boldsymbol{u}^\star)$ *is said to be* optimal *if it is admissible and*

$$J[\boldsymbol{x}^\star, \boldsymbol{u}^\star] \leqslant J[\boldsymbol{x}, \boldsymbol{u}]$$

for all admissible trajectories $(\boldsymbol{x}, \boldsymbol{u})$.
It is said to be locally optimal *if it is admissible and there exist* $\delta > 0$ *such that*

$$J[\boldsymbol{x}^\star, \boldsymbol{u}^\star] \leqslant J[\boldsymbol{x}, \boldsymbol{u}]$$

for all admissible trajectories $(\boldsymbol{x}, \boldsymbol{u})$ *in a neighborhood of* $(\boldsymbol{x}^\star, \boldsymbol{u}^\star)$*, that is,* $||\boldsymbol{x}^\star - \boldsymbol{x}||_{L^\infty([t_0, t_{\text{f}}])} \leqslant \delta$, $||\boldsymbol{u}^\star - \boldsymbol{u}||_{L^\infty([t_0, t_{\text{f}}])} \leqslant \delta$.

In this terminology, $\boldsymbol{u}^\star$ is the optimal control and $\boldsymbol{x}^\star$ is the optimal state trajectory.

Equivalent formulations and generalizations

The presented formulation of the standard optimal control problem can be reformulated or extended to address a wider class of problems than the considered ODE-constrained optimal control problem over the fixed time horizon $[t_0, t_{\text{f}}]$ with path and end point constraints.

Interior point constraints The constraint functions (1.1d), (1.1f) and (1.1e) cover a wide range of common settings. They can be extended to include inner time point constraints, which represent conditions imposed on a finite number m of grid points $\{t_i\} \subset [t_0, t_{\text{f}}]$, $0 \leqslant i \leqslant m-1$, for instance

$$\boldsymbol{r}_{\text{eq}} : (\mathbb{R}^n)^m \times \mathbb{R}^{n_{\text{p}}} \to \mathbb{R}^{n_{\text{r}_{\text{eq}}}}, \ \boldsymbol{r}_{\text{eq}}(\{\boldsymbol{x}(t_i)\}, \boldsymbol{p}) = \boldsymbol{0}, \ \{t_i\} \subset [t_0, t_{\text{f}}].$$

The constraints may exhibit a coupling in time. One specific example are periodicity constraints, e.g.

$$\boldsymbol{r}^0(\boldsymbol{x}(t_0)) - \boldsymbol{r}^{\text{f}}(\boldsymbol{x}(t_{\text{f}})) = 0$$

wherein $\boldsymbol{r}^0$ and $\boldsymbol{r}^{\text{f}}$ contain permutations of the state components.

Objective function formulation The performance index $J[\boldsymbol{x}, \boldsymbol{u}]$ in (OCP) is formulated in form of a Bolza problem consisting of an integral contribution, the Lagrange objective with

integrand $l(\boldsymbol{x}(t), \boldsymbol{u}(t), \boldsymbol{p})$, evaluated on the whole time horizon $[t_0, t_f]$ and an end–point contribution, the Mayer objective $m(\boldsymbol{x}(t_f), \boldsymbol{p})$, evaluated only at the end point t_f. Equivalent formulations that contain only one of the two terms are called Lagrange problem and Mayer problem, respectively. For the equivalence, consider first the conversion of a Lagrange problem to a Mayer problem with a reformulated objective function

$$m(\boldsymbol{x}(t_f), \boldsymbol{p}) = z(t_f)$$

where z is an additional state variable which follows the differential equation

$$\dot{z} = l(\boldsymbol{x}(t), \boldsymbol{u}(t), \boldsymbol{p})$$

with initial value $z(t_0) = 0$. Mayer problems are readily reduced to Lagrange problems considering the objective function

$$\int_{t_0}^{t_f} z(\boldsymbol{x}(t), \boldsymbol{u}(t)) \mathrm{d}t$$

where z is an additional state variable with differential equation

$$\dot{z}(t) = 0, \quad z(t_0) = t_f^{-1} m(\boldsymbol{x}(t_f), \boldsymbol{p}).$$

Similarly, both objective formulations are equivalent to Bolza problems.

Controllable parameters The model parameters $\boldsymbol{p} \in \mathbb{R}^{n_p}$ may be considered to be controllable in which case

$$\begin{aligned} \min_{\boldsymbol{x},\boldsymbol{u},\boldsymbol{p}} \quad & J[\boldsymbol{x}, \boldsymbol{u}, \boldsymbol{p}] \\ \text{s.t.} \quad & (1.1a) - (1.1f). \end{aligned}$$

The model parameters can be replaced by additional state variables such that

$$\tilde{\boldsymbol{x}} = \begin{bmatrix} \boldsymbol{x} \\ \boldsymbol{p} \end{bmatrix}$$

The initial values $x_{0,n}, \ldots, x_{0,p+n-1}$ of the new variables are considered free and the ODE right hand side function is augmented such that

$$\tilde{\boldsymbol{f}}(\tilde{\boldsymbol{x}}(t), \boldsymbol{u}(t)) = \begin{bmatrix} \boldsymbol{f}(\boldsymbol{x}(t), \boldsymbol{u}(t), \boldsymbol{p}) \\ \boldsymbol{0} \end{bmatrix}.$$

Variable time horizons A time transformation replacing t with τ

$$t(\tau) := t_0 + z\tau, \quad z := t_f - t_0.$$

allows to investigate the optimal control problem on the simplified time horizon $[t_0, t_f] \overset{\text{def}}{=} [0, 1] \subset \mathbb{R}$. With $\dfrac{\mathrm{d}}{\mathrm{d}\tau} = \dfrac{\mathrm{d}}{\mathrm{d}t} z$, the ODE is now given by

$$\dot{\boldsymbol{x}}(\tau) = z \cdot \boldsymbol{f}\big(\boldsymbol{x}(t(\tau)), \boldsymbol{u}(t(\tau)), \boldsymbol{p}\big).$$

Variable length horizons including a free initial and/or a free final time can be conceptually formulated by including z as a global model parameter subject to optimization

$$\begin{aligned}
\min_{\boldsymbol{x},\boldsymbol{u},z} \quad & J[\boldsymbol{x},\boldsymbol{u},z] \\
\text{s.t.} \quad & \dot{\boldsymbol{x}}(\tau) = z \cdot \boldsymbol{f}\big(\boldsymbol{x}(t(\tau)),\boldsymbol{u}(t(\tau)),\boldsymbol{p}\big) && \tau \in [0,1] \text{ a.e.} \\
& \dot{z}(\tau) = 1 \\
& \boldsymbol{x}(t_0) = \boldsymbol{x}_0(\boldsymbol{p}) \\
& \boldsymbol{u}(t(\tau)) \in U(t(\tau)) && \tau \in [0,1] \text{ a.e.} \\
& z(t_0) = 0 \\
& \mathbf{0} \geqslant \boldsymbol{c}\big(\boldsymbol{x}(t(\tau)),\boldsymbol{u}(t(\tau)),\boldsymbol{p}\big) && \tau \in [0,1] \text{ a.e.} \\
& \mathbf{0} \geqslant \boldsymbol{r}_{\text{in}}(\boldsymbol{x}(t(1)),\boldsymbol{p}) \\
& \mathbf{0} = \boldsymbol{r}_{\text{eq}}(\boldsymbol{x}(t(1)),\boldsymbol{p}).
\end{aligned}$$

Non-autonomous system Problem (OCP) is formulated as an autonomous problems with no explicit time dependence in the model equations. Any non-autonomous system in which the equations $\boldsymbol{f}, l$, etc. depend explicitly on time can be readily transformed into this form. To this end, an additional state variable z is introduced that replaces the explicit occurrences of the time t and is governed by the ODE

$$\dot{z}(t) = 1, \quad z(t_0) = 0$$

with fixed final value $z(t_\text{f}) = t_\text{f}$.

Linear Semi-Implicit differential algebraic equation (DAE) The class of optimal control problems using system of ODEs to describe the dynamic process OCP may be extended to that of a semi–implicit index one DAE systems with differential states $\boldsymbol{x}(\cdot) \in \mathbb{R}^n$ and algebraic states $\boldsymbol{z}(\cdot) \in \mathbb{R}^{n_\text{z}}$ satisfying

$$\begin{aligned}
\boldsymbol{A}(\boldsymbol{x}(t),\boldsymbol{z}(t),\boldsymbol{u}(t),\boldsymbol{p})\,\dot{\boldsymbol{x}}(t) &= \boldsymbol{f}(\boldsymbol{x}(t),\boldsymbol{z}(t),\boldsymbol{u}(t),\boldsymbol{p}) \quad t \in [t_0,t_\text{f}] \text{ a.e.} \\
\mathbf{0} &= \boldsymbol{g}(\boldsymbol{x}(t),\boldsymbol{z}(t),\boldsymbol{u}(t),\boldsymbol{p}) \quad t \in [t_0,t_\text{f}] \text{ a.e..}
\end{aligned}$$

It is assumed that the left hand side matrix $\boldsymbol{A}$ and the Jacobian $\frac{\mathrm{d}}{\mathrm{d}\boldsymbol{z}}\boldsymbol{g}$ are regular. Using the implicit function theorem, the algebraic state trajectory $\boldsymbol{z}$ can then be regarded as an implicit function $\boldsymbol{z}(t) = \boldsymbol{g}^{-1}(\boldsymbol{x}(t),\boldsymbol{u}(t),\boldsymbol{p})$ of the differential state and control trajectories.
For more information and for the numerical solution of semi–implicit index one DAE systems, we refer to [3, 4, 12, 118]

1.2 Pontryagin's minimum principle

Pontryagin's minimum principle of optimal control, historically also known as Pontryagin's maximum principle or simply maximum principle, gives the necessary conditions for a trajectory $(\boldsymbol{x}^\star,\boldsymbol{u}^\star)$ to be optimal. It was developed in the mid 1950s under the leadership of Pontryagin, cf. [122]. The following exposition is based on the textbook [35]. We assume that the optimal control function $\boldsymbol{u}^\star$ is non-singular and can hence be determined using Pontryagin's minimum principle.

We state the theorem for a simplified version of (OCP) with only equality and inequality end-

point constraints.

$$\begin{aligned} \min_{\boldsymbol{x},\boldsymbol{u}} \quad & J[\boldsymbol{x},\boldsymbol{u}] := \int_{t_0}^{t_\mathrm{f}} l(\boldsymbol{x}(t),\boldsymbol{u}(t),\boldsymbol{p})\,\mathrm{d}t + m(\boldsymbol{x}(t_\mathrm{f}),\boldsymbol{p}) && \text{(OCP')} \\ \text{s.t.} \quad & \dot{\boldsymbol{x}}(t) = \boldsymbol{f}(\boldsymbol{x}(t),\boldsymbol{u}(t),\boldsymbol{p}) && t \in [t_0,t_\mathrm{f}] \text{ a.e.} \\ & \boldsymbol{x}(t_0) = \boldsymbol{x}_0(\boldsymbol{p}) \\ & \boldsymbol{u}(t) \in U(t) && t \in [t_0,t_\mathrm{f}] \text{ a.e.} \\ & \boldsymbol{0} \geqslant \boldsymbol{r}_\mathrm{in}(\boldsymbol{x}(t_\mathrm{f}),\boldsymbol{p}) \\ & \boldsymbol{0} = \boldsymbol{r}_\mathrm{eq}(\boldsymbol{x}(t_\mathrm{f}),\boldsymbol{p}) \end{aligned}$$

As before, we consider an autonomous system with a fixed final time. At the end of this section, we remark about the extension to control path constraints and to mixed control state constraints.
It is useful to define the Hamiltonian function.

Definition 1.2.1 *The Hamiltonian function associated with* (OCP') *is defined as*

$$H(\boldsymbol{x}(t),\boldsymbol{u}(t),\lambda^0,\boldsymbol{\lambda}(t)) = \boldsymbol{\lambda}(t) f(\boldsymbol{x}(t),\boldsymbol{u}(t),\boldsymbol{p}) + \lambda^0 l(\boldsymbol{x}(t),\boldsymbol{u}(t),\boldsymbol{p}).$$

with adjoint function $\boldsymbol{\lambda}^T(t) \in \mathbb{R}^n$ *and constant* λ^0.

The notation $\partial_{\boldsymbol{u}} = \frac{\partial}{\partial \boldsymbol{u}}$ always stands for the partial (Fréchet) derivative.

Pontryagin's minimum principle asserts that the solution trajectory together with an associated adjoint function and constraint multipliers satisfy a two-point boundary value problem for state and adjoint equations.

Theorem 1.2.1 (Pontryagin's minimum principle, cf. [35, Theorem 4.2i]) *If* $\boldsymbol{u}^\star$ *and the associated state trajectory* $\boldsymbol{x}^\star$ *are a solution of* (OCP') *on* $[t_0,t_\mathrm{f}]$*, then there exists a constant* $\lambda^0 \geqslant 0$*, an absolutely continuous adjoint function* $\boldsymbol{\lambda}^T(t) \in \mathbb{R}^n$ *and multiplier vectors* $\boldsymbol{\zeta}^T \in \mathbb{R}^{n_{\mathrm{r_{eq}}}}$ *and* $\boldsymbol{\nu}^T \in \mathbb{R}^{n_{\mathrm{r_{in}}}}$ *satisfying the following conditions:*

1. *Nontriviality of the adjoints:*

$$(\lambda^0,\boldsymbol{\lambda}(t)) \neq \boldsymbol{0} \;\; \text{on } [t_0,t_\mathrm{f}] \text{ a.e.}$$

2. *State equation:*

$$\dot{\boldsymbol{x}}^\star(t) = \boldsymbol{f}(\boldsymbol{x}^\star(t),\boldsymbol{u}^\star(t),\boldsymbol{p}) \;\; \text{on } [t_0,t_\mathrm{f}] \text{ a.e.}$$

3. *Initial condition:*

$$\boldsymbol{x}^\star(t_0) = \boldsymbol{x}_0^\star(\boldsymbol{p})$$

4. *Adjoint equation:*

$$\dot{\boldsymbol{\lambda}}(t) = -\boldsymbol{\lambda}(t)\partial_{\boldsymbol{x}} \boldsymbol{f}(\boldsymbol{x}^\star(t),\boldsymbol{u}^\star(t),\boldsymbol{p}) - \lambda^0\,\partial_{\boldsymbol{x}} l(\boldsymbol{x}^\star(t),\boldsymbol{u}^\star(t),\boldsymbol{p}) \;\; \text{on } [t_0,t_\mathrm{f}] \text{ a.e.}$$

5. *Transversality condition:*

$$\boldsymbol{\lambda}(t_\mathrm{f}) = \lambda^0\,\partial_{\boldsymbol{x}} m(\boldsymbol{x}^\star(t_\mathrm{f}),\boldsymbol{p}) + \boldsymbol{\zeta}^T \partial_{\boldsymbol{x}} \boldsymbol{r}_\mathrm{eq}(\boldsymbol{x}^\star(t_\mathrm{f}),\boldsymbol{p}) + \boldsymbol{\nu}^T \partial_{\boldsymbol{x}} \boldsymbol{r}_\mathrm{in}(\boldsymbol{x}^\star(t_\mathrm{f}),\boldsymbol{p})$$

6. *Constraints:*

$$\boldsymbol{r}_{\text{eq}}(\boldsymbol{x}(t_{\text{f}}),\boldsymbol{p})=\boldsymbol{0},\ \boldsymbol{r}_{\text{in}}(\boldsymbol{x}(t_{\text{f}}),\boldsymbol{p})\leqslant\boldsymbol{0}$$

7. *Complementary slackness:*

$$\boldsymbol{\nu}^T\boldsymbol{r}_{\text{in}}(\boldsymbol{x}(t_{\text{f}}),\boldsymbol{p})=\boldsymbol{0},\ \boldsymbol{\nu}\geqslant\boldsymbol{0}$$

8. *Minimum condition:*

$$H(\boldsymbol{x}^\star(t),\boldsymbol{u}^\star(t),\lambda^0,\boldsymbol{\lambda}(t))=\min_{\boldsymbol{u}\in U(t)}H(\boldsymbol{x}^\star(t),\boldsymbol{u}(t),\lambda^0,\boldsymbol{\lambda}(t))\ \ \textit{on}\ [t_0,t_{\text{f}}]\ \text{a.e.}$$

If $\boldsymbol{u}(t)$ takes on values in the interior of $U(t)$ for all $t\in[t_0,t_{\text{f}}]$ a.e., then we can infer from the minimum condition that

$$\partial_{\boldsymbol{u}}H(\boldsymbol{x}^\star(t),\boldsymbol{u}^\star(t),\lambda^0,\boldsymbol{\lambda}(t))=\boldsymbol{0}\quad\forall t\in[t_0,t_{\text{f}}]\ \text{a.e.}\tag{1.3}$$

properly supported by second-order relations, often referred to as Legendre conditions, e.g., [35, 28]:

Definition 1.2.2 *The solution trajectory* $(\boldsymbol{x}^\star,\boldsymbol{u}^\star,\lambda^0,\boldsymbol{\lambda})$ *satisfies the* Legendre necessary condition *if, in a neighborhood of* $\boldsymbol{u}^\star$*,*

$$d^T\partial^2_{\boldsymbol{u}^2}H(\boldsymbol{x}^\star(t),\boldsymbol{u}^\star(t),\lambda^0,\boldsymbol{\lambda}(t))d\geqslant 0\quad\forall d\in\mathbb{R}^{n_u},\ \forall t\in[t_0,t_{\text{f}}]\ \textit{a.e.}.$$

Under additional requirements using derivative information to describe local minimizers of the Hamiltonian, it can be ensured that the inner minimization problem in the minimum condition of Theorem 1.2.1 can be solved by using Equation (1.3).

Definition 1.2.3 *The solution trajectory* $(\boldsymbol{x}^\star,\boldsymbol{u}^\star,\lambda^0,\boldsymbol{\lambda})$ *satisfies the* strong Legendre condition *if, in a neighborhood of* $\boldsymbol{u}^\star$*,* $\forall t\in[t_0,t_{\text{f}}]$ *a.e.*

$$d^T\partial^2_{\boldsymbol{u}^2}H(\boldsymbol{x}^\star(t),\boldsymbol{u}^\star(t),\lambda^0,\boldsymbol{\lambda}(t))d\geqslant\alpha\ \textit{for some}\ \alpha>0\ \textit{and arbitrary}\ d\in\mathbb{R}^{n_u}.$$

Simple control constraints of the form

$$\boldsymbol{u}(t)\in\boldsymbol{U}(t)\subseteq\mathbb{R}^{n_{\text{u}}},\quad t\in[t_0,t_{\text{f}}]\ \text{a.e.}$$

e.g. with $\boldsymbol{U}(t)=[\boldsymbol{u}_{\min}(t),\boldsymbol{u}_{\max}(t)]$ can be transferred to the inner minimization problem. To this end, we define the extended Hamiltonian

$$\begin{aligned}H^\mu(\boldsymbol{x}^\star(t),\boldsymbol{u}^\star(t),\lambda^0,\boldsymbol{\lambda}(t))=H(\boldsymbol{x}^\star(t),\boldsymbol{u}^\star(t),\lambda^0,\boldsymbol{\lambda}(t))\\-\boldsymbol{\mu}_0(\boldsymbol{u}^\star-\boldsymbol{u}_{\min}(t))+\boldsymbol{\mu}_1(\boldsymbol{u}^\star-\boldsymbol{u}_{\max}(t))\end{aligned}$$

with multipliers $\boldsymbol{\mu}_0^T,\boldsymbol{\mu}_1^T\in\mathbb{R}^{n_{\text{u}}}$.
More complicated mixed state-control constraints and pure state constraints require a more complex theory that is subject to recent research [59, 128, 68, 28].

1.3 Overview of solution methods

Methods for the solution of optimal control problems of the type (OCP) can be classified into dynamic programming, indirect methods and direct methods. *Dynamic programming* is based

on *Bellman's Principle of Optimality* [13]. We refer to [117, 20] for more information. *Indirect methods* are based on Pontryagin's minimum conditions and follow the principle of first optimizing, then discretizing the problem instance. After applying the optimality conditions in function space, the resulting two-point boundary value problem for the state and adjoint variables is solved by numerical methods.
For large-scale, real-world optimal control problems with different types of constraints, *direct methods* are often the method of choice. This class of methods adheres the principle of first discretizing, then optimizing. They can be divided into *direct collocation*, e.g. cf. [22], *direct single shooting* and *direct multiple shooting* methods. We focus on the last method which forms a hybrid approach combining the shooting method of solving an IVP together with a possibly problem-dependent discretization. Advantages compared to collocation are the lower dimension of the resulting NLP and the fixed structure that can be exploited by tailored solvers. Compared to single shooting methods, it permits an easy initialization of the state trajectory variables and exhibits improved stability and efficiency of the IVP and the boundary value problem (BVP) solution process.

1.4 The direct multiple shooting method for optimal control

The direct multiple shooting method for optimal control has its origins in the diploma thesis [121], supervised by Hans Georg Bock, and was first published in [27]. Extensions can be found in e.g. [3, 26, 40, 92, 93, 133]. The direct multiple shooting code `MUSCOD-II` is described in detail in [91]. For the following description of the multiple shooting method, we follow the overviews given in [82]. For a detailed exposition including many of the possible extensions in the formulation of the optimal control problem, we refer to [94].
We consider the numerical solution of the following class of OCP that have been introduced in the beginning of this chapter as (OCP)

$$
\begin{aligned}
\min_{\boldsymbol{x},\boldsymbol{u}} \quad & \int_{t_0}^{t_\mathrm{f}} l(\boldsymbol{x}(t),\boldsymbol{u}(t),\boldsymbol{p})\mathrm{d}t + m(\boldsymbol{x}(t_\mathrm{f}),\boldsymbol{p}) \\
\text{s.t.} \quad & \dot{\boldsymbol{x}}(t) = \boldsymbol{f}(\boldsymbol{x}(t),\boldsymbol{u}(t),\boldsymbol{p}) && t \in [t_0, t_\mathrm{f}] \text{ a.e.} \\
& \boldsymbol{x}(t_0) = \boldsymbol{x}_0(\boldsymbol{p}) \\
& \boldsymbol{u}(t) \in U(t) && t \in [t_0, t_\mathrm{f}] \text{ a.e.} \\
& \boldsymbol{0} \geqslant \boldsymbol{c}(\boldsymbol{x}(t),\boldsymbol{u}(t),\boldsymbol{p}) && t \in [t_0, t_\mathrm{f}] \text{ a.e.} \\
& \boldsymbol{0} \geqslant \boldsymbol{r}_\mathrm{in}(\boldsymbol{x}(t_\mathrm{f}),\boldsymbol{p}) \\
& \boldsymbol{0} = \boldsymbol{r}_\mathrm{eq}(\boldsymbol{x}(t_\mathrm{f}),\boldsymbol{p})
\end{aligned}
$$

1.4.1 Discretized optimal control problem

The first step of the direct multiple shooting method is a discretization of the continuous time horizon $[t_0, t_\mathrm{f}]$ into N_shoot not necessarily equidistant intervals with

$$t_0 < t_1 < \ldots < t_{N_\mathrm{shoot}-1} < t_{N_\mathrm{shoot}} = t_\mathrm{f}.$$

Based on this so-called multiple shooting grid $\mathcal{T} = \{t_0, \ldots, t_{N_\mathrm{shoot}}\}$ a discretization method for the continuous control and state trajectories and for the constraints is defined using the building blocks

(I) the control discretization with parameter vector $\boldsymbol{q}$ and control functions $\hat{\boldsymbol{u}}(t;\boldsymbol{q})$,

(II) the state parametrization with parameter vector $\boldsymbol{s}$ and state trajectories $\boldsymbol{x}(t;\boldsymbol{s},\boldsymbol{q})$,

(III) the constraint discretization.

(I) Control discretization A computationally tractable representation of the infinite-dimensional control trajectory $\boldsymbol{u}(\cdot)$ is obtained by a discretization on the multiple shooting grid $\mathcal{T}$: On each interval $[t_j, t_{j+1}]$, $0 \leqslant j \leqslant N_{\text{shoot}} - 1$, and for each control function $1 \leqslant i \leqslant n_{\text{u}}$, we choose locally supported basis functions $\hat{\boldsymbol{u}}_i^{(j)}$ that are parameterized by a vector of finitely many control parameters $\boldsymbol{q}_i^{(j)} \in \mathbb{R}^{n_{\text{q}_i(j)}}$

$$\hat{\boldsymbol{u}}_i^{(j)} : [t_j, t_{j+1}] \times \mathbb{R}^{n_{\text{q}_i}^{(j)}} \longrightarrow \mathbb{R}.$$

Popular choices for the basis functions include piecewise constant controls ($n_{\text{q}_i(j)} = 1$)

$$\hat{\boldsymbol{u}}_i^{(j)}(t, q_i^{(j)})) = q_i^{(j)}, \tag{1.5}$$

piecewise linear controls ($n_{\text{q}_i(j)} = 2$)

$$\hat{\boldsymbol{u}}_i^{(j)}(t, \boldsymbol{q}_i^{(j)}) = \frac{t_{j+1} - t}{t_{j+1} - t_j} q_{i,1}^{(j)} + \frac{t - t_j}{t_{j+1} - t_j} q_{i,2}^{(j)}, \tag{1.6}$$

or piecewise cubic spline controls ($n_{\text{q}_i(j)} = 4$) with appropriately chosen spline function coefficients $\boldsymbol{\beta}$

$$\hat{\boldsymbol{u}}_i^{(j)}(t, \boldsymbol{q}_i^{(j)}) = \sum_{k=1}^{4} q_{i,k}^{(j)} \beta_k \left(\frac{t - t_j}{t_{j+1} - t_j} \right)^{k-1}. \tag{1.7}$$

If the discretized control trajectory is required to be continuous, we have to impose additional control continuity conditions in all points of the control discretization grid $\mathcal{T}$. For instance, for piecewise linear controls, the following constraints

$$0 = \hat{\boldsymbol{u}}_i^{(j)}(t_{j+1}, \boldsymbol{q}^{(j)}) - \hat{\boldsymbol{u}}_{i+1}^{(j)}(t_{j+1}, \boldsymbol{q}^{(j+1)}), \quad 0 \leqslant j \leqslant N_{\text{shoot}} - 1 \tag{1.8}$$

guarantee continuity along the multiple shooting horizon.

(II) State parameterization In contrast to single shooting methods, multiple shooting methods also introduce a parametrization of the state trajectory $\boldsymbol{x}(\cdot)$ on the multiple shooting grid $\mathcal{T}$ resulting in N_{shoot} IVPs with initial values $\boldsymbol{s}^{(j)} \in \mathbb{R}^n$ on the intervals $[t_j, t_{j+1}]$

$$\dot{\boldsymbol{x}}^{(j)}(t) = \boldsymbol{f}(\boldsymbol{x}^{(j)}(t), \hat{\boldsymbol{u}}^{(j)}(t, \boldsymbol{q}^{(j)}), \boldsymbol{p}), \quad t \in [t_j, t_{j+1}] \text{ a.e., } 0 \leqslant j \leqslant N_{\text{shoot}} - 1 \tag{1.9a}$$

$$\boldsymbol{x}^{(j)}(t_j) = \boldsymbol{s}^{(j)}. \tag{1.9b}$$

For the state parametrization $N_{\text{shoot}} - 1$ additional matching conditions

$$\boldsymbol{0} = \boldsymbol{x}^{(j)}(t_{j+1};\ t_j, \boldsymbol{s}^{(j)}, \boldsymbol{q}^{(j)}) - \boldsymbol{s}^{(j+1)}, \quad 0 \leqslant j \leqslant N_{\text{shoot}} - 1 \tag{1.10}$$

are required to ensure continuity of the obtained trajectory $\boldsymbol{x}(\cdot)$ on the time horizon $[t_0, t_{\text{f}}]$. Here, $\boldsymbol{x}^{(j)}(\cdot;\ t_j, \boldsymbol{s}^{(j)}, \boldsymbol{q}^{(j)})$ denotes the state trajectory obtained as the solution of the IVP (1.9) on the interval $[t_j, t_{j+1}]$ when starting in the initial value $\boldsymbol{x}(t_j) = \boldsymbol{s}^{(j)}$ and applying the control $\boldsymbol{u}(t) = \hat{\boldsymbol{u}}^{(j)}(t, \boldsymbol{q}^{(j)})$ with final value $\boldsymbol{x}^{(j)}(t_{j+1};\ t_j, \boldsymbol{s}^{(j)}, \boldsymbol{q}^{(j)})$ at time point t_{j+1}.
Hence, the evaluation of the each matching condition (1.10) requires the solution of an IVP, which allows the use of highly efficient adaptive IVP solvers, e.g. [4, 3, 12, 118], within the

direct multiple shooting method. Adaptive solvers employ error estimators to choose stepsizes and orders adaptively and are able to generate solutions that approximate the analytical solution with a prescribed error guarantee while remaining efficient by avoiding unnecessarily small stepsizes.

(III) Constraint discretization The path constraint $\boldsymbol{c}(\cdot)$ is discretized on $\mathcal{T}$ by enforcing a satisfaction on the multiple shooting grid only,

$$\mathbf{0} \leqslant \boldsymbol{c}^{(j)}(\boldsymbol{s}^{(j)}, \hat{\boldsymbol{u}}^{(j)}(t_j, \boldsymbol{q}^{(j)}), \boldsymbol{p}), \quad 0 \leqslant j \leqslant N_{\text{shoot}}. \tag{1.11}$$

In rare cases, the discretization may introduce violations of the path constraints between the shooting nodes for the optimal trajectory $(\boldsymbol{x}^\star, \boldsymbol{u}^\star)$ obtained as solution of the discretized problem shows. One possibility is to choose a finer, possibly adapted shooting grid for the constraint discretization. Alternatively, a semi–infinite programming algorithm for tracking of constraint violations in the interior of shooting intervals is discussed in [123, 124].

The nonlinear problem The resulting $(N_{\text{shoot}}+1)n + N_{\text{shoot}}n_{\text{q}}$ unknown variables from the application of the direct multiple shooting discretization to problem (OCP), here assuming $n_{\text{q}_i(j)}$ to be identical for all nodes and controls, are

$$\boldsymbol{y} \overset{\text{def}}{=} \begin{bmatrix} \boldsymbol{s}^{(0)} & \boldsymbol{q}^{(0)} & \dots & \boldsymbol{s}^{(N_{\text{shoot}}-1)} & \boldsymbol{q}^{(N_{\text{shoot}}-1)} & \boldsymbol{s}^{(N_{\text{shoot}})} \end{bmatrix}. \tag{1.12}$$

The resulting discretized optimal control problem reads

$$\min_{\boldsymbol{s},\boldsymbol{q}} \quad \sum_{j=0}^{N_{\text{shoot}}} l^{(j)}(\boldsymbol{s}^{(j)}, \boldsymbol{q}^{(j)}, \boldsymbol{p}) \tag{DOCP}$$

$$\text{s.t.} \quad \mathbf{0} = \boldsymbol{x}^{(j)}(t_{j+1};\ t_j, \boldsymbol{s}^{(j)}, \boldsymbol{q}^{(j)}) - \boldsymbol{s}^{(j+1)} \qquad 0 \leqslant j \leqslant N_{\text{shoot}} - 1 \tag{1.13a}$$

$$\mathbf{0} \geqslant \boldsymbol{c}^{(j)}(\boldsymbol{s}^{(j)}, \hat{\boldsymbol{u}}^{(j)}(t_j, \boldsymbol{q}^{(j)}), \boldsymbol{p}) \qquad 0 \leqslant j \leqslant N_{\text{shoot}} \tag{1.13b}$$

$$\mathbf{0} = \boldsymbol{r}_{\text{eq}}(\boldsymbol{s}^{(N_{\text{shoot}})}, \boldsymbol{p}) \tag{1.13c}$$

$$\mathbf{0} \geqslant \boldsymbol{r}_{\text{in}}(\boldsymbol{s}^{(N_{\text{shoot}})}, \boldsymbol{p}) \tag{1.13d}$$

Here, the Mayer term $m(\boldsymbol{s}^{(N_{\text{shoot}})}, \boldsymbol{p})$ has been expressed as final term

$$l^{(N_{\text{shoot}})}(\boldsymbol{s}^{(N_{\text{shoot}})}, \boldsymbol{q}^{(N_{\text{shoot}})}, \boldsymbol{p})$$

of the objective.

The discretized optimal control problem is a large but highly structured, constrained nonlinear program (NLP) and is solved by a tailored sequential quadratic programming (SQP) [67, 125] or other Newton-type methods preserving the specific structure of the Jacobian and the Hessian matrix resulting from the matching conditions (1.13a).

A convergence criterion to check whether convergence to a local optimum has been achieved is defined as the so-called *Karush–Kuhn–Tucker (KKT) tolerance* taking into account the weighted sum of possible objective function improvement and constraint violations[38, 93]. For the formula, we refer to [94, Section 3.2.2]. The acceptable KKT tolerance ε_{KKT} has the same units as the objective function.

1.4.2 Sensitivity generation

When we solve the discretized optimal control problem (DOCP) with a gradient-based method, the objective and constraints (1.13a)–(1.13d) as well as their first and possibly second order derivatives with respect to the discretized variables $\boldsymbol{s}$ and $\boldsymbol{q}$ must be evaluated at different points.
The functions l, m, $\boldsymbol{f}$, $\boldsymbol{c}$ and $\boldsymbol{r}$ are explicitly formulated as analytic functions and their derivatives can be evaluated, e.g., by using algorithmic differentiation (AD), cf. [65], or symbolic differentiation by writing down directly the analytic derivatives. For the important matching conditions (1.13a), the state trajectories $\boldsymbol{x}^{(j)}(\cdot;\ t_j, \boldsymbol{s}^{(j)}, \boldsymbol{q}^{(j)})$, which are given implicitly as solutions of the ODE (1.1a), as well as their derivatives need to be evaluated. The derivatives of this solution representation in the direction of the initial values $s^{(j)}$ and the discretized controls $q^{(j)}$, assumed for an arbitrary but fixed shooting node j with $1 \leqslant j \leqslant N_{\text{shoot}}$

$$\frac{d\boldsymbol{x}^{(j)}(\cdot;\ t_j, \boldsymbol{s}^{(j)}, \boldsymbol{q}^{(j)})}{d\boldsymbol{s}^{(j)}} \text{ and } \frac{d\boldsymbol{x}^{(j)}(\cdot;\ t_j, \boldsymbol{s}^{(j)}, \boldsymbol{q}^{(j)})}{d\boldsymbol{q}^{(j)}},$$

are called sensitivities in order to distinguish them from derivatives of analytic functions whose evaluation can be easily handled.

Finite differences

A straightforward approach to obtain the sensitivities of the IVP's solution at the end point $\boldsymbol{x}^{(j)}(t_{j+1};\ t_j, \boldsymbol{s}^{(j)}, \boldsymbol{q}^{(j)})$, or of intermediate shooting points, with respect to the initial values $\boldsymbol{s}^{(j)}$ and control parameters $\boldsymbol{q}^{(j)}$ is to apply a finite difference procedure to the solution method. For one-sided finite differences with a small perturbation factor $h > 0$, we obtain the state sensitivities with respect to $s_i^{(j)}$, $0 \leqslant i \leqslant n-1$, by

$$\begin{aligned}\frac{d\boldsymbol{x}^{(j)}(t_{j+1};\ t_j, \boldsymbol{s}^{(j)}, \boldsymbol{q}^{(j)})}{ds_i^{(j)}} &= \frac{\boldsymbol{\eta}(t_{j+1}; t_j, \boldsymbol{s}^{(j)} + he_i, \boldsymbol{q}^{(j)}) - \boldsymbol{\eta}(t_{j+1}; t_j, \boldsymbol{s}^{(j)}, \boldsymbol{q}^{(j)})}{h} \\ &\quad + \mathcal{O}(\mathtt{tol}/h) + \mathcal{O}(h)\end{aligned} \tag{1.14}$$

where $\boldsymbol{\eta}(t_{j+1}; t_j, \boldsymbol{s}^{(j)}, \boldsymbol{q}^{(j)})$ denotes the approximation of the IVP's solution $\boldsymbol{x}(t_{j+1})$ obtained when starting at time t_j with initial values $\boldsymbol{s}^{(j)}$ and e_i is the ith unit vector. $\mathtt{tol}$ is the local error bound, i.e., the integration tolerance of the forward solver. The optimal choice of perturbation is $h = \mathtt{tol}^{\frac{1}{2}}$. This means very tight integration tolerances are required to obtain sufficiently precise approximations of the IVP sensitivities.
This approach is referred to as external numerical differentiation because it treats the IVP solution method as a black box to which finite differences are applied *externally*. Several complications may occur when using adaptive and possibly different discretization grids $\{t_k\}$, pivoting in linear algebra subroutines, and iterative or inexact solvers causing nondifferentiabilities of the mapping $\boldsymbol{\eta}$ for the unperturbed and the perturbed values. This can lead to a decrease in precision or even inconsistent derivatives.

Variational Differential Equations

One way of computing the sensitivities that can be much more efficient than the previous finite difference scheme is to compute the sensitivities by following the principle of internal numerical differentiation (IND) introduced by Bock [24, 25]. It is based on the idea of differentiating

the discretization scheme used to compute an approximation of the nominal solution. Therefore, it avoids the previoiusly mentioned numerical difficulties and allows re-using certain internal information of the integration scheme.
The principle of IND is equivalent to numerically solving the nominal ODE system augmented by the corresponding variational differential equation (VDE), a technique that we will make use of in a later chapter. For this approach, we define the sensitivity matrices $\boldsymbol{x}_{\boldsymbol{s}}^{(j)}$ and $\boldsymbol{x}_{\boldsymbol{q}}^{(j)}$ as

$$\begin{aligned}\boldsymbol{x}_{\boldsymbol{s}}^{(j)} &:= \frac{d\boldsymbol{x}^{(j)}}{d\boldsymbol{s}^{(j)}} = \left(\frac{d\boldsymbol{x}_i^{(j)}(\cdot;\ t_j, \boldsymbol{s}^{(j)}, \boldsymbol{q}^{(j)})}{d\boldsymbol{s}_k^{(j)}}\right)_{1\leqslant i,k\leqslant n} \\ \boldsymbol{x}_{\boldsymbol{q}}^{(j)} &:= \frac{d\boldsymbol{x}_i^{(j)}}{d\boldsymbol{q}^{(j)}} = \left(\frac{d\boldsymbol{x}_i^{(j)}(\cdot;\ t_j, \boldsymbol{s}^{(j)}, \boldsymbol{q}^{(j)})}{d\boldsymbol{q}_k^{(j)}}\right)_{1\leqslant i\leqslant n, 1\leqslant k\leqslant n_{\mathrm{q}}}.\end{aligned}$$

The (forward) VDE corresponding to the dynamics

$$\begin{aligned}\dot{\boldsymbol{x}}^{(j)}(t) &= \boldsymbol{f}(\boldsymbol{x}^{(j)}(t), \hat{\boldsymbol{u}}^{(j)}(t, \boldsymbol{q}^{(j)}), \boldsymbol{p}) \\ \boldsymbol{x}^{(j)}(t_j) &= \boldsymbol{s}^{(j)}\end{aligned}$$

can now be formulated as

$$\begin{aligned}\dot{\boldsymbol{x}}_{\boldsymbol{s}}^{(j)}(t) &= \frac{\partial \boldsymbol{f}}{\partial \boldsymbol{x}}\boldsymbol{x}_{\boldsymbol{s}}^{(j)}(t), && \boldsymbol{x}_s(t_0) = I \\ \dot{\boldsymbol{x}}_{\boldsymbol{q}}^{(j)}(t) &= \frac{\partial \boldsymbol{f}}{\partial \boldsymbol{x}}\boldsymbol{x}_{\boldsymbol{q}}^{(j)}(t) + \frac{\partial \boldsymbol{f}}{\partial \boldsymbol{u}}\frac{\partial \hat{\boldsymbol{u}}}{\partial \boldsymbol{q}}, && \boldsymbol{x}_q(t_0) = \boldsymbol{0}.\end{aligned}$$

This approach also allows to exploit sparsity patterns in the Jacobians $\frac{\partial \boldsymbol{f}}{\partial \boldsymbol{x}}$ and $\frac{\partial \boldsymbol{f}}{\partial \boldsymbol{u}}$ of the ODE system's right-hand side.

2 Optimal control under uncertainty

We describe the main problem of optimal control under uncertainty in an informal manner by introducing the uncertain optimal control problem as an extension of parametric optimal control. We proceed with an overview of risk measures and a survey of existing solution methods for uncertainty propagation in dynamical systems and in optimal control problems.

2.1 From parametric optimal control to optimal control under uncertainty

In *parametric optimal control* or *optimal control with perturbations*, the model parameters $\boldsymbol{p} \in \mathbb{R}^{n_\mathrm{p}}$ are not fixed but instead vary according to different realizations. Under standard regularity assumptions together with the assumption of a sufficiently small variation of the parameters, the optimality condition hold also for the perturbed state trajectory $\boldsymbol{x}(t) = \boldsymbol{x}(t;\boldsymbol{p})$. This can be derived from stability and sensitivity analysis of solutions to parametric optimal control problems, compare, e.g., [74, 103] or Appendix B for an introduction to perturbation theory of mathematical problems.
A major extension is *optimal control under uncertainty*. Similarly assuming a dependence on unknown parameters, it is not based on the limiting assumption of a sufficiently small variation. Instead, it is assumed that the parameter domain has a certain structure, e.g., a set of a certain form or even derive from a measure or probability space. In this thesis, we consider the special assumption that the unknown parameters represent a random vector ξ on a probability space $(\Omega, \mathcal{F}, \mathrm{P})$ with finite or infinite support $\mathcal{S} \subseteq \mathbb{R}^d$. Here, d is the dimension of the uncertainty.

Before setting up the uncertain version of the optimal control problem, we give an informal introduction to probability-theoretic concepts. For precise definitions and more details we refer the reader to Appendix A. $\xi(\omega)$ represents the outcome of the random vector $\xi : \Omega \to \mathbb{R}^d$ if the realization $\omega \in \Omega$ occurs. By working with a probability measure P on Ω, the random variables induce a probability distribution on $\mathbb{R}^d$ with cumulative distribution function (CDF) F_ξ defined by taking $F_\xi(z)$ to be the probability assigned by P to the set of $\omega \in \Omega$ such that $\xi(\omega) \leqslant z$. The corresponding probability density function (PDF) is denoted by $\rho_\xi(z)$.
In optimal control problems, the parameters affect the state variables which evolve in time. At any arbitrary but fixed time point $\tau \in [t_0, t_\mathrm{f}]$, the state variables $x_\tau(\xi) = \boldsymbol{x}(\tau;\xi)$ can itself be considered as an $\mathbb{R}^n$-valued random vector with propagated distribution function $F_{\boldsymbol{x}_\tau}$ and propagated probability density function $\rho_{\boldsymbol{x}_\tau}$. By means of a nonlinear transformation $\eta(\xi)$, they can be expressed in terms of ξ, which can simplify the computation of integrals, etc. While ξ is usually assumed to be a continuous random variable, the propagated random vector $\boldsymbol{x}_\tau$ may not be continuous – due to the nonlinear dependence η on ξ – but can be expressed via ρ_ξ:

$$\mathrm{P}(\boldsymbol{x}_\tau \leqslant c) = \mathrm{P}(\eta(\xi) \leqslant c) = \mathrm{P}(\{\xi \in \mathcal{S} \mid \eta(\xi) \leqslant c\}) = \int_{\{\xi \in \mathcal{S} \mid \eta(\xi) \leqslant c\}} \rho_\xi(\xi)\mathrm{d}\xi. \tag{2.1}$$

Determining the set $\{\xi \in \mathcal{S} \mid \eta(\xi) \leqslant c\}$ and therefore the mapping η of the parameter distri-

bution onto the state variables or onto the constraints are the main difficulties in analyzing the effects of the random inputs ξ on the optimal control problem.
A prototype optimal control problem under uncertainty can be formulated as follows.

Definition 2.1.1 *The optimal control problem under uncertainty is an optimal control problem affected by random variables $\xi : \Omega \to \mathbb{R}^d$ with support $\mathcal{S}$*

$$\min_{x,u} \quad \Upsilon\big(J[x,u]\big) \tag{UOCP}$$

$$\text{s.t.} \quad \dot{x}(t) = f(x(t;\xi),u(t),\xi) \qquad t \in [t_0,t_f] \text{ a.e., } \xi \in \mathcal{S} \tag{2.2a}$$

$$x(t_0) = x_0(\xi) \qquad \xi \in \mathcal{S} \tag{2.2b}$$

$$u(t) \in U(t) \qquad t \in [t_0,t_f] \text{ a.e.} \tag{2.2c}$$

$$0 \geqslant \Phi\big(c(x(t;\xi),u(t),\xi)\big) \qquad t \in [t_0,t_f] \text{ a.e.} \tag{2.2d}$$

$$0 = \Psi\big(r_{eq}(x(t_f;\xi),\xi)\big) \tag{2.2e}$$

$$0 \geqslant \Psi\big(r_{in}(x(t_f;\xi),\xi)\big) \tag{2.2f}$$

where Υ, Φ and Ψ represent adequately chosen risk measures for the objective and constraint function.

Regardless of the type of considered uncertain parameters, e.g., "random" uncertain parameters as we have introduced them or "deterministic" uncertain parameters bound to take values from a certain set, the theory and the solution of optimal control under uncertainty is more complicated than in its absence. The main question is how the uncertainty affects the solution. We distinguish between two necessary tasks, which may overlap. In Section 2.3 we describe techniques for propagating and quantifying the uncertainty within the problem. Problems in optimization or in optimal control pose the additional challenge, which is often an advantage, of taking a robustification decisions. This can be achieved by applying one of the risk measures that we describe in Section 2.2 to the objective function and the constraints.

2.2 Introduction to risk measures

The amount of risk in a quantity of interest, e.g. the constraint $c(x,u,\xi)$, can loosely be regarded as the degree of uncertainty in its deviation about the nominal value. *Risk measures* assign a value to the random variable that quantifies the risk of loss or of another measure of performance. There is a wide choice of eligible risk measures that varies in their efficiency and cost of numerical computation. Loosely spoken, a risk measure is acceptable if it does not underestimate in some way the possibility of failure. Consequently, we seek for a performance guarantee even in the presence of uncertainty.

Simple surrogates for the risk are obtained by using moment-based risk measure. The most popular one is obtained by summing the mean and the standard deviation multiplied by a constant that depends on the required risk level

$$\Psi(c(x,u,\xi)) = \mathrm{E}\big[c(x,u,\xi)\big] + c_\delta \sqrt{\mathrm{Var}\big[c(x,u,\xi)\big]}. \tag{2.3}$$

This risk measure only leads to acceptable results in the rare case that the distribution of x can be completely described by the first two moments. This happens for instance if the input distribution of ξ is sufficiently simple and x depends linearly or nearly linearly on ξ because outputs resulting from linear transformations have the same distribution as the uncertain in-

puts. In general, using only low-order moments does not lead to a safe approximations for general nonlinear transformations without simplifying assumptions.

Arguably the most natural formulation of quantifying the variation of a random variable is by probabilistic constraints, also called chance constraints, in which the desired constraints are to hold at least with a specified probability:

$$\mathrm{P}\big(\boldsymbol{c}(\boldsymbol{x},\boldsymbol{u},\boldsymbol{\xi}) \leqslant \mathbf{0}\big) \geqslant 1-\delta. \tag{2.4}$$

Compared to worst-case, also called "min-max" risk measures, in which the constraint is to be satisfied for all possible realizations, they leave room for a small bounded number of constraint violations due to extreme outcomes that are infeasible to be satisfied or lead to a degraded performance. Therefore, chance constraints are a natural way of guaranteeing constraint satisfaction under uncertainty.
Computation methods for chance constraints can be divided into three major classes: (i) simulation methods; (ii) numerical integration and (iii) analytical methods [96]. The computation of chance constraints by

$$\mathrm{P}\big(\boldsymbol{c}(\boldsymbol{x},\boldsymbol{u},\boldsymbol{\xi}) \leqslant \mathbf{0}\big) = \mathrm{P}(\{\boldsymbol{\xi} \in \mathcal{S} \mid \boldsymbol{c}(\boldsymbol{x},\boldsymbol{u},\boldsymbol{\xi}) \leqslant \mathbf{0}\}) = \int_{\{\boldsymbol{\xi}\in\mathcal{S} \mid \boldsymbol{c}(\boldsymbol{x},\boldsymbol{u},\boldsymbol{\xi})\leqslant\mathbf{0}\}} \rho_{\boldsymbol{\xi}}(\boldsymbol{\xi})\mathrm{d}\boldsymbol{\xi}$$

involves multidimensional integration over a set in $\mathbb{R}^d$ which is difficult to determine. Consequently, there is little hope of finding a closed form expression for the distribution. A popular way of approximating the integral is by using a Monte Carlo sampling (MCS) average approximation, but the required huge number of samples of the random quantity may destroy either the satisfaction guarantee or the computational efficiency. One alternative is to apply the MCS instead to a so-called surrogate model, a sufficiently accurate approximate model describing the random dependence of the quantity of interest. This can be computationally much more tractable than a MCS applied to the original optimal control problem.
If we consider one-dimensional chance constraints for $c : \mathbb{R}^n \times \mathbb{R}^{n_\mathrm{u}} \times \mathbb{R}^d \to \mathbb{R}$

$$\mathrm{P}\big(c(\boldsymbol{x},\boldsymbol{u},\boldsymbol{\xi}) \leqslant \mathbf{0}\big) \geqslant 1-\delta, \tag{2.5}$$

we can use an equivalent formulation with a scalar value describing the $(1-\delta)$-quantile $q_{1-\delta}$ or value-at-risk (VaR)

$$\mathrm{VaR}_{1-\delta}(c(\boldsymbol{x},\boldsymbol{u},\boldsymbol{\xi})) := q_{1-\delta}(c(\boldsymbol{x},\boldsymbol{u},\boldsymbol{\xi})) = \inf\{\gamma \mid F_c(\gamma) \geqslant 1-\delta\}. \tag{2.6}$$

The VaR answers the question: what is the maximum loss with a specified confidence level of $1-\delta$?
For one-dimensional constraints, the satisfaction of (2.4) is equivalent to

$$\mathrm{VaR}_{1-\delta}(c(\boldsymbol{x},\boldsymbol{u},\boldsymbol{\xi})) \leqslant 0 \tag{2.7}$$

or

$$\min \gamma \text{ s.t. } \mathrm{P}\big(c(\boldsymbol{x},\boldsymbol{u},\boldsymbol{\xi}) \leqslant \gamma\big). \tag{2.8}$$

Thus, this formulation naturally extends chance constraints to the objective functional.
Despite being widely used, chance constraints or the VaR formulation are not free of criticism. The fact that they do not take into account the extreme loss beyond the $(1-\delta)$-quantile can be a positive or negative property depending on the application: it means a disregard towards ex-

treme outcomes, hence robustness against outliers and extremely heavy losses. Another critic comes with the fact that both formulations are inherently non-convex, thus violating the diversification principle in finance and economics and leading to disadvantages for optimization procedures if the underlying problem is convex. To overcome these drawbacks, the axiomatic framework of coherency as an indicator for when a risk measure preserves the properties of the underlying system was developed within finance and economics by Artzner and coworkers [7] and extended by Rockafellar [129]. A coherent replacement of the VaR was found by the conditional value-at-risk (CVaR) as the tightest convex approximation to individual chance constraints [112]. With the same confidence level, VaR is a lower bound for CVaR, hence less conservative.

Our focus in this thesis is not on convex risk measures because the dependence of $\boldsymbol{x}(t;\xi)$ and therefore of $\boldsymbol{c}(\cdot)$ on ξ is not convex. Rather, we seek risk measures that lead to the best objective value for optimal control problems while remaining acceptable under uncertainty. In other words, they should provide a safe application-dependent guarantee of feasibility with as few conservatism as possible.

2.3 Existing approaches to optimal control under uncertainty

Existing methods can be roughly divided into two groups, based on (i) deterministic methods such as the worst-case guarantee approach, and (ii) stochastic or statistical design techniques that employ a probabilistic description of the uncertainty to define robustness measures and lead to a guarantee with a high probability. In both cases, linearization is often applied for simplification but only leads to a reasonable reformulation in some cases, e.g., if the uncertain parameter do not deviate too much from their nominal value or the curvatures of the involved functions with respect to the uncertainty are bounded. Usually it cannot capture nonlinear effects of the considered class of constrained, nonlinear optimal control problems.

In the following, we explain and classify the existing techniques in more detail. Our method of choice must be able to capture the nonlinear uncertainty propagation within the dynamical system and be tractable for optimal control in which the minimization of the objective and the solution of the dynamic model proceeds simultaneously. A further consideration is the assumption that we can only control the system in a nonanticipative open-loop mode with no measurements available and without possibility to react to disturbances online during the process operation.

2.3.1 Classical robust control

Classical robust control assumes that the uncertain parameters arise from some compact uncertainty set $\mathcal{S}$. It was developed to overcome the limitations of the Kalman filter [79, 44]. The first developments concerned linear control systems with set constrained disturbances [153]. For a more detailed exposition of the development of robust control theory, we refer to the textbooks [154, 46].
Commonly used bounded uncertainty sets are polytopes, given with bounds $\xi_{\min}, \xi_{\max} \in \mathbb{R}^d$,

$$\mathcal{S} = \{\xi \in \mathbb{R}^d \mid \xi_{\min} \leqslant \xi \leqslant \xi_{\max}\} \tag{2.9}$$

ellipsoids, given with mean $\bar{\xi} \in \mathbb{R}^d$, covariance matrix $\Sigma \in \mathbb{R}^{d\times d}$ and scalar $\gamma > 0$

$$\mathcal{S} = \{\xi \in \mathbb{R}^d \mid (\xi - \bar{\xi})^T \Sigma^{-1} (\xi - \bar{\xi}) \leqslant \gamma\}. \tag{2.10}$$

or the more general norm-constrained set, given with mean $\bar{\xi} \in \mathbb{R}^d$, invertible matrix $\Sigma \in \mathbb{R}^{d\times d}$ and parameter $1 \leqslant q \leqslant \infty$ for the scaled Hölder q-norm

$$\mathcal{S} = \{\xi \in \mathbb{R}^d \mid \left|\left|\xi - \bar{\xi}\right|\right|_{\Sigma,q} \leqslant 1\}. \tag{2.11}$$

Some uncertainty sets allow for an interpretation in terms of confidence level sets for random variables. For instance the first set can be interpreted in terms of a confidence level set of a uniformly distributed variable and the second set coincides to the confidence level of a Gaussian distribution with critical value γ corresponding to a prescribed probability level $1-\delta$.
For contributions on the analysis of ellipsoidal methods for linear dynamic systems, we refer to Kurzhanski, Valyi, and Varaiya [86, 87]. Particularly in control theory, polytopic uncertainty sets are also common, e.g., [21, 41, 23].

Worst-case design is concerned with optimizing the worst possible outcome of the uncertain-but-bounded parameter set. The term robust counterpart formulation was coined by Ben-Tal and Nemirovski [14] in robust optimization. In this formulation, the optimizer chooses $\boldsymbol{u}$ first while an adverse player can arbitrarily choose the uncertainty realizations ξ and $\boldsymbol{x}(\xi)$ afterwards. This leads to a min-max optimization problem with a bilevel structure. For optimal control for which we assume that the dynamics must be satisfied for almost all uncertainty realizations, it leads to the following form:

Example 2.3.1 (Min-max formulation)

$$\begin{aligned}
\min_{\boldsymbol{u}\in U(t)} \ & \max_{\boldsymbol{x},\xi\in\mathcal{S}} J[\boldsymbol{x},\boldsymbol{u}] \\
\text{s.t.} \ & \max_{\boldsymbol{x},\xi\in\mathcal{S}} \boldsymbol{c}(\boldsymbol{x},\boldsymbol{u},\xi) \leqslant \boldsymbol{0} \\
\text{s.t.} \ & \dot{\boldsymbol{x}} = \boldsymbol{f}(\boldsymbol{x},\boldsymbol{u},\xi) \qquad \forall \xi \in \mathcal{S} \\
& \boldsymbol{x}(t_0) = \boldsymbol{x}_0
\end{aligned}$$

The computationally tractable cases are robust linear, convex and semidefinite programs and have first been studied by Ben-Tal and Nemiosvski [14, 15] and Ghaoui [58]. A related view is semi-infinite programming for which we refer to [70] for a recommendable overview article. In this formulation, the constraints have to be satisfied for all possible uncertainty realizations arising from $\mathcal{S}$. This leads to an infinite number of constraints that must be regarded at any time point τ, and has the following form for an optimal control problem:

Example 2.3.2 (Semi-infinite formulation)

$$\begin{aligned}
\min_{\boldsymbol{x},\boldsymbol{u}\in U(t)} \ & J[\boldsymbol{x},\boldsymbol{u}] \\
\text{s.t.} \ & \dot{\boldsymbol{x}} = \boldsymbol{f}(\boldsymbol{x},\boldsymbol{u},\xi) \quad \forall \xi \in \mathcal{S} \\
& \boldsymbol{x}(t_0) = \boldsymbol{x}_0 \\
& \boldsymbol{0} \geqslant \boldsymbol{c}(\boldsymbol{x},\boldsymbol{u},\xi) \quad \forall \xi \in \mathcal{S}
\end{aligned}$$

Under certain simplifying assumptions on the functions and the uncertainty set, the sub maximization problem can be eliminated by linearization of the model functions using the nominal value of ξ. If the functional dependence on the uncertain parameters is linear or shows only small curvalture, or if the underlying maximization problem has its solution always on the boundary of the uncertainty set, the result is a conservative robustification. In optimal control, this approach was used by Ma and Braatz [101], Nagy and Braatz [110, 109] and Diehl et al. [41, 42, 43].

Recent developments in robust control and uncertain dynamical systems is driven by *reachability analysis* and *set-based methods*, cf., e.g., [72].

2.3.2 Unscented transform and the sigma point approach

The Kalman filter [79] only provides an optimal solution for linear systems by maintaining a consistent estimate of the first two moments of the state distribution. To improve on it, the unscented transform (UT) was developed by Julier [78] as a general method for approximating nonlinear transformations of probability distributions. In control and filtering applications, the UT, especially in the form of the unscented Kalman filter (UKF), has largely replaced the extended Kalman filter (EKF), which simply uses a linearization by Taylor approximation around the mean.

The UT proceeds by applying the nonlinear function transformation to a discrete distribution of so-called *sigma points* with specific weights computed to be able to capture a set of known statistics of an unknown distribution. For simple distributions such as the normal distribution, the given mean and covariance information can be exactly encoded and propagated. The mean and covariance of the transformed set of points then represents the desired transformed estimate.

The disadvantage of these approaches lie in the fact that they do not lead to a conservative approximation for general nonlinearly propagated distributions. The main advantage is its simplicity and it has been applied in optimal control, see [69, 145].

2.3.3 Classical stochastic optimal control

Stochastic and statistical techniques to optimization and optimal control under uncertainty assume that the uncertainty has a probabilistic description. The probabilistic description may range from a probability distribution, which can completely characterize the uncertainty, to a continuous or discrete set of possible scenarios together with a corresponding probability of occurrence or with a number of given probability statistics such as moments.

Similar to robust control based on deterministic principles, linearization of the system trajectories is often used for propagating the uncertainty through the dynamical system. This can be done by applying the linear transformation to a finite number of lower moments, e.g. applied to the mean and the variance, we obtain

$$\mathrm{E}\left[A\xi\right] = A\bar{\xi} \text{ and } \mathrm{E}\left[(A\xi)(A\xi)^T\right] = \mathrm{E}\left[A\xi\xi^T A^T\right] = A\Sigma_\xi A^T.$$

A natural interpretation of constraints in the presence of randomness are chance constraints which have been developed by Charnes, Cooper, and Symonds in [36], Miller and Wagner [107], as well as by Prekopa [126]. In engineering science, chance-constrained optimization and chance-constrained optimal control is coined reliability-based design. In Section 2.2, we gave a theoretical introduction into this topic which plays an important part in this thesis. The first studied problems in chance constrained optimization were linear programs, exploiting heavily the convexity of the feasible region resulting in the case of quasi-concavely distributed uncertain variables [135].

Applied to (UOCP), chance constraints lead to a performance guarantee for the original problem. In the case of joint chance constraints, the guarantee holds for at least $(1-\delta)$% of all possible realizations of the uncertain parameters. There are different possibilities of how to apply chance constraints to the objective and constraints function.

Example 2.3.3 (Risk-neutral objective, joint chance-constrained OCP)

$$\begin{aligned}
\min_{\boldsymbol{x},\boldsymbol{u}\in U(t)} \quad & \mathrm{E}[J[\boldsymbol{x},\boldsymbol{u}]] \\
\text{s.t.} \quad & \dot{\boldsymbol{x}} = \boldsymbol{f}(\boldsymbol{x},\boldsymbol{u},\xi) && \forall \xi \in \mathcal{S} \\
& \boldsymbol{x}(t_0) = \boldsymbol{x}_0 \\
& 1-\delta \leqslant \underbrace{\mathrm{P}\big(\boldsymbol{c}(\boldsymbol{x},\boldsymbol{u},\xi) \leqslant \boldsymbol{0}\big)}_{\mathrm{P}\left(c_j(\boldsymbol{x},\boldsymbol{u},\xi)\leqslant 0,\ j=1,\ldots,n_\mathrm{c}\right)}
\end{aligned}$$

The multidimensional integral in Example 2.3.3 is over $\mathbb{R}^{n_\mathrm{c}}$. Computationally more tractable is the formulation with individual chance constraints, which leads to a guaranteed constraint satisfaction rate of $\sum_{j=1}^{n_\mathrm{c}}(1-\delta_j)\,\%$.

Example 2.3.4 (Risk-neutral objective, individual chance-constrained OCP)

$$\begin{aligned}
\min_{\boldsymbol{x},\boldsymbol{u}\in U(t)} \quad & \mathrm{E}[J[\boldsymbol{x},\boldsymbol{u}]] \\
\text{s.t.} \quad & \dot{\boldsymbol{x}} = \boldsymbol{f}(\boldsymbol{x},\boldsymbol{u},\xi) && \forall \xi \in \mathcal{S} \\
& \boldsymbol{x}(t_0) = \boldsymbol{x}_0 \\
& 1-\delta_j \leqslant \mathrm{P}\big(c_j(\boldsymbol{x},\boldsymbol{u},\xi) \leqslant 0\big) && j = 1,\ldots,n_\mathrm{c}
\end{aligned}$$

A certain attitude towards risk, either a risk preference or a risk averseness, can be expressed by incorporating chance constraints also for the objective value instead of the risk-neutral mean formulation.

Example 2.3.5 (Risk-averse/seeking objective, individual chance-constrained OCP)

$$\begin{aligned}
\min_{\boldsymbol{x},\boldsymbol{u}\in U(t)} \quad & \gamma \\
\text{s.t.} \quad & \dot{\boldsymbol{x}} = \boldsymbol{f}(\boldsymbol{x},\boldsymbol{u},\xi) && \forall \xi \in \mathcal{S} \\
& \boldsymbol{x}(t_0) = \boldsymbol{x}_0 \\
& 1-\delta_0 \leqslant \mathrm{P}\left(J[\boldsymbol{x},\boldsymbol{u}] \leqslant \gamma\right) \\
& 1-\delta_j \leqslant \mathrm{P}\big(c_j(\boldsymbol{x},\boldsymbol{u},\xi) \leqslant 0\big) && j = 1,\ldots,n_\mathrm{c}
\end{aligned}$$

2.3.4 Sampling and scenario-based approaches

In scenario or sampling approaches, the uncertainty space is discretized into a finite number of N samples or scenarios $\Delta = \{\xi^{(1)},\ldots,\xi^{(N)}\}$ of ξ and the original problem is solved only on Δ. This leads to an enlarged optimal control problem with state dimension $\mathbb{R}^{nN}$ and control dimension $\mathbb{R}^{n_\mathrm{u}}$. The objective is formulated as a weighted sum of the objectives for the different scenarios.

Example 2.3.6 (Sampling/scenario-OCP)

$$\begin{aligned}
\min_{\boldsymbol{x}^{(1)},\ldots,\boldsymbol{x}^{(N)}\in\mathbb{R}^n,\boldsymbol{u}\in U(t)} \quad & \sum_{m=1}^{N} J[\boldsymbol{x}^{(m)},\boldsymbol{u}]\,w^{(m)} \\
\text{s.t.} \quad & \dot{\boldsymbol{x}}^{(m)} = \boldsymbol{f}(\boldsymbol{x}^{(m)},\boldsymbol{u},\xi^{(m)}) && m = 1,\ldots,N \\
& \boldsymbol{x}^{(m)}(t_0) = \boldsymbol{x}_0 \\
& \boldsymbol{0} \geqslant \boldsymbol{c}(\boldsymbol{x}^{(m)},\boldsymbol{u},\xi^{(m)}) && m = 1,\ldots,N
\end{aligned}$$

The main concern towards this approach lies in the feasibility of the constraints. That is, does the satisfaction of $\boldsymbol{c}(\boldsymbol{x}^{(m)}, \boldsymbol{u}, \xi^{(m)}) \leqslant \boldsymbol{0}$ for all scenarios infer the satisfaction of $\boldsymbol{c}(\boldsymbol{x}, \boldsymbol{u}, \xi) \leqslant \boldsymbol{0}$ for all possible parameter realizations within the critical subspace for a given probability level $\delta > 0$? In other words, if formulated in terms of a probability space, does

$$\boldsymbol{c}(\boldsymbol{x}^{(m)}, \boldsymbol{u}, \xi^{(m)}) \leqslant \boldsymbol{0},\ m = 1, \dots, N \implies \mathrm{P}\big(\boldsymbol{c}(\boldsymbol{x}, \boldsymbol{u}, \xi) \leqslant \boldsymbol{0}\big) \geqslant 1 - \delta \tag{2.18}$$

hold?
Scenario-based sampling has been applied to optimal control in, e.g., [30, 31], who also provide a satisfaction guarantee for convex problems with a reasonable bound on the number of samples.

MCS methods are widely used for uncertainty quantification in many fields. Similarly to scenario-based approaches, they proceed by solving an enlarged optimal control problem over a finite set of possible realizations $\xi^{(1)}, \dots, \xi^{(N_{\mathrm{MC}})}$, which are now randomly sampled from the distribution of ξ. A point-wise approximation of the constraint $c : \mathbb{R}^n \times \mathbb{R}^{n_\mathrm{u}} \times \mathbb{R}^d \to \mathbb{R}$ is then constructed via

$$\mathrm{P}\big(c(\boldsymbol{x}, \boldsymbol{u}, \xi) \leqslant 0\big) = \int_{(-\infty, 0]^d} c(\boldsymbol{x}, \boldsymbol{u}, \xi) \rho(\xi) \mathrm{d}\xi \approx \sum_{m=1}^{N_{\mathrm{MC}}} c(\boldsymbol{x}^{(m)}, \boldsymbol{u}, \xi^{(m)})\, w^{(m)}$$

for appropriately chosen weights $\{w^{(m)}\}_{m=1,\dots,N_{\mathrm{MC}}}$. Using the law of large numbers and the central limit theorem [48], MCS provides a consistent convergence rate of $O(n^{-1/2})$ independent of the dimension of ξ and applicable to arbitrary probability distributions. Consequently, the feasibility of the constraints via (2.18) can be guaranteed. Unfortunately, in practical applications and in particular for nonlinear optimal control problems, the convergence rate is too slow to be of practical use. Certain techniques, e.g., quasi Monte Carlo (QMC), Latin-Hypercube MC or variance reduction techniques may allow for a speed-up. However, the required large number of realizations for obtaining high accuracy is still prohibitively high for optimal control. Nevertheless, some applications to optimal control were reported in the literature, cf. [34, 100].

2.3.5 Recourse decisions

Recourse decisions, cf. [149], allow, after taking an initial decision, for taking a second decision. This operation could counteract bad consequences or take advantage of good consequences. A similar approach is multistage programming where decisions are made successively in order to use the additional information that enters into the problem when the realization of an uncertain parameter takes place, e.g. to ensure that the constraints are satisfied. In model predictive control (MPC), scenario tree approaches in which the description of the uncertainty evolves in form of a scenario tree, are popular [98, 97, 90].

2.3.6 Spectral methods and the polynomial chaos method

Sampling approaches provide a point-wise estimate of the random quantities. A substantially different view on the resolution of the model equations is provided by spectral methods which reconstruct the functional dependency of the solution $\boldsymbol{x}$ on the random input ξ

$$\boldsymbol{x}(\xi) = \sum_{k=0}^{\infty} \boldsymbol{x}_k \phi_k(\xi) \tag{2.19}$$

by means of a set of basis functionals ϕ_k and deterministic coefficients $\boldsymbol{x}_k$. Such a series representation requires in most cases additional regularity assumptions on the solution, e.g., $\boldsymbol{x}(\xi)$ being L^2-measurable with respect to the underlying probability space. Spectral methods provide a simpler surrogate model of adjustable complexity and adjustable approximation quality. These surrogate models can be used, e.g., for approximation of the probability density function by application of MCS or of other techniques. This can save several orders of magnitudes in the computational cost compared to direct MCS.

The different types of spectral methods vary in the type of basis functionals and the derivation of the coefficients which can be carried out analytically, by sampling techniques or by projection techniques. Our main focus in this thesis is the polynomial chaos (PC) method, a spectral method in which Equation (2.19) represents a generalized global Fourier expansion, called polynomial chaos expansion, in a random polynomial basis. When using more general probability distributions such as the normal distribution, this method is also referred to as generalized polynomial chaos (gPC). First practical use of the gPC fracemwork can be found in sparse and linear system, often complicated by high dimensionality in state or uncertain parameter space originating from a discretization of PDE or stochastic processes. Application areas vary amongst computational fluid dynamics [57, 151, 89], aerodynamic design [134], mechanics [147] and geology [114]. Current work primarily addresses this setting. Examples for recent applications to stochastic optimal control of PDEs include [37, 155, 85, 84] as well as in shape and topology optimization [134, 147]. The first works of gPC in control systems with ordinary differential equations empirically studied questions such as convergence and stability on small test problems [73, 75, 55] or linear systems [138, 54]. Applications to real-world optimal control problems can be found in, e.g., [111, 80, 18], and the review article [81]. For recent work on the use of gPC for solving stochastic model predictive control, consider [76, 105, 106]. Fagiano [52] uses gPC to design a controller that induces convergence of the expected value of the state to the origin and satisfies state constraints in expectation.

2.3.7 Optimal control of stochastic differential equations

So far we have considered the uncertain inputs to be (random) variables. An extension of this parametric uncertainty framework is the inclusion of a stochastic process ζ_t into the vector field function which results in a pathwise (explicit) ODE

$$\dot{\boldsymbol{x}}(t) = \boldsymbol{f}(\boldsymbol{x}, \boldsymbol{u}, \zeta_t).$$

This formulation is called random differential equations (RDE) [83].
A further extension are stochastic differential equations (SDE)

$$\dot{\boldsymbol{x}}(t) = \boldsymbol{f}(\boldsymbol{x}, \boldsymbol{u}) + \boldsymbol{g}(\boldsymbol{x}, \boldsymbol{u})\zeta_t,$$

where the random process ζ_t with known covariance is called noise or stochastic forcing. This extension is equivalent to the RDE formulation if ζ_t is sufficiently regular [83, 66] The class of RDE can be analysed pathwise with the usual methods of deterministic calculus, taking into account that the solution is only continuously differentiable but not further differentiable in time [83, 66] while the second class is usually tackled by the L^2 convergence results given by the Îto stochastic calculus.
The most popular SDE, also called Îto SDE, is

$$\mathrm{d}\boldsymbol{x}_t = \boldsymbol{f}(\boldsymbol{x}_t, \boldsymbol{u}) + \boldsymbol{g}(\boldsymbol{x}_t, \boldsymbol{u})\mathrm{d}W_t$$

where W_t is the Wiener process.

Instead of these two continuous approaches, it is sometimes possible to obtain a finite approximation of the stochastic process ζ_t by using the Karhunen-Loeve expansion [95], a technique similar to the principal component analysis. If the noise is amenable to a finite-dimensional approximation, e.g. if it has a non-zero correlation window, then the number of terms of the expansion will be finite and can be replaced by a finite number of independent random variables.

3 Convergence analysis of the polynomial chaos surrogate

This chapter contains a thorough analysis of the uncertain optimal control problem in a slightly simpler form. We include a summary of the most important definitions and results of spectral projections with orthogonal polynomials, which also form the foundation of the polynomial chaos method described thereafter. We apply the polynomial chaos method to the uncertain optimal control problem in order to derive the corresponding polynomial chaos surrogate problem. Similar to the deterministic problem version in Section 1.2, we discuss well-posedness and necessary optimality conditions. The major contribution is the proof of convergence of the polynomial chaos surrogates in the last part of this chapter.

3.1 Problem definition

Having introduced the considered problem class in Section 2.1, we consider a slightly simpler set-up of the uncertain nonlinear optimal control problem with final state constraints and with expected value robustification:

Definition 3.1.1 *The* uncertain optimal control problem *is given by*

$$\min_{\boldsymbol{u},\boldsymbol{x}} \quad \mathrm{E}\Big[\int_{t_0}^{t_\mathrm{f}} l(\boldsymbol{x}(t;\xi),\boldsymbol{u}(t),\xi)\mathrm{d}t + m(\boldsymbol{x}(t;\xi),\xi)\Big] \tag{UOCP}$$

$$\text{s.t.} \quad \dot{\boldsymbol{x}}(t;\xi) = \boldsymbol{f}(\boldsymbol{x}(t;\xi),\boldsymbol{u}(t),\xi) \qquad t\in[t_0,t_\mathrm{f}]\ a.e.,\ \xi\in\mathcal{S} \tag{3.1a}$$

$$\boldsymbol{x}(t_0) = \boldsymbol{x}_0(\xi) \qquad \xi\in\mathcal{S} \tag{3.1b}$$

$$\boldsymbol{u}(t)\in U(t) \qquad t\in[t_0,t_\mathrm{f}]\ a.e. \tag{3.1c}$$

$$\boldsymbol{0} \geqslant \mathrm{E}\big[\boldsymbol{r}_\mathrm{in}(\boldsymbol{x}(t_\mathrm{f};\xi),\xi)\big] \tag{3.1d}$$

$$\boldsymbol{0} = \mathrm{E}\big[\boldsymbol{r}_\mathrm{eq}(\boldsymbol{x}(t_\mathrm{f};\xi),\xi)\big]. \tag{3.1e}$$

The problem is influenced by uncertain inputs which form a d-dimensional, continuous random variable

$$\xi = (\xi_1,\ldots,\xi_d) : \Omega \to \mathbb{R}^d$$

independently distributed in each dimension over a probability space $(\Omega,\mathcal{F},\mathrm{P})$ with joint density function $\rho(\xi)$ and support $\mathcal{S}$.

Similar to the deterministic version of the problem, we make the following assumptions on the involved functions.

Assumption 3.1 *For each realization $\xi(\omega),\ \omega\in\Omega$ a.s. the function $\boldsymbol{f}$ is Lipschitz–continuous in $\boldsymbol{x}$ and $\boldsymbol{u}$ on $[t_0,t_\mathrm{f}]$ with bounded Lipschitz-continuous derivative in $\boldsymbol{x}$. The expectations of the objective and constraint functions $\mathrm{E}[l]$, $\mathrm{E}[m]$, $\mathrm{E}\big[\boldsymbol{r}_\mathrm{eq}\big]$ and $\mathrm{E}[\boldsymbol{r}_\mathrm{in}]$ are continuously differentiable in $\boldsymbol{x}$. We assume that the constraints are compatible, in particular, that there is an admissible pair $(\boldsymbol{x},\boldsymbol{u})$ satisfying (3.1a)–(3.1e).*

We may pose the following constraint qualification on the terminal constraints at $\boldsymbol{x}^\star(t_\mathrm{f};\boldsymbol{\xi}(\omega))$, $\omega \in \Omega$ a.s.

$$\operatorname{rank}\begin{pmatrix} \partial_{\boldsymbol{x}} \mathrm{E}\big[\boldsymbol{r}_{\mathrm{eq}}(\boldsymbol{x}^\star(t_\mathrm{f};\boldsymbol{\xi}),\boldsymbol{\xi})\big] & \mathbf{0} \\ \partial_{\boldsymbol{x}} \mathrm{E}\big[\boldsymbol{r}_{\mathrm{in}}(\boldsymbol{x}^\star(t_\mathrm{f};\boldsymbol{\xi}),\boldsymbol{\xi})\big] & \operatorname{diag}\big(\mathrm{E}\big[\boldsymbol{r}_{\mathrm{in}}(\boldsymbol{x}^\star(t_\mathrm{f};\boldsymbol{\xi}),\boldsymbol{\xi})\big]\big) \end{pmatrix} = n_{\mathrm{r_{eq}}} + n_{\mathrm{r_{in}}}. \tag{3.2}$$

Under Assumption 3.1, the IVP (3.1a)–(3.1b) has a unique solution $\boldsymbol{x}(\cdot;\boldsymbol{\xi}) = \boldsymbol{x}_{\boldsymbol{u}}(\cdot;\boldsymbol{\xi})$ for any admissible control function $\boldsymbol{u} \in \mathcal{U}$ and for each fixed random outcome $\omega \in \Omega$ a.s.

We assume in the following that (UOCP) has an optimal solution $(\boldsymbol{x}_{\boldsymbol{u}^\star}, \boldsymbol{u}^\star)$. At each time instance, $\boldsymbol{x}_{\boldsymbol{u}^\star}$ is assumed to have finite variance with respect to the underlying probability space. In other words, using the definition of $L^2_\rho(\mathcal{S})$, the L^2-space with weight function ρ over the set $\mathcal{S}$, we pose the following assumption.

Assumption 3.2 *The optimal state trajectories $\boldsymbol{x}_{\boldsymbol{u}^\star}$ are $L^2_\rho(\mathcal{S})$-measurable, i.e., at any arbitrary but fixed time point $\tau \in [t_0, t_\mathrm{f}]$*

$$\boldsymbol{x}_{\boldsymbol{u}^\star}(\tau;\cdot) \in L^2_\rho(\mathcal{S}).$$

This is the fundamental assumption of the polynomial chaos method and can be extended to any admissible control.

Lemma 3.1.1 *Given Assumptions 3.1 and 3.2,*

$$\boldsymbol{x}_{\boldsymbol{u}}(\tau;\cdot) \in L^2_\rho(\mathcal{S})$$

holds for any $\boldsymbol{u} \in \mathcal{U}$.

Proof *Let $\boldsymbol{x}_{\boldsymbol{u}^\star}(\tau;\cdot)$ be the optimal state trajectory for which we have $\|\boldsymbol{x}_{\boldsymbol{u}^\star}(\tau;\cdot)\|_{L^2(\mathcal{S})} < \infty$ and let $\boldsymbol{u} \in \mathcal{U}$. The triangle inequality for an arbitrary but fixed point in time τ yields*

$$\|\boldsymbol{x}_{\boldsymbol{u}}(\tau;\cdot)\|_{L^2(\mathcal{S})} \leqslant \|\boldsymbol{x}_{\boldsymbol{u}}(\tau;\cdot) - \boldsymbol{x}_{\boldsymbol{u}^\star}(\tau;\cdot)\|_{L^2(\mathcal{S})} \; + \; \|\boldsymbol{x}_{\boldsymbol{u}^\star}(\tau;\cdot)\|_{L^2(\mathcal{S})}. \tag{3.3}$$

Consider the state and control trajectory at a fixed but arbitrary random realization $\bar{\xi}$. By Lipschitz-continuity of $\boldsymbol{f}$ in $\boldsymbol{x}$ and $\boldsymbol{u}$ and by applying the Gronwall Inequality, there is a constant $M < \infty$ such that

$$\big|\big|\boldsymbol{x}_{\boldsymbol{u}}(\cdot;\bar{\xi}) - \boldsymbol{x}_{\boldsymbol{u}^\star}(\cdot;\bar{\xi})\big|\big|_{L^\infty([t_0,t_\mathrm{f}])} \leqslant M \, ||\boldsymbol{u} - \boldsymbol{u}^\star||_{L^\infty([t_0,t_\mathrm{f}])} < \infty.$$

This implies that for any arbitrary but fixed point in time τ,

$$\big|\big|\boldsymbol{x}_{\boldsymbol{u}}(\tau;\bar{\xi}) - \boldsymbol{x}_{\boldsymbol{u}^\star}(\tau;\bar{\xi})\big|\big| < \infty$$

thus

$$\|\boldsymbol{x}_{\boldsymbol{u}}(\tau;\cdot) - \boldsymbol{x}_{\boldsymbol{u}^\star}(\tau;\cdot)\|_{L^2(\mathcal{S})} < \infty.$$

This proves the desired bound $\|\boldsymbol{x}_{\boldsymbol{u}}(\tau;\cdot)\|_{L^2(\mathcal{S})} < \infty$. □

3.2 Spectral projections with orthogonal polynomials

Before we can explain the polynomial chaos method for uncertainty quantification and apply it to optimal control under uncertainty, we give an introduction to the theory of spectral projections with orthogonal polynomials. Spectral methods rely on the approximation of the exact solution by series of orthogonal polynomials with an order of convergence that is bounded only by the regularity of the exact solution.
The goal of this section is to lay out the theory necessary for the remainder of this chapter. In particular, we need a-priori estimates related to the spectral convergence rate of the polynomial expansion for different families of the classical orthogonal polynomials, i.e. error estimates for the truncation error, limited only by the regularity in the parameter space.
The references used in this section are Szego [144] for general orthogonal polynomials, Canuto and Quarteroni [33] for results on weighted Sobolev spaces in bounded domains and Shen et al. [136] for results on weighted Sobolev spaces in unbounded domains.

Throughout this section, we use the following notation. The partial derivative with respect to z is denoted by $\partial_z = \frac{\partial}{\partial z}$. $I \subseteq \mathbb{R}$ stands for an open or closed interval and $\mathcal{S} = I^d$ denotes the Cartesian product whose variables are denotes by $\xi = (\xi_1, \dots, \xi_d)$. The weight function in the considered weighted Hilbert and Sobolev spaces typically arise as probability density functions – up to a scaling factor – hence is denoted by a subscript ρ. If the weight function is not relevant or if it is clear from the context, we drop the subscript.

3.2.1 Weighted L^p and Sobolev spaces

We first define the weighted L^p and Sobolev spaces of Hilbert type over the open set $\mathcal{S}$.

Definition 3.2.1 *Let $\mathcal{S} \subseteq \mathbb{R}^d$ be a domain. A weight function $\rho : \mathcal{S} \to [0, \infty]$ is a non-negative, integrable function. The weight function ρ is separable if it can be written as $\rho(\xi) = \prod_{j=1}^{d} \rho_j(\xi_j)$.*

Weight functions are closely related to the concept of probability measures. A separable weight function corresponds to independent random variables.

Example 3.2.1 (Gaussian measure) *The weight function*

$$\rho(\xi) = \frac{1}{(2\pi)^{d/2}} \exp\left(-\frac{\xi^T \xi}{2}\right)$$

defines the Gaussian measure $\mu(\xi)$ by setting $\mu(\xi) = \rho(\xi)\mathrm{d}\xi$. If the components ξ_j, $1 \leqslant j \leqslant d$, are independent to each other, then the weight function is separable

$$\rho(\xi) = \prod_{j=1}^{d} \frac{1}{\sqrt{2\pi}} \exp\left(-\frac{\xi_j^2}{2}\right).$$

Definition 3.2.2 *The* weighted L^p-space *on $\mathcal{S} \subseteq \mathbb{R}^d$ is defined as*

$$L^p_\rho(\mathcal{S}) = \{v | v \text{ measurable and } ||v||_{L^p_\rho(\mathcal{S})} < \infty\}$$

where

$$||v||_{L^p_\rho(\mathcal{S})} = \left(\int_{\mathcal{S}} |v(\xi)|^p \rho(\xi)\mathrm{d}\xi\right)^{\frac{1}{p}} \quad \text{for } 0 < p < \infty.$$

For $p = \infty$, the space of essentially bounded functions $L^\infty(\mathcal{S})$ is defined similarly with the norm

$$||v||_{L^\infty(\mathcal{S})} = \text{ess sup}_{\mathcal{S}} \left|v(\xi)\right|.$$

We assume that the weight function is chosen such that $L^2_\rho = L^2_\rho(\mathcal{S})$ forms a Hilbert space with the norm

$$\|v\|_{L^2(\mathcal{S})} = \langle v, v\rangle^{\frac{1}{2}}_{L^2(\mathcal{S})}$$

induced by the inner product

$$\left\langle u(\xi), v(\xi)\right\rangle_{L^2(\mathcal{S})} = \left(\int_{\mathcal{S}} u(\xi)v(\xi)\rho(\xi)\mathrm{d}\xi\right)^{\frac{1}{2}}.$$

In this case, there exist a complete orthogonal system of polynomial basis functions $\{\phi_k\}$ that can be normalized such that

$$\left\langle \phi_k(\xi), \phi_j(\xi)\right\rangle_{L^2(\mathcal{S})} = \int_{\mathcal{S}} \phi_k(\xi)\phi_j(\xi)\rho(\xi)\mathrm{d}\xi = \delta_{kj} \quad \forall k, j.$$

This set can be constructed by the Gram-Schmidt orthogonalization procedure [127].

Example 3.2.2 *The Hermite polynomials form a complete orthogonal basis for the Hilbert space $L^2(\mathbb{R}^d, \mu)$ with the Gaussian measure μ.*

Similar to the weighted L^p-spaces, we can define the weighted Sobolev spaces.

Definition 3.2.3 *The* weighted Sobolev spaces *are defined as*

$$W^{l,p}_\rho(\mathcal{S}) = \left\{v \in L^p_\rho(\mathcal{S}) \mid D_{\boldsymbol{m}} v \in L^p_\rho(\mathcal{S})\ \forall \boldsymbol{m} \in \mathbb{N}^d \text{ with } |\boldsymbol{m}| \leqslant l\right\}$$

with derivative operator $D_{\boldsymbol{m}} v = \dfrac{\partial^{|\boldsymbol{m}|} v}{\partial^{m_1}\xi_1 \ldots \partial^{m_d}\xi_d}$ *and multi-index* $\boldsymbol{m} = (m_1, \ldots, m_d) \in \mathbb{N}^d$ *with* $|\boldsymbol{m}| := \sum_{j=1}^d m_j$.

The space

$$W^{l,2}_\rho(\mathcal{S}) =: H^l_\rho,\ l \geqslant 0,$$

forms a Hilbert space equipped with the norm

$$||v||_{H^l_\rho} = \sum_{|\boldsymbol{m}|\leqslant l} \|D_{\boldsymbol{m}} v\|_{L^2(\mathcal{S})}.$$

If ξ is a random variable with probability measure P over the sample space Ω, we regard $\mathcal{S} \subseteq \mathbb{R}^d$ as the support of the pdf of ξ. The inner product in the Hilbert space is determined by the probability density function (PDF) ρ of the random variables

$$\left\langle u(\xi), v(\xi)\right\rangle_{L^2(\mathcal{S})} = \int_{\mathcal{S}} u(\xi(\omega))v(\xi(\omega))\,\mathrm{dP}(\omega) = \int_{\mathcal{S}} u(\xi)v(\xi)\rho(\xi)\mathrm{d}\xi.$$

The first and second moment of the random variable is defined by $\langle \xi \rangle_{L^2(\mathcal{S})} = \mathrm{E}[\xi]$ and $\|\xi\|^2_{L^2(\mathcal{S})} = \mathrm{E}[\xi^2]$, respectively.

3.2.2 Generalized Fourier series

Let $\phi_0(\xi), \ldots, \phi_{M_p-1}(\xi)$ be a sequence of multidimensional polynomials in $\xi = (\xi_1, \ldots, \xi_d)$ orthonormal with respect to $L^2_\rho(\mathcal{S})$. The polynomials are assumed to be separable in each dimension, i.e.,

$$\phi_k(\xi) = \prod_{j=1}^{d} \phi_{k,j}(\xi_j).$$

The total degree of $\phi_k(\xi)$ is defined by

$$\deg(\phi_k(\xi)) := \sum_{j=1}^{d} \deg(\phi_{k,j}(\xi_j)),$$

and is assumed to be at most p.
Consider the generated space of polynomials of degree at most p

$$S_p = \mathrm{span}\{\boldsymbol{\phi}_0(\xi), \ldots, \phi_{M_p-1}(\xi)\}.$$

An orthogonal projection

$$\Pi_p : L^2_\rho(\mathcal{S}) \to S_p$$

of a function $f \in L^2_\rho(\mathcal{S})$ onto S_p is defined by

$$\langle f - \Pi_p f, \phi_k \rangle_{L^2(\mathcal{S})} = 0 \text{ for } k = 0, \ldots, M_p - 1.$$

A generalized Fourier series is an expansion

$$\Pi_p f = \sum_{k=0}^{M_p-1} c_k(f)\phi_k(\xi)$$

of a function f based on a system of orthogonal polynomials. The Fourier coefficients are defined by

$$c_k(f) := \langle f, \phi_k \rangle_{L^2(\mathcal{S})}.$$

and satisfy Parseval's identity

$$\sum_{k=0}^{\infty} |c_k(f)|^2 = \|f\|^2_{L^2(\mathcal{S})}. \tag{3.4}$$

The Fourier series $\Pi_p f$ is the L^2_ρ-best approximation of f, for which

$$\|f - \Pi_p f\|_{L^2(\mathcal{S})} = \min_{g \in S_p} \|f - g\|_{L^2(\mathcal{S})}.$$

3.2.3 Classical orthogonal polynomials

The classical orthogonal polynomials, which correspond each to a specific weight function ρ on the open set $I \subseteq \mathbb{R}$, generate most of the common continuous probability distributions. In higher dimensions with $d > 1$ independent random variables, the weights $\rho(\xi)$ are tensorized on $\mathcal{S} = I^d$.
Our goal in this section is to derive a-priori estimates related to the spectral convergence rate of the polynomial expansion for the different families of classical orthogonal polynomials, i.e. error estimates for the truncation error, limited only by the regularity in the parameter space.

Orthogonal polynomials on bounded domains

The Jacobi polynomials are the orthogonal polynomials with respect to a weight function of the form

$$\rho(\xi_j) = (1-\xi_j)^\alpha (1+\xi_j)^\beta \ , \alpha, \beta > -1 \text{ on } I = (-1,1).$$

They include the Chebychev polynomials

$$\alpha = \beta = -\frac{1}{2} \text{ with weight function } \rho(\xi_j) = (1-\xi_j^2)^{-1/2}$$

and the Legendre polynomials

$$\alpha = \beta = 0 \text{ with weight function } \rho(\xi_j) = 1.$$

It is a well-known fact (see [144, Section 7.32]), that the Jacobi polynomials reach the maximum and minimum of their absolute value at $\xi_j = 1$ and $\xi_j = -1$, respectively, provided that $\alpha, \beta \geqslant -\frac{1}{2}$. Since

$$\phi_k^{(\alpha,\beta)}(1) = \frac{\Gamma(k+\alpha+1)}{k!\alpha+1} = O(k^\alpha) \text{ and } \phi_k^{(\alpha,\beta)}(-1) = \frac{\Gamma(k+\beta+1)}{k!\beta+1} = O(k^\beta) \quad \forall k \geqslant 0,$$

it follows that

$$\|\phi_k\|_{L^\infty(\mathcal{S})} = O(1) \quad \forall k \geqslant 0.$$

In the following, we focus on the Legendre polynomials for their correspondence to the uniform distributions. The results equally apply to the Chebychev polynomials [33] and more general types of Jacobi weights [136, Chapter 3.5].

Definition 3.2.4 (Legendre polynomials) *The n-th Legendre polynomial $L_n(\xi_j)$, $\xi_j \in \mathbb{R}$ is defined by*

$$L_0(\xi_j) = 1$$
$$L_n(\xi_j) = \frac{1}{2^n n!} \frac{d^n}{d\xi_j^n} \left((\xi_j^2 - 1)^n \right) \quad n \geqslant 1.$$

They are solutions to the Legendre's differential equation

$$\frac{d}{d\xi_j} \left((1-\xi_j^2) \frac{d}{d\xi_j} L_n(\xi_j) \right) + n(n+1) L_n(\xi_j) = 0$$

normalized such that $L_n(1) = 1$.

The associated orthonormal system $\{\phi_k\}_{k=0}^{\infty}$ with $\|\phi_k\|_{L^2(\mathcal{S})} = 1 \ \forall k$ is given by

$$\phi_k = \lambda_k L_k, \quad k \geqslant 0$$

with normalization factor

$$\lambda_k = (k + 1/2)^{1/2}.$$

The sequence of Legendre polynomials satisfies the recurrence

$$(n+1)L_{n+1}(\xi_j) = (2n+1)\xi_j L_n(\xi_j) - nL_{n-1}(\xi_j), \quad L_0(\xi_j) = 1, \quad L_1(\xi_j) = \xi_j.$$

and the following relation for the derivative

$$\frac{d}{d\xi_j} L_{n+1}(\xi_j) = 2\lambda_n L_n(\xi_j) + 2\lambda_{n-2} L_{n-2}(\xi_j) + \ldots + \begin{cases} 2\lambda_1 L_1(\xi_j) & \text{if } n \text{ odd} \\ 2\lambda_2 L_2(\xi_j) & \text{if } n \text{ even} \end{cases} \tag{3.5}$$

A-priori estimates of the spectral convergence rate of the expansion can be derived by using the characterization of the classical orthogonal polynomials as eigenfunctions of some second-order linear differential operator and by finding bounds for the derivative of the expansion and the expansion of the derivative.

Theorem 3.2.1 (Spectral bound, Theorem 2.25 of [33]) *For $0 \leqslant k \leqslant m$, define*

$$\mathfrak{h}(k,m) = \begin{cases} \frac{2m+1-4k}{2}, & \text{if } \ k \geqslant 1, \\ \frac{2m-3k}{2}, & \text{if } k \in [0,1) \end{cases}.$$

Then, for any $v \in H_\rho^m(\mathcal{S})$,

$$\left|\left|v - \Pi_p v\right|\right|_{H_\rho^k} \leqslant C p^{-\mathfrak{h}(k,m)} \, ||v||_{H_\rho^m}.$$

In some cases, it is useful to consider inverse inequalities, which hold for finite-dimensional spaces.

Theorem 3.2.2 (Inverse inequality, Lemma 2.4 of [33]) *Suppose $0 \leqslant k \leqslant m$. Then,*

$$||v||_{H_\rho^m} \leqslant C p^{2(m-k)} \, ||v||_{H_\rho^k}$$

for any $v \in S_p$.

In Section 3.5, we make use of the following bound for compact spaces $\mathcal{S}$ introduced in [6, Equation 2.3]: there exist a constant C_s and a parameter h depending only on ρ and on d such that for $v \in L_\rho^2$

$$\max\left\{\|v\|_{L^\infty(\mathcal{S})}, \left\|\partial_{\xi_1} v\right\|_{L^\infty(\mathcal{S})}, \ldots, \left\|\partial_{\xi_d} v\right\|_{L^\infty(\mathcal{S})}\right\} < C_s \sum_{k=0}^{\infty} |c_k(v)| \, (\deg \phi_k)^h. \tag{3.6}$$

For our purposes it is sufficient to consider the above bound for finite $v \in S_p$, which we derive from scratch in the following. With the further regularity assumption $v \in H_\rho^k$ we can show boundedness: L^∞ can be continuously embedded into $H_\rho^k(\mathcal{S})$ whenever $k > \frac{d}{2}$. This can be

seen by considering the Fourier transform $\hat{v}(\theta) \in L^2_\rho(\mathbb{R}^d)$ of $v(\xi) \in L^2_\rho(\mathbb{R}^d)$

$$\begin{aligned}\sup_{\mathcal{S}} \left|v(\xi)\right| &\leqslant \frac{1}{(2\pi)^d} \int_{R^d} |\hat{v}(\theta)| \, \mathrm{d}\theta \\ &\leqslant \frac{1}{(2\pi)^d} \underbrace{\left(\int_{R^d} \frac{\mathrm{d}\theta}{(1+|\theta|^2)^k} \right)^{1/2}}_{:= C_k < \infty \text{ iff } k > d/2} \left(\int_{R^d} |\hat{v}(\theta)|^2 (1+|\theta|^2)^k \mathrm{d}\theta \right)^{1/2}.\end{aligned}$$

The claim $\|v\|_{L^\infty(\mathcal{S})} \leqslant C \, ||v||_{H^k_\rho}$ follows by noting the equivalence, cf. e.g. [17],

$$H^k(\mathbb{R}^n) = \left\{ f \in L^2_\rho(\mathbb{R}^n) : \mathcal{F}^{-1}\left[(1+|\theta|^2)^{\frac{k}{2}} \mathcal{F} f \right] \in L^2_\rho(\mathbb{R}^n) \right\}.$$

Using the inverse inequalities, or directly computing the norms of the derivative of the different orthonormal polynomials, we can find a constant C and a parameter m depending only on the weight function ρ such that for $1 \leqslant j \leqslant d$

$$\left\| \partial_{\xi_j} v \right\|_{L^2(\mathcal{S})} \leqslant C p^m \|v\|_{L^2(\mathcal{S})} \text{ for } v \in S_p.$$

Consequently, by Parseval's identity 3.4 and the L^∞-embedding, there exist a constant C_s' and a parameter h' depending on only ρ and on d such that for $v \in S_p$

$$\max\left\{ \|v\|_{L^\infty(\mathcal{S})}, \left\| \partial_{\xi_1} v \right\|_{L^\infty(\mathcal{S})}, \ldots, \left\| \partial_{\xi_d} v \right\|_{L^\infty(\mathcal{S})} \right\} \leqslant C_s' p^{h'} \sum_{k=0}^{M_p - 1} |c_k(v)|. \tag{3.7}$$

Orthogonal polynomials on unbounded domains

In unbounded domains, the weights are usually of exponential type in order to preserve integrability of the weighted polynomials. We consider the Hermite polynomials, which can be defined in two different ways as "probabilists'" or "physicist'" and derived from each other by rescaling. The weight functions for the two types are defined as follows

$$\rho(\xi_j) = e^{-\xi_j^2/2} \text{ and } \rho(\xi_j) = \exp\left(-\xi_j^2\right) \text{ on } I = \mathbb{R}, \text{ respectively.}$$

For the Laguerre polynomials, the weights are defined as

$$\rho(\xi_j) = \exp\left(-\xi_j\right) \text{ on } I = (0, \infty).$$

The weight function of the "probabilists'" Hermite polynomials corresponds to the Normal distribution, thus we focus on this class.

Definition 3.2.5 (Hermite polynomials) *The n-th (probabilist) Hermite polynomial $H_n(\xi_j)$, $\xi_j \in \mathbb{R}$ is defined by*

$$\begin{aligned} H_0(\xi_j) &= 1 \\ H_n(\xi_j) &= (-1)^n \exp\left(\frac{\xi_j^2}{2}\right) \frac{\mathrm{d}^n}{\mathrm{d}\xi_j^n} \left(\exp\left(-\frac{\xi_j^2}{2} \right) \right) \quad n \geqslant 1. \end{aligned}$$

Example 3.2.3 *The Hermite polynomials up to second order two for $\xi = (\xi_1, \xi_2)$ are given by*

$$\begin{aligned}
\phi_0(\xi) &= \phi_0^0(\xi_1)\phi_0^1(\xi_2) = 1\\
\phi_0(\xi) &= \phi_1^0(\xi_1)\phi_1^1(\xi_2) = \xi_1\\
\phi_0(\xi) &= \phi_2^0(\xi_1)\phi_2^1(\xi_2) = \xi_2\\
\phi_0(\xi) &= \phi_3^0(\xi_1)\phi_3^1(\xi_2) = \xi_1^2 - 1\\
\phi_0(\xi) &= \phi_4^0(\xi_1)\phi_4^1(\xi_2) = \xi_1\xi_1\\
\phi_0(\xi) &= \phi_5^0(\xi_1)\phi_5^1(\xi_2) = \xi_2^2 - 1.
\end{aligned}$$

Denote by

$$\lambda_m = (\sqrt{2\pi}n!)^{-\frac{1}{2}}$$

the normalization term such that $\phi_k = \lambda_k H_k$ and $\|\phi_k\|_{L^2(\mathcal{S})} = 1,\ k \geqslant 0$.
The sequence of normalized Hermite polynomials satisfies the recurrence

$$(n+1)^{\frac{1}{2}}\phi_{n+1}(\xi_j) = \xi_j\phi_n(\xi_j) - n^{\frac{1}{2}}\phi_{n-1}(\xi_j), \quad H_0(\xi_j) = 1, \quad H_1(\xi_j) = \xi_j$$

and the following relation for the derivative

$$\frac{\mathrm{d}}{\mathrm{d}\xi_j}\phi_n(\xi_j) = n^{\frac{1}{2}}\phi_{n-1}(\xi_j). \tag{3.8}$$

The derivation of the spectral error estimates is similar to the orthogonal polynomials on bounded domains and uses the characterization of the classical orthogonal polynomials as eigenfunctions of some second-order linear differential operator.

Theorem 3.2.3 (Spectral bound, Theorem 2.25 of [16]) *Let $0 \leqslant k \leqslant m$ and define*

$$\mathfrak{h}(k,m) = \frac{m-k}{2}.$$

Then, for $v \in H_\rho^m(\mathcal{S})$,

$$\left|\left|v - \Pi_p v\right|\right|_{H_\rho^k} \leqslant Cp^{-\mathfrak{h}(k,m)}\,||v||_{H_\rho^m}.$$

For similar results for the Laguerre polynomials, we refer to [16], and for inverse inequalities, we refer to [16, Theorem 2.21, 2.24].

As before, by computing the derivative of the different orthonormal polynomials, we can find a constant C independent of any function and p and a parameter m depending only on ρ such that

$$\left\|\partial_{\xi_j} v\right\|_{L^2(\mathcal{S})} \leqslant Cp^m\|v\|_{L^2(\mathcal{S})} \text{ for } v \in S_p.$$

For Hermite polynomials, the constant $m = \frac{1}{2}$ follows from differentiating the expansion and from relation (3.8),

$$\partial_{\xi_j} v = \partial_{\xi_j}\sum_{k=0}^{p}\hat{v}_k\phi_k = \sum_{k=1}^{p}\hat{v}_k k^{\frac{1}{2}}\phi_{k-1}.$$

3.3 The polynomial chaos transformation

The polynomial chaos method, which belongs to the class of spectral methods, is a popular uncertainty quantification method. A short introduction and a literature review can be found under Section 2.3.6.

In this section, we aim to provide a simple and compact introduction to this topic. Therefore, we neglect the time dependence of the state variables that are considered to be random variables $x : \Omega \to \mathbb{R}$ affected by an $\mathbb{R}^d$-valued random input vector $\boldsymbol{\xi} = \boldsymbol{\xi}(\omega)$.

3.3.1 Basic development

Early development took place in 1938 when Wiener introduced the notion of *homogeneous chaos* as the span of Hermite polynomial functionals of a Gaussian process [150] and in 1947 when Cameron and Martin proved that the Fourier-Hermite series expansion, which can be constructed with the homogeneous chaos, converges to any L^2-measurable functional [32]. More than 50 years later, the techniques were rediscovered under the notion of generalized polynomial chaos (gPC) and extended to several continuous and discrete probability distributions other than the Gaussian measure, cf. [57, 152, 151].

The polynomial chaos transformation applies a polynomial expansion to approximate the dependence of the propagated random states on the random input parameters ξ, which are assumed to be independent, see Remark 3.1.

In their seminal work, Cameron and Martin [32] proved that any random functional $x \in L^2((\Omega, \mathcal{F}, \mathrm{P}))$ on a probability space $(\Omega, \mathcal{F}, \mathrm{P})$ can be expanded into an L^2-converging series $\sum_{k=0}^{M_p-1} \hat{x}_k \phi_k(\boldsymbol{\xi})$ of a countable collection of independent Gaussian random variables $\boldsymbol{\xi} : \Omega \to \mathbb{R}^d$ for some $d \geqslant 1$ with Gaussian probability law P and a sequence of Hermite polynomials $\{\phi_i\}$.

The original polynomial chaos expansion was written in the form, cf. [89],

$$\begin{aligned} x(\boldsymbol{\xi}(\omega)) = c_0 H_0 + \sum_{i_1=1}^{\infty} c_{i_1} H_1(\xi_{i_1}(\omega)) + \sum_{i_1=1}^{\infty} \sum_{i_2=1}^{i_1} c_{i_1 i_2} H_2(\xi_{i_1}(\omega), \xi_{i_2}(\omega)) \\ + \sum_{i_1=1}^{\infty} \sum_{i_2=1}^{i_1} \sum_{i_3=1}^{i_2} c_{i_1 i_2 i_3} H_3(\xi_{i_1}(\omega), \xi_{i_2}(\omega), \xi_{i_3}(\omega)) + \dots, \end{aligned} \tag{3.9}$$

where $H_d(\xi_{i_1}(\omega), \dots, \xi_{i_d}(\omega))$ denotes the multidimensional Hermite polynomial of order d in terms of the multidimensional independent standard Gaussian random variable $\boldsymbol{\xi} = (\xi_{i_1}, \dots, \xi_{i_d})$ and $c_{i_1 \dots i_d}$ are the coefficients.

Relation (3.9) can be reordered and rewritten in a simpler standard notation with multidimensional Hermite basis polynomials $\phi_k(\boldsymbol{\xi}(\omega))$ and coefficients $\hat{x}_k$, here exemplary for $d = 2$,

i.e., $\xi = (\xi_1, \xi_2)$:

$$\begin{aligned} x(\xi(\omega)) &= c_0 H_0 + \sum_{i_1=1}^{\infty} c_{i_1} H_1(\xi_{i_1}(\omega)) + \sum_{i_1=1}^{\infty} \sum_{i_2=1}^{i_1} c_{i_1 i_2} H_2(\xi_{i_1}(\omega), \xi_{i_2}(\omega)) \\ &\quad + \sum_{i_1=1}^{\infty} \sum_{i_2=1}^{i_1} \sum_{i_3=1}^{i_2} c_{i_1 i_2 i_3} H_3(\xi_{i_1}(\omega), \xi_{i_2}(\omega), \xi_{i_3}(\omega)) + \dots \\ &= c_0 H_0 + c_1 H_1(\xi_1(\omega)) + c_2 H_1(\xi_2(\omega)) + c_{11} H_2(\xi_1(\omega), \xi_1(\omega)) \\ &\quad + c_{21} H_2(\xi_2(\omega), \xi_1(\omega)) + c_{22} H_2(\xi_2(\omega), \xi_2(\omega)) \\ &\quad + c_{111} H_3(\xi_1(\omega), \xi_1(\omega), \xi_1(\omega)) + \dots \\ &= \hat{x}_0 \phi_0(\xi_1(\omega), \xi_2(\omega)) + \hat{x}_1 \phi_1(\xi_1(\omega), \xi_2(\omega)) + \hat{x}_2 \phi_2(\xi_1(\omega), \xi_2(\omega)) \\ &\quad + \hat{x}_3 \phi_3(\xi_1(\omega), \xi_2(\omega)) + \hat{x}_4 \phi_4(\xi_1(\omega), \xi_2(\omega)) + \hat{x}_5 \phi_5(\xi_1(\omega), \xi_2(\omega)) \\ &\quad + \hat{x}_6 \phi_6(\xi_1(\omega), \xi_2(\omega)) + \dots . \end{aligned} \tag{3.10}$$

In general, the multivariate basis polynomials can be expressed as products of univariate basis polynomials $\phi_{i,j}(\xi_j(\omega))$ for $i \geqslant 0,\ 1 \leqslant j \leqslant d$ with the help of multi-indices to define a mixed set of multivariate polynomials. This decoupling is possible due to the use of independent random variables. For instance, for (3.10) we obtain

$$\begin{aligned} x(\xi(\omega)) = \hat{x}_0 \underbrace{\phi_0(\xi_1(\omega), \xi_2(\omega))}_{\phi_{0,1}(\xi_1(\omega))\phi_{0,2}(\xi_2(\omega))} + \hat{x}_1 \underbrace{\phi_1(\xi_1(\omega), \xi_2(\omega))}_{\phi_{1,1}(\xi_1(\omega))\phi_{0,2}(\xi_2(\omega))} + \hat{x}_2 \underbrace{\phi_2(\xi_1(\omega), \xi_2(\omega))}_{\phi_{0,1}(\xi_1(\omega))\phi_{1,2}(\xi_2(\omega))} \\ + \hat{x}_3 \underbrace{\phi_3(\xi_1(\omega), \xi_2(\omega))}_{\phi_{2,1}(\xi_1(\omega))\phi_{0,2}(\xi_2(\omega))} + \hat{x}_4 \underbrace{\phi_4(\xi_1(\omega), \xi_2(\omega))}_{\phi_{1,1}(\xi_1(\omega))\phi_{1,2}(\xi_2(\omega))} + \hat{x}_5 \underbrace{\phi_5(\xi_1(\omega), \xi_2(\omega))}_{\phi_{0,1}(\xi_1(\omega))\phi_{2,2}(\xi_2(\omega))} + \dots . \end{aligned}$$

The coefficients that realize the L^2-convergence

$$\left\| x - \sum_{i=0}^{M_p - 1} \hat{x}_k \phi_k(\xi) \right\|_{L^2(\mathcal{S})} \xrightarrow{p \to \infty} 0. \tag{3.11}$$

are computed in a Fourier-like manner using a Galerkin projection

$$\hat{x}_k := \left\langle x(\xi), \phi_k(\xi) \right\rangle_{L^2(\mathcal{S})}, \quad k = 0, 1, \dots$$

as defined in Section 3.2.2.
The convergence rate of the expansion is limited by the regularity of the solution $x(\xi)$ and can be exponentially fast for smooth convergence. The a-priori error estimate

$$\left\| x - \sum_{i=0}^{M_p - 1} \hat{x}_k \phi_k(\xi) \right\|_{L^2(\mathcal{S})} \leqslant C p^{-\frac{m}{2}} ||x||_{H^m},$$

where H^m is the Sobolev space weighted by the Gaussian measure, is provided by Theorem 3.2.1 for spectral expansions with Hermite polynomials.
For a p-th order approximation, a total number of M_p multidimensional basis polynomials are required where

$$M_p = \text{card}\{\phi_k(\xi) \mid \deg(\phi_k(\xi)) = \sum_{0 \leqslant j \leqslant d} \phi_{k_j}(\xi_j) \leqslant p\}$$

denotes the number of multivariate polynomials of total degree at most p.
The exact expression for M_p is given by the following well-known lemma, cf. e.g. [8].

Lemma 3.3.1 *The number of terms in a p-th order approximation corresponding to the number of monomials of degree at most p in d variables is*

$$M_p = \binom{p+d}{d} = \frac{(d+p)!}{d!p!}.$$

Proof (e.g. [8]) *There is exactly one monomial of degree 0. For $k \geqslant 1$, the number of monomials of degree exactly k in d variables is given by [29]*

$$\binom{k+d-1}{d-1}.$$

Thus, the number of monomials of degree at most p in d variables is

$$M_p = 1 + \sum_{k=1}^{p} \binom{k+d-1}{d-1} = \binom{p+d}{d} = \frac{(d+p)!}{d!p!}.$$

This is equal to the number of orthogonal polynomials of degree at most p in d variables, which can be obtained from the set of monomials by an orthogonalization procedure. □

The benefit of the polynomial chaos series representation $x^{(p)}(\xi) = \sum_{k=0}^{M_p-1} \hat{x}_k \phi_k(\xi)$ lies in the decomposition of the stochastic equations into deterministic coefficients $\hat{x}$ and random basis functions $\phi_i(\xi)$. The orthogonality property allows for computing the statistical moments of the expanded variables from the deterministic coefficients, e.g.,

$$\mathrm{E}\left[x^{(p)}\right] = \hat{x}_0, \ \mathrm{Var}\left[x^{(p)}\right] = \mathrm{E}\left[(x^{(p)})^2\right] - \mathrm{E}\left[x^{(p)}\right]^2 = \sum_{i=1}^{M_p-1} \hat{x}_i^2.$$

Lemma 3.3.2 *The k-th moment of the p-order polynomial chaos approximation $x^{(p)}$ is*

$$\mathrm{E}\left[(x^{(p)})^k\right] = \sum_{0 \leqslant i_1, \ldots, i_k \leqslant M_p - 1} \hat{x}_{i_1} \ldots \hat{x}_{i_k} \left\langle \phi_{i_1}(\xi) \ldots \phi_{i_k}(\xi) \right\rangle_{L^2(\mathcal{S})}.$$

Proof

$$\begin{aligned} \mathrm{E}\left[(x^{(p)})^k\right] &= \mathrm{E}\left[\sum_{i_1=0}^{M_p-1} \hat{x}_{i_1} \phi_{i_1}(\xi) \ldots \sum_{i_k=0}^{M_p-1} \hat{x}_{i_k} \phi_{i_k}(\xi) \right] \\ &= \sum_{0 \leqslant i_1, \ldots, i_k \leqslant M_p - 1} \hat{x}_{i_1} \ldots \hat{x}_{i_k} \, \mathrm{E}\left[\phi_{i_1}(\xi) \ldots \phi_{i_k}(\xi)\right] \end{aligned}$$

□

3.3.2 Choice of basis

For most of the common continuous and discrete distribution, there exists a direct correspondence between the probability distribution and the weight function of the orthogonal polynomials. The polynomial families used in gPC derive from the Askey scheme [151, 5] of hypergeometric polynomials and can be traced back to the classical orthogonal polynomials described

	distribution	polynomials	support	probability density/mass
continuous	Gaussian	Hermite	$\mathbb{R}$	$\frac{1}{\sqrt{2\pi}}\exp\left(-\frac{-\xi^2}{2}\right)$
	Gamma	Laguerre	$[0,\infty)$	$\exp(-\xi)$
	Beta	Jacobi	$[a,b]$	$\frac{b-a}{2}(1-\xi)^{\alpha}(1+\xi)^{\beta}$
	Uniform	Legendre	$[a,b]$	$\frac{b-a}{2}$
discrete	Poisson(λ)	Charlier	$\{0,1,\ldots\}$	$\exp(-\lambda)\frac{\lambda^k}{k!}$
	Binomial(n,p)	Krawtchouk	$\{0,1,\ldots,n\}$	$\binom{n}{k}p^k(1-p)^r$
	Negative binomial (r,p)	Meixner	$\{0,1,\ldots\}$	$\binom{k+r-1}{k}p^k(1-p)^r$
	Hypergeometric (N,K,n)	Hahn	$\{0,1,\ldots,n\}$	$\frac{\binom{K}{k}\binom{N-K}{n-k}}{\binom{N}{n}}$

Table 3.1: Orthogonal polynomials from the Askey scheme and their corresponding continuous or discrete probability distribution.

in Section 3.2.3. A selection of probability distributions with their orthogonal polynomials is listed in Table 3.1. An extension of the fundamental L^2-convergence result to expansion in polynomials more general than Hermite polynomials, provided the existence of moments of any order, can be found in [51].

The optimal choice of basis functions $\{\phi_i(\xi)\}$ that best captures the uncertainty behavior with the lowest expansion order cannot be predetermined, as the distribution of $x(\xi)$ is not known. A heuristic choice is to select the polynomial family that is orthogonal to the probability space of the input distribution instead.

A generalization of polynomial chaos techniques towards arbitrary discrete, continuous, or discretized continuous probability measures, which can be specified either analytically in form of a the density or distribution functions, via statistics of the distribution such as moments, numerically as histogram or as raw data sets, is coined arbitrary polynomial chaos (aPC) [113]. The polynomials can be generated by some orthogonalization procedure, e.g. the Gram-Schmidt procedure [127].

A final remark concerns the basic assumption of the use of independent random variables.

Remark 3.1 (Dependent random variables) *Dependent random variables ζ must be transformed to a set of independent random variables ξ by a nonlinear change of variables. The dimension of ξ should thereby be chosen to represent the number of distinct sources of randomness in the particular problem. That is, it can be smaller than the dimension of the dependent random variables ζ. Different methods are described in [49].*

3.3.3 Intrusive and non-intrusive methods

To obtain expressions for the coefficients $\hat{x}_0,\ldots,\hat{x}_k$, a projection of $x(\xi)$ or of the model equations against the selected basis functions is computed as follows:

$$\hat{x}_k := \langle x,\phi_k\rangle_{L^2(\mathcal{S})} = \int_{\mathcal{S}} x(\xi)\phi_k(\xi)\mathrm{d}\xi, \quad k=0,1,\ldots.$$

In practice, a truncated basis is used which results in a finite-dimensional approximation

$$\hat{x}_k := \left\langle x^{(p)}, \phi_k \right\rangle_{L^2(\mathcal{S})} = \int_{\mathcal{S}} x^{(p)}(\xi)\phi_k(\xi)\mathrm{d}\xi, \quad k = 0, \ldots, M_p - 1. \tag{3.12}$$

There exist two approaches for computing or approximating the inner product:

1. The *intrusive* spectral projection approach carries out the analytic computations as far as possible by using elementary operations, interchanging sum and integral and exploiting orthogonality. The inner product of products of standard orthogonal polynomials

$$\begin{aligned}&\left\langle \phi_{i_1}(\xi), \ldots, \phi_{i_k}(\xi) \right\rangle_{L^2(\mathcal{S})} \\ &= \left\langle \phi_{i_{1,1}}(\xi_1), \ldots, \phi_{i_{k,1}}(\xi_1) \right\rangle_{L^2(\mathcal{S})} \cdots \left\langle \phi_{i_{1,d}}(\xi_d), \ldots, \phi_{i_{k,d}}(\xi_d) \right\rangle_{L^2(\mathcal{S})} \in \mathbb{R}\end{aligned}$$

   can be computed analytically using the dimension-independence and possibly be stored for later reuse. Provided that the involved functions can be expressed as polynomials in ξ, this leads to a fully deterministic system. For nonlinear problems with non-polynomial expressions, this may be achieved in some cases through a nonlinear transformation by using additional differential or algebraic states.

2. The more popular alternative, which can be applied to any kind of system, including blackbox systems, is referred to as *non-intrusive* spectral projection. Its main difference is the use of a numerical integration rule instead of direct algebraic manipulation to compute the Galerkin projection integral. We describe only the use of a grid-based quadrature and refer to the literature for other methods to approximate the integral 3.12, such as sampling or regression methods [50, 49, 8].

   We first consider one-dimensional quadrature rules for ξ_j over $I_j \subseteq \mathbb{R}$ where $1 \leqslant j \leqslant d$. An N_Q-point one-dimensional Gaussian quadrature rule $\{(\xi_j^{(m)}, w_j^{(m)})\}_{m=1,\ldots,N_\mathrm{Q}}$ involes nodes $\{\xi_j^{(m)}\}_{m=1,\ldots,N_\mathrm{Q}}$ selected as the zeros of an N_Q-th order one-dimensional polynomial $\phi_{N_\mathrm{Q},j}(\xi_j)$ and specific formulas for the weights $\{w_j^{(m)}\}_{m=1,\ldots,N_\mathrm{Q}}$ [60], which depend on the underlying random space. Examples are Gauss-Hermite, Gauss-Legendre, Gauss-Laguerre, generalized Gauss-Laguerre, and Gauss-Jacobi rules. The integral is then computed as follows

$$\int_{I_j} x^{(p)}(\xi_j)\phi_{k,j}(\xi_j)\mathrm{d}\xi_j \approx \sum_{m=1}^{N_\mathrm{Q}} x^{(p)}(\xi_j^{(m)})\ \phi_{k,j}(\xi_j^{(m)})w_j^{(m)}.$$

   An N_Q-point Gaussian quadrature rule integrates exactly all one-dimensional polynomials of degree at most $2N_\mathrm{Q} - 1$, see [60] for more information. For multidimensional quadrature, either a tensor grid of one-dimensional quadrature rules or Smolyak sparse grids [141] can be used.

   Setting $w^{(m)} = w_1^{(m)} \cdot \ldots \cdot w_d^{(m)}$, the inner product (3.12) is computed by

$$\hat{x}_k = \int_{\mathcal{S}} x^{(p)}(\xi)\phi_k(\xi)\mathrm{d}\xi \approx \sum_{m=1}^{N_\mathrm{Q}} x^{(p)}(\xi^{(m)})\ \phi_k(\xi^{(m)})w^{(m)}. \tag{3.13}$$

   The integrand in (3.13) involves polynomials of order up to p in each dimension for the evaluation of ϕ_k and of order exactly p in each dimension for evaluation of the PC

model $x^{(p)}(\xi)$. Consequently, to obtain good accuracy in these coefficients, a Gaussian quadrature order of $\frac{2p+1}{2}$, i.e., of $p+1$, is necessary and sufficient in each dimension.

In practical problems, the Galerkin projection and hence the Gauss quadrature is not directly applied to $x^{(p)}$ but to the model function $f(x^{(p)})$, e.g., for optimal control problems the Galerkin projection is applied to

$$\frac{\mathrm{d}}{\mathrm{dt}}\boldsymbol{x}^{(p)}(t;\xi) = \boldsymbol{f}(\boldsymbol{x}^{(p)}(t;\xi), \boldsymbol{u}(t), \xi).$$

In this case, the evaluation of the model function requires a numerical quadrature in the form, for $i = 1, \dots, n$,

$$\hat{f}_{k,i} = \int_{\mathcal{S}} f_i(\boldsymbol{x}^{(p)}(t;\xi), \boldsymbol{u}(t), \xi)\phi_k(\xi)\,\mathrm{d}\xi \tag{3.14}$$

$$s \approx \sum_{m=1}^{N_\mathrm{Q}} f_i(\boldsymbol{x}^{(p)}(t;\xi^{(m)}), \boldsymbol{u}(t), \xi^{(m)})\ \phi_k(\xi^{(m)})\, w^{(m)} \tag{3.15}$$

and the order of the integrand is $p+q \geqslant 2p$ where $q \geqslant p$ and $q = p$ only if f is linear. Thus a minimal Gaussian quadrature order of $p+1$ is necessary but might not be sufficiently large to give exact results. In particular if the model functions $\boldsymbol{f}$ are highly nonlinear, the Gauss quadrature gives only an approximation of the true solution.

3.3.4 Advantages and limits

There are several distinctive features of the polynomial chaos method, which make them attractive for optimal control problems. It can deal with nonlinear models and several different input distributions. Moments of any order can be analytically computed by the use of Lemma 3.3.2. The non-intrusive polynomial chaos method is easily applicable to blackbox systems, as they often arise in practical optimal control problems where all or a part of the model can only be evaluated as the output of a simulator. Furthermore, the approximation quality, which corresponds to the expansion order is adjustable depending on the available computational resources. Already a polynomial chaos surrogate model with an expansion order as low as $p = 2$ is able to capture significant nonlinear effects that deviate from the input distribution. Due to the exponential increase of the required number of terms M_p with the dimension d, cf. Lemma 3.3.1, the method is best suitable for low to moderate uncertainty dimensions. This is often satisfied for nonlinear optimal control applications.
As the convergence speed depends on the regularity of the solution with respect to the probability space of the expansion, the selected polynomial basis may not be adequate for capturing the nonlinear, possibly asymmetric uncertainty propagation. Possible remedies for the case that the basis cannot adequately represent the propagated uncertainty distribution are a decomposition of the uncertainty space [148] or basis adaption, e.g., [99]. For further references, we refer to the previous works listed in Section .

3.4 Properties of the polynomial chaos surrogate optimal control problem

The polynomial chaos procedure derived in Section 3.3 can be applied to the uncertain optimal control problem (UOCP). The resulting polynomial chaos surrogate problem is a deterministic, nonlinear optimal control problem with large state space

$$\hat{\boldsymbol{x}} = (\hat{\boldsymbol{x}}_0, \dots, \hat{\boldsymbol{x}}_{M_p-1}) = (\hat{x}_{0,0}, \dots, \hat{x}_{0,n-1}, \dots, \hat{x}_{M_p-1,0}, \dots, \hat{x}_{M_p-1,n-1}),$$
$$\hat{\boldsymbol{x}} \in W^{1,\infty}([t_0, t_\mathrm{f}], \mathbb{R}^{nM_p})$$

and controls

$$\boldsymbol{u} \in L^\infty([t_0, t_\mathrm{f}], \mathbb{R}^{n_\mathrm{u}}).$$

The new state equations are obtained by an orthogonal projection of $\boldsymbol{f}$ onto the basis functions,

$$\dot{\hat{\boldsymbol{x}}}_k = \left\langle \boldsymbol{f}(\boldsymbol{x}^{(p)}, \boldsymbol{u}, \boldsymbol{\xi}), \phi_k \right\rangle_{L^2(\mathcal{S})} =: \hat{\boldsymbol{f}}_k(\hat{\boldsymbol{x}}, \boldsymbol{u}) \quad \text{for } k = 0, \dots, M_p - 1 \tag{3.16}$$

as described in Section 3.3.3.
By a slight abuse of notation, we use a simplified way of formulating the expected value objective and constraints, cf. 3.3.2,

$$\hat{l} = \mathrm{E}[l] = \langle l, \phi_0 \rangle_{L^2(\mathcal{S})}, \ \hat{m} = \mathrm{E}[m] = \langle m, \phi_0 \rangle_{L^2(\mathcal{S})},$$
$$\hat{\boldsymbol{r}}_\mathrm{eq} = \mathrm{E}\big[\boldsymbol{r}_\mathrm{eq}\big] = \left\langle \boldsymbol{r}_\mathrm{eq}, \phi_0 \right\rangle_{L^2(\mathcal{S})}, \ \hat{\boldsymbol{r}}_\mathrm{in} = \mathrm{E}[\boldsymbol{r}_\mathrm{in}] = \langle \boldsymbol{r}_\mathrm{in}, \phi_0 \rangle_{L^2(\mathcal{S})}.$$

The resulting polynomial chaos surrogate problem is given by

$$\min_{\boldsymbol{u}, \hat{\boldsymbol{x}}} \quad \int_{t_0}^{t_\mathrm{f}} \hat{l}(\hat{\boldsymbol{x}}(t), \boldsymbol{u}(t)) \mathrm{d}t + \hat{m}(\hat{\boldsymbol{x}}(t_\mathrm{f})) \tag{OCP^p}$$

$$\text{s.t.} \quad \dot{\hat{\boldsymbol{x}}}_k(t) = \hat{\boldsymbol{f}}_k(\hat{\boldsymbol{x}}(t), \boldsymbol{u}(t)), \qquad t \in [t_0, t_\mathrm{f}] \text{ a.e., } 0 \leqslant k \leqslant M_p - 1 \tag{3.17a}$$
$$\boldsymbol{u}(t) \in U(t) \qquad t \in [t_0, t_\mathrm{f}] \text{ a.e.} \tag{3.17b}$$
$$\hat{\boldsymbol{x}}(t_0) = (\boldsymbol{x}_0, \boldsymbol{0}, \dots, \boldsymbol{0}) \tag{3.17c}$$
$$\boldsymbol{0} \geqslant \hat{\boldsymbol{r}}_\mathrm{in}(\hat{\boldsymbol{x}}(t_\mathrm{f})) \tag{3.17d}$$
$$\boldsymbol{0} = \hat{\boldsymbol{r}}_\mathrm{eq}(\hat{\boldsymbol{x}}(t_\mathrm{f})). \tag{3.17e}$$

As in Chapter 1 for the deterministic OCP, we denote by

$$\partial_{\hat{\boldsymbol{x}}_k} \mathrm{r}_\mathrm{eq} := \frac{\partial(\mathrm{r}_{\mathrm{eq}\,0}, \dots, \mathrm{r}_{\mathrm{eq}\,n_{\mathrm{r}_\mathrm{eq}}})}{\partial(\hat{x}_{k,0}, \dots, \hat{x}_{k,n-1})}$$

the $n_{\mathrm{r}_\mathrm{eq}} \times n$ Jacobian matrix of an arbitrary function r_eq. Similar notations hold for the other functions and variables.

3.4.1 Well-posedness

The following lemma implies that the optimal control surrogate problem (OCP^p) is well-posed and consequently has a unique solution $(\hat{\boldsymbol{x}}, \boldsymbol{u})$. The regularity of the objective as well as of the end point constraint follows from Assumption 3.1:

Lemma 3.4.1 *The function $\hat{\boldsymbol{f}}$ is Lipschitz-continuous in $\hat{\boldsymbol{x}}$ and $\boldsymbol{u}$ on $[t_0, t_f]$ a.e. with bounded Lipschitz-continuous derivatives in $\hat{\boldsymbol{x}}$.*

Proof *Take $0 \leqslant k \leqslant M_p - 1$ arbitrary but fixed. By construction,*

$$\hat{f}_k(\hat{\boldsymbol{x}}, \boldsymbol{u}) = \int_{\mathcal{S}} \boldsymbol{f}(\boldsymbol{x}^{(p)}(t;\xi), \boldsymbol{u}(t), \xi)\ \phi_k(\xi)\ \rho(\xi)\ \mathrm{d}\xi.$$

By Assumption 3.1, there exist constants $C_1, C_2, C_3 < \infty$ such that

$$C_1 = \sup_{t\in[t_0,t_f]} \left|\left|\partial_u \boldsymbol{f}(\boldsymbol{x},\boldsymbol{u},\xi)\right|\right|,\ C_2 = \sup_{t\in[t_0,t_f]} \left|\left|\partial_{\boldsymbol{x}} \boldsymbol{f}(\boldsymbol{x},\boldsymbol{u},\xi)\right|\right|,\ C_3 = \sup_{t\in[t_0,t_f]} \left|\left|\partial^2_{\boldsymbol{x}^2} \boldsymbol{f}(\boldsymbol{x},\boldsymbol{u},\xi)\right|\right|.$$

We show that the Lipschitz constants of the projected functions $\hat{\boldsymbol{f}}_k$ with respect to $\boldsymbol{u}$ and to $\hat{\boldsymbol{x}} = (\hat{\boldsymbol{x}}_0, \ldots, \hat{\boldsymbol{x}}_{M_p-1})$ and the Lipschitz constants of $\frac{\partial \hat{f}_k}{\partial \hat{\boldsymbol{x}}}$ with respect to $\hat{\boldsymbol{x}}$ are bounded. First,

$$\begin{aligned}
||\partial_{\boldsymbol{u}} \boldsymbol{f}_k|| &= \left|\left|\partial_{\boldsymbol{u}} \int_{\mathcal{S}} \boldsymbol{f}(\boldsymbol{x}^{(p)}, \boldsymbol{u}, \xi)\ \phi_k(\xi)\ \rho(\xi)\mathrm{d}\xi\right|\right| = \left|\left|\int_{\mathcal{S}} \partial_{\boldsymbol{u}} \boldsymbol{f}(\boldsymbol{x}^{(p)}, \boldsymbol{u}, \xi)\ \phi_k(\xi)\ \rho(\xi)\mathrm{d}\xi\right|\right| \\
&\leqslant \int_{\mathcal{S}} \underbrace{\left|\left|\partial_{\boldsymbol{u}} \boldsymbol{f}(\boldsymbol{x}^{(p)}, \boldsymbol{u}, \xi)\right|\right|}_{\leqslant C_1} \left|\phi_k(\xi)\right|\ \rho(\xi)\ \mathrm{d}\xi \leqslant C_1\, \mathrm{E}\left|\phi_k(\xi)\right| = C_1 M_k.
\end{aligned}$$

For the derivatives with respect to the new states we apply the chain rule

$$\frac{\partial}{\partial \hat{\boldsymbol{x}}_j} f(\boldsymbol{x}^{(p)}, \boldsymbol{u}, \xi) = \frac{\partial}{\partial \boldsymbol{x}} f(\boldsymbol{x}^{(p)}, \boldsymbol{u}, \xi) \frac{\partial}{\partial \hat{\boldsymbol{x}}_j} \boldsymbol{x}^{(p)} = \partial_{\boldsymbol{x}} f(\boldsymbol{x}^{(p)}, \boldsymbol{u}, \xi)\, \phi_j.$$

W.l.o.g., we only show boundedness for the second derivative. This follows by applying the chain rule twice:

$$\begin{aligned}
\left|\left|\partial^2_{\hat{\boldsymbol{x}}_j \hat{\boldsymbol{x}}_l} \boldsymbol{f}_k\right|\right| &= \left|\left|\partial^2_{\hat{\boldsymbol{x}}_j \hat{\boldsymbol{x}}_l} \int_{\mathcal{S}} \boldsymbol{f}(\boldsymbol{x}^{(p)}(t), \boldsymbol{u}(t))\phi_k(\xi)\rho(\xi)\mathrm{d}\xi\right|\right| \\
&= \left|\left|\int_{\mathcal{S}} \partial_{\hat{\boldsymbol{x}}_j} \left(\partial_{\hat{\boldsymbol{x}}_l} \boldsymbol{f}(\boldsymbol{x}^{(p)}, \boldsymbol{u}, \xi)\right) \phi_k(\xi)\ \rho(\xi)\mathrm{d}\xi\right|\right| \\
&= \left|\left|\int_{\mathcal{S}} \partial^2_{\boldsymbol{x}^2} \boldsymbol{f}(\boldsymbol{x}^{(p)}, \boldsymbol{u}, \xi)\phi_l(\xi)\phi_j(\xi)\phi_k(\xi)\rho(\xi)\mathrm{d}\xi\right|\right| \\
&\leqslant C_3\, \mathrm{E}\left|\phi_l(\xi)\phi_j(\xi)\phi_k(\xi)\right| = C_3 M_{i,j,k} \quad \textit{for } 1 \leqslant j, l \leqslant M_p - 1
\end{aligned}$$

It remains to ensure that the absolute (mixed) moments $M_{\boldsymbol{\alpha}}$ of ϕ are bounded, where

$$M_{\boldsymbol{\alpha}} := \mathrm{E}\left|\phi_{\alpha_1}(\xi) \ldots \phi_{\alpha_m}(\xi)\right| \textit{ for a multi-index } \boldsymbol{\alpha} \in \mathbb{N}^m,\ 0 < m < \infty.$$

To this end, note that $\phi_{\alpha_1}(\xi) \cdot \ldots \cdot \phi_{\alpha_m}(\xi)$ is a polynomial in ξ. Thus M_α can be upper bounded by a sum of absolute moments of ξ, and $\mathrm{E}\left[|\xi|^l\right] < \infty$ iff the l-th moment exists, which is a necessary assumption for the polynomial chaos method [51]. □

3.4.2 Optimality conditions

Given the adjoint function $\hat{\boldsymbol{\lambda}}^T(t) = (\hat{\boldsymbol{\lambda}}_0^T(t), \dots, \hat{\boldsymbol{\lambda}}_{M_p-1}^T(t)) \in \mathbb{R}^{nM_p}$ and the constant $\lambda^0 \in \mathbb{R}$ associated with (OCP^p), we formulate the Hamiltonian function similarly to Section 1.2

$$\hat{H}(\hat{\boldsymbol{x}}^\star(t), \boldsymbol{u}^\star(t), \lambda^0, \hat{\boldsymbol{\lambda}}(t)) = \sum_{l=0}^{M_p-1} \hat{\boldsymbol{\lambda}}_l(t) \hat{\boldsymbol{f}}_l(\hat{\boldsymbol{x}}^\star(t), \boldsymbol{u}^\star(t)) + \lambda^0 \hat{l}(\hat{\boldsymbol{x}}^\star(t), \boldsymbol{u}^\star(t)). \tag{3.18}$$

The notation $\partial_{\boldsymbol{u}} = \frac{\partial}{\partial \boldsymbol{u}}$ always stands for the partial (Fréchet) derivative.

The existence of the adjoints as well as the necessary optimality conditions is given in the following theorem, cf. [35, Theorem 4.2i].

Theorem 3.4.2 (Pontryagin's minimum principle) *If $\boldsymbol{u}^\star$ and the associated state trajectory $\hat{\boldsymbol{x}}^\star$ are a solution of (OCP^p), then there exists a constant $\lambda^0 \geqslant 0$, an absolutely continuous adjoint function $\hat{\boldsymbol{\lambda}}^T(t) \in \mathbb{R}^{nM_p}$ and multiplier vectors $\boldsymbol{\zeta}^T \in \mathbb{R}^{n_{r_{\text{eq}}}}$, $\boldsymbol{\nu}^T \in \mathbb{R}^{n_{r_{\text{in}}}}$ satisfying the following conditions:*

1. *Nontriviality of the adjoints:*

$$(\lambda^0, \hat{\boldsymbol{\lambda}}(t)) \neq \boldsymbol{0} \quad \text{on } [t_0, t_f]$$

2. *State equation:*

$$\frac{\mathrm{d}}{\mathrm{d}t}\hat{\boldsymbol{x}}^\star(t) = \hat{\boldsymbol{f}}(\hat{\boldsymbol{x}}^\star(t), \boldsymbol{u}(t)) \quad \text{on } [t_0, t_f] \text{ a.e.}$$

3. *Initial condition:*

$$\hat{\boldsymbol{x}}^\star(t_0) = (\boldsymbol{x}_0, \boldsymbol{0} \dots, \boldsymbol{0})$$

4. *Adjoint equation: for $k = 0, \dots, M_p - 1$*

$$\frac{\mathrm{d}}{\mathrm{d}t}\hat{\boldsymbol{\lambda}}_k(t) = -\sum_{l=0}^{M_p-1} \hat{\boldsymbol{\lambda}}_l(t) \partial_{\hat{\boldsymbol{x}}_k} \hat{\boldsymbol{f}}_l(\hat{\boldsymbol{x}}^\star(t), \boldsymbol{u}^\star(t)) - \lambda^0 \partial_{\hat{\boldsymbol{x}}_k} \hat{l}(\hat{\boldsymbol{x}}^\star(t), \boldsymbol{u}^\star(t))$$

   on $[t_0, t_f]$ a.e.

5. *Transversality condition: for $k = 0, \dots, M_p - 1$*

$$\hat{\boldsymbol{\lambda}}_k(t_f) = \lambda^0 \partial_{\hat{\boldsymbol{x}}_k} \hat{m}(\hat{\boldsymbol{x}}^\star(t_f)) + \boldsymbol{\zeta} \partial_{\hat{\boldsymbol{x}}_k} \hat{\boldsymbol{r}}_{\text{eq}}(\hat{\boldsymbol{x}}^\star(t_f)) + \boldsymbol{\nu} \partial_{\hat{\boldsymbol{x}}_k} \hat{\boldsymbol{r}}_{\text{in}}(\hat{\boldsymbol{x}}^\star(t_f))$$

6. *Constraints:*

$$\hat{\boldsymbol{r}}_{\text{eq}}(\hat{\boldsymbol{x}}^\star(t_f)) = \boldsymbol{0}, \ \hat{\boldsymbol{r}}_{\text{in}}(\hat{\boldsymbol{x}}^\star(t_f)) \leqslant \boldsymbol{0}$$

7. *Complementary slackness:*

$$\boldsymbol{\nu} \hat{\boldsymbol{r}}_{\text{in}}(\hat{\boldsymbol{x}}^\star(t_f)) = 0, \ \boldsymbol{\nu} \geqslant \boldsymbol{0}$$

8. *Minimum condition:*

$$\hat{H}(\hat{\boldsymbol{x}}^\star(t), \boldsymbol{u}^\star(t), \lambda^0, \hat{\boldsymbol{\lambda}}(t)) = \min_{\boldsymbol{u}\in U(t)} \hat{H}(\hat{\boldsymbol{x}}^\star(t), \boldsymbol{u}(t), \lambda^0, \hat{\boldsymbol{\lambda}}(t)) \;\; on\; [t_0, t_f]\; a.e.$$

Using the polynomial chaos approximation of the adjoint state

$$\boldsymbol{\lambda}^{(p)}(t;\xi) := \sum_{l=0}^{M_p-1} \hat{\boldsymbol{\lambda}}_l(t)\phi_l(\xi),$$

the Hamiltonian function 3.18 can be written in an alternative form

$$\begin{aligned}\mathcal{H}(\boldsymbol{x}^{(p)\star}, \boldsymbol{u}^\star, \lambda^0, \boldsymbol{\lambda}^{(p)}) &= \sum_{l=0}^{M_p-1} \hat{\boldsymbol{\lambda}}_l(t)^T \left\langle \boldsymbol{f}(\boldsymbol{x}^{(p)\star}, \boldsymbol{u}^\star, \xi), \phi_l \right\rangle_{L^2(\mathcal{S})} + \lambda^0 \left\langle l(\boldsymbol{x}^{(p)\star}, \boldsymbol{u}^\star) \right\rangle_{L^2(\mathcal{S})} \\ &= \left\langle (\sum_{l=0}^{M_p-1} \hat{\boldsymbol{\lambda}}_l \phi_l)^T \boldsymbol{f}(\boldsymbol{x}^{(p)\star}, \boldsymbol{u}^\star, \xi) + \lambda^0 l(\boldsymbol{x}^{(p)\star}, \boldsymbol{u}^\star, \xi) \right\rangle_{L^2(\mathcal{S})} \\ &= \mathrm{E}\big[(\boldsymbol{\lambda}^{(p)})^T \boldsymbol{f}(\boldsymbol{x}^{(p)\star}, \boldsymbol{u}^\star, \xi) + \lambda^0 l(\boldsymbol{x}^{(p)\star}, \boldsymbol{u}^\star, \xi)\big]. \end{aligned} \tag{3.19}$$

From the minimum condition, we can infer that

$$\partial_{\boldsymbol{u}} \mathcal{H}(\boldsymbol{x}^{(p)\star}(t;\xi), \boldsymbol{u}^\star(t), \lambda^0, \boldsymbol{\lambda}^{(p)}(t;\xi)) = \boldsymbol{0} \quad \forall t \in [t_0, t_f] \text{ a.e.}$$

properly supported by a second-order condition

$$d^T \partial^2_{\boldsymbol{u}^2} \mathcal{H}(\boldsymbol{x}^{(p)\star}(t;\xi), \boldsymbol{u}^\star(t), \lambda^0, \boldsymbol{\lambda}^{(p)}(t;\xi)) d \geqslant 0 \quad \forall d \in \mathbb{R}^{n_u},\; \forall t \in [t_0, t_f] \text{ a.e..}$$

Further, we assume a strong second-order sufficient condition for sufficiently large orders p that allows to express the control as a function of states and adjoints.

Assumption 3.3 *The solution trajectory* $(\boldsymbol{x}^{(p)\star}, \boldsymbol{u}^\star, \lambda^0, \boldsymbol{\lambda}^{(p)})$ *satisfies the* strong Legendre condition *for all polynomial chaos orders* $p \geqslant q$ *for some* $q \geqslant 0$*, that is,* $\forall t \in [t_0, t_f]$ *a.e.*

$$\begin{aligned} &d^T \partial^2_{\boldsymbol{u}^2} \mathcal{H}(\boldsymbol{x}^{(p)\star}(t;\xi), \boldsymbol{u}^\star(t), \lambda^0, \boldsymbol{\lambda}^p(t;\xi)) d \\ &= d^T \mathrm{E}\big[(\boldsymbol{\lambda}^p)^T \partial^2_{\boldsymbol{u}^2} \boldsymbol{f}(\boldsymbol{x}^{(p)\star}(t;\xi), \boldsymbol{u}^\star(t), \xi) + \lambda^0 \partial^2_{\boldsymbol{u}^2} l(\boldsymbol{x}^{(p)\star}(t;\xi), \boldsymbol{u}^\star(t), \xi)\big] d \\ &\geqslant \alpha \end{aligned}$$

for some $\alpha > 0$ *and arbitrary* $d \in \mathbb{R}^{n_u}$.

To this end, we assume that $\boldsymbol{u}(t)$ takes on values in the interior of $U(t)$ for all $t \in [t_0, t_f]$ a.e., therefore we preclude *bang-bang* or *singular* controls. If $\boldsymbol{u}(t)$ takes on values on the boundary of $U(t)$, the control constraints can be transferred to the inner minimization problem by forming the extended Hamiltonian

$$\mathcal{H}^\mu(\boldsymbol{x}^{(p)\star}, \boldsymbol{u}^\star, \lambda^0, \boldsymbol{\lambda}^{(p)}) = \mathcal{H}(\boldsymbol{x}^{(p)\star}, \boldsymbol{u}^\star, \lambda^0, \boldsymbol{\lambda}^{(p)}) - \boldsymbol{\mu}_0(\boldsymbol{u}^\star - \boldsymbol{u}_{\min}) + \boldsymbol{\mu}_1(\boldsymbol{u}^\star - \boldsymbol{u}_{\max})$$

with multipliers $\boldsymbol{\mu}_0^T, \boldsymbol{\mu}_1^T \in \mathbb{R}^{n_u}$ and control set $U(t) = [\boldsymbol{u}_{\min}(t), \boldsymbol{u}_{\max}(t)]$.

Remark 3.2 *The optimality condition of* (OCP^p) *are required to hold only for the mean value, i.e.,*

$$\boldsymbol{0} = \partial_{\boldsymbol{u}} \mathcal{H}(\boldsymbol{x}^\star, \boldsymbol{u}^\star, \lambda^0\, \boldsymbol{\lambda}) = \mathrm{E}\big[(\boldsymbol{\lambda}^{(p)})^T \partial_{\boldsymbol{u}} \boldsymbol{f}(\boldsymbol{x}^{(p)\star}, \boldsymbol{u}^\star, \xi) + \lambda^0\, \partial_{\boldsymbol{u}} l(\boldsymbol{x}^{(p)\star}, \boldsymbol{u}^\star, \xi)\big].$$

In contrary, the Hamiltonian function associated to (UOCP) with adjoint function $\boldsymbol{\lambda} = \boldsymbol{\lambda}(t;\xi)$ is

$$H(\boldsymbol{x}^\star, \boldsymbol{u}^\star, \lambda^0\,\boldsymbol{\lambda}) := \boldsymbol{\lambda}^T \boldsymbol{f}(\boldsymbol{x}^\star, \boldsymbol{u}^\star, \xi) + \lambda^0\, l(\boldsymbol{x}, \boldsymbol{u}^\star, \xi)$$

and leads to a more restricted form

$$\mathbf{0} = \partial_{\boldsymbol{u}} H(\boldsymbol{x}^\star, \boldsymbol{u}^\star, \lambda^0\,\boldsymbol{\lambda}) = (\boldsymbol{\lambda}^{(p)})^T \partial_{\boldsymbol{u}} \boldsymbol{f}(\boldsymbol{x}^{(p)\star}, \boldsymbol{u}^\star, \xi) + \lambda^0\, \partial_{\boldsymbol{u}} l(\boldsymbol{x}^{(p)\star}, \boldsymbol{u}^\star, \xi)$$

required to hold for any realization $\xi(\omega),\ \omega \in \Omega$.

3.5 Proof of convergence

We state and prove our main result that the sequence $(\boldsymbol{x}^{(p)}, \boldsymbol{u})$, constructed from the solution $(\hat{\boldsymbol{x}}_0, \ldots, \hat{\boldsymbol{x}}_{M_p-1}, \boldsymbol{u})$ of (OCP^p), converges as p increases and approximates the solution $(\boldsymbol{x}^\star, \boldsymbol{u}^\star)$ of (UOCP) arbitrarily well in Theorem 3.5.1 and Corollary 3.5.2. Therefore, we consider the states and adjoints at an arbitrary but fixed time instance $t \in [t_0, t_f]$.
The first part is posed upon a compactness assumption on the underlying random space for which alternatives will be discussed at the end of this section.

Assumption 3.4 *$\mathcal{S}$ is compact.*

The second paragraph of the following proof including the bounds (3.20) and (3.21) are motivated by the work of Anitescu [6, Theorem 3.10] who shows convergence of the PC approximation for parametric nonlinear programming problems. Note that bound (3.21) is always satisfied if the functions m, $\boldsymbol{r}_{\text{in}}$ and $\boldsymbol{r}_{\text{eq}}$ in (UOCP) are linear.

Theorem 3.5.1 (Convergence) *Let $(\hat{\boldsymbol{x}}_0, \ldots, \hat{\boldsymbol{x}}_{M_p-1}, \boldsymbol{u}^{(p)}, \lambda^{0(p)}, \hat{\boldsymbol{\lambda}}_0, \ldots, \hat{\boldsymbol{\lambda}}_{M_p-1})$ be the solution of (OCP^p) satisfying the strong second-order condition in Assumption 3.3 for all sufficiently large p. Let $\boldsymbol{\zeta}^{(p)} \in \left(\mathbb{R}^{n_{\text{req}}}\right)^\star$, $\boldsymbol{\nu}^{(p)} \in \left(\mathbb{R}^{n_{\text{rin}}}\right)^\star$ be the corresponding constraint multipliers.*
Suppose that Assumption 3.4 holds and that there exist constants $\tilde{C}_x,\ \tilde{C}_\lambda > 0$ such that $\forall t \in [0, t_f]$

$$\sum_{k=0}^{M_p-1} \left|\left| \frac{\mathrm{d}}{\mathrm{d}t} \hat{\boldsymbol{x}}_k(t) \right|\right| (\deg \phi_k)^h < \tilde{C}_x, \tag{3.20}$$

$$\sum_{k=0}^{M_p-1} \left|\left| \frac{\mathrm{d}}{\mathrm{d}t} \hat{\boldsymbol{\lambda}}_k(t) \right|\right| (\deg \phi_k)^h < \tilde{C}_\lambda,\ \sum_{k=0}^{M_p-1} \left|\left| \hat{\boldsymbol{\lambda}}_k(t_f) \right|\right| (\deg \phi_k)^h < \tilde{C}_\lambda, \tag{3.21}$$

where h is the parameter from the bound (3.6) in Section 3.2. Further suppose that there exist a constant $\tilde{C} > 0$ such that

$$\lambda^{0(p)}, \left|\left| \boldsymbol{\nu}^{(p)} \right|\right|, \left|\left| \boldsymbol{\zeta}^{(p)} \right|\right| < \tilde{C}. \tag{3.22}$$

Then, we can construct a bounded sequence $\{(\boldsymbol{x}^{(p)}, \boldsymbol{u}^{(p)}, \boldsymbol{\lambda}^{(p)})\}$ with

$$\boldsymbol{x}^{(p)} = \sum_{i=0}^{M_p-1} \hat{\boldsymbol{x}}_i(t)\phi_i(\xi) \text{ and } \boldsymbol{\lambda}^{(p)}(\xi) = \sum_{i=0}^{M_p-1} \hat{\boldsymbol{\lambda}}_i(t)\phi_i(\xi)$$

containing a convergent subsequence whose limit is a feasible solution to (UOCP).

Proof 1. *First, we show that Equation (3.20) extends to similar bounds for $\hat{\boldsymbol{x}}_k$ and $\hat{\boldsymbol{\lambda}}_k$.*

By the mean value theorem, there exists $\tau \in (0, t_f)$ *with*

$$||\hat{\boldsymbol{x}}_k(t)|| \leqslant \left|\left|\frac{\mathrm{d}}{\mathrm{d}t}\hat{\boldsymbol{x}}_k(\tau)\right|\right| t_f + ||\hat{\boldsymbol{x}}_k(0)||\,.$$

Consequently, and since $\hat{\boldsymbol{x}}_k(0) = 0$ *for* $k > 0$*, we can find a constant* C_x *such that*

$$\begin{aligned}\sum_{k=0}^{M_p-1} ||\hat{\boldsymbol{x}}_k(t)||\,(\deg\phi_k)^h &\leqslant \sum_{k=0}^{M_p-1}\left(t_f\left|\left|\frac{\mathrm{d}}{\mathrm{d}t}\hat{\boldsymbol{x}}_k(\tau)\right|\right|(\deg\phi_k)^h + ||\hat{\boldsymbol{x}}_k(0)||\right)\\ &\leqslant \underbrace{||\hat{\boldsymbol{x}}_0(0)||}_{given} + t_f\underbrace{\sum_{k=0}^{M_p-1}||\hat{\boldsymbol{x}}_k(\tau)||\,(\deg\phi_k)^h}_{<\tilde{C}_x} < C_x. \end{aligned} \tag{3.23}$$

In the same way, a constant C_λ *can be chosen. To this end, for some* $\tau \in (0, t_f)$*, we note*

$$\left|\left|\hat{\boldsymbol{\lambda}}_k(t)\right|\right| \leqslant \left|\left|\frac{\mathrm{d}}{\mathrm{d}t}\hat{\boldsymbol{\lambda}}_k(\tau)\right|\right| t_f + \left|\left|\hat{\boldsymbol{\lambda}}_k(t_f)\right|\right|,$$

and

$$\begin{aligned}&\sum_{k=0}^{M_p-1}\left|\left|\hat{\boldsymbol{\lambda}}_k(t)\right|\right|(\deg\phi_k)^h \leqslant \sum_{k=0}^{M_p-1}\left(\left|\left|\frac{\mathrm{d}}{\mathrm{d}t}\hat{\boldsymbol{\lambda}}_k(\tau)\right|\right| t_f + \left|\left|\hat{\boldsymbol{\lambda}}_k(t_f)\right|\right|\right)(\deg\phi_k)^h\\ &\leqslant t_f\underbrace{\sum_{k=0}^{M_p-1}\left|\left|\frac{\mathrm{d}}{\mathrm{d}t}\hat{\boldsymbol{\lambda}}_k(\tau)\right|\right|(\deg\phi_k)^h}_{<\tilde{C}_\lambda} + \underbrace{\sum_{k=0}^{M_p-1}\left|\left|\hat{\boldsymbol{\lambda}}_f(t_f)\right|\right|(\deg\phi_k)^h}_{<\tilde{C}_\lambda} < C_\lambda. \end{aligned} \tag{3.24}$$

2. *Assume* $p < \infty$*. Using Equation* (3.23) *and applying the bound* (3.6) *to*

$$\boldsymbol{x}^{(p)}(t) = \sum_{i=0}^{M_p-1}\hat{\boldsymbol{x}}_i(t)\phi_i(\xi) \in L^2(\mathcal{S})$$

by setting $c_i(\boldsymbol{x}^{(p)}(t)) = \begin{cases}\hat{\boldsymbol{x}}_i(t) & 0 \leqslant i \leqslant M_p - 1\\ 0 & i \geqslant M_p\end{cases}$*, we obtain*

   (a) *uniform boundedness:* $\left\|\boldsymbol{x}^{(p)}(t)\right\|_{L^\infty(\mathcal{S})} \leqslant C_s\sum_{k=0}^{M_p-1}||\hat{\boldsymbol{x}}_k(t)||\,(\deg\phi_k)^h < C_sC_x$

   (b) *equicontinuity:* $\forall\xi_0, \xi_1 \in \Omega$

$$\left|\left|\boldsymbol{x}^{(p)}(t;\xi_0) - \boldsymbol{x}^{(p)}(t;\xi_1)\right|\right| \leqslant \left\|\sup_{1\leqslant j\leqslant d}\partial_{\xi_j}\boldsymbol{x}(t)\right\|_{L^\infty(\mathcal{S})}\left|\left|\xi_0 - \xi_1\right|\right| \leqslant C_sC_x\left|\left|\xi_0 - \xi_1\right|\right|.$$

Equally, Equation (3.20) *and bound* (3.6) *can be applied to*

$$\frac{\mathrm{d}}{\mathrm{d}t}\boldsymbol{x}^{(p)}(t) = \sum_{i=0}^{M_p-1}\frac{\mathrm{d}\hat{\boldsymbol{x}}_i}{\mathrm{d}t}(t)\phi_i(\xi) \in L^2_\rho(\mathcal{S})$$

to obtain equicontinuity and uniform boundedness of $\frac{\mathrm{d}}{\mathrm{d}t}\boldsymbol{x}^{(p)}(t)$.

Thus, $\left\{\boldsymbol{x}^{(p)}(t)\right\}$ *as well as* $\left\{\frac{\mathrm{d}}{\mathrm{d}t}\boldsymbol{x}^{(p)}(t)\right\}$ *are uniform Lipschitz continuous in* ξ. *Similar arguments apply to the gPC approximation of the adjoint states,* $\left\{\boldsymbol{\lambda}^{(p)}(t)\right\}$ *and* $\left\{\frac{\mathrm{d}}{\mathrm{d}t}\boldsymbol{\lambda}^{(p)}(t)\right\}$, *which are by construction also contained in* $L^2_\rho(\mathcal{S})$.

We apply the Arzela-Ascoli Theorem, cf. [35, Theorem 9.1i] to obtain a uniformly converging subsequence, taking into account that the multipliers $\lambda^{0(p)}$, $\boldsymbol{\nu}^{(p)}$, $\zeta^{(p)}$ *are uniformly bounded,*

$$\left\{\left(\boldsymbol{x}^{(p_k)}(t), \boldsymbol{\lambda}^{(p_k)}(t), \frac{\mathrm{d}}{\mathrm{d}t}\boldsymbol{x}^{(p_k)}(t), \frac{\mathrm{d}}{\mathrm{d}t}\boldsymbol{\lambda}^{(p_k)}(t), \lambda^{0(p_k)}, \boldsymbol{\nu}^{(p_k)}, \zeta^{(p_k)}\right)\right\} \subset \left\{\left(\boldsymbol{x}^{(p)}(t), \boldsymbol{\lambda}^{(p)}(t), \frac{\mathrm{d}}{\mathrm{d}t}\boldsymbol{x}^{(p)}(t), \frac{\mathrm{d}}{\mathrm{d}t}\boldsymbol{\lambda}^{(p)}(t), \lambda^{0(p)}, \boldsymbol{\nu}^{(p)}, \zeta^{(p)}\right)\right\}$$

with limiting functions

$$\left(\boldsymbol{x}^{(\infty)}(t), \boldsymbol{\lambda}^{(\infty)}(t), \frac{\mathrm{d}}{\mathrm{d}t}\boldsymbol{x}^{(\infty)}(t), \frac{\mathrm{d}}{\mathrm{d}t}\boldsymbol{\lambda}^{(\infty)}(t), \lambda^{0(\infty)}, \boldsymbol{\nu}^{(\infty)}, \zeta^{(\infty)}\right)$$

that are Lipschitz continuous and contained in $L^\infty(\mathcal{S})$.

3. *Fix* $\varepsilon > 0$ *and choose* p_k' *such that* $\forall p_k \geqslant p_k'$ $\forall t \in [t_0, t_\mathrm{f}]$

$$\left\|\boldsymbol{x}^{(p_k)}(t) - \boldsymbol{x}^{(\infty)}(t)\right\|_{L^\infty(\mathcal{S})} < \varepsilon \text{ and } \left\|\boldsymbol{\lambda}^{(p_k)}(t) - \boldsymbol{\lambda}^{(\infty)}(t)\right\|_{L^\infty(\mathcal{S})} < \varepsilon.$$

Select an index $q \in \{p_k\}$ *with* $q \geqslant p_k'$.

$(\boldsymbol{x}^{(q)}(t), \boldsymbol{\lambda}^{(q)}(t))$ *is constructed from the solution to* (OCP^p) *with control law* $\boldsymbol{u}^{(q)}(t)$ *and satisfies*

$$0 = \partial_{\boldsymbol{u}}\mathcal{H}(\boldsymbol{x}^{(q)}(t), \boldsymbol{u}^{(q)}(t), \lambda^{0(q)}, \boldsymbol{\lambda}^{(q)}(t)) \text{ on } [t_0, t_\mathrm{f}] \text{ a.e.}$$

with $\tilde{H}$ *defined in* (3.19).

By Assumption (3.3), $\partial^2_{\boldsymbol{u}^2}\mathcal{H}(\boldsymbol{x}^{(q)}(t), \boldsymbol{u}^{(q)}(t), \lambda^{0(q)}, \boldsymbol{\lambda}^{(q)}(t))$ *is invertible. Thus, we can apply the implicit function theorem to determine a Lipschitz continuous mapping*

$$\Gamma : B^\infty_\varepsilon(\boldsymbol{x}^{(q)}(t), \lambda^{0(q)}, \boldsymbol{\lambda}^{(q)}(t)) \to \mathbb{R}^{n_\mathrm{u}}$$

in the ε*-neighborhood of* $(\boldsymbol{x}^{(q)}(t), \lambda^{0(q)}, \boldsymbol{\lambda}^{(q)}(t))$ *with*

$$\boldsymbol{u}(t) = \Gamma(\boldsymbol{x}(t), \lambda^0, \boldsymbol{\lambda}(t)) \iff \partial^2_{u^2}\mathcal{H}(\boldsymbol{x}(t), \boldsymbol{u}(t), \lambda^0, \boldsymbol{\lambda}(t)) = 0.$$

Defining

$$\boldsymbol{u}^{(p_k)}(t) = \Gamma(\boldsymbol{x}^{(p_k)}(t), \lambda^{0(p_k)}, \boldsymbol{\lambda}^{(p_k)}(t)) \text{ and } \boldsymbol{u}^{(\infty)}(t) = \Gamma(\boldsymbol{x}^{(\infty)}(t), \lambda^{0(\infty)}, \boldsymbol{\lambda}^{(\infty)}(t)),$$

we deduce

$$\lim_{k\to\infty} \boldsymbol{u}^{(p_k)}(t) = \boldsymbol{u}^{(\infty)}(t).$$

4. *In the last step, we show that the limit* $(\boldsymbol{x}^{(\infty)}(t), \boldsymbol{u}^{(\infty)}(t), \lambda^{0(\infty)}, \boldsymbol{\lambda}^{(\infty)}(t), \boldsymbol{\nu}^{(\infty)}, \zeta^{(\infty)})$ *of the convergent subsequence* $\left\{(\boldsymbol{x}^{(p_k)}(t), \boldsymbol{u}^{(p_k)}(t), \lambda^{0(p_k)}, \boldsymbol{\lambda}^{(p_k)}(t), \boldsymbol{\nu}^{(p_k)}, \zeta^{(p_k)})\right\}_{l \geqslant 0}$ *is feasible for* (UOCP).

   For ease of notation, we drop the arbitrary but fixed index $t \in [t_0, t_f]$.

   Any $(\boldsymbol{x}^{(p_k)}, \lambda^{0(p_k)}, \boldsymbol{\lambda}^{(p_k)}, \boldsymbol{u}^{(p_k)}, \boldsymbol{\nu}^{(p_k)}, \zeta^{(p_k)})$ *satisfies the following equations*

$$\frac{\mathrm{d}}{\mathrm{d}t}\boldsymbol{x}^{(p_k)}(t;\xi) = \sum_{k=0}^{M_{(p_k)}-1} \left\langle \boldsymbol{f}(\boldsymbol{x}^{(p_k)}, \boldsymbol{u}^{(p_k)}), \phi_k \right\rangle_{L^2(\mathcal{S})} \phi_k, \tag{3.25}$$

$$\begin{aligned}\frac{\mathrm{d}}{\mathrm{d}t}\boldsymbol{\lambda}^{(p_k)}(t;\xi) = &- \sum_{k=0}^{M_{p_k}-1} \left\langle \left(\boldsymbol{\lambda}^{(p_k)}\right) \partial_{\boldsymbol{x}} \boldsymbol{f}(\boldsymbol{x}^{(p_k)}, \boldsymbol{u}^{(p_k)}), \phi_k \right\rangle_{L^2(\mathcal{S})} \phi_k \\ &- \lambda^{0(p)} \partial_{\boldsymbol{x}} l(\boldsymbol{x}^{(p_k)}, \boldsymbol{u}^{(p_k)}),\end{aligned} \tag{3.26}$$

$$\begin{aligned}\boldsymbol{\lambda}^{(p)}(t_f;\xi) = &\lambda^{0(p)} \partial_{\boldsymbol{x}} \mathrm{E}\left[m(\boldsymbol{x}^{(p)}(t_f;\xi))\right] + \left(\boldsymbol{\nu}^{(p)}\right) \partial_{\boldsymbol{x}} \mathrm{E}\left[\boldsymbol{r}_{\mathrm{eq}}(\boldsymbol{x}^{(p)}(t_f;\xi))\right] \\ &+ \left(\zeta^{(p)}\right) \partial_{\boldsymbol{x}} \mathrm{E}\left[\boldsymbol{r}_{\mathrm{in}}(\boldsymbol{x}^{(p)}(t_f;\xi))\right].\end{aligned} \tag{3.27}$$

   This follows from their construction as the solution of (OCP^p), *thus satisfying*

$$\begin{aligned}\frac{\mathrm{d}}{\mathrm{d}t}\hat{\boldsymbol{x}}_k(t) &= \left\langle \boldsymbol{f}(\boldsymbol{x}^{(p)}, \boldsymbol{u}), \phi_k \right\rangle_{L^2(\mathcal{S})}, \\ \frac{\mathrm{d}}{\mathrm{d}t}\hat{\boldsymbol{\lambda}}_k(t) &= -\sum_{l=0}^{M_p-1} \hat{\boldsymbol{\lambda}}_l \frac{\partial}{\partial \hat{\boldsymbol{x}}_k} \left\langle \boldsymbol{f}(\boldsymbol{x}^{(p)}, \boldsymbol{u}), \phi_l \right\rangle_{L^2(\mathcal{S})} - \lambda^{0(p)} \frac{\partial}{\partial \hat{\boldsymbol{x}}_k} \hat{l}_0(\boldsymbol{x}^{(p)}, \boldsymbol{u}) \\ &= -\frac{\partial}{\partial \hat{\boldsymbol{x}}_k} \left\langle \left(\sum_{l=0}^{M_p-1} \hat{\boldsymbol{\lambda}}_l \phi_l \right) \boldsymbol{f}(\boldsymbol{x}^{(p)}, \boldsymbol{u}) \right\rangle_{L^2(\mathcal{S})} - \frac{\partial}{\partial \hat{\boldsymbol{x}}_k} \left\langle \lambda^{0(p)} l(\boldsymbol{x}^{(p)}, \boldsymbol{u}) \right\rangle_{L^2(\mathcal{S})} \\ &= -\frac{\partial}{\partial \hat{\boldsymbol{x}}_k} \left\langle \left(\boldsymbol{\lambda}^{(p)}\right) \boldsymbol{f}(\boldsymbol{x}^{(p)}, \boldsymbol{u}) + \lambda^{0(p)} l(\boldsymbol{x}^{(p)}, \boldsymbol{u}) \right\rangle_{L^2(\mathcal{S})} \\ &= \left\langle -\left(\boldsymbol{\lambda}^{(p)}\right) \partial_{\boldsymbol{x}} \boldsymbol{f}(\boldsymbol{x}^{(p)}, \boldsymbol{u}) - \lambda^{0(p)} \partial_{\boldsymbol{x}} l(\boldsymbol{x}^{(p)}, \boldsymbol{u}), \phi_k \right\rangle_{L^2(\mathcal{S})}, \text{ and} \\ \hat{\boldsymbol{\lambda}}_k(t_f) &= \lambda^{0(p)} \frac{\partial}{\partial \hat{\boldsymbol{x}}_k} \hat{m}(\boldsymbol{x}^{(p)}(t_f;\xi)) + \boldsymbol{\nu}^{(p)} \frac{\partial}{\partial \hat{\boldsymbol{x}}_k} \hat{\boldsymbol{r}}_{\mathrm{eq}}(\boldsymbol{x}^{(p)}(t_f;\xi)) \\ &\quad + \zeta^{(p)} \frac{\partial}{\partial \hat{\boldsymbol{x}}_k} \hat{\boldsymbol{r}}_{\mathrm{in}}(\boldsymbol{x}^{(p)}(t_f;\xi)) \\ &= \frac{\partial}{\partial \hat{\boldsymbol{x}}_k} \left\langle \lambda^{0(p)} m(\boldsymbol{x}^{(p)}(t_f;\xi)) + \boldsymbol{\nu}^{(p)} \boldsymbol{r}_{\mathrm{eq}}(\boldsymbol{x}^{(p)}(t_f;\xi)) + \zeta^{(p)} \boldsymbol{r}_{\mathrm{in}}(\boldsymbol{x}^{(p)}(t_f;\xi)) \right\rangle_{L^2(\mathcal{S})} \\ &= \left\langle \lambda^{0(p)} \partial_{\boldsymbol{x}} m(\boldsymbol{x}^{(p)}(t_f;\xi)) + \boldsymbol{\nu}^{(p)} \partial_{\boldsymbol{x}} \boldsymbol{r}_{\mathrm{eq}}(\boldsymbol{x}^{(p)}(t_f;\xi)) + \zeta^{(p)} \partial_{\boldsymbol{x}} \boldsymbol{r}_{\mathrm{in}}(\boldsymbol{x}^{(p)}(t_f;\xi)), \phi_k \right\rangle_{L^2(\mathcal{S})}.\end{aligned}$$

   Using Equations (3.25)–(3.27) *and the results of 2., we derive*

$$\begin{aligned}&\lim_{k\to\infty} \sum_{j=0}^{M_{p_k}-1} \left\langle \boldsymbol{f}(\boldsymbol{x}^{(p_k)}, \boldsymbol{u}^{(p_k)}), \phi_j \right\rangle_{L^2(\mathcal{S})} \phi_j = \sum_{j=0}^{\infty} \left\langle \boldsymbol{f}(\lim_{k\to\infty} \boldsymbol{x}^{(p_k)}, \lim_{k\to\infty} \boldsymbol{u}^{(p_k)}), \phi_j \right\rangle_{L^2(\mathcal{S})} \phi_j \\ &= \sum_{j=0}^{\infty} \left\langle \boldsymbol{f}(\boldsymbol{x}^{(\infty)}, \boldsymbol{u}^{(\infty)}), \phi_j \right\rangle_{L^2(\mathcal{S})} \phi_j = \boldsymbol{f}(\boldsymbol{x}^{(\infty)}, \boldsymbol{u}^{(\infty)}),\end{aligned}$$

and consequently

$$\dot{\boldsymbol{x}}^{(\infty)} = \lim_{k\to\infty} \frac{\mathrm{d}}{\mathrm{d}t}\boldsymbol{x}^{(p_k)} = \boldsymbol{f}(\boldsymbol{x}^{(\infty)}, \boldsymbol{u}^{(\infty)}).$$

Similarly for the adjoint states,

$$\begin{aligned}
&\lim_{k\to\infty} \sum_{j=0}^{M_{p_k}-1} \left\langle -\boldsymbol{\lambda}^{(p_k)}\partial_{\boldsymbol{x}}\boldsymbol{f}(\boldsymbol{x}^{(p_k)}, \boldsymbol{u}^{(p_k)}) - \lambda^{0(p_k)}\partial_{\boldsymbol{x}} l(\boldsymbol{x}^{(p_k)}, \boldsymbol{u}^{(p_k)}), \phi_j \right\rangle_{L^2(\mathcal{S})} \phi_j \\
&= -\sum_{j=0}^{\infty} \left\langle (\boldsymbol{\lambda}^{(\infty)})\partial_{\boldsymbol{x}}\boldsymbol{f}(\boldsymbol{x}^{(\infty)}, \boldsymbol{u}^{(\infty)}) + \lambda^{0(\infty)}\partial_{\boldsymbol{x}} l(\boldsymbol{x}^{(\infty)}, \boldsymbol{u}^{(\infty)}), \phi_j \right\rangle_{L^2(\mathcal{S})} \phi_j \\
&= -(\boldsymbol{\lambda}^{(\infty)})\partial_{\boldsymbol{x}}\boldsymbol{f}(\boldsymbol{x}^{(\infty)}, \boldsymbol{u}^{(\infty)}) - \lambda^{0(p)}\partial_{\boldsymbol{x}} l(\boldsymbol{x}^{(\infty)}, \boldsymbol{u}^{(\infty)}).
\end{aligned}$$

Consequently

$$\dot{\boldsymbol{\lambda}}^{(\infty)} = -(\boldsymbol{\lambda}^{(\infty)})\partial_{\boldsymbol{x}}\boldsymbol{f}(\boldsymbol{x}^{(\infty)}, \boldsymbol{u}^{(\infty)}) - \lambda^{0(\infty)}\partial_{\boldsymbol{x}} l(\boldsymbol{x}^{(\infty)}, \boldsymbol{u}^{(\infty)})$$

and

$$\begin{aligned}
\boldsymbol{\lambda}^{(\infty)}(t_\mathrm{f}; \xi) = \lambda^{0(\infty)}\partial_{\boldsymbol{x}} m(\boldsymbol{x}^{(\infty)}(t_\mathrm{f}, \xi)) + \boldsymbol{\nu}^{(\infty)}\partial_{\boldsymbol{x}}\boldsymbol{r}_\mathrm{eq}(\boldsymbol{x}^{(\infty)}(t_\mathrm{f}; \xi)) \\
+ \boldsymbol{\zeta}^{(\infty)}\partial_{\boldsymbol{x}}\boldsymbol{r}_\mathrm{in}(\boldsymbol{x}^{(\infty)}(t_\mathrm{f}; \xi)).
\end{aligned}$$

For the constraints, we obtain

$$\boldsymbol{r}_\mathrm{eq}(\boldsymbol{x}^{(\infty)}(t_\mathrm{f}; \xi)) = \lim_{k\to\infty} \boldsymbol{r}_\mathrm{eq}(\boldsymbol{x}^{(p_k)}(t_\mathrm{f}; \xi)) = \boldsymbol{0},$$

$$\boldsymbol{\zeta}^{(\infty)}\boldsymbol{r}_\mathrm{in}(\boldsymbol{x}^{(\infty)}(t_\mathrm{f}; \xi)) = \lim_{k\to\infty} \boldsymbol{\zeta}^{(p_k)}\boldsymbol{r}_\mathrm{eq}(\boldsymbol{x}^{(p_k)}(t_\mathrm{f}; \xi)) = \boldsymbol{0}$$

and

$$\boldsymbol{\zeta}^{(p_k)} \geqslant \boldsymbol{0}\ \forall k \ \Rightarrow\ \boldsymbol{\zeta}^{(\infty)} = \lim_{k\to\infty} \boldsymbol{\zeta}^{(p_k)} \geqslant \boldsymbol{0}.$$

□

It remains to show that the limit that $(\boldsymbol{x}^{(p)}(t), \boldsymbol{u}^{(p)}(t))$ converges to is the sought solution. For this task, we introduce a random perturbation $\delta(t; \xi)$ into the formulation of problem (UOCP).

Definition 3.5.1 (Perturbed Uncertain Optimal Control Problem)

$$\begin{aligned}
\min_{\boldsymbol{x},\boldsymbol{u}} \quad & \mathrm{E}[J[\boldsymbol{x}, \boldsymbol{u}]] && && \text{(PUOCP)} \\
\text{s.t.} \quad & \dot{\boldsymbol{x}}(t; \xi) = \boldsymbol{f}(\boldsymbol{x}(t; \xi), \boldsymbol{u}(t), \xi) - \delta(t; \xi), && t \in [t_0, t_\mathrm{f}]\ a.e.,\ \xi = \xi(\omega),\ \omega \in \Omega\ \text{a.s.} \\
& \boldsymbol{x}(t_0) = \boldsymbol{x}_0 \\
& \boldsymbol{u}(t) \in U(t) && t \in [t_0, t_\mathrm{f}]\ a.e. \\
& \boldsymbol{0} \geqslant \mathrm{E}\left[\boldsymbol{r}_\mathrm{in}(\boldsymbol{x}(t_\mathrm{f}; \xi), \xi)\right] \\
& \boldsymbol{0} = \mathrm{E}\left[\boldsymbol{r}_\mathrm{eq}(\boldsymbol{x}(t_\mathrm{f}; \xi), \xi)\right]
\end{aligned}$$

Corollary 3.5.2 (Consistency) *Suppose* (UOCP) *has an optimum solution* $(\boldsymbol{x}^\star(t;\xi),\boldsymbol{u}^\star(t))$ *that is* L^2*-measurable and assume* $\boldsymbol{x}^{(p)}(t;\xi)$ *is the polynomial chaos projection corresponding to the optimal solution* $(\hat{\boldsymbol{x}}^{(p)},\boldsymbol{u}^{(p)})$ *of* (OCP^p)*. Then, for any fixed but arbitrary* $t\in[0,t_\mathrm{f}]$*,*

$$\lim_{p\to\infty}\boldsymbol{x}^{(p)}(t;\cdot)=\boldsymbol{x}^\star(t;\cdot)\ \text{in}\ L^2_\rho(\mathcal{S}).$$

Proof *Fix* $t\in[t_0,t_\mathrm{f}]$ *to some arbitrary value. We consider* (PUOCP) *with a perturbation defined by the error resulting from the p-th-order polynomial chaos approximation of* $\boldsymbol{f}$*,*

$$\delta^{(p)}(t;\xi)=\sum_{k=0}^{\infty}\left\langle\boldsymbol{f}(\boldsymbol{x}(t;\xi),\boldsymbol{u}(t),\xi(\omega)),\phi_k\right\rangle_{L^2(\mathcal{S})}\phi_k-\sum_{k=0}^{M_p-1}\left\langle\boldsymbol{f}(\boldsymbol{x}(t;\xi),\boldsymbol{u}(t),\xi(\omega)),\phi_k\right\rangle_{L^2(\mathcal{S})}\phi_k$$

for $\omega\in\Omega$*.*
Note that the objective and end point constraint function are not affected by any perturbation defined in this way since they are evaluated at their expected values, and

$$\mathrm{E}\left[\delta^{(p)}(t;\xi)\right]=\left\langle\boldsymbol{f}(\boldsymbol{x}(t;\xi),\boldsymbol{u}(t),\xi(\omega)),\phi_0\right\rangle_{L^2(\mathcal{S})}-\left\langle\boldsymbol{f}(\boldsymbol{x}(t;\xi),\boldsymbol{u}(t),\xi(\omega)),\phi_0\right\rangle_{L^2(\mathcal{S})}\equiv 0.$$

For $p=\infty$*, in which case* $\delta^{(p)}\equiv 0$*, the optimal solution is given by* $(\boldsymbol{x}^\star,\boldsymbol{u}^\star)$ *and is unique by assumption. For each finite p with perturbation* $\delta^{(p)}$*, the optimal solution is by construction* $(\hat{\boldsymbol{x}}^{(p)},\boldsymbol{u}^{(p)})$*, the unique optimal solution corresponding to* (OCP^p)*. Since* $\boldsymbol{f}$ *is globally Lipschitz continuous in its arguments, we obtain, with the help of 3.1.1 for any admissible* $\boldsymbol{u}\in\mathcal{U}$*,*

$$y(t;\xi):=\boldsymbol{f}(\boldsymbol{x}(t;\xi),\boldsymbol{u}(t),\xi)\in L^2_\rho(\mathcal{S})\quad\forall t\in[t_0,t_\mathrm{f}].$$

Consequently $\boldsymbol{y}$ *admits itself a decomposition*

$$\boldsymbol{y}(t;\xi)=\sum_{k=0}^{\infty}\left\langle\boldsymbol{f}(\boldsymbol{x}(t;\xi),\boldsymbol{u}(t),\xi),\phi_k\right\rangle_{L^2(\mathcal{S})}\phi_k$$

for which

$$\begin{aligned}\left\|\delta^{(p)}\right\|_{L^2(\mathcal{S})}&=\left\|\sum_{k=0}^{\infty}\left\langle\boldsymbol{f}(\boldsymbol{x},\boldsymbol{u},\xi),\phi_k\right\rangle_{L^2(\mathcal{S})}\phi_k-\sum_{k=0}^{M_p-1}\left\langle\boldsymbol{f}(\boldsymbol{x},\boldsymbol{u},\xi),\phi_k\right\rangle_{L^2(\mathcal{S})}\phi_k\right\|_{L^2(\mathcal{S})}\\&=\left\|\boldsymbol{y}-\Pi_p\boldsymbol{y}\right\|_{L^2(\mathcal{S})}\xrightarrow{p\to\infty}0.\end{aligned}$$

Consequently, $0=\lim_{p\to\infty}\left\|\boldsymbol{x}^{(p)}-\boldsymbol{x}^\star\right\|_{L^2(\mathcal{S})}=\left\|\boldsymbol{x}^{(\infty)}-\boldsymbol{x}^\star\right\|_{L^2(\mathcal{S})}$. □

3.5.1 Non-compact uncertainty sets

We give an informal description about how to deal with non-compactly supported random variables for which Theorem 3.5.1 does not directly apply.
A condition for the spectral convergence rate of the polynomial chaos expansion of a random variable is the existence of moments of any order [51]. An equivalent and very natural assumption is the sufficiently rapid decay of the tails of the PDF, that is,

$$t^l\,\mathrm{P}(|\boldsymbol{x}|>t)<\infty\quad\forall l.$$

For instance, this is satisfied for the Normal distribution and the exponential distribution that

have exponentially decaying tails. For such well-behaved random variables with rapidly decaying tails, we can restrict $\mathcal{S}$ to some compact subset $\tilde{\mathcal{S}} \subseteq \mathcal{S}$ in which case the convergence results from Theorem 3.5.1 applies. By

$$||\boldsymbol{x}||_{L^2_\rho(\mathcal{S})} < \infty \implies ||\boldsymbol{x}||_{L^2_\rho(\tilde{\mathcal{S}})} < \infty,$$

the truncated random variable is L^2-measurable. The truncated density function $\rho(\boldsymbol{\xi})$ is obtained by

$$\tilde{\rho}(\boldsymbol{\xi}) = \begin{cases} \frac{\rho(\boldsymbol{\xi})}{W(\tilde{\mathcal{S}})} & \text{if } \boldsymbol{\xi} \in \tilde{\mathcal{S}} \\ 0 & \text{if } \boldsymbol{\xi} \neq \tilde{\mathcal{S}} \end{cases}$$

where the scaling factor $W(\tilde{\mathcal{S}})$ ensures that $\int_{\tilde{\mathcal{S}}} \tilde{\rho}(\boldsymbol{\xi}) \mathrm{d}\boldsymbol{\xi} = 1$. Using the Gram-Schmidt orthogonalization procedure, the corresponding orthogonal polynomial family can be generated.

4 Fast numerical solution methods

This chapter presents the algorithmic counterpart of the preceding theoretical chapter, containing as a major contribution the adaptive algorithm for the fast solution of the uncertain optimal control problem. As a second algorithmic improvement, we present a fast structure-exploiting derivative generation, published in the article [19].

4.1 Adaptive algorithm

While a high expansion order results in a surrogate problem that is difficult to solve computationally it may be unavoidable to capture the nonlinear effects of the uncertainty propagation and to guarantee valid results. Considering the expansion order p_i for each of the n states $x_i(t;\xi)$ separately, p_i is related to the sensitivity of x_i to the uncertainty. For instance, if $p_i = 0$ then x_i is deterministic and if $p_i = 1$ then x_i is of the same distribution family as ξ. On the contrary, if the propagated density varies a lot from the original density, e.g., is asymmetric with non-negligible tail behavior while the input density is symmetric, then p_i must be sufficiently high. For such problems, the computational resources are usually a limiting factor and a trade-off on the accuracy must often be accepted.

To prevent a blowup in the number of new surrogate states, we make the observation that the nature and the sensitivity of the dependence on the input uncertainty varies among the different states. This idea leads to an adaptive strategy for optimal control problems in which we consider error estimates for each state separately and adapt the expansion order accordingly. In each iteration, the previously found solution is refined until all state expansions have converged.

4.1.1 Algorithm

We denote by $\boldsymbol{p} = (p_0, \ldots, p_{n-1})$ the joint expansion order for all states. The state coefficient corresponding to x_i with expansion order p_i are summarized as $\hat{\boldsymbol{x}}_{\cdot,i}^{(p_i)} = (\hat{x}_{0,i}^{(p_i)}, \ldots, \hat{x}_{M_{p_i}-1,i}^{(p_i)})$. Let p_i and p_i^{old} be the current expansion order and the expansion order of the previous iteration respectively. $\delta_i^{(p_i,p_i^{\text{old}})}$ denotes the error estimate and $\delta_i^{(p_i)} := \delta_i^{(p_i,p_i-1)}$.

The adaptive strategy is based on the following procedure: if the current error estimate is higher than a threshold, then the order p_i is increased, otherwise it is set back to the order of the previous iteration by disregarding the added states. The algorithm terminates if all states have converged to their optimal expansion order. An outline of the adaptive algorithm is given in Algorithm 1.

Algorithm 1 Adaptive polynomial chaos for optimal control

Input: gPC basis $\{\phi_i\}$, max. order $\boldsymbol{p}^{\max}$, threshold ε_{AD}, initial guess $\boldsymbol{u}_{\text{init}}$
solve deterministic OCP
store solution $\boldsymbol{u}^{(0)}$, $\hat{\boldsymbol{x}}^{(0)}$
$\boldsymbol{p}^{\text{old}} \leftarrow \mathbf{0}$, $\boldsymbol{p} \leftarrow \mathbf{1}$
while $\boldsymbol{p} \leqslant \boldsymbol{p}^{\max}$ **do**
  construct gPC-surrogate with coefficients $\hat{\boldsymbol{x}}_{\cdot,i}^{(p_i)}$ for $i = 1, \dots, n$
  solve OCP^p with control guess $\boldsymbol{u}^{(\boldsymbol{p}_{\text{old}})}$
  store solution $\boldsymbol{u}^{(\boldsymbol{p})}$, $\hat{\boldsymbol{x}}^{(\boldsymbol{p})}$
  for $i = 1, \dots, n$ **do**
    if $\delta_i^{(p_i, p_i^{\text{old}})} < \varepsilon_{\text{AD}}$ **then**
      $p_i \leftarrow p_i^{\text{old}}$ {p_i^{old} was optimal, convergence achieved for x_i}
    else
      $p_i^{\text{old}} \leftarrow p_i$
      $p_i \leftarrow p_i + 1$ {p_i not sufficient}
    end if
  end for
  if $\max_i \delta_i^{(p_i, p_i^{\text{old}})} < \varepsilon_{\text{AD}}$ **then**
    return {convergence achieved for all states}
  end if
end while

4.1.2 Error estimates

For the construction of the error estimates, we consider the L^2-error of state x_i, $i = 1, \dots, n$

$$\left\| x_i^{(\infty)}(t;\cdot) - x_i^{(p_i)}(t;\cdot) \right\|_{L^2(\mathcal{S})}^2 = \underbrace{\sum_{k=0}^{M_{p_i}-1} \left| \hat{x}_{k,i}(t) - \hat{x}_{k,i}^{(p_i)}(t) \right|^2}_{(1)} + \underbrace{\sum_{k \geqslant M_{p_i}} \left| \hat{x}_{k,i}(t) \right|^2}_{(2)},$$

consisting of two terms: (1) the difference between the computed M_p coefficients of the surrogate model $\hat{x}_{k,i}^{(p_i)}$ and the unknown optimal coefficients $\hat{x}_{k,i}$ up to that order, plus (2) the infinitesimal higher-order unknown optimal coefficients. By Lemma 3.1.1 we can assume that $x_i \in L_w^2(\Omega)$ for any admissible control $\boldsymbol{u}$, consequently we have (2) $\xrightarrow{p \to \infty}$ 0 . The difference (1) depends on the difference between the optimal control surrogate solutions for different expansion orders and can be expected to vanish if the solution converges as shown in Theorem 3.5.1. An a-posteriori error estimate for each state $i = 0, \dots, n-1$ can be defined accordingly by

$$\left\| x_i^{(p_i)}(t) - x_i^{(q_i)}(t) \right\|_{L^2(\mathcal{S})}^2 = \sum_{k=0}^{M_{q_i}-1} \left| \hat{x}_{k,i}^{(p_i)}(t) - \hat{x}_{k,i}^{(q_i)}(t) \right|^2 + \sum_{k=M_{q_i}}^{M_{p_i}-1} \left| \hat{x}_{k,i}^{(p_i)}(t) \right|^2 \quad \text{for} \quad p_i \geqslant q_i.$$

The definition gives rise to an error estimate $\delta_i^{(p_i, q_i)}$ applicable as refinement criterion for the

adaptive algorithm by setting

$$\delta_i^{(p_i,q_i)} := \left\| \sum_{k=M_{q_i}}^{M_{p_i}-1} \left| \hat{x}_{k,i}^{(p_i)}(t) \right|^2 \right\|_{L^\infty([0,t_f])} \tag{4.1}$$

or by using the scaled version

$$\delta_i^{(p_i,q_i)} := \left\| \frac{1}{\tilde{\sigma}_i^{(p_i)}(t)} \sum_{k=M_{q_i}}^{M_{p_i}-1} \left| \hat{x}_{k,i}^{(p_i)}(t) \right|^2 \right\|_{L^\infty([0,t_f])} . \tag{4.2}$$

For the scaling factor, we can use the standard deviation of $x_i^{(p_i)}$, computed according to Lemma 3.3.2,

$$\sigma_i^{(p_i)}(t) := \left(\sum_{k=1}^{M_{p_i}-1} \left| \hat{x}_{k,i}^{(p_i)}(t) \right|^2 \right)^{1/2}, \tag{4.3}$$

or the following estimate of the standard deviation

$$\tilde{\sigma}_i^{(p_i)}(t) := \left(\sum_{r=1}^{p_i} \sum_{k=M_{r-1}}^{M_r-1} \left| \hat{x}_{k,i}^{(p_i)}(t) \right|^2 \right)^{1/2}$$

that can be implemented without the additional cost of storing the whole sequence $\hat{x}_{0,i}^{(p_i)}, \ldots, \hat{x}_{M_{p_i}-1,i}^{(p_i)}$ in each iteration.

4.2 Fast derivative generation

The surrogate optimal control problem resulting from the polynomial chaos method is transformed into a nonlinear optimization problem by the direct multiple shooting method for optimal control problems as described in Section 1.4. The resulting discretized optimal control problem is typically solved by a Newton-type method, which requires the efficient computation of the first and second derivatives of the objective function and constraints. One of the most costly steps is the computation of the sensitivities, that is, the derivatives of the differential states with respect to the initial values and controls. Here, this is done by solving the variational differential equation as described in Section 1.4.2, which additionally requires the efficient and reliable computation of the model function derivatives

$$\frac{\partial \hat{f}_{k,i}(\hat{\boldsymbol{x}}(t), \boldsymbol{u}(t))}{\partial \hat{x}_{l,j}}, \quad \frac{\partial \hat{f}_{k,i}(\hat{\boldsymbol{x}}(t), \boldsymbol{u}(t))}{\partial u_{l,j}} \quad 0 \leqslant k, l \leqslant M_p - 1,\ 0 \leqslant i, j \leqslant n-1.$$

As in Section 3.3, we use the following notation and ordering for the polynomial chaos coefficients that form the new differential states of the projected optimal control problem:

$$\hat{\boldsymbol{x}} = (\hat{\boldsymbol{x}}_0, \ldots, \hat{\boldsymbol{x}}_{M_p-1}) = (\hat{x}_{0,0}, \ldots, \hat{x}_{0,n-1}, \hat{x}_{1,0}, \ldots, \hat{x}_{1,n-1}, \ldots, \hat{x}_{M_p-1,0}, \ldots, \hat{x}_{M_p-1,n-1}).$$

The derivatives are collected in the $nM_p \times nM_p$ model state Jacobian of the projected system

$$\begin{aligned}\hat{J}_x[t] &= \left(\frac{\partial \hat{f}_{k,i}(\hat{\boldsymbol{x}}(t), \boldsymbol{u}(t))}{\partial \hat{x}_{l,j}}\right)_{0 \leqslant k,l \leqslant M_p-1,\ 0 \leqslant i,j \leqslant n-1} \\ &= \begin{pmatrix} \frac{\partial \hat{f}_{0,0}}{\partial \hat{x}_{0,0}} & \cdots & \frac{\partial \hat{f}_{0,0}}{\partial \hat{x}_{0,n-1}} & \cdots & \frac{\partial \hat{f}_{0,0}}{\partial \hat{x}_{M_p-1,0}} & \cdots & \frac{\partial \hat{f}_{0,0}}{\partial \hat{f}_{M_p-1,n-1}} \\ \vdots & & & \ddots & & & \vdots \\ \frac{\partial f_{M_p-1,n-1}}{\partial \hat{x}_{0,0}} & \cdots & \frac{\partial \hat{f}_{M_p-1,n-1}}{\partial \hat{x}_{n-1,0}} & \cdots & \frac{\partial \hat{f}_{M_p-1,n-1}}{\partial \hat{x}_{M_p-1,0}} & \cdots & \frac{\partial \hat{f}_{M_p-1,n-1}}{\partial \hat{x}_{M_p-1,n-1}} \end{pmatrix}\end{aligned}$$

and in the $nM_p \times n_\mathrm{u}$ model control Jacobian of the projected system

$$\begin{aligned}\hat{J}_u[t] &= \left(\frac{\partial \hat{f}_{k,i}(\hat{\boldsymbol{x}}(t), \boldsymbol{u}(t))}{\partial u_j}\right)_{0 \leqslant k \leqslant M_p-1,\ 0 \leqslant i \leqslant n-1,\ 0 \leqslant j \leqslant n_\mathrm{u}-1} \\ &= \begin{pmatrix} \frac{\partial \hat{f}_{0,0}}{\partial u_0} & \cdots & \frac{\partial \hat{f}_{0,0}}{\partial u_{n_\mathrm{u}-1}} \\ & \vdots & \\ \frac{\partial f_{M_p-1,n-1}}{\partial u_0} & \cdots & \frac{\partial \hat{f}_{M_p-1,n-1}}{\partial_{n_\mathrm{u}-1}} \end{pmatrix}\end{aligned}$$

In order to analyze the computational costs for different techniques for computing the Jacobians of the surrogate model, we make the following specifications: by c we denote the maximum cost to evaluate $f_i,\ i = 0, \ldots, n-1$, i.e.,

$$c := \max_{i=0,\ldots,n-1} \mathrm{cost}(f_i).$$

Consequently, the cost to evaluate f is equal to $\mathrm{cost}(\boldsymbol{f}) = nc$. Finally, the cost of applying the Galerkin projection from Equation (3.12) to $\boldsymbol{f}$ in order to obtain the projected system $\hat{\boldsymbol{f}}$ is

$$\mathrm{cost}(\hat{\boldsymbol{f}}) = M_p N_\mathrm{Q} nc.$$

4.2.1 Computation by finite differences

The standard method for computing $\hat{J}_x[t]$ and $\hat{J}_u[t]$ applies a finite difference approximation to the nominal trajectory $\hat{\boldsymbol{f}}(\hat{\boldsymbol{x}}(t), \boldsymbol{u}(t))$ and a perturbed trajectory as explained in Section 1.4.2

$$\begin{aligned}\frac{\partial \hat{\boldsymbol{f}}}{\partial \hat{x}_{j,l}} = \frac{1}{h}\big(&\hat{\boldsymbol{f}}(\hat{x}_{0,0}(t), \ldots, \hat{x}_{j,l}(t) + h, \ldots, \hat{x}_{M_p-1,n-1}(t), \boldsymbol{u}(t)) \\ &- \hat{\boldsymbol{f}}(\hat{x}_{0,0}(t), \ldots, \hat{x}_{j,l}(t), \ldots, \hat{x}_{M_p-1,n-1}(t), \boldsymbol{u}(t))\big) + O(h).\end{aligned}$$

This approach requires computing at least nM_p perturbed trajectories plus one nominal trajectory which results in costs of order

$$\mathrm{cost}(FD_x) = nM_p \cdot \mathrm{cost}(\hat{\boldsymbol{f}}) \approx M_p^2 N_\mathrm{Q} cn^2$$

for the state Jacobian $\hat{J}_x[t]$ and costs of order

$$\mathrm{cost}(FD_u) = n_\mathrm{u} \cdot \mathrm{cost}(\hat{\boldsymbol{f}}) \approx M_p N_\mathrm{Q} cnn_\mathrm{u}$$

for the control Jacobian $\hat{J}_u[t]$.

4.2.2 Computation by sparse Galerkin projection

Instead of the commonly used finite difference approximation, we can apply a sparse Galerkin projection to obtain the model Jacobians. In the first step, we write down the Jacobians of the original system

$$J_x[t] = \frac{\partial \boldsymbol{f}}{\partial \boldsymbol{x}} \in \mathbb{R}^{n\times n},\ J_u[t] = \frac{\partial \boldsymbol{f}}{\partial \boldsymbol{u}} \in \mathbb{R}^{n\times n_u}.$$

Since n, the size of the original system, is small compared to nM_p, the size of the projected system, the computational cost of computing J_x and J_u is negligible compared to the computational cost of deriving the Jacobians $J_{\hat{x}}$ and $J_{\hat{u}}$ of the projected system. In many cases, the derivatives can easily be written down analytically at modeling stage or, in case of a blackbox system, are returned without additional cost.
In the second step, we apply an orthogonal projection as in the projection equation (3.12) to J_x and J_u and obtain, by making use of the chain rule,

$$\begin{aligned}\frac{\partial \hat{f}_{k,i}}{\partial \hat{x}_{l,j}} &= \frac{\partial}{\partial \hat{x}_{l,j}} \left\langle f_i(\boldsymbol{x}^{(p)}, \boldsymbol{u}, \xi), \boldsymbol{\phi}_k \right\rangle = \left\langle \frac{\partial}{\partial \hat{x}_{l,j}} f_i(\boldsymbol{x}^{(p)}, \boldsymbol{u}, \xi), \boldsymbol{\phi}_k \right\rangle \\ &= \left\langle \frac{\partial f_i(\boldsymbol{x}^{(p)}, \boldsymbol{u}, \xi)}{\partial x_j^{(p)}} \frac{\partial x_j^{(p)}}{\partial \hat{x}_{l,j}}, \boldsymbol{\phi}_k \right\rangle = \left\langle \partial_{x_j} f_i(\boldsymbol{x}^{(p)}, \boldsymbol{u}, \xi) \cdot \boldsymbol{\phi}_l, \boldsymbol{\phi}_k \right\rangle\end{aligned}$$

while for the control Jacobian

$$\frac{\partial \hat{f}_{k,i}}{\partial u_j} = \frac{\partial}{\partial u_j} \left\langle f_i(\boldsymbol{x}^{(p)}, \boldsymbol{u}, \xi), \boldsymbol{\phi}_k \right\rangle_{L^2(\mathcal{S})} = \left\langle \frac{\partial}{\partial u_j} f_i(\boldsymbol{x}^{(p)}, \boldsymbol{u}, \xi), \boldsymbol{\phi}_k \right\rangle_{L^2(\mathcal{S})}.$$

Compared to the finite difference approximation, this approach does not suffer from truncation error. Additionally, it opens the possibility to exploit the sparsity present in $J_x = \frac{\partial \boldsymbol{f}}{\partial \boldsymbol{x}}$ and $J_u = \frac{\partial \boldsymbol{f}}{\partial \boldsymbol{u}}$ since any zero element remains zero after projection, e.g., here for the state derivatives:

$$\frac{\partial f_i}{\partial x_j} = 0 \Longrightarrow \frac{\partial \hat{f}_{k,i}}{\partial \hat{x}_{l,j}} = 0 \ \text{ for } \ 0 \leqslant k, l \leqslant M_p - 1.$$

This can reduce the number of necessary function evaluations and projection operations by at least a factor S_x and S_u proportional to the inverse of the fraction of nonzero elements in J_x and J_u, respectively. Here, the sparsity factors S_x and S_u are defined as follows

$$\begin{aligned}S_x &:= \frac{n^2}{\sum_{i=0}^{n-1} \operatorname{card}\left\{0 \leqslant j \leqslant n-1 \mid \frac{\partial f_i}{\partial x_j} \neq 0\right\}} = \frac{n^2}{\sum_{i=0}^{n-1} n_x^i} \\ &\leqslant \frac{n^2 M_p^2}{\sum_{k=0}^{M_p-1} \sum_{i=0}^{n-1} \operatorname{card}\left\{(l,j) \mid 0 \leqslant l \leqslant M_p - 1, 0 \leqslant j \leqslant n-1,\ \frac{\partial \hat{f}_{k,i}}{\partial \hat{x}_{l,j}} \neq 0\right\}} =: \hat{S}_x,\end{aligned} \tag{4.4}$$

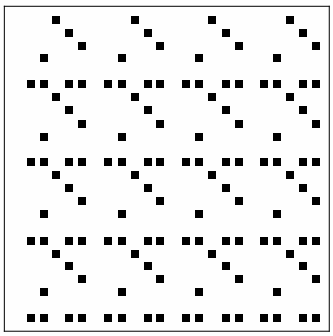

Figure 4.1: Sparsity pattern of $\hat{J}_x$ for container crane problem ($S_x = 4.2,\ M_p = 4$).

whereas n_x^i denotes the number of nonzero entries of the state gradient of f_i, and in the case of the control Jacobian,

$$S_u := \frac{n \cdot n_u}{\sum_{i=0}^{n-1} \operatorname{card}\left\{0 \leqslant j \leqslant n-1 \mid \frac{\partial f_i}{\partial u_j} \neq 0\right\}} = \frac{n \cdot n_u}{\sum_{i=0}^{n-1} n_u^i}$$
$$\leqslant \frac{nM_p \cdot n_u}{\sum_{k=0}^{M_p-1} \sum_{i=0}^{n-1} \operatorname{card}\left\{0 \leqslant j \leqslant n_\mathrm{u}-1 \mid \frac{\partial \hat{f}_i}{\partial u_j} \neq 0\right\}} =: \hat{S}_u,$$

whereas n_u^i denotes the number of the nonzero entries of the control gradient of f_i. Figure 4.1 shows an example of the sparsity pattern of the projected Jacobian $J_{\hat{x}}$.

Consequently, instead of the full Jacobians, only the reduced sparse Jacobians J_x^{spa} and J_u^{spa} with information about the sparsity structure are required to be stored and projected. The full procedure is given in Algorithm 2.

Algorithm 2 Sparse derivative projection

Input: gPC quadrature grid $\left\{(\xi^{(m)}, \rho^{(m)})\right\}_{m=1}^{N_\mathrm{Q}}$, sparse Jacobian J_x^{spa}, J_u^{spa}

evaluate sparse Jacobian J_x^{spa} and J_u^{spa} at $(\boldsymbol{x}(t, \xi^{(m)}), \boldsymbol{u}(t))$ for $m = 1, \ldots, N_\mathrm{Q}$
for $k = 0, \ldots, M_p - 1$ **do**
  for $l = 0, \ldots, M_p - 1$ **do**
    project J_x^{spa} on $\phi_l \phi_k \to \hat{J}_x^{\mathrm{spa}}$
  end for
  project J_u^{spa} on $\phi_k \to \hat{J}_u^{\mathrm{spa}}$
end for

With the notation from Section 4.4, the total computational effort of this method is of order

$$\operatorname{cost}(DP_x) = M_p^2 N_\mathrm{Q} \operatorname{cost}(J_x^{\mathrm{spa}}) = M_p^2 N_\mathrm{Q} c \sum_{i=0}^{n-1} n_x^i$$

for the state Jacobian and costs of order

$$\text{cost}(DP_u) = M_p N_Q \text{cost}(J_u^{\text{spa}}) = M_p N_Q c \sum_{i=0}^{n-1} n_u^i$$

for the control Jacobian. Therefore, the savings resulting from using the sparse projection approach compared to the finite difference approach is proportional to

$$\frac{\text{cost}(DP_x) - \text{cost}(FD_x)}{\text{cost}(DP_x)} \approx 1 - S_x^{-1} \quad \text{and} \quad \frac{\text{cost}(DP_u) - \text{cost}(FD_u)}{\text{cost}(DP_u)} \approx 1 - S_u^{-1}.$$

5 A new approach to chance constrained optimal control

We first introduce the polynomial chaos approach to reachable set propagation and show how to implement it into direct methods for optimal control problems. Thereafter, we show how to apply the developed techniques to the reformulation of chance constraints in the considered problem class. All results of this chapters are published in the article [18].

5.1 The polynomial chaos approach to reachable set propagation

We start with a description of the reachability problem considered in this chapter and explain how it can be approximated with the help of the polynomial chaos surrogate.

5.1.1 Conditional reachable sets

Given $\mathcal{S} \subseteq \mathbb{R}^d$, the finite or infinite support of ξ, we call the set $\mathcal{U}_\delta \subseteq \mathcal{S}$ the initial uncertainty set. We make the following assumption.

Assumption 5.1 *$\mathcal{U}_\delta \subseteq \mathbb{R}^d$ is compact.*

The compactness assumption covers our main application, the reformulation of chance constraints. In particular, it includes all infinitely supported probability distributions with finite variance as long as the constraint satisfaction level is smaller than 1 while for finite supported distributions the required satisfaction level may be equal to 1 and consequently include all possible realizations similar to the worst case robustification approach described in Section 2.3.1.

Definition 5.1.1 *The reachable set conditioned on $\mathcal{U}_\delta$ at time point $\tau \in [t_0, t_f]$ for a fixed control trajectory $\boldsymbol{u}(\cdot)$ is given by*

$$\begin{aligned}\mathcal{X}_\delta(\tau;\mathcal{U}_\delta) = \{\boldsymbol{y} \in \mathbb{R}^n \mid \exists\, \boldsymbol{x}(\cdot) \text{ solution of } \dot{\boldsymbol{x}} = f(\boldsymbol{x}(t;\xi), \boldsymbol{u}(t), \xi) \text{ a.e. on } [t_0, \tau] \\ \text{with } \boldsymbol{x}(t_0) = \boldsymbol{x}_0,\ \boldsymbol{x}(\tau) = \boldsymbol{y} \text{ for } \xi \in \mathcal{U}_\delta\}.\end{aligned} \tag{5.1}$$

For ease of notation, we drop the dependence on the control and initial state.
We use the explicit functional mapping of the polynomial chaos method to derive an approximation by solving a subproblem.

Problem 1 *Given $\boldsymbol{x}^{(p)}(t;\xi) = \sum_{k=0}^{M_p-1} \hat{\boldsymbol{x}}_k \phi_k$, we can compute a p-th order approximation of $\mathcal{X}_\delta(\tau;\mathcal{U}_\delta)$ by solving a polynomial optimization problem to find*

$$\mathcal{X}_\delta{}^{(p)}(\tau;\mathcal{U}_\delta) = [\min_{\xi\in\mathcal{U}_\delta} \boldsymbol{x}^{(p)}(\tau;\xi),\ \max_{\xi\in\mathcal{U}_\delta} \boldsymbol{x}^{(p)}(\tau;\xi)].$$

Convergence of this estimator with increasing order to the exact term $\mathcal{X}_\delta(\tau;\mathcal{U}_\delta)$ is shown in the following lemma by invoking an additional regularity assumption. The bound on the order m of the Sobolev space follows by ensuring that $\mathfrak{h}(\cdot,\cdot) > 0$ in Theorem 3.2.1 and Theorem 3.2.3.

Lemma 5.1.1 *Assume $\boldsymbol{x} \in H^m(\mathcal{S})$ for $m > \max\left\{\frac{3}{4}, d - \frac{1}{2}\right\}$. Then*

$$\lim_{p\to\infty} \mathcal{X}_\delta^{(p)}(\tau;\mathcal{U}_\delta) = \mathcal{X}_\delta(\tau;\mathcal{U}_\delta).$$

Proof 1. *Define $\boldsymbol{\nu}(\xi) := \sqrt{\rho(\xi)}\boldsymbol{x}(\xi) \in L^2(\mathcal{S})$. By application of the Sobolev embedding theorem, cf. [1, Theorem 4.11], $\boldsymbol{\nu} \in H^k(\mathcal{S})$ implies boundedness of $\boldsymbol{\nu}$ since $L^\infty(\mathcal{S})$ can be continuously embedded into the Sobolev space $H^k(\mathcal{S})$ whenever $k > \frac{d}{2}$ which applies to the chosen m. Consequently, for a domain-dependent constant C_S,*

$$||\boldsymbol{\nu}||_{L^\infty(\mathcal{S})} \leqslant C_S\, ||\boldsymbol{\nu}||_{H^k(\mathcal{S})}$$

assuming $\boldsymbol{\nu} \in H^k(\mathcal{S})$. Now we consider the functions $\mathbf{v}(\xi)$ and $\mathbf{x}(\xi)$ defined as the restrictions of $\boldsymbol{\nu}(\xi)$ and $\boldsymbol{x}(\xi)$, respectively, to $\mathcal{U}_\delta$. It follows that

$$||\mathbf{v}||_{L^\infty(\mathcal{U}_\delta)} \leqslant C_S\, ||\mathbf{v}||_{H^k(\mathcal{U}_\delta)}$$

and, taking into account that

$$C_\rho := \min_{\mathcal{U}_\delta} \rho(\xi) > 0$$

is a constant bounded away from zero, we obtain

$$\max_{\mathcal{U}_\delta} \left|\mathbf{x}(\xi)\right| \leqslant C_\rho^{-1} \max_{\mathcal{U}_\delta} \left|\sqrt{\mathbf{v}(\xi)}\right| \leqslant C_S C_\rho^{-1}\, ||\mathbf{v}||_{H^k(\mathcal{U}_\delta)} = C_S C_\rho^{-1}\, ||\mathbf{x}||_{H^k_\rho(\mathcal{U}_\delta)}\,.$$

2. *Define similarly $\mathbf{x}^{(\mathbf{p})}(\xi)$ to be the restriction of $\boldsymbol{x}^{(p)}(\xi)$ to $\mathcal{U}_\delta$.*

   Uniform convergence follows by applying the previous arguments for the first estimate to obtain

$$\max_{\mathcal{U}_\delta} \left|\mathbf{x} - \mathbf{x}^{(\mathbf{p})}\right| \leqslant C_S C_\rho^{-1} \left|\left|\mathbf{x} - \mathbf{x}^{(\mathbf{p})}\right|\right|_{H^k(\mathcal{U}_\delta)} \leqslant \underbrace{C_S C_\rho^{-1} C_k}_{C}\, p^{-\mathfrak{h}(k,m)}\, ||\mathbf{x}||_{H^m(\mathcal{U}_\delta)}\,,$$

   and by choosing m and $k > \frac{d}{2}$ appropriately such that the function $\mathfrak{h}(\cdot,\cdot)$ in Theorem 3.2.1 and in Theorem 3.2.3 is positive.

3. *Given the uniform convergence of $\mathbf{x}^{(\mathbf{p})}$ and the boundedness of $\mathbf{x}$ and hence $\mathbf{x}^{(\mathbf{p})}$, we can now show convergence of the extreme values. Fix $\varepsilon > 0$. Choose $q \in \mathbb{N}$ such that*

$$\forall \xi \in \mathcal{U}_\delta \quad \forall p \geqslant q: \quad \mathbf{x}(\xi) - \varepsilon < \mathbf{x}^{(\mathbf{p})}(\xi) < \mathbf{x}(\xi) + \varepsilon$$

   It follows that

$$\begin{aligned} \forall \xi \in \mathcal{U}_\delta: \quad \mathbf{x}(\xi) - \varepsilon &\leqslant \max_{\xi\in\mathcal{U}_\delta} \mathbf{x}^{(\mathbf{p})}(\xi) \\ \mathbf{x}^{(\mathbf{p})}(\xi) &\leqslant \max_{\xi\in\mathcal{U}_\delta} \mathbf{x}(\xi) - \varepsilon \end{aligned}$$

   and consequently

$$\begin{aligned} \max_{\xi\in\mathcal{U}_\delta} \mathbf{x}(\xi) - \varepsilon &\leqslant \max_{\xi\in\mathcal{U}_\delta} \mathbf{x}^{(\mathbf{p})}(\xi) \\ \max_{\xi\in\mathcal{U}_\delta} \mathbf{x}^{(\mathbf{p})}(\xi) &\leqslant \max_{\xi\in\mathcal{U}_\delta} \mathbf{x}(\xi) + \varepsilon \end{aligned}$$

resulting in

$$\left| \max_{\xi \in \mathcal{U}_\delta} \mathbf{x}(\xi) - \max_{\xi \in \mathcal{U}_\delta} \mathbf{x}^{(\mathbf{p})}(\xi) \right| \leqslant \varepsilon.$$

The same argument can be applied to the infimum. Thus, $\min_{\xi \in \mathcal{U}_\delta} \mathbf{x}^{(\mathbf{p})}(\tau;\xi)$ *and* $\max_{\xi \in \mathcal{U}_\delta} \mathbf{x}^{(\mathbf{p})}(\tau;\xi)$ *converge to* $\min_{\xi \in \mathcal{U}_\delta} \mathbf{x}(\tau;\xi)$ *and* $\max_{\xi \in \mathcal{U}_\delta} \mathbf{x}(\tau;\xi)$*, respectively.* □

An immediate consequence is that the rate of convergence is determined by

$$|\max_{\xi \in \mathcal{U}_\delta} \boldsymbol{x}(\xi) - \max_{\xi \in \mathcal{U}_\delta} \boldsymbol{x}^{(p)}(\xi)| \leqslant \max_{\xi \in \mathcal{U}_\delta} |\boldsymbol{x}(\xi) - \boldsymbol{x}^{(p)}(\xi)| \leqslant C\, p^{-\mathfrak{h}(d,m)}\, ||\boldsymbol{x}||_{H^m},$$

where $\mathfrak{h}$ is positive and depends on the polynomial basis, e.g., for Hermite polynomials,

$$\mathfrak{h}(d,m) = \frac{1}{2}\left(m - (\frac{d}{2} + \varepsilon)\right)$$

for $\varepsilon > 0$ arbitrary, cf. Theorem 3.2.3.

5.1.2 Solving the polynomial subproblem

In the following, we present two computational approaches for solving Problem1 in order to approximate the reachable set.
For an illustration of the complexity of finding a solution to this polynomial subproblem and a verification of the accuracy of the resulting polynomial chaos surrogate, consider the following example.

Example 5.1.1 *Figure 5.1 (values taken from the uncertain container crane problem described in Section 6.1) illustrates the functional dependence of the state variable* $\boldsymbol{x}(t;\xi)$ *on the uncertain parameter* ξ *over time for a given control policy* $\bar{\boldsymbol{u}}$*. This example shows the common behavior of the dependency becoming more asymmetric as time evolves, starting from linear for early times and evolving to a non-monotone function with multiple extrema giving evidence that the propagated distribution deviates significantly from the initial distribution. For verification, the true functional mapping obtained by computing the solution of the (deterministic) ODE given* $\bar{\boldsymbol{u}}$ *on a grid of* ξ *is included as sampled data points. The data points show almost complete agreement with the PC surrogate trajectories.*

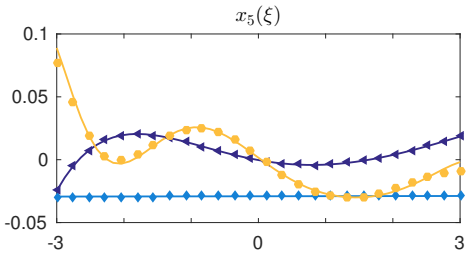

Figure 5.1: 9-th-order PC surrogate $\boldsymbol{x}^{(9)}(\xi)$ visualizing the dependence of the state $\boldsymbol{x}_5(t;\xi)$ on ξ and sampled points of the deterministic ODE on a grid of $\xi \in [-3,3]$ at time $t = 0.44$s (blue diamonds), $t = 5.0$s (dark triangles), $t = t_f = 9$s (light-colored circles).

Method 1: Discretization of the stochastic space

A straightforward approach for solving the polynomial subproblem, easily generalizable for high-dimensional uncertainty, employs a (problem-adapted) discretization of the domain $\mathcal{U}_\delta$ to approximately find the location of the extrema. For the conducted numerical experiments in Section 6.2, we select tensor product grids of Chebyshev nodes with, e.g., $n_j = p^j$ points per dimension. Chebyshev nodes are distributed more densely towards the edges of the domain, where the majority of the global extrema are likely to be located. This behavior is also illustrated in Example 5.1.1 and in partcular Figure 5.1. For the generation of Chebyshev nodes, we have used the Chebfun software package [45]. This approach yields a total of

$$N_P = n_1 \dots n_d \sim p^d$$

points to check, where we assume that the boundaries are included in the chosen point set.
An example of the application to a practical optimal control problem can be found in the numerical section, cf. Remark 6.2.

Method 2: Root search

The second method that we propose builds on a reformulation of the polynomial subproblem as a root search for a multivariate polynomial of degree at most $(p-1)^d$ over a compact set $\mathcal{U}_\delta$:

Problem 2 *Given* $f(\xi) := x^{(p)}(\tau;\xi)$*, find* $\xi^\star = (\xi_1^\star, \dots, \xi_d^\star) \in \mathcal{U}_\delta$ *such that*

$$\mathbf{0} = \nabla f(\xi^\star).$$

To obtain the exact solution, the method needs to identify all local extrema, a maximum of $(p-1)^d$, and compare their values to the ones at the boundary, a maximum of 2^d. The problem of real polynomial root finding can be solved in various ways, e.g., by finding the eigenvalues of the companion matrix in case of a one-dimensional polynomial or with a subdivision algorithm in the general case, e.g. [137].
For the multidimensional case, we use a decomposed Newton method with

$$N_d \sim (p-1)^d$$

subsets. To ensure that each subset contains at most one root and that the Newton method can be applied, we pose the following assumptions.

Assumption 5.2

(i) $H := \nabla^2 f(\xi^\star)$ *is non-singular at* $\xi^\star$.
(ii) $\nabla f(\xi)$ *has bounded derivatives.*

Non-singularity of H in a neighborhood of $\xi^\star$ implies that $\nabla f(\xi)$ has only simple and well-conditioned roots that admit an isolation. Requirement (ii) can be ensured by imposing $x \in H^m(\mathcal{S})$ similarly as in Lemma 5.1.1.
A combined Newton-bisection procedure, outlined in Algorithm 3, with a fixed number of steps to avoid nondifferentiability issues caused by adaptivity is applied to each subset in order to approximate the root. As a safeguarding measure, a bisection step in the direction of the Newton step to the middle of the interval is taken whenever the Newton step falls outside the

Algorithm 3 Multidimensional Newton-Raphson with root-bracketing

Input: functions $\nabla \boldsymbol{f}$, $H := \nabla^2 \boldsymbol{f}$, domain $[\boldsymbol{l}, \boldsymbol{h}] = [l_1, h_1] \times \ldots \times [l_d, h_d] \subseteq \mathbb{R}^d$
fixed number of steps N_{step}
for $j = 1, \ldots, d$ **do**
  if $\nabla \boldsymbol{f}(l_j) > \boldsymbol{0} > \nabla \boldsymbol{f}(h_j)$ **then**
    exchange l_j, h_j
  end if
end for
set starting point $\xi^{(0)} \leftarrow \frac{1}{2}(\boldsymbol{l} + \boldsymbol{h})$
evaluate $\nabla \boldsymbol{f}^{(0)} = \nabla \boldsymbol{f}(\xi^{(0)})$, $H^{(0)} = H(\xi^{(0)})$
for $k = 1, \ldots, N_{\text{step}}$ **do**
  compute Newton step $\xi^{(k)} \leftarrow \xi^{(k-1)} - \left(H^{(k-1)}\right)^{-1} \nabla \boldsymbol{f}^{(k-1)}$
  $i = \text{argmin}_{j=1,\ldots,d} \left\{ (h_j - \xi_j^{(k)})(\xi_j^{(k)} - l_j) \right\}$
  if $(h_i - \xi_i^{(k)})(\xi_i^{(k)} - l_i) < 0$ **then**
    compute bisection step $\xi_i^B \leftarrow l_i + \frac{1}{2}(h_i - l_i)$
    set step length $\alpha_i = \dfrac{\xi_i^B - \xi_i^{(k-1)}}{\xi_i^{(k)} - \xi_i^{(k-1)}}$
    compute modified Newton step $\xi^{(k)} \leftarrow \xi^{(k-1)} - \alpha_i \left(H^{(k-1)}\right)^{-1} \nabla \boldsymbol{f}^{(k-1)}$
  end if
  evaluate $\nabla \boldsymbol{f}^{(k)} = \nabla \boldsymbol{f}(\xi^{(k)})$, $H^{(k)} = H(\xi^{(k)})$
  for $j = 1, \ldots, d$ **do**
    if $\nabla \boldsymbol{f}^{(k)}(l_j) < \boldsymbol{0}$ **then**
      $l_j \leftarrow \xi_j^{(k)}$
    else
      $h_j \leftarrow \xi_j^{(k)}$
    end if
  end for
end for

subset in at least one dimension. Further remarks related to numerical experiments can be found in Remark 6.1.
The computational cost for one run of Algorithm 3 for one-dimensional problems is moderate given the fixed number of iterations, e.g. $N_{\text{step}} = 10$, and the fast polynomial function evaluation. The significant factor for multidimensional systems is the effort to obtain $H^{-1}(\xi)$. Additionally to the obtained root in each of the N_d subsets, we need to check the boundaries, thus resulting in

$$N_P = N_d + N_d 2^d \sim p^d$$

points to check.

Summary of computational cost of the chance constraint evaluation

In summary, the computational costs of both methods as well as the number N_P of points to check is polynomial in p and exponential in d. Both methods can be considered as improved sampling methods, leading to $N_P \sim p^d$ simple linear constraints per original uncertain constraint. The subproblem solution becomes part of the evaluation of the robustified constraint. Solving the surrogate optimal control problem, e.g. by the direct multiple shooting method, requires that first and possibly second order derivatives are well-defined and computable. Under standard nondegeneracy assumptions, per discretization node at most one of the newly introduced constraints is active near the solution. Thus, the additional computational effort is restricted to evaluating the constraint residuals, which are provided analytically as polynomials using the PC-surrogate, but does not usually involve computing more than one active constraint per node.

5.2 Chance constraint reformulation

In this section, we show how to use the reachable sets conditioned on an initial set $\mathcal{U}_\delta$ to reformulate chance constraints with a guaranteed satisfaction level.
Given a maximum allowable violation rate $\delta > 0$ and the multivariate constraint function $\boldsymbol{c} : \mathbb{R}^n \times \mathbb{R}^{n_u} \times \mathbb{R}^d \to \mathbb{R}^{n_c}$, a probabilistic formulation of the constraints $\boldsymbol{c}(\boldsymbol{x}(t;\xi), \boldsymbol{u}(t), \xi) \leqslant 0$ is given by

$$\mathrm{P}\left(\boldsymbol{c}(\boldsymbol{x}(t;\xi), \boldsymbol{u}(t), \xi) \leqslant \boldsymbol{0}\right) \geqslant 1 - \delta.$$

In other words, the joint failure probability

$$\mathrm{P}\left(\boldsymbol{c}(\boldsymbol{x}(t;\xi), \boldsymbol{u}(t), \xi) > \boldsymbol{0}\right)$$

of the constraints

$$c_0(\boldsymbol{x}(t;\xi), \boldsymbol{u}(t), \xi) \leqslant 0, \ldots, c_{n_c-1}(\boldsymbol{x}(t;\xi), \boldsymbol{u}(t), \xi) \leqslant 0$$

must not exceed the maximum allowable failure level δ.
Individual chance constraints

$$\mathrm{P}\left(c_j(\boldsymbol{x}(t;\xi), \boldsymbol{u}(t), \xi) \leqslant 0\right) \geqslant 1 - \delta_j \text{ for } j = 0, \ldots, n_c - 1, \tag{5.2}$$

allow for a violation of each constraint of at most δ_j. Since they involve only one-dimensional

integration, they are easier to compute.
Comparing both formulations, joint chance constraints lead to a performance guarantee for the whole problem while individual chance constraints pose bounds for each constraint separately. A sufficient, although over-conservative, condition for ensuring feasibility of individual chance constraints in the joint chance constrained problem is to enforce the sum of individual violation probabilities to be less than the total violation probability. This is a consequence of Bonferroni's inequality [47, p. 31]:

$$\begin{aligned}&\mathrm{P}\big(c_0(\boldsymbol{x}(t;\xi),\boldsymbol{u}(t),\xi)>0,\dots,c_{n_\mathrm{c}-1}(\boldsymbol{x}(t;\xi),\boldsymbol{u}(t),\xi)>0\big)\\&=\mathrm{P}\left(\bigcap_{j=0}^{n_\mathrm{c}-1} c_j(\boldsymbol{x}(t;\xi),\boldsymbol{u}(t),\xi)>0\right)\leqslant\sum_{j=0}^{n_\mathrm{c}-1}\mathrm{P}\big(c_j(\boldsymbol{x}(t;\xi),\boldsymbol{u}(t),\xi)>0\big)\leqslant\sum_{j=0}^{n_\mathrm{c}-1}\delta_j\leqslant\delta.\end{aligned}$$

W.l.o.g., we consider the chance constraint $\boldsymbol{c}:\mathbb{R}^n\to\mathbb{R}^{n_\mathrm{c}}$ for an arbitrary but fixed $t\in[t_0,t_\mathrm{f}]$ and arbitrary but fixed admissible control function $\boldsymbol{u}(t)$. Using the polynomial chaos approximation of the state variables, we can express the dependence of $\boldsymbol{c}$ on ξ explicitly by a multivariate function $\boldsymbol{h}:\mathbb{R}^d\to\mathbb{R}^{n_\mathrm{c}}$ defined for an arbitrary but fixed $t\in[t_0,t_\mathrm{f}]$ as

$$\boldsymbol{h}(\xi)=\boldsymbol{c}(\boldsymbol{x}^p(t;\xi),\boldsymbol{u}(t)).$$

Depending on the structure of $\boldsymbol{c}$, the root-finding problem might involve a polynomial of higher degree than the expansion order p or even a non-polynomial multivariate function. In the following proposition, which is based on elementary probability and set theory, we derive the reformulation of chance constraints using reachable sets.

Lemma 5.2.1 *Let $\boldsymbol{h}:\mathbb{R}^d\to\mathbb{R}^{n_\mathrm{c}}$ be a measurable transformation and $\mathcal{U}_\delta\subseteq\mathbb{R}^d$ such that*

$$\mathrm{P}\big(\xi\in\mathcal{U}_\delta\big)\geqslant 1-\delta$$

for a given $\delta>0$. Denote the image set of $\mathcal{U}_\delta$ under $\boldsymbol{h}$ by $\mathcal{X}_\delta=\boldsymbol{h}(\mathcal{U}_\delta)\subseteq\mathbb{R}^{n_\mathrm{c}}$. Then

$$\mathrm{P}\big(\boldsymbol{h}(\xi)\in\mathcal{C}\big)\geqslant 1-\delta$$

whenever $\mathcal{X}_\delta\subseteq\mathcal{C}$.

Proof *Denote by*

$$\boldsymbol{h}^{-1}(\mathcal{X}_\delta)=\{\xi\in X\mid\boldsymbol{h}(\xi)\in\mathcal{X}_\delta\}$$

the pre-image of $\mathcal{X}_\delta$ under $\boldsymbol{h}$. By elementary properties of the pre-image,

$$\mathcal{U}_\delta\subseteq\boldsymbol{h}^{-1}(\boldsymbol{h}(\mathcal{U}_\delta)) \tag{5.3}$$

and therefore, by monotonicity,

$$\mathrm{P}\big(\xi\in\mathcal{U}_\delta\big)\leqslant\mathrm{P}\big(\xi\in\boldsymbol{h}^{-1}(\boldsymbol{h}(\mathcal{U}_\delta))\big). \tag{5.4}$$

Then, by a change of variables,

$$1-\delta=\mathrm{P}\big(\xi\in\mathcal{U}_\delta\big)\leqslant\mathrm{P}\big(\xi\in\boldsymbol{h}^{-1}(\boldsymbol{h}(\mathcal{U}_\delta))\big)=\mathrm{P}\big(\boldsymbol{h}(\xi)\in\mathcal{X}_\delta\big)\leqslant\mathrm{P}\big(\boldsymbol{h}(\xi)\in\mathcal{C}\big)$$

assuming $\mathcal{X}_\delta\subseteq\mathcal{C}$. □

Remark 5.1 *(i) Measurability of $\boldsymbol{h}$ is implied by continuity of $\boldsymbol{c}$ and $\boldsymbol{x}$.*

(ii) Equality in Equation (5.3) and (5.4) occurs if $\boldsymbol{h}$ is injective. In general, we get an over-approximation of the chance constraint. The reason is the intentional avoidance of computing the inverse transformation $\boldsymbol{h}^{-1}$, which requires the availability of an expression for $\boldsymbol{x}(t;\xi)$. Assuming the use of the polynomial chaos surrogate for $\boldsymbol{x}(t;\xi)$, this would be equivalent to computing the inverse of a non-monotone, possibly multidimensional, higher-order polynomial. This seems to be a more difficult problem, and without further limiting information, the inverse function can in the best case only be expected to be well approximated locally.

Example 5.2.1 *$\mathrm{P}\big(\boldsymbol{h}(\xi) \in [a,b]\big) \geqslant 1-\delta$ is satisfied if for some set $\mathcal{U}_\delta$ constructed such that $\mathrm{P}\big(\xi \in \mathcal{U}_\delta\big) \geqslant 1-\delta$ it holds that*

$$a \leqslant \min_{\xi \in \mathcal{U}_\delta} \boldsymbol{h}(\xi) \quad \text{and} \quad \max_{\xi \in \mathcal{U}_\delta} \boldsymbol{h}(\xi) \leqslant b.$$

Remark 5.2 (Choice of the uncertainty set $\mathcal{S}$)

(i) $\mathcal{U}_\delta$ is chosen to be a closed set that covers $(1-\delta)\cdot 100\%$ of the population corresponding to the distribution of ξ. Bounds are given by the corresponding (one- or two-sided) quantile of ξ.

(ii) There are different choices leading to the same coverage probability. The resulting ambiguity can be avoided by selecting the smallest such interval $\mathcal{U}_\delta$ or by taking information about the problem structure into account.

Example 5.2.2 *Given Gaussian input distribution with maximum violation rate $\delta = 5\%$, there is an infinite number of possibilities for $\mathcal{U}_\delta$, e.g., $[-1.96, 1.96]$ (left tail 2.5%, right tail 2.5%), $[-2.242, 1.781]$ (left tail 1.25%, right tail 3.75%), $[-2.576, 1.696]$ (left tail 0.5%, right tail 4.5%), of which $\mathcal{U}_\delta = [-1.96, 1.96]$ is the smallest.*

$\mathcal{X}_\delta$ is the propagated reachable set of the function $\boldsymbol{c}(\boldsymbol{x}^p(\xi))$ for $\xi \in \mathcal{U}_\delta$ and covers at least $(1-\delta)\cdot 100\%$ of the population. This means that no matter of how complex the chance constraint is, it can be traced back to the probability that ξ, which follows a well-known distribution, is contained in some intervals $\mathcal{U}_\delta$. For the practical computation, we can use the estimation developed in the previous chapter. Additionally to the convergence proved in Lemma 5.1.1, we prove convergence of the chance constraint approximation by showing convergence in distribution, including the special cases of nonlinear constraint functions $\boldsymbol{c}(\cdot)$, multidimensional uncertainties $d > 1$ and joint chance constraints with > 1 that seek the simultaneous satisfaction of several constraints with one given probability.

Lemma 5.2.2 *For the constraint function $\boldsymbol{c} : \mathbb{R}^n \to \mathbb{R}^{n_c}$, there is a sequence of PC-approximations $\big\{\boldsymbol{c}^{(p)}(\boldsymbol{x}(\xi))\big\}$ with*

$$\mathrm{P}\big(\boldsymbol{c}^{(p)}(\boldsymbol{x}(\xi)) \in \mathcal{C}\big) \xrightarrow{p\to\infty} \mathrm{P}\big(\boldsymbol{c}(\boldsymbol{x}(\xi)) \in \mathcal{C}\big)$$

for arbitrary $\mathcal{C} \subseteq \mathbb{R}^{n_c}$.

Proof *First, note that $\mathcal{C} \subseteq \mathbb{R}^{n_c}$ is a continuity set of $\boldsymbol{c}$ as $\boldsymbol{c}$ and $\boldsymbol{x}$ are continuous. Depending on the dimension of $\boldsymbol{c}$ we consider different cases.*

(i) If $c : \mathbb{R} \to \mathbb{R}$, i.e., c depends only on a one-dimensional variable x, we set

$$c^{(p)} := c(x^{(p)}(\xi)),$$

i.e., the p-th order PC surrogate of $c(x(\xi))$. It is a well-known fact that the mean-square convergence of $x^{(p)}$ implies convergence in probability, which implies convergence in distribution, cf. [48], and this proves the statement. The last two convergence modes extend to all continuous functions c by the continuous mapping theorem, in particular also for nonlinear c, for which mean-square convergence need not hold.

(ii) If $c : \mathbb{R}^{\tilde{n}} \to \mathbb{R}$ with $1 < \tilde{n} \leqslant n$, we can introduce an additional uncertain state variable $y(t, \xi) = c(\boldsymbol{x}(t, \xi))$ into the uncertain optimal control problem defined by the ODE

$$\dot{y}(t) = \frac{\mathrm{d}}{\mathrm{d}t} c(\boldsymbol{x}(t)),\ y(t_0) = c(\boldsymbol{x}(t_0)).$$

Expanding $y^{(p)} = \sum_{i=0}^{M_p} y_i \phi_i(\xi)$ leads to new state variables $y_0(t), \ldots, y_{M_p}(t)$ specified by the ODE

$$\dot{y}_k = \left\langle \dot{y}^{(p)}, \phi_k \right\rangle_{L^2(\mathcal{S})},\ k = 0, \ldots, M_p.$$

Writing

$$c^{(p)}(\boldsymbol{x}(t, \xi)) := y^{(p)}(\boldsymbol{x}(t, \xi))$$

leads to a mean-square convergence for $c^{(p)}$ from which follows

$$\mathrm{P}\left(c^{(p)}(\boldsymbol{x}(\xi)) \in \mathcal{C}\right) \xrightarrow{p \to \infty} \mathrm{P}\left(c(\boldsymbol{x}((\xi)) \in \mathcal{C}\right).$$

(iii) If $\boldsymbol{c} : \mathbb{R}^{\tilde{n}} \to \mathbb{R}^{n_c}$ with $1 < \tilde{n} \leqslant n$ and $n_\mathrm{c} > 1$, we need to show convergence jointly for n_c constraint functions with sets $\mathcal{C}_1, \ldots, \mathcal{C}_{n_\mathrm{c}} \in \mathbb{R}$

$$\mathrm{P}\left(c_1^{(p)}(\boldsymbol{x}(\xi)) \in \mathcal{C}_1, \ldots, c_{n_\mathrm{c}}^{(p)}(\boldsymbol{x}(\xi)) \in \mathcal{C}_{n_\mathrm{c}}\right) \xrightarrow{p \to \infty} \mathrm{P}\left(c_1(\boldsymbol{x}(\xi)) \in \mathcal{C}_1, \ldots, c_{n_\mathrm{c}}(\boldsymbol{x}(\xi)) \in \mathcal{C}_{n_\mathrm{c}}\right).$$

By using the same arguments as in case (ii) for nonlinear c_j and otherwise setting

$$c_j^{(p)}(\boldsymbol{x}(\xi)) := c_j(\boldsymbol{x}^{(p)}(\xi)),$$

we may assume that

$$c_j^{(p)}(\boldsymbol{x}(\xi)) \xrightarrow{p \to \infty} c_j(\boldsymbol{x}(\xi))$$

in $L^2(\mathcal{S})$ for $j = 1, \ldots, n_\mathrm{c}$.

The events $\{c_j^{(p)}(\boldsymbol{x}(\xi)) \in \mathcal{C}_j\}$, similarly as $\left\{c_j(\boldsymbol{x}(\xi)) \in \mathcal{C}_j\right\}$, are generally not mutually independent. A necessary and sufficient condition for weak convergence in the joint distribution is that each linear combination of constraint functions converges to the corresponding limiting linear combination, cf. [48, Theorem 5.1.8]. To this end, we have to show that for all

constants $\forall \boldsymbol{\alpha} \in \mathbb{R}^{n_c}$

$$\alpha_1 c_1^{(p)} + \ldots + \alpha_{n_c} c_{n_c}^{(p)} \xrightarrow{p\to\infty} \alpha_1 c_1 + \ldots + \alpha_{n_c} c_{n_c} \quad \textit{in distribution.}$$

This simply follows from the fact that L^2*-convergence of the polynomial chaos expansion is preserved under linear combination.* □

Thus, for joint chance constraints

$$\mathrm{P}\left(c_1(\boldsymbol{x}(\xi)) \in \mathcal{C}_1, \ldots, c_{n_c}(\boldsymbol{x}(\xi)) \in \mathcal{C}_{n_c}\right) \geqslant 1-\delta,$$

we require the constraints

$$h_j(\mathcal{U}_\delta) = c_j(\boldsymbol{x}(\xi)) \subseteq \mathcal{C}_j$$

to hold over the same set $\mathcal{U}_\delta$ for $1 \leqslant j \leqslant n_c$.

Remark 5.3 (Multidimensional uncertainty)
Under the independence assumption of the polynomial chaos method, cf. Remark 3.1, the bounds of a multidimensional uncertainty set $\mathcal{U}_\delta = I_1 \times \ldots \times I_d$ *can be selected by*

$$\begin{aligned}\mathrm{P}\left(\xi \in \mathcal{U}_\delta\right) &= \int_{I_1} \ldots \int_{I_d} \rho_\xi(\xi_1, \ldots, \xi_d)\, \mathrm{d}\xi_1 \ldots \mathrm{d}\xi_d \\ &= \prod_{i=1,\ldots,d} \int_{I_i} p_{\xi_i}(\xi_i)\, \mathrm{d}\xi_i = \prod_{i=1,\ldots,d} \mathrm{P}(\xi_i \in I_i).\end{aligned}$$

The polynomial subproblem now involves the one- or multi-variate function $\mathbf{c}$ *with* d *variables over a* d*-dimensional interval. From a practical viewpoint, we can select the* I_i *to be sets that satisfy*

$$\mathrm{P}(\xi_i \in I_i) \geqslant (1-\delta)^{\frac{1}{d}} \textit{ for } i = 1, \ldots, d$$

to obtain $\mathrm{P}\left(\xi \in \mathcal{U}_\delta\right) \geqslant 1-\delta$*. This illustrates how the conservatism resulting from the over-approximation of chance constraints, cf. Remark 5.1, is often increased for higher-order uncertainty.*

6 Numerical results

We analyze the performance of the methods developed in the previous chapters using two nonlinear optimal control benchmark problems that are inspired by real-world processes. Additionally, the last part of this chapter contains an industrial application, a challenging nonlinear optimal control problem modeling an adsorption refrigeration system – which for the first time is considered under uncertainty.

The resulting polynomial chaos surrogate problems are solved with the direct multiple shooting method for optimal control [27] described in Section 1.4 using the software package MUSCOD-II [71]. The standard accuracy ε_{KKT} for the solution of the discretized optimal control problems is computed in form of the KKT-tolerance, as described at the end of Section 1.4.1.

The performance of the adaptive algorithm described in Section 4.1 is measured in terms of the total run time required to find a solution of the surrogate problem with an expansion order that is sufficient to capture the nonlinear uncertainty propagation. It is compared to the standard approach of solving the surrogate problem with an a-priori defined order. In addition to the full adaptive algorithm, we assess the use of the "optimal" expansion order returned by the adaptive algorithm to solve the problem in a single run. This may be useful for repeated solution, e.g., in a feedback loop. Both benchmark problems show a significant performance gain without loss of accuracy, which can be attributed to the smaller problem sizes and the iterative search procedure for the full adaptive algorithm.
The sparse Jacobian projection for the fast derivative generation developed in Section 4.2 is compared to the standard method implementing finite differences. For both benchmark problems, the performance speed-up agrees with the theoretically predicted gain proportional to the sparsity factors of 2.8 and 4.2.
In the robustification studies, we illustrate the tradeoff between low cost objective, chance constraint satisfaction and variance minimization. The main intention is to demonstrate the suitability of the reachable set computation developed in Chapter 5 for the approximation of chance constraints in nonlinear optimal control problems.

Computing Environment The computational results for the two benchmark optimal control problems have been obtained on a 64–bit *Ubuntu Linux 16.04* system powered by an *Intel Core i7 6700* CPU with 32 GB main memory available.
For the industrial application, a 64–bit *Windows 7* system powered by an *Intel Core i7 4800MQ* CPU with 8 GB main memory available has been used.
In both cases, a single core of the available four physical cores of the CPU has been used.

6.1 Container crane

The following model of the optimal control of a container crane has been developed in [131] and is characterized by a strong nonlinear dynamics.

6.1.1 Control problem

The aim of the container crane problem is to transfer containers from a ship to a cargo truck, specified by a fixed initial and desired final position while minimizing the swing during the transfer operation. The crane is driven by a hoist motor and a trolley drive motor, and the six differential states constitute the trolley position, the hoist cable length, the load swing angle, the trolley velocity, the hoist cable velocity and the load swing velocity.
The optimal control problem with time horizon $t_0 = 0,\ t_\mathrm{f} = 9$ is formulated as follows:
$\forall t \in [t_0, t_\mathrm{f}]$ a.e.

$$
\begin{aligned}
\min_{\boldsymbol{x},\boldsymbol{u}}\ & \frac{1}{2}\int_{t_0}^{t_\mathrm{f}} x_2^2(t) + x_5^2(t)\,\mathrm{d}t \quad \text{s.t.} \\
& \dot{x}_0(t) = x_3(t) \\
& \dot{x}_1(t) = x_4(t) \\
& \dot{x}_2(t) = x_5(t) \\
& \dot{x}_3(t) = u_0(t) + 1.76 \cdot 9.81\ \beta\ x_2(t) \\
& \dot{x}_4(t) = u_1(t) \\
& \dot{x}_5(t) = -\frac{u_0 + (1.0 + 1.76\ \alpha)9.81\ x_2(t) + 2\ \beta\ x_4(t) x_5(t)}{x_1(t)} \\
& \boldsymbol{x}(t_0) = (0, 22, 0, 0, -1, 0) \\
& |x_3(t)| \leqslant 2.5 \\
& \left|x_4(t)\right| \leqslant 1.0 \\
& |x_5(t)| \leqslant 0.035 \\
& |u_0(t)| \leqslant 2.83374 \\
-0.80865 & \leqslant u_1(t) \leqslant 0.71265 \\
& \boldsymbol{x}(t_\mathrm{f}) \in [\boldsymbol{x}_{\min_\mathrm{f}}, \boldsymbol{x}_{\max_\mathrm{f}}]
\end{aligned}
$$

with two parameters α and β with nominal values $\bar{\alpha} = \bar{\beta} = 1$ that model the influence of the uncertainty, e.g., due to fluctuating environmental or operating conditions.
The final state condition is determined by

$$
\begin{aligned}
\boldsymbol{x}_{\min_\mathrm{f}} &= (9.9, 13.9, -0.001, 2.4, -0.001, -0.001) \\
\boldsymbol{x}_{\max_\mathrm{f}} &= (11, 14.1, 0.001, 2.6, 0.001).
\end{aligned}
$$

For a multiple shooting discretization of $N_\mathrm{shoot} = 25$ and a KKT-tolerance of $\varepsilon_\mathrm{KKT} = 10^{-6}$, the computation time is 0.1s resulting in a deterministic optimum value of $4.396 \cdot 10^{-3}$.

6.1.2 Uncertainty analysis

We consider two uncertainty scenarios:

1. $d = 1$: $\alpha \sim \mathcal{N}(1, 0.4)$ (i.e., mean $\mu = 1$, standard deviation $\sigma_{\text{dev}} = 0.4$)
2. $d = 2$: $\alpha \sim \mathcal{N}(1, 0.4)$, $\beta \sim \mathcal{N}(1, 0.1)$

For an illustration of the control trajectories and the state trajectories of the problem under uncertainty and in the deterministic case, we refer to Figures 6.1 and 6.2, respectively. The effects of the uncertainty on the state variables at different time instances can be observed in Figures 6.3 and 6.4 which show the probability density function (PDF) of the states for the test case $d = 1$ and $d = 2$, respectively.

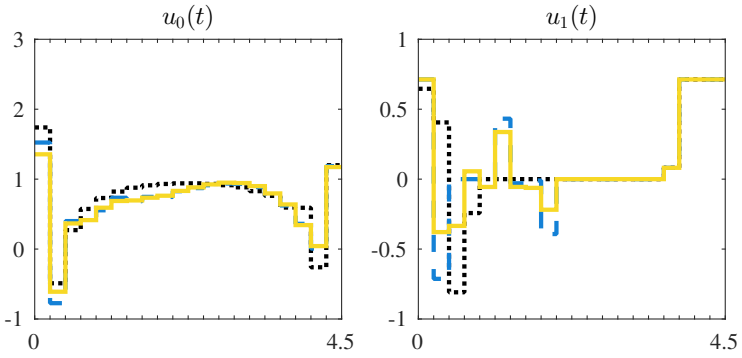

Figure 6.1: Container crane optimal control law. Deterministic, case $d = 1$ and $d = 2$ are plotted as dark dotted, dashed and light-colored solid lines, resp. Termination criterion: $\varepsilon_{\text{KKT}} = 10^{-8}$.

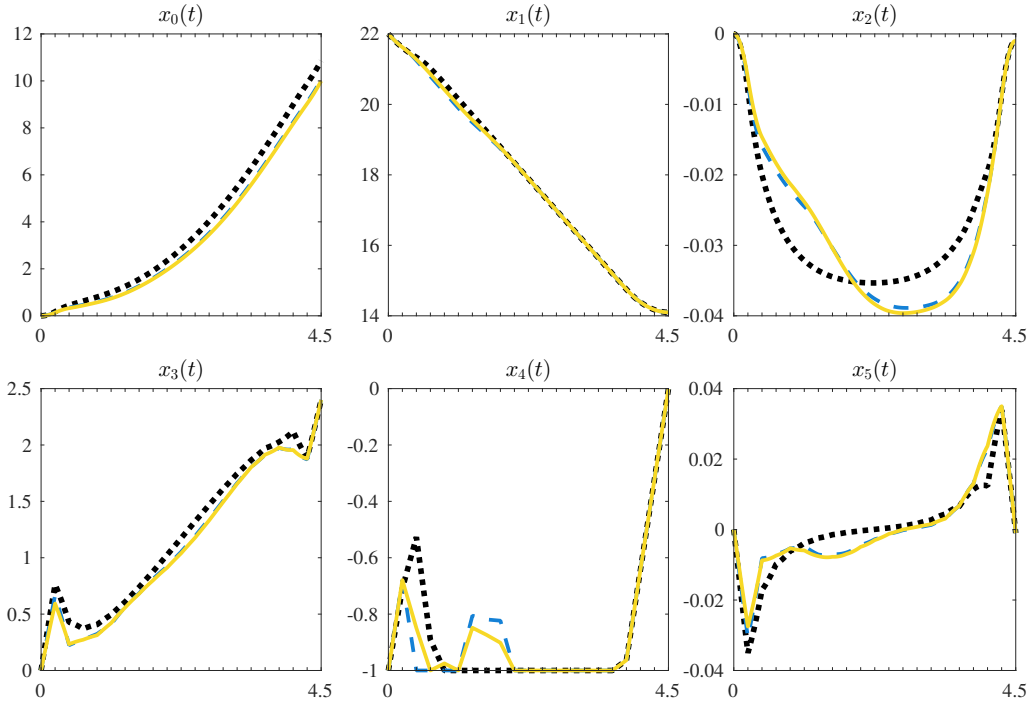

Figure 6.2: Container crane optimal process behavior. Deterministic, case $d = 1$ and $d = 2$ are plotted as dark dotted, dashed and light-colored solid lines, resp. Termination criterion: $\varepsilon_{\text{KKT}} = 10^{-8}$.

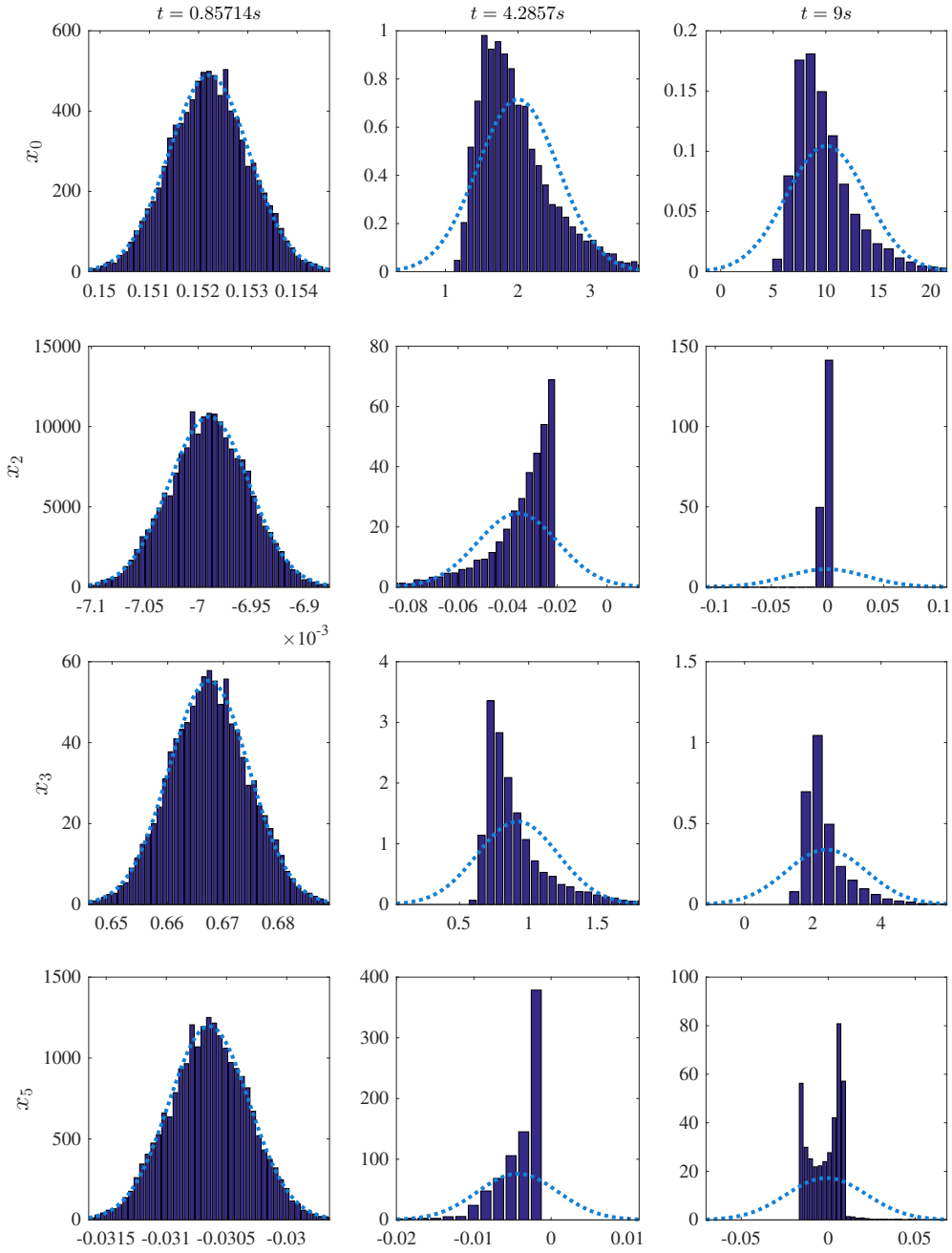

Figure 6.3: Sampled PDF ($N_{\mathrm{MC}} = 10,000$) of container crane problem with $d = 1$ for all states influenced by uncertainty. Dotted light curve depicts Gaussian fit with abscissa ranging over $[-3\sigma_{\mathrm{dev}}, 3\sigma_{\mathrm{dev}}]$. Termination criterion: $\varepsilon_{\mathrm{KKT}} = 10^{-8}$.

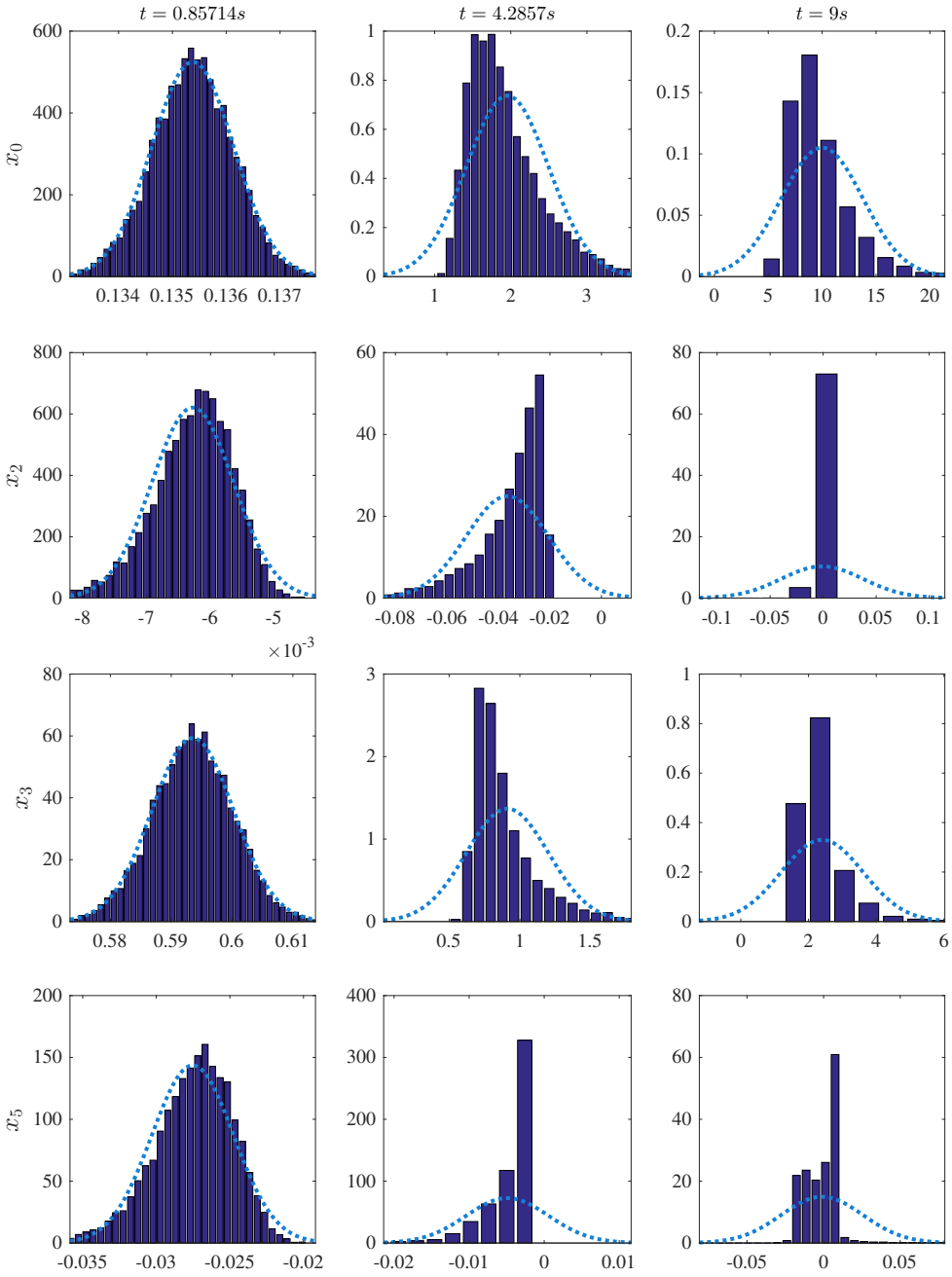

Figure 6.4: Sampled PDF ($N_{\mathrm{MC}} = 10,000$) of container crane problem with $d = 2$ for all states influenced by uncertainty. Dotted light curve depicts Gaussian fit with abscissa ranging over $[-3\sigma_{\mathrm{dev}}, 3\sigma_{\mathrm{dev}}]$. Termination criterion: $\varepsilon_{\mathrm{KKT}} = 10^{-8}$.

6.1.3 Derivative projection

Figures 6.5 and 6.6 illustrate the reduction in run time of the proposed derivative projection compared to the standard method based on a finite difference derivative approximation for the test case $d = 1$ and $d = 2$, respectively. The actual speed-up corresponds well to the savings with sparsity factor $S_x = 4.2$ given by the predicted trajectory $t_{\mathrm{DP}} = \frac{t_{\mathrm{FD}}}{S_x}$. Due to the short solution times in the one-dimensional test case, the computational overhead present in the sparse derivative generation is still visible in Figure 6.5.

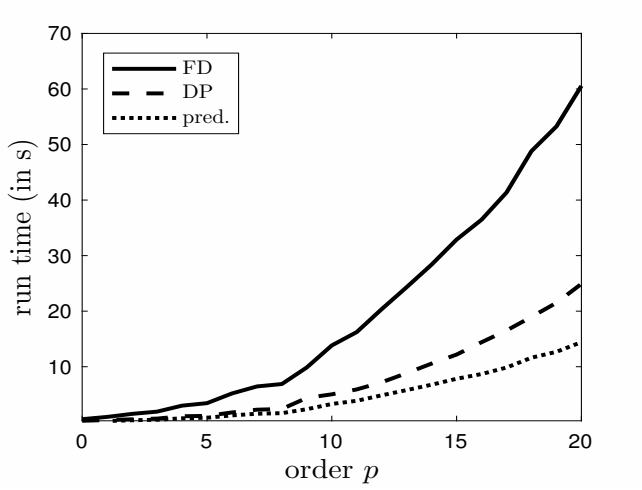

Figure 6.5: Illustration of smaller run times for container crane problem with derivative projection (DP) compared to finite difference derivatives (FD) and predicted trajectory for $d = 1$. Termination criterion: $\varepsilon_{\mathrm{KKT}} = 10^{-6}$.

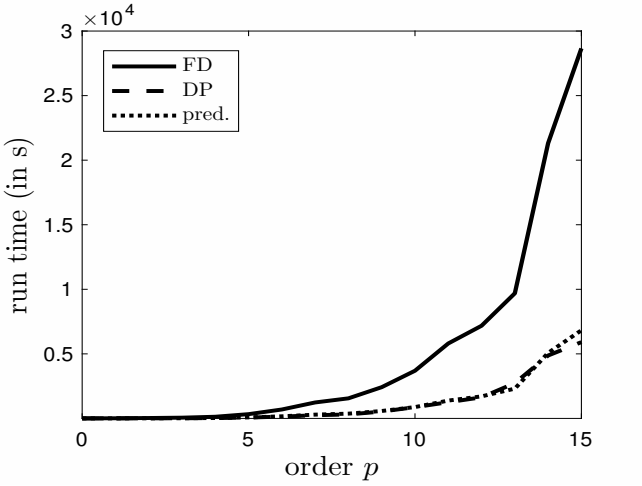

Figure 6.6: Illustration of smaller run times for container crane problem with derivative projection (DP) compared to finite difference derivatives (FD) and predicted trajectory for $d = 2$. Termination criterion: $\varepsilon_{\mathrm{KKT}} = 10^{-6}$.

6.1.4 Adaptive algorithm

We set the adaptive refinement threshold to $\varepsilon_{\text{AD}} = 10^{-6}$. The decay of the error estimates $\delta^{(p)}$ for the adaptive refinement is plotted in Figure 6.7. For the test case $d = 1$, the algorithm terminates after 2.5s with objective value $6.265 \cdot 10^{-3}$ and optimal adaptive order $\boldsymbol{p}^{\text{opt},1} = \{10, 0, 9, 10, 0, 10\}$. For the test case $d = 2$, the overall run time is 5:05min leading to an objective value of $6.455 \cdot 10^{-3}$ and an optimal adaptive order $\boldsymbol{p}^{\text{opt},2} = \{12, 0, 11, 12, 0, 12\}$.
The results of the single run of the surrogate problem with fixed order chosen to be sufficiently high for accurate results and the single run with the optimal orders returned by the adaptive algorithm are compared in Table 6.2. For a better comparison of the standard approach and the proposed adaptive algorithm, we refer to Figure 6.8 for a plot of the run times for different expansion orders.

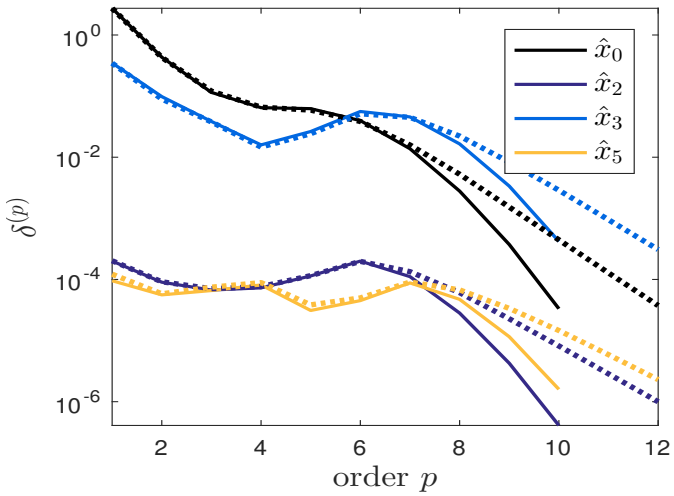

Figure 6.7: Decay of error estimates for uncertain states for container crane problem. Dotted and solid curves correspond to $d = 1$ and $d = 2$, resp. Different colors correspond to different state indices (deterministic states omitted). Termination criterion: $\varepsilon_{\text{KKT}} = 10^{-6}$.

	fixed order	optimal order	adaptive algorithm
p	$\{10, \ldots, 10\}$	$\{10, 0, 9, 10, 0, 10\}$	–
M_p	$\{11, \ldots, 11\}$	$\{11, 1, 10, 11, 1, 11\}$	–
# states	66	45	–
obj. value	$6.263 \cdot 10^{-3}$	$6.263 \cdot 10^{-3}$	$6.265 \cdot 10^{-3}$
run time [s]	5.03	2.51	2.54

Table 6.1: Results container crane for single run with predefined fixed order, single run with optimal adapted order and adaptive algorithm for $d = 1$. Termination criterion: $\varepsilon_{\text{AD}} = \varepsilon_{\text{KKT}} = 10^{-6}$.

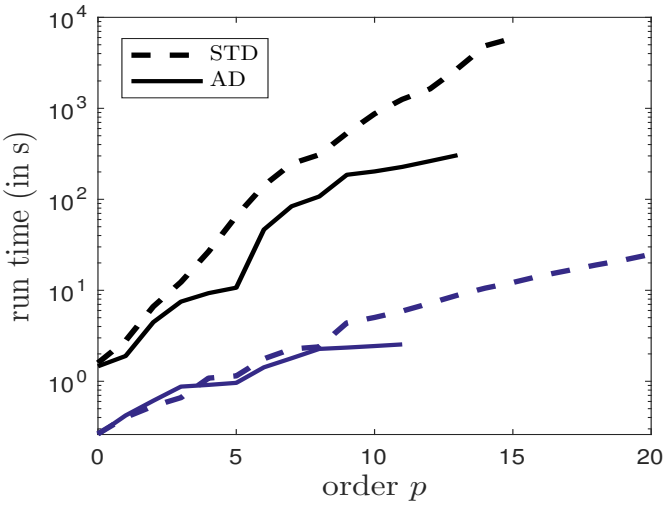

Figure 6.8: Illustration of smaller run times of adaptive algorithm compared to standard method for different polynomial orders for container crane problem. The two lower and two higher curves correspond to $d = 1$ and $d = 2$, resp. Termination criterion: $\varepsilon_{\text{KKT}} = \varepsilon_{\text{AD}} = 10^{-6}$.

	fixed order	optimal order	adaptive algorithm
p	$\{12, \ldots, 12\}$	$\{12, 0, 11, 12, 0, 12\}$	–
M_p	$\{91, \ldots, 91\}$	$\{91, 1, 78, 91, 1, 91\}$	–
# states	546	353	–
obj. value	$6.454 \cdot 10^{-3}$	$6.453 \cdot 10^{-3}$	$6.455 \cdot 10^{-3}$
run time [mm:ss]	27:14	11:51	05:05

Table 6.2: Results container crane for single run with predefined fixed order, single run with optimal adapted order and adaptive algorithm for $d = 2$. Termination criterion: $\varepsilon_{\text{AD}} = \varepsilon_{\text{KKT}} = 10^{-6}$.

6.1.5 Chance constraint reformulation

The effects of the uncertainty on the state variables at different time instances for the one-dimensional uncertainty are illustrated in the probability density function plots in Figure 6.3. As can be observed in the corresponding Figure 6.4 for the two-dimensional uncertainty, this case does not lead to majorly different effects. Thus we restrict the analysis for this example problem to the case $d = 1$ with $\alpha \sim \mathcal{N}(1, 0.4)$. The used polynomial chaos order is $p = 9$, $M_p = 10$.

The state constraint

$$x_5(t, \xi) \in [-0.03, 0.045]$$

on the load swing velocity is to be satisfied in almost all cases and can be formulated in form of a two-sided chance constraint for $t \in [0, t_f]$ with

$$\mathrm{P}\big(x_5(t, \xi) \in [-0.03, 0.045]\big) = \mathrm{P}\big(x_5(t, \xi) \geqslant -0.03,\ x_5(t, \xi) \leqslant 0.045\big) \geqslant 0.95.$$

The other inequality constraints in the problem formulation are formulated for the mean values only.
For the chance constraint computation, we consider the three different approximations:

(i) Mean constraint: $\mathrm{E}\big[x_5(t, \xi)\big] \in [-0.03, 0.045]$

(ii) Two-sided mean-variance approximation/Gaussian fit: constraints

$$\mathrm{E}\big[x_5(t, \xi)\big] - 1.96\sqrt{\mathrm{Var}\big[x_5(t, \xi)\big]} \geqslant -0.03 \text{ and}$$
$$\mathrm{E}\big[x_5(t, \xi)\big] + 1.96\sqrt{\mathrm{Var}\big[x_5(t, \xi)\big]} \leqslant 0.045$$

where $c_{0.025} = 1.96$ corresponds to the two sided 2.5%-quantile of the normal distribution.

(iii) Chance constraint formulation using a 95%-reachable set: constraints

$$-0.03 \leqslant \min_{\xi \in \mathcal{S}} x_5(t, \xi) \text{ and } \max_{\xi \in \mathcal{S}} x_5(t, \xi) \leqslant 0.045$$

where $\mathcal{S} = [-2.576, 2.576]$ is the smallest set with $\mathrm{P}\big(\xi \in \mathcal{S}\big) = 0.95$.

Remark 6.1 *For this example, the chance constraint in (iii) is approximated using Method 1 of Section 5.1.2 on a uniform decomposition of $N_P = p-1$ subsets with a fixed number of $N_{step} = 10$ Newton-bisection steps on each subset. It is verified empirically that these choices are sufficient to identify all roots up to machine accuracy. That is, using adaptivity a lower number of steps would have been selected in all cases. No issues with nondifferentiability from the bisection safeguard were observed.*

Formulation (ii) does not lead to a feasible problem formulation and is therefore omitted in the results. The issue that the normal distribution is not a good approximation can be observed in the in Figure 6.3 depicting an estimation of the true probability density function and the normal distribution fit for all states influences by the uncertainty at different time instances.
Figures 6.9 and 6.10 show the associated control and state trajectories. A Monte Carlo sampling of the state trajectory of interest illustrating the extent of the sampled trajectories for different

uncertainty realizations is depicted in Figure 6.11. Table 6.3 summarizes the results and the dimensions of the surrogate problems after the multiple shooting discretization. The chance constraint reformulation leads to a lower constraint violation rate than the required 5%, which is violated by a large extent for the expected value robustification. In this example, the final variance for the solution with the chance constraint robustification is larger than the final variance of the solution with expected value robustification. The reason is that it interferes with the explicit variance minimization imposed in the objective function

$$\mathrm{E}\left[\frac{1}{2}\int_0^{t_\mathrm{f}} x_2^2(t,\xi)+x_5^2(t,\xi)\,\mathrm{d}t\right]=\frac{1}{2}\int_0^{t_\mathrm{f}}\mathrm{E}\left[x_2^2(t,\xi)\right]+\mathrm{E}\left[x_5^2(t,\xi)\right]\,\mathrm{d}t.$$

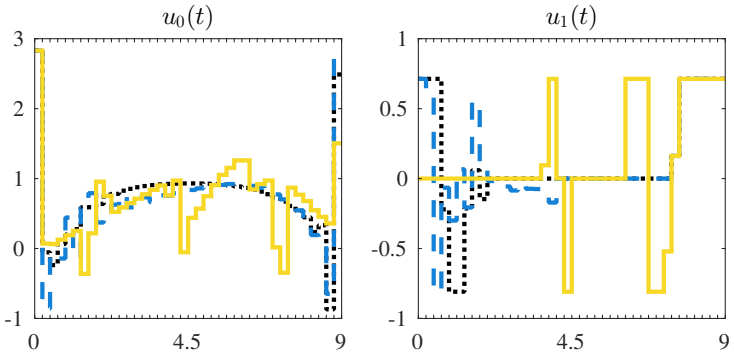

Figure 6.9: Robustified version of container crane optimal control law. Deterministic, mean value bounds (case (i)) and chance constraint robustification (case (iii)) are plotted as dark dotted, dashed and light-colored solid lines, resp.

	det.	(i)	(iii)
objective	$4.31\cdot10^{-3}$	$6.13\cdot10^{-3}$	$7.30\cdot10^{-3}$
final variance $\mathrm{Var}[x_5(t_\mathrm{f})]$	–	$5.0\cdot10^{-4}$	$9.2\cdot10^{-3}$
max. constraint violation [%]	–	50.4	1.0
computation time [ss]	0.8	14.7	11.1
NLP variables	386	2582	2582
equality constraints	280	2440	2440
inequality constraints	$736+12$ $=748$	$5164+12+20\cdot2$ $=5216$	$5164+12+2\cdot10\cdot40$ $=5976$

Table 6.3: Properties of the optimal solutions obtained for the robustified container crane problem. Constraint violations have been computed by $N_\mathrm{MC}=10,000$ samples over $\mathbb{R}$ using the obtained optimal control law. Last section contains the NLP dimensions after the multiple shooting discretization with $N_\mathrm{shoot}=40$.

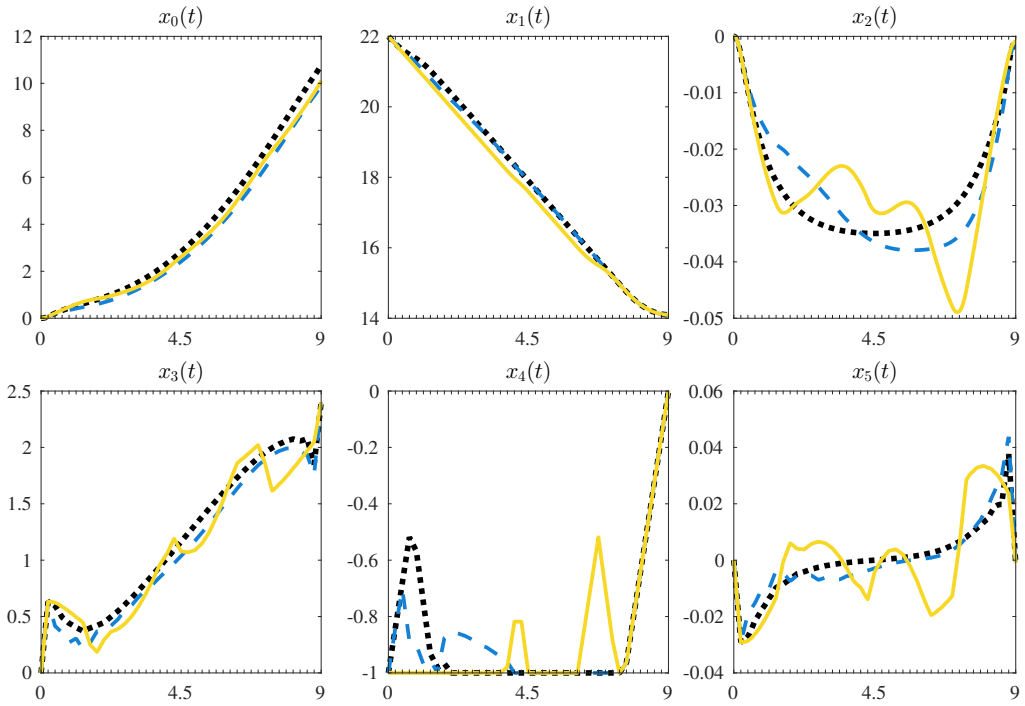

Figure 6.10: Robustified version of container crane optimal process behavior. Deterministic, mean value bounds (case (i)) and chance constraint robustification (case (iii)) are plotted as dark dotted, dashed and light-colored solid lines, resp.

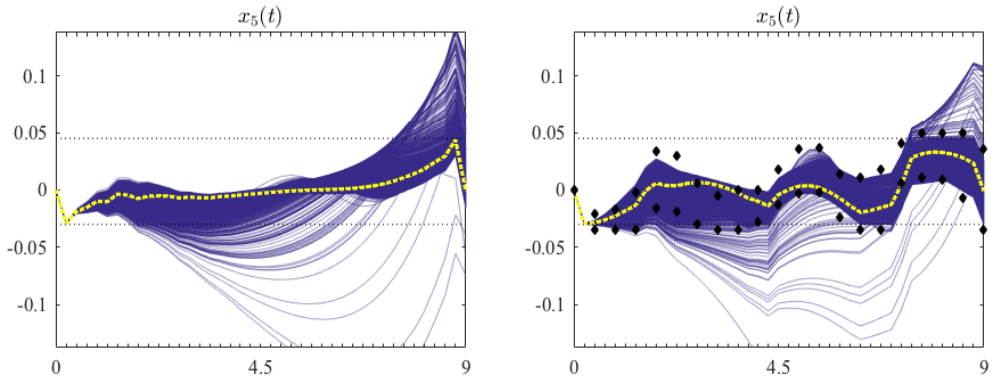

Figure 6.11: Sampled trajectories ($N_{\mathrm{MC}} = 10,000$) of state $x_5(t, \xi)$ of robustified container crane problem given optimal controls for average constraint (i) (left) and chance constraint approximation (iii) (right). The light-colored dotted trajectory is the nominal solution. Triangle-shaped markers illustrate the extreme trajectories for the 95%-quantile (case (iii)).

6.2 Semi-batch fermentation process

The challenge of the second test problem modeling the control of a fermentation process in a semi-batch reactor lies within the larger problem size.

6.2.1 Control problem

The semi-batch fermentation process describes the fermentation of a product P produced by a biomass B in a semi-batch reactor given substrates S_1 and S_2 and a nutrient G. The state variables are composed of the corresponding concentrations, the crop rate, the amount of product generated and the volume balances of the substrate feeds. The control variables are the substrate feed rates and the crop rate. It has been used as a benchmark problem in [18]. The optimal control task is to minimize the accumulated amount of substrates fed, while maximizing the accumulated yield of the product on a normalized time horizon $[t_0, t_f] = [0, 1]$:

$$\min_{\boldsymbol{x},\boldsymbol{u}} \quad \frac{S_1(t_f) + \frac{1}{2}S_2(t_f)}{P(t_f)} \tag{6.1a}$$

$$\text{s.t.} \quad \dot{x}(t) = \boldsymbol{f}(\boldsymbol{x}(t), \boldsymbol{u}(t), \boldsymbol{p}) \qquad t \in [t_0, t_f] \text{ a.e.} \tag{6.1b}$$

$$\boldsymbol{x}(t_0) = \boldsymbol{x}_0 \tag{6.1c}$$

$$\boldsymbol{0} \geqslant \boldsymbol{c}(\boldsymbol{x}(t), \boldsymbol{u}(t)) \qquad t \in [t_0, t_f] \text{ a.e.} \tag{6.1d}$$

$$\tag{6.1e}$$

The process model (6.1b) is as follows:

$$\begin{aligned}
\dot{c}_p(t) &= \mu_p c_B(t) c_{S_1}(t) c_{S_2}(t) - c_p(t)\frac{u_0(t)+u_1(t)}{V(t)},\\
\dot{c}_{S_1}(t) &= 0.42\,\frac{u_0(t)}{V(t)} - c_{S_1}\frac{u_0(t)+u_1(t)}{V(t)}\\
&\quad - 10\cdot 10^4\cdot\, c_B(t) c_{S_1}(t) c_{S_2}(t) c_G(t) - \gamma_{p,S_1}\, c_B(t) c_{S_1}(t) c_{S_2}(t),\\
\dot{c}_{S_2}(t) &= 0.333\,\frac{u_0(t)}{V(t)} - c_{S_1}\frac{u_0(t)+u_1(t)}{V(t)}\\
&\quad - 5000\, c_B(t) c_{S_1}(t) c_{S_2}(t) - \gamma_{p,S_2}\, c_B(t) c_{S_1}(t) c_{S_2}(t) c_G(t),\\
\dot{c}_B(t) &= 20\cdot 10^4\, c_B(t) c_{S_1}(t) c_{S_2}(t) c_G(t) - c_B(t)\frac{u_0(t)+u_1(t)}{V(t)},\\
\dot{c}_G(t) &= -5\cdot 10^4\, c_B(t) c_{S_1}(t) c_{S_2}(t) c_G(t) - c_G(t)\frac{u_0(t)+u_1(t)}{V(t)},\\
\dot{V}(t) &= u_0(t) + u_1(t) - u_2(t),\\
\dot{P}(t) &= u_2(t) c_p + (u_0(t)+u_1(t)-u_2(t)) c_p\\
&\quad + V(t)\left(\mu_p\, c_B(t) c_{S_1}(t) c_{S_2}(t) - c_p(t)\frac{u_0(t)+u_1(t)}{V(t)}\right),\\
\dot{S}_1(t) &= 0.42\, u_0(t),\\
\dot{S}_2(t) &= 0.333\, u_1(t)
\end{aligned}$$

with parameters μ_G, μ_p, γ_{g,S_1}, γ_{g,S_2}, γ_{p,S_1}, γ_{p,S_2}, $\gamma_{g,G}$, $c_{S_1}^{in}$, $c_{S_2}^{in}$ as listed in Table 6.4.
State and control bounds (6.1d) as well as initial values (6.1c) are listed in Table 6.5.

For a multiple shooting discretization of $N_{shoot} = 20$ and a KKT-tolerance of $\varepsilon_{KKT} = 10^{-6}$, the computation time is 0.4s resulting in a deterministic optimum value of 5.208.

Symbol	Description	Nominal value
μ_{G}	Growth rate of B	$20 \cdot 10^4$
μ_{p}	Product generation rate	$5.0 \cdot 10^3$
$\gamma_{\mathrm{g,S_1}}$	Consumption of S_1 due to growth	$10 \cdot 10^4$
$\gamma_{\mathrm{g,S_2}}$	Consumption of S_2 due to growth	$0.5 \cdot 10^4$
$\gamma_{\mathrm{p,S_1}}$	Consumption of S_1 due to production	$2.0 \cdot 10^4$
$\gamma_{\mathrm{p,S_2}}$	Consumption of S_2 due to production	$1.5 \cdot 10^3$
$\gamma_{\mathrm{g,G}}$	Consumption of G due to growth	$5.0 \cdot 10^4$
$c_{\mathrm{S_1}}^{\mathrm{in}}$	Feed concentration of S_1	$4.2 \cdot 10^{-1}$
$c_{\mathrm{S_2}}^{\mathrm{in}}$	Feed concentration of S_2	$3.33 \cdot 10^{-1}$

Table 6.4: Parameters for the fermenter process model.

	c_{p}	$c_{\mathrm{S_1}}$	$c_{\mathrm{S_2}}$	c_{B}	c_{G}	V	p	S_1	S_2	u_0	u_1	u_2
min	0	0	0	0	0	0.3	0	0	0	0	0	0
max	0.1	0.04	0.03	0.1	0.45	0.1	0.05	0.2	0.025	15	1	30
$\boldsymbol{x}(t_0)$	0	0.03	0.03	0.01	0.1	0.3	0	0.009	0.009	-	-	-

Table 6.5: Bounds and initial values of differential states and controls for the fermentation process.

6.2.2 Uncertainty analysis

We consider the two uncertainty scenarios:

1. $d = 2$:

$$\mu_{\mathrm{G}} \sim 10^4 \cdot \mathcal{N}(20, 4),\ \gamma_{\mathrm{g,S_2}} \sim 10^4 \cdot \mathcal{N}(0.5, 1.25)$$

2. $d = 3$:

$$\mu_P \sim \mathcal{N}(5 \cdot 10^3, 400),\ \gamma_{\mathrm{p,S_1}} \sim \mathcal{N}(20 \cdot 10^3, 2 \cdot 10^3),\ \gamma_{\mathrm{p,S_2}} \sim \mathcal{N}(1.5 \cdot 10^3, 300)$$

For an illustration of the control and state trajectories, we refer to Figure 6.12 and Figure 6.13, respectively. The effect of the uncertainty on the state variables at different point in time can be observed in the Figures 6.14 and 6.15, respectively, illustrating the probability desnity functions of the state variables.

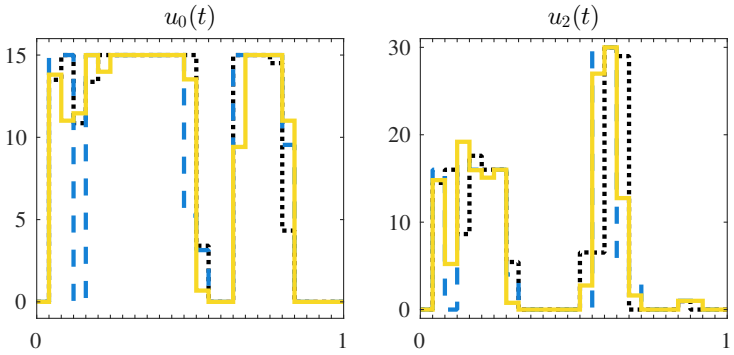

Figure 6.12: Fermentation process optimal control law. Deterministic, case $d = 2$ and $d = 3$ are plotted as dark dotted, dashed and light-colored solid lines, resp. Termination criterion: $\varepsilon_{\text{KKT}} = 10^{-8}$.

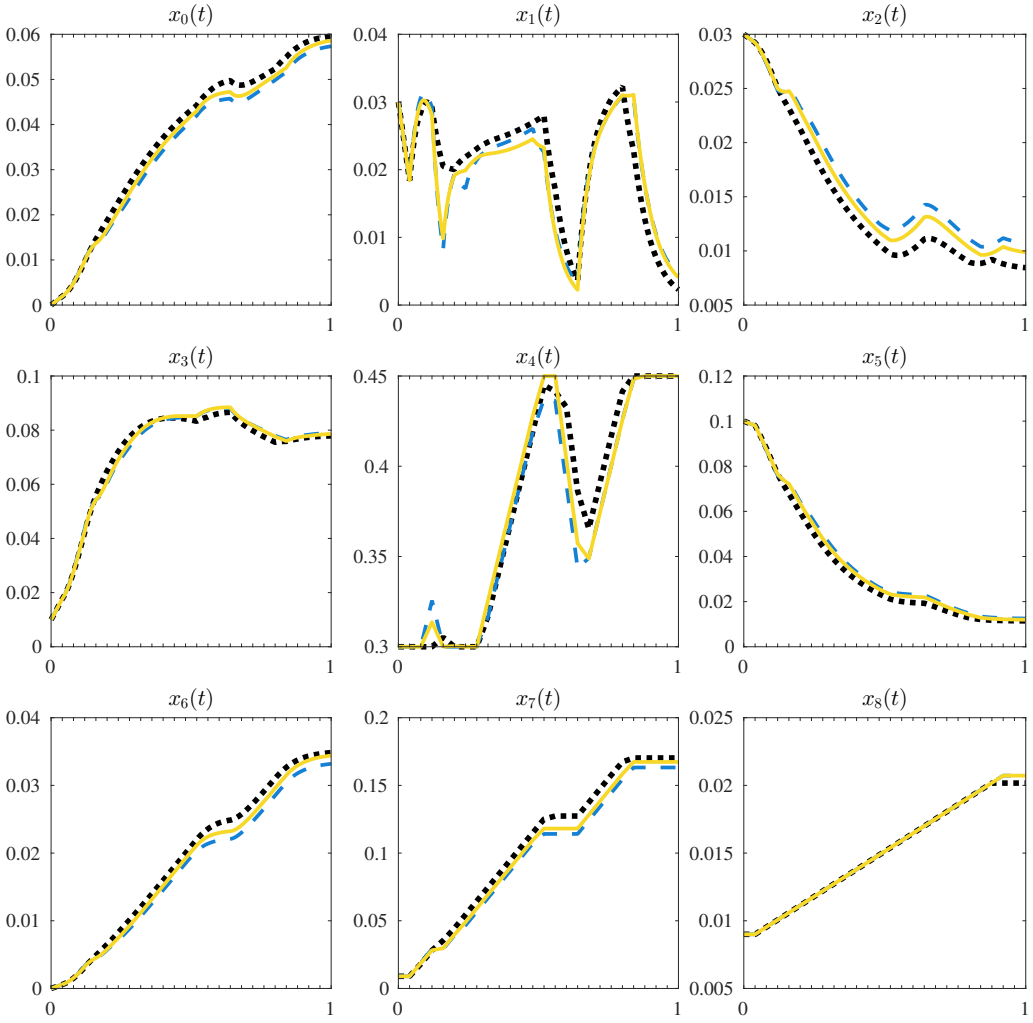

Figure 6.13: Fermentation process optimal process behavior. Deterministic, case $d = 2$ and $d = 3$ are plotted as dark dotted, dashed and light-colored solid lines, resp. Termination criterion: $\varepsilon_{\text{KKT}} = 10^{-8}$.

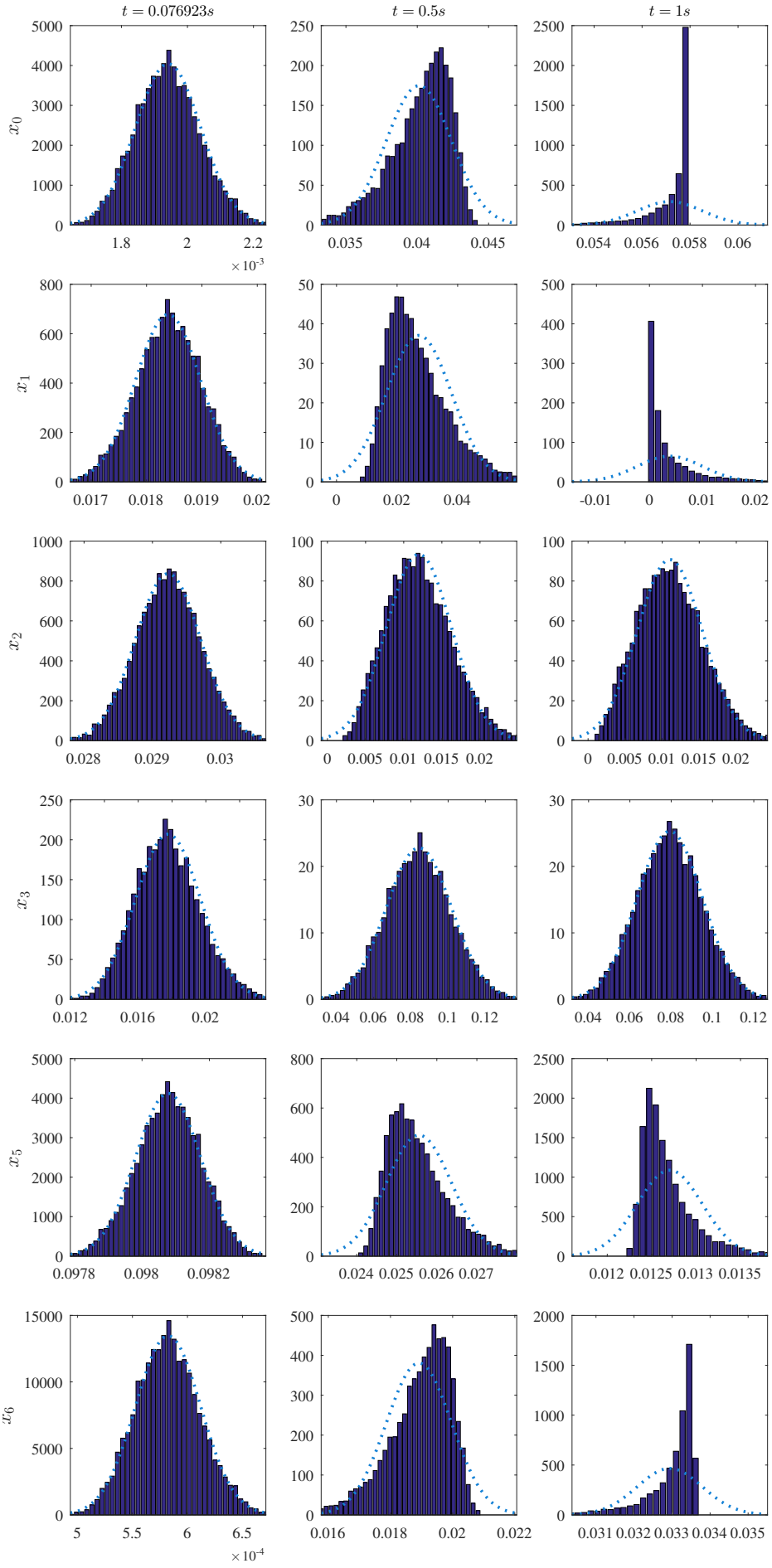

Figure 6.14: Sampled PDF ($d = 2$, $N_{\mathrm{MC}} = 10,000$) of fermentation process for uncertain states. Dotted light curve depicts Gaussian fit over $[-3\sigma_{\mathrm{dev}}, 3\sigma_{\mathrm{dev}}]$.

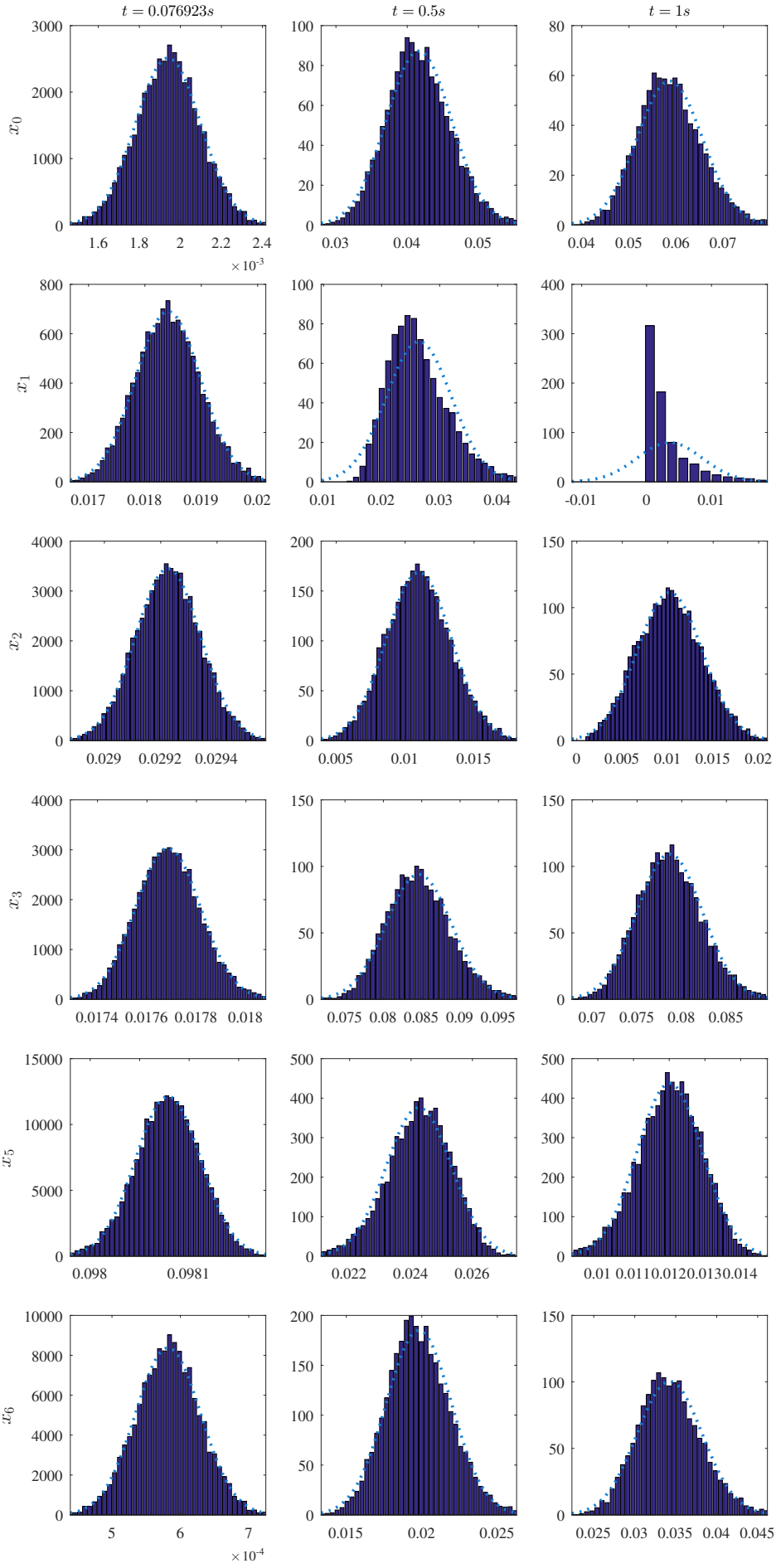

Figure 6.15: Sampled PDF ($d = 3$, $N_{\mathrm{MC}} = 10,000$) of fermentation process for uncertain states. Dotted light curve depicts Gaussian fit over $[-3\sigma_{\mathrm{dev}}, 3\sigma_{\mathrm{dev}}]$.

6.2.3 Derivative projection

Figures 6.16 and 6.17 illustrate the reduction in run time of the proposed derivative projection compared to the standard method based on a finite difference derivative approximation for the two test cases. The actual speed-up corresponds well to the savings with sparsity factor $S_x = 2.79$ given by the predicted trajectory $t_{\text{DP}} = \frac{t_{\text{FD}}}{S_x}$.

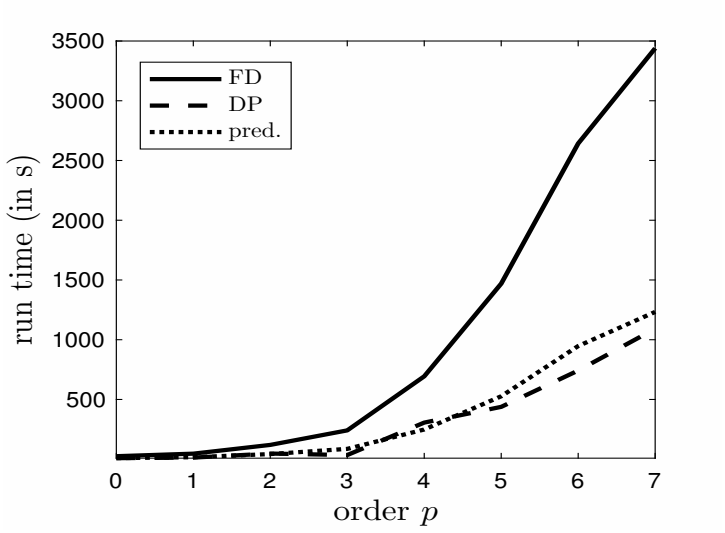

Figure 6.16: Illustration of smaller run times for the soultion of uncertain fermentation process ($d = 2$) with derivative projection (DP) compared to finite difference derivatives (FD). Termination criterion: $\varepsilon_{\text{KKT}} = 10^{-6}$.

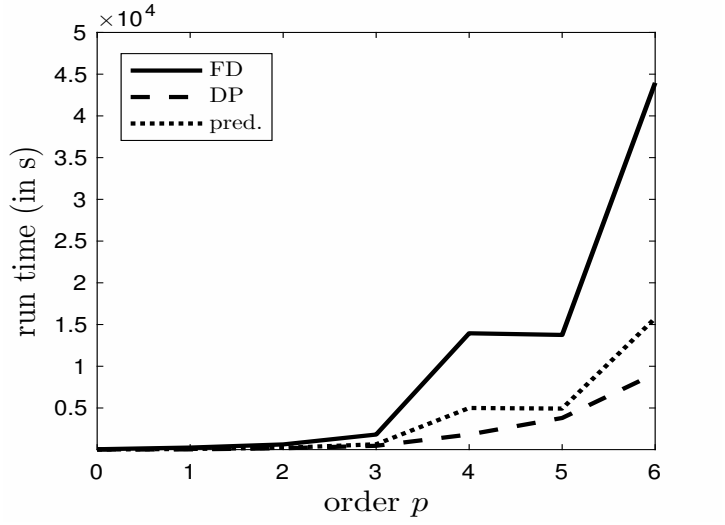

Figure 6.17: Illustration of smaller run times for the soultion of uncertain fermentation process ($d = 3$) with derivative projection (DP) compared to finite difference derivatives (FD). Termination criterion: $\varepsilon_{\text{KKT}} = 10^{-6}$.

6.2.4 Adaptive algorithm

We set the adaptive refinement threshold $\varepsilon_{\text{AD}} = 10^{-7}$ because the solution shows a higher sensitivity to the selected error tolerance. The decay of the state error estimates $\delta^{(p)}$ for the adaptive refinement is plotted in Figure 6.18. Compared to the first test problem, the convergence is faster, cf. Figure 6.18, which can be attributed to the smaller degree of nonlinearity in the dynamics. For the test case $d = 2$, the algorithm terminates after 27s with objective value 5.2582 and returns an optimal order of $\boldsymbol{p}^{\text{opt},2} = \{3,6,2,4,0,1,2,0,0\}$. For test case $d = 3$, the adaptive algorithm terminates after 7:34min with objective value 5.2287 and returns an optimal order of $\boldsymbol{p}^{\text{opt},3} = \{4,5,2,2,0,1,2,0,0\}$.
The results of the single run of the surrogate problem with fixed order chosen to be sufficiently high for accurate results and the single run with the obtained optimal orders are compared in the Tables 6.6 and 6.7 for the two test cases. For a better comparison of the standard approach and the proposed adaptive algorithm, we refer to Figure 6.19 which shows a plot of the run times for different expansion orders. It can be seen that the adaptive algorithm leads to a further run time reduction and a more precise objective value.

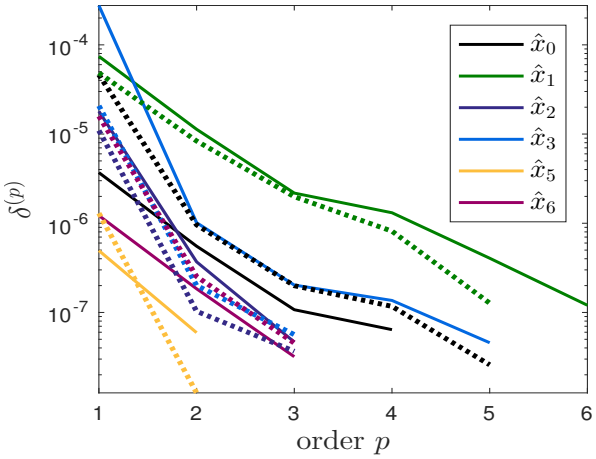

Figure 6.18: Decay of error estimates for uncertain states for fermentation process. Dotted and solid curves correspond to $d = 2$ and $d = 3$, resp., while colors correspond to different state indices (deterministic states omitted). Termination criterion: $\varepsilon_{\text{r}} = 10^{-7}$, $\varepsilon_{\text{KKT}} = 10^{-6}$.

	fixed order	optimal order	ad. alg
p	$\{6,\dots,6\}$	$\{3,6,2,4,0,1,2,0,0\}$	–
# states	252	71	–
obj. value	5.2879	5.273	5.2582
run time [mm:ss]	12:09	02:55	00:27

Table 6.6: Results fermentation process for single run with predefined fixed order and single run with optimal adapted order for test example $d = 2$. Termination criterion: $\varepsilon_{\text{KKT}} = 10^{-6}$.

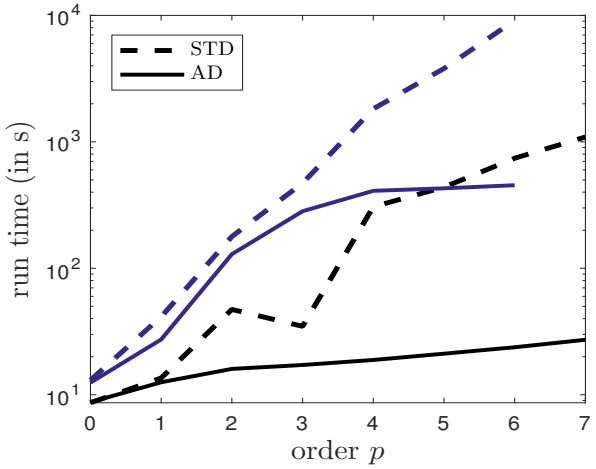

Figure 6.19: Illustration of smaller run times for adaptive algorithm compared to standard approach for fermentation process. Blue upper and black lower curves correspond to $d = 2$ and $d = 3$, resp. Termination criterion: $\varepsilon_r = 10^{-7}$, $\varepsilon_{KKT} = 10^{-6}$.

	fixed order	optimal order	ad. alg
p	$\{5,\ldots,5\}$	$\{4,5,2,2,0,1,2,0,0\}$	–
# states	504	128	–
obj. value	5.2849	5.2786	5.2287
run time [h:mm:ss]	1:03:08	0:09:32	0:07:34

Table 6.7: Results fermentation process for single run with predefined fixed order and single run with optimal adapted order for test example $d = 3$. Termination criterion: $\varepsilon_{KKT} = 10^{-6}$.

6.2.5 Chance constraint reformulation

In this part, we consider only the two-dimensional uncertainty because it shows a more interesting behavior. The uncertain inputs are

$$\mu_G \sim 10^4 \cdot \mathcal{N}(20,4),\ \gamma_{g,S_2} \sim 10^4 \cdot \mathcal{N}(0.5,1.25)$$

and the employed polynomial chaos order is

$$\boldsymbol{p} = \{3,6,2,4,0,1,2,0,0\},\ \boldsymbol{M_p} = \{10,28,6,15,1,3,6,1,1\}.$$

The effects of the uncertainty on the state variables at different time instances can be observed in Figure 6.14 depicting an estimation of the true probability density function and the normal distribution fit for all states influences by the uncertainty at different time instances.
The upper bound on the substrate concentration

$$c_{S_1}(t,\xi) \leqslant 0.04$$

is critical and may only be violated in a well-defined number of cases. To meet this requirement, we add a chance constraint allowing for a constraint violation in at most $\delta = 2\%$ of all possible outcomes

$$\mathrm{P}\left(c_{S_1}(t,\xi) \leqslant 0.04\right) \geqslant 0.98.$$

We compare different constraint reformulations:

(i) Mean constraint: $\mathrm{E}\left[c_{S_1}(t,\xi)\right] \leqslant 0.04$

(ii) Mean-variance constraint:

$$\mathrm{E}\left[c_{S_1}(t,\xi)\right] + 2.0537\sqrt{\mathrm{Var}\left[c_{S_1}(t,\xi)\right]} \leqslant 0.04$$

where $c^u_{0.2} = 2.0537$ corresponds to the upper 2%-quantile of the normal distribution.

(iii) 98%-chance constraint:

$$\max_{\xi \in \mathcal{S}}\ c_{S_1}(t,\xi) \leqslant 0.04$$

using the uncertainty set $\mathcal{S} = [-2.574, 2.574] \times [-2.574, 2.574]$ with $\mathrm{P}\left(\xi \in \mathcal{S}\right) \geqslant 0.98$.

Figures 6.20 and 6.21 show the control and state trajectories corresponding to the different strategies.
Table 6.8 summarizes the benchmarks and includes the dimensions of the surrogate problems after the multiple shooting discretization. The chance constraint reformulation leads to a significantly lower constraint violation rate than the required 2%, which is violated in the two other cases.

Remark 6.2 *In this example, we have used the Chebyshev discretization of Method 2 in Section 5.1.2 for the computation of the chance constraint reformulation (iii). The number of selected Chebyshev points is* $N_P = 18^2 = 324$. *It can be seen from the computation times in Table 6.8 that the effort of the additional linear inequality constraints is negligible compared to the effort related to the high-dimensional state space of the surrogate problem and the increased effort to find a solution in the presence of tight constraints.*

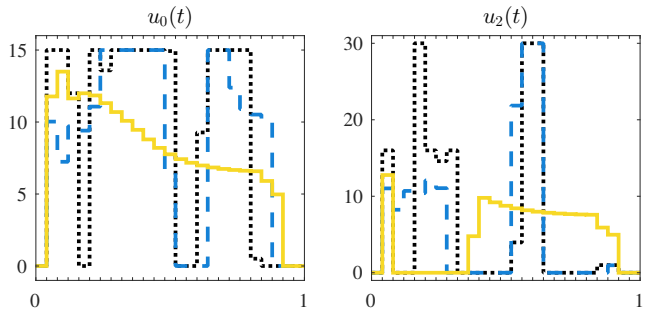

Figure 6.20: Robustified version of optimal control law of fermentation process (u_1 shows nearly constant behavior and is omitted). Deterministic (no uncertainty present), mean-variance bound (case (ii)) and chance constrained robustification (case (iii)) are plotted as dark dotted, dashed and light-colored solid lines, resp.

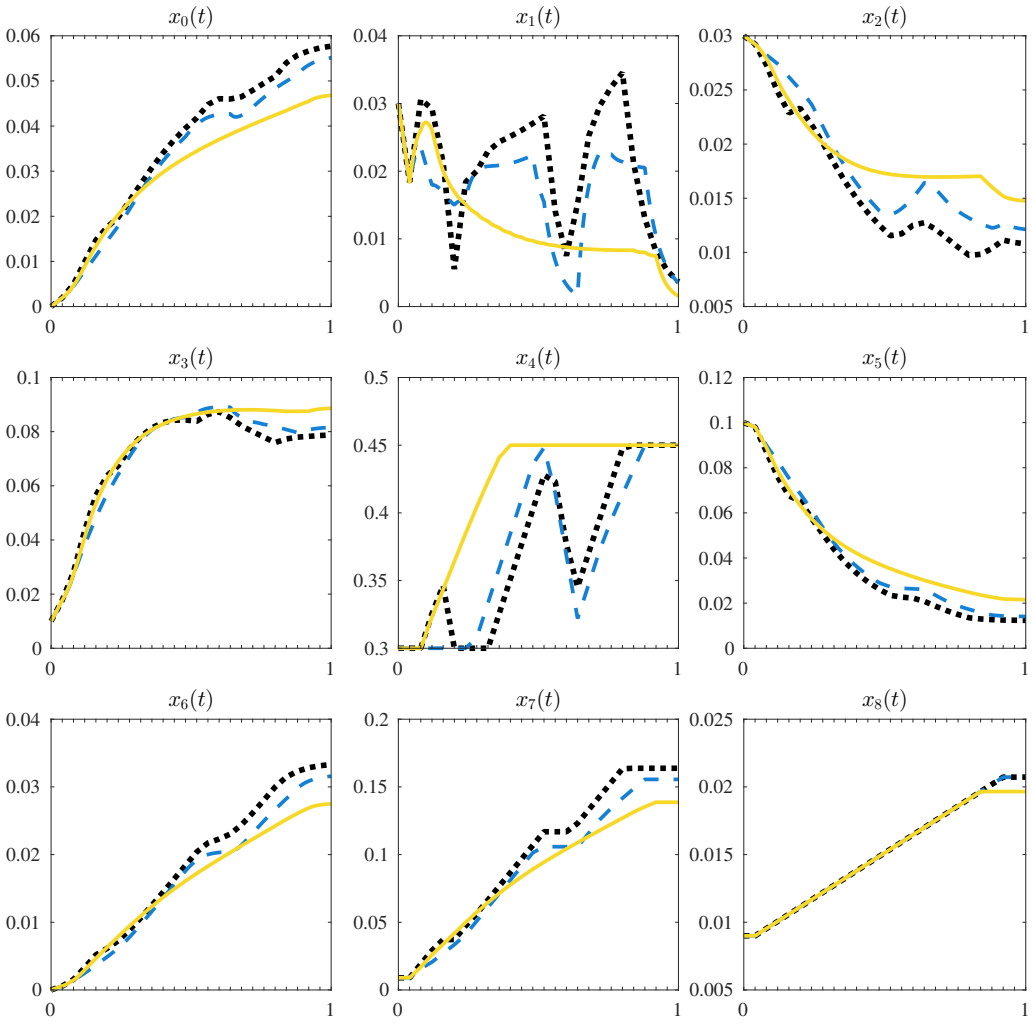

Figure 6.21: Robustified version of optimal process behavior of fermentation process. Deterministic, mean-variance bound (case (ii)) and chance constrained robustification (case (iiia), (iiib)) are plotted as dark dotted, dashed and light-colored solid lines, resp.

A Monte Carlo sampling of the state trajectory of interest $c_{S_1}(t)$ illustrating the extend of the sampled trajectories for different uncertainty realizations is depicted in Figure 6.22. The overall extent of the trajectories can be seen to be significantly smaller in the solutions corresponding to the chance constraint reformulation. This property is also indicated by the smaller propagated variance, which is implicitly enforced by satisfying the chance constraints. Compared to the container crane problem, the inclusion of chance constraints has an inherent variance minimization effect.

	det.	(i)	(ii)	(iii)
objective	5.176	5.233	5.257	5.403
$\mathrm{Var}\, c_{S_1}(t_f)$	–	$3.91 \cdot 10^{-5}$	$2.77 \cdot 10^{-5}$	$0.62 \cdot 10^{-5}$
constraint violation [%]	–	27.45	3.96	0.08
run time [mm:ss]	00:01	09:54	09:33	03:54
NLP variables	309	1921	1921	1921
equality constraints	225	1775	1775	1775
inequality constraints	618	$2 \cdot 1921 + 26$	$2 \cdot 1921 + 26$	$2 \cdot 1921 + 324 \cdot 25$
		3868	3868	11942

Table 6.8: Properties of the optimal solutions obtained for the robustified fermentation process. Constraint violation rates for different strategies have been computed from $N_{\mathrm{MC}} = 10,000$ samples over $\mathbb{R}^2$ using the obtained optimal control law. Last section contains the NLP dimensions after the multiple shooting discretization with $N_{\mathrm{shoot}} = 25$.

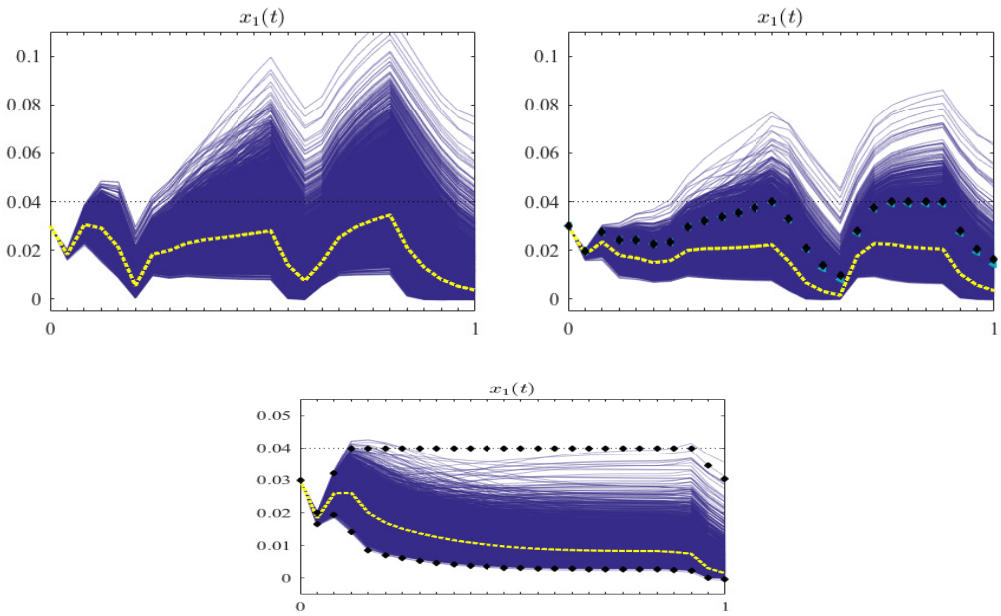

Figure 6.22: Sampled trajectories ($N_{\mathrm{MC}} = 10,000$) of $x_1(t, \xi)$ of robustified fermentation process given optimal controls for average constraint (i) (upper left), Gaussian fit (ii) (upper right) and chance constraint approximation (iii) (lower). The light-colored dotted trajectory is the nominal solution. Dark triangular- and diamond-shaped markers illustrate computed and sampled mean-variance bound (case (ii)) and computed extreme trajectories for the 99%-quantile (case (iii)), resp.

6.3 Application: Adsorption chiller

In this section, we present numerical results for an industrial application, a challenging nonlinear optimal control problem modeling an adsorption refrigeration system under uncertainty. The process model of an adsorption chiller was developed by the Chair of Technical Thermodynamics LTT of the RWTH Aachen University. The focus of this case study is a first feasibility study of a real industrial application under uncertainty.

6.3.1 Adsorption chiller cycle

Adsorption chillers or heat pumps use the physical process of adsorption for thermal compression of the working fluid. The advantage of these systems is the efficient use of solar or waste heat to meet cooling and heating demands, therefore allowing an environmentally friendly provision of heating and cooling demands.
The one-bed adsorption chiller consists of one adsorber bed, a condenser and an evaporator. The main components of the adsorber bed are the heat exchanger and the attached adsorbent material. There are different choices of combinations of adsorbent material, e.g. silica gel or zeolite, and working fluid or refrigerant, e.g. water. The adsorber is connected to the evaporator and to the condenser via butterfly valves and between condenser and evaporator there is a condensate reflux connection. For a picture and the scheme of the adsorption chiller test stand, see Figures 6.23 and 6.24. For a scheme of the structure of the adsorption chiller model, see Figure 6.25.

Figure 6.23: Picture of the adsorption chiller test stand.
Source: *Chair of Technical Thermodynamics LTT, RWTH Aachen*

The basic working principle of the adsorption cycle is to condense the refrigerant at high pressure/temperature and evaporate it at low pressure/temperature. The simple one-bed adsorption cooling cycle is divided into four different phases: isosteric cooling, adsorption, isosteric heating and desorption.
In the isosteric cooling, the adsorbent is cooled until the pressures of the adsorbent material is equal to the low pressure of the evaporator. In the adsorption phase, using hot water from the external waste heat source, e.g. the solar collector, the refrigerant vaporizes in the evaporator and streams into the adsorber in order to be adsorbed. Due to the low pressure, the evaporation happens at low temperature, extracting heat from its surroundings and thereby producing the

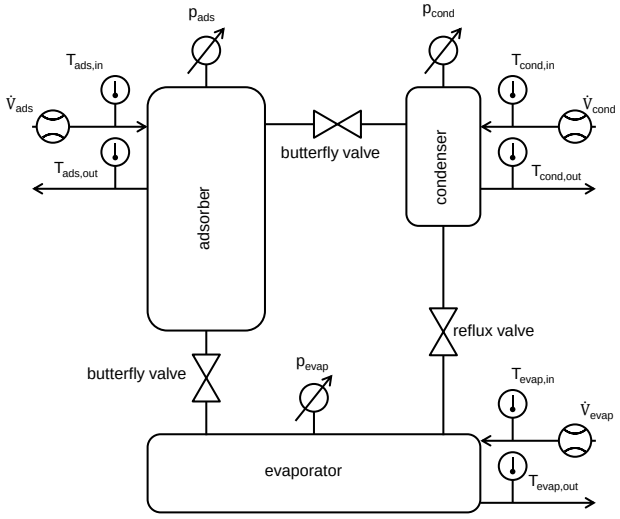

Figure 6.24: Scheme of the adsorption chiller test stand consisting of one adsorber bed, a condenser and an evaporator chamber. Additionally, the temperature, pressure and volume flow sensors are pictured.
Source: *Chair of Technical Thermodynamics LTT, RWTH Aachen*

useful "cold". The adsorption phase is finished when the adsorbent is saturated. With the use of hot water, the adsorbed refrigerant is again evaporated. The adsorbent pressure rises until it reaches the condenser pressure. The desorbed vapor streams out of the adsorber to the condenser which is cooled down. The desorption phase ends when the maximal temperature of the adsorbent and minimal loading is reached.
The adsorption cycle is a batch process. For quasi-continuous cooling, at least two sorbent beds are needed, which operate in counter-phase. In a two-bed adsorber, the sorbent in the first compartment (adsorption department) adsorbs the steam entering from the evaporator and produces the useful "cold", while the sorbent in the second compartment is regenerated using hot water from the external waste heat source. If the sorption material in the adsorption compartment is saturated, the chambers are switched over in their function.

Lanzerath et al. propose a lumped model for the adsorbent in which only the heat exchangers are discretized in flow direction. Further assumptions are reported in the corresponding paper [88]. The inlet water temperatures and volume flows are given by measurement data. To transform this simulation model to a model suited for optimization, three modifications are done: i) removing discretizations, ii) simplifying adsorber heat exchanger, iii) approximating measurement data by smooth functions. The model is built modularly in Modelica using the adsorption energy systems library developed at RWTH Aachen University [9]. The fluid properties and the heat exchangers are based on the TIL library by TLK Thermo [61].

6.3.2 Control problem

To compare the performance of adsorption chillers to the performance of conventional compression chillers, the two performance indicators *coefficient of performance (COP)* and *specific cooling power (SCP)* are used. The COP measures the efficiency of the plant whereas the SCP measures the system's power density.
The COP is defined by the ratio of the used heat Q_{evap}, which is the heat transferred during the evaporation process, and the expended heat Q_{heating} consisting of the heat required to heat up

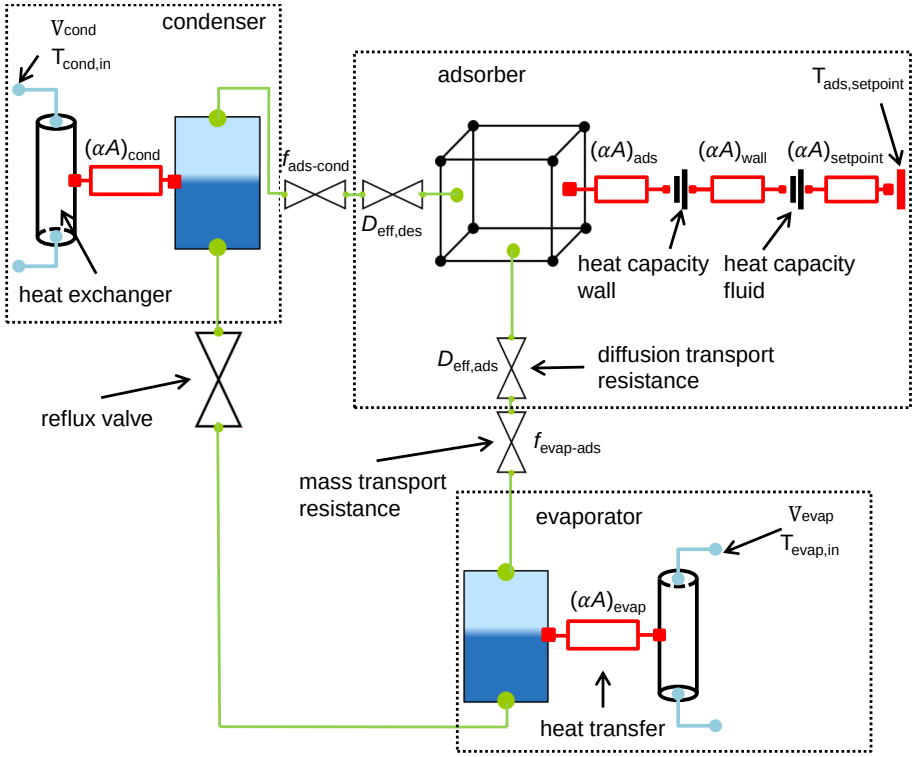

Figure 6.25: Structure of the adsorption chiller model with the three components: evaporator, condenser and adsorber. Each component consists of sub-models for heat exchangers, heat capacities, tubes and equilibrium models for the refrigerant water and the adsorbent. The reflux connection between the condenser and the evaporator is realised by a valve model. The connection between the adsorber and the condenser respectively the evaporator is modelled by a double valve model describing convective and diffusion resistances. The connections to the heat exchangers respectively the heat capacities are realized via heat transfer models. To simplify the representation the heat losses are omitted.
Source: *Chair of Technical Thermodynamics LTT, RWTH Aachen*

the adsorber and the heat needed for the desorption process:

$$\mathrm{COP} = \frac{Q_{\mathrm{evap}}}{Q_{\mathrm{heating}}}.$$

For the SCP indicator, the used heat is divided by the adsorbent mass m_{sor} and the time for an entire cycle t_{cycle}:

$$\mathrm{SCP} = \frac{Q_{\mathrm{evap}}/t_{\mathrm{cycle}}}{m_{\mathrm{sor}}}.$$

To improve system properties, an optimization of the adsorber bed design can be carried out. Design choices include the heat exchanger geometry, the adsorbent configuration and the combination of working fluid and adsorbent material. In most cases, one must accept a trade-off between COP and SCP. For instance, a large heat exchanger surface promotes a high SCP but the resulting increase in mass of the heat exchanger lowers the COP. A similar relationship holds for the cycle times that constitute the durations of the adsorption and the desorption cycle. Assuming for simplicity that the adsorption and desorption cycle times are equal, then long cycle times promote a high COP whereas short cycle times promote a high SCP [2, 39, 132].

An appropriate optimal control problem is to find a cycle time and possibly design parameter choices that lead to maximum cooling power per period, assuming there is enough cheap waste heat available. The process is restricted to periodic operation. Depending on the model complexity, one can determine different duration times for isosteric cooling, adsorption, isosteric heating, desorption and, if applied, durations of heat recovery and mass recovery [63].

The resulting optimal control problem with differential state variables $\boldsymbol{x}(t)$ and algebraic state variables $\boldsymbol{z}(t)$ reads

$$\min_{\boldsymbol{x},\boldsymbol{z},\boldsymbol{p},t_{\text{cycle}}} \quad -Q_{\text{evap}}(t_{\text{cycle}})/Q_{\text{heating}}(t_{\text{cycle}}) \tag{6.3a}$$

$$-Q_{\text{evap}}(t_{\text{cycle}})/(t_{\text{cycle}} \cdot m_{\text{sor}}) \tag{6.3b}$$

$$\text{s.t.} \quad \dot{\boldsymbol{x}}(t) = \boldsymbol{f}(t,\boldsymbol{x}(t),\boldsymbol{z}(t),\boldsymbol{p}) \qquad t \in [t_0, t_{\text{cycle}}] \text{ a.e.} \tag{6.3c}$$

$$\boldsymbol{0} = \boldsymbol{g}(t,\boldsymbol{x}(t),\boldsymbol{z}(t),\boldsymbol{p}) \qquad t \in [t_0, t_{\text{cycle}}] \text{ a.e.} \tag{6.3d}$$

$$\boldsymbol{u}(t) \in U(t) \qquad t \in [t_0, t_{\text{cycle}}] \text{ a.e.} \tag{6.3e}$$

$$\boldsymbol{0} \geqslant \boldsymbol{c}(t,\boldsymbol{x}(t),\boldsymbol{z}(t),\boldsymbol{p}) \qquad t \in [t_0, t_{\text{cycle}}] \text{ a.e.} \tag{6.3f}$$

$$\boldsymbol{0} = \boldsymbol{x}(t_0) - \boldsymbol{r}(\boldsymbol{x}(t_{\text{cycle}})) \tag{6.3g}$$

In this formulation, there are no continuous controls required as the system is controlled purely by the horizon length and design parameter choices. The path constraints (6.3f) comprise typically the bounds on the variables, the parameters and the time horizon. The constraint (6.3g) on the initial and final state value, where $\boldsymbol{r}$ contains permutations of the state variables and the initial value can be a free variable, ensures the period operation of the system.
The dynamic DAE process (6.3c)–(6.3d) is provided as a blackbox system in form of a dynamic Modelica model, which is encapsulated in a functional mock-up unit (FMU). Via the standardized Functional Mock-up Interface (FMI), the dynamic model is connected to the optimization algorithm. For more details on the technical realisation, see Gräber et al. [64].

For the following case study under uncertainty, we use a model with two adsorber beds and equal adsorption and desorption times. The adsorption cycle is modeled by 39 differential states describing mainly the fluid density and temperature in the evaporator and in the condenser, the temperature and water uptake of the two adsorber beds and the temperature values of the discretized heat exchangers for the condenser, evaporator and the two adsorbers. Additional state variables, e.g. $Q_{\text{evap}}(t)$, $Q_{\text{heating}}(t)$ model the heat flows. There are 21 parameters describing the geometric design and the heat and mass transfer of the components. The optimization variables are composed of the cycle time t_{cycle} and the three parameters describing the lengths l_{ads}, l_{evp}, l_{cond} of the evaporator, condenser and adsorbers. For different formulations of the adsorption chiller optimal control problem using, e.g., multi-stage system and algebraic variables, we refer to [62, 63, 10, 11].

6.3.3 Uncertainty analysis

The calibration of the parameter values with the measurement data suffers from deviating operating conditions, e.g., changing availability of solar or waste heat, different temperatures, filling levels etc. In particular the outcomes for the diffusion transport resistance D for the adsorption and desorption process and the heat transfer coefficients (αA) of the evaporator, condenser and the adsorbers are affected. For a detailed analysis of the model accuracy after calibration of the parameters, we refer to Lanzerath et al. [88].

For this initial uncertainty quantification study, we consider one uncertain parameter D_{ads},

normally distributed with nominal value $\overline{D}_{\text{ads}} = 1.8 \cdot 10^{-10}\,\text{m}^2/\text{s}$ and with a standard deviation of 7.5% up to 15% of the nominal value.

One of the main challenges that arises when incorporating uncertainty into Problem (6.3) is the appropriate reformulation of the periodicity conditions (6.3f) that are imposed as equality constraints comprising the deterministic initial state and the final state that is influenced by the uncertainty.

A straight-forward reformulation using the mean value $\mathrm{E}\big[\boldsymbol{r}(\boldsymbol{x}(t_{\text{cycle}}))\big]$ is as follows:

$$\boldsymbol{x}(t_0) - \mathrm{E}\big[\boldsymbol{r}(\boldsymbol{x}(t_{\text{cycle}}))\big] = \boldsymbol{0}.$$

In the presence of uncertainty, this formulation is rather restrictive and in most cases results in an infeasible problem formulation. Therefore, a reformulation as inequality constraints using a target set $[-\varepsilon\,|\boldsymbol{x}(t_0)|\,, \varepsilon\,|\boldsymbol{x}(t_0)|]$ with a small parameter $\varepsilon \in [0,1)$, scaled in magnitude by the deterministic initial value, is advisable. This results in the two constraints

$$\boldsymbol{x}(t_0) - \mathrm{E}\big[\boldsymbol{r}(\boldsymbol{x}(t_{\text{cycle}}))\big] \leqslant \varepsilon\,|\boldsymbol{x}(t_0)|\,, \tag{6.4}$$
$$\boldsymbol{x}(t_0) - \mathrm{E}\big[\boldsymbol{r}(\boldsymbol{x}(t_{\text{cycle}}))\big] \geqslant -\varepsilon\,|\boldsymbol{x}(t_0)|\,. \tag{6.5}$$

A higher degree of robustness than the mean value formulation (6.4)–(6.5) can offer is given by a chance constraint based formulation with

$$\mathrm{P}\Big(\big|\boldsymbol{x}(t_0) - \mathrm{E}\big[\boldsymbol{r}(\boldsymbol{x}(t_{\text{cycle}}))\big]\big| \leqslant \varepsilon\,|\boldsymbol{x}(t_0)|\Big) \geqslant 0.99.$$

Larger or smaller bounds than 0.99 are possible and depend on the application. The chance constraint can be readily incorporated into the optimal control problem with the methodology developed in Chapter 5.

Robustified optimal control problem The reformulated optimal control problem with chance constraint robustification reads

$$\min_{\boldsymbol{x},\boldsymbol{p},t_{\text{cycle}},\varepsilon} \quad -\mathrm{E}\big[Q_{\text{evap}}(t_{\text{cycle}})/(t_{\text{cycle}} \cdot m_{\text{sor}})\big] + c\varepsilon \tag{6.6a}$$
$$\text{s.t.} \quad \dot{\boldsymbol{x}}(t) = \boldsymbol{f}(t, \boldsymbol{x}(t), \boldsymbol{p}) \qquad t \in [t_0, t_{\text{cycle}}] \text{ a.e.} \tag{6.6b}$$
$$0.99 \geqslant \mathrm{P}\Big(\big|\boldsymbol{x}(t_0) - \mathrm{E}\big[\boldsymbol{r}(\boldsymbol{x}(t_{\text{cycle}}))\big]\big| \leqslant \varepsilon\,|\boldsymbol{x}(t_0)|\Big) \tag{6.6c}$$
$$\boldsymbol{u}(t) \in U(t) \qquad t \in [t_0, t_{\text{cycle}}] \text{ a.e.} \tag{6.6d}$$
$$\boldsymbol{0} \geqslant \mathrm{E}[\boldsymbol{c}(t, \boldsymbol{x}(t), \boldsymbol{p})] \qquad t \in [t_0, t_{\text{cycle}}] \text{ a.e.} \tag{6.6e}$$
$$\text{COP} = \mathrm{E}\big[Q_{\text{evap}}(t_{\text{cycle}})/Q_{\text{heating}}(t_{\text{cycle}})\big] \tag{6.6f}$$

Instead of considering the original multi-objective problem with two simultaneous objective functions (6.3a) and (6.3b), we fix one of the objectives to COP = 0.14. The offset ε that is scaled by an appropriate constant c is minimized in order to ensure that the target set is as small as possible. Consequently, the periodicity constraint under uncertainty is nearly satisfied while retaining the problem feasibility. It is customary to set the scaling factor c to a large value, here $c = 10000$, such that $c\varepsilon$ is of the same magnitude as the SCP. The initial standard deviation is set to $\sigma_{D_{\text{ads}}} = 0.075 \cdot \overline{D}_{\text{ads}}$.

To obtain the deterministic surrogate optimal control problems, we used a polynomial chaos order of $p = 3$. In the reformulation of the chance constraints, we used Method 2 in Section 5.1.2 with $N_P = 10$ Chebyshev points. Both values turned out to be sufficient to capture

the low or moderate nonlinear effects. For the solution of the optimal control problem, we set the termination criterion to $\varepsilon_{\text{KKT}} = 10^{-5}$ for the discretized optimization problem and use an integration tolerance of 10^{-7}.

The results for the deterministic optimal control problem and the uncertain optimal control problem with mean value and with chance constraint robustification are summarized in Table 6.9. As expected the offset ε is 0 for the deterministic version and the periodic equality constraints are satisfied while for the uncertain problem versions a small deviation of approximately 1% is necessary. Because of the larger offset, they result in a higher SCP of 171.2 W/kg^{-1} for the chance constraint robustification and a slightly larger outcome of 170.4 W/kg^{-1} for the mean value robustification versus 125.3 W/kg^{-1} for the deterministic case.
The effects of the uncertainty on the state variables at different time instances can be observed in Figure 6.26 which shows the state density functions for the uncertain problem with chance constraint robustification. Note that the mean value robustification gives similar density plots. Due to the high state dimensionality, we depict only a selection of the state variables: evaporator temperature T_{evap}, condenser fluid density ρ_{cond}, heating transferred during the evaporation process Q_{evap}, expended heat Q_{heating}, fluid temperature of second adsorber heat exchanger $T_{\text{hx–fluid,ads2}}$ and wall temperature of second adsorber heat exchanger $T_{\text{hx–wall,ads2}}$.

	SCP [W/kg^{-1}]	t_{cycle}[s]	l_{ads}[mm^2]	l_{evp}	l_{cond}	ε
chance constraint	170.4	110.8	7.00	3.00	4.60	$1.46 \cdot 10^{-2}$
mean value	171.2	110.0	7.00	3.00	4.59	$1.44 \cdot 10^{-2}$
deterministic	125.3	184.6	7.68	2.31	4.55	0

Table 6.9: Optimal control results for periodic adsorber problem for chance constraint robustification, mean value robustification and deterministic version. The initial standard deviation is $\sigma_{D_{\text{ads}}} = 0.075 \cdot \overline{D}_{\text{ads}}$ and COP=14%.

For an evaluation of the effects of the periodic constraints on the uncertainty propagation, we consider Problem 6.6 with fixed initial states $\boldsymbol{x}(t_0) = \boldsymbol{x}_0$. Hence, the uncertainty propagation through the forward problem takes place without being influenced by the periodic state condition. For this test, we set the initial standard deviation to $\sigma_{D_{\text{ads}}} = 0.15 \cdot \overline{D}_{\text{ads}}$.

The results for the deterministic optimal control problem and the uncertain optimal control problem with mean value robustification and with chance constraint robustification are summarized in Table 6.10. As expected the offset ε modeling the violation of the equality constraints is significantly smaller for the deterministic version. Contrary to the periodic problem, which has more degrees of freedom, a small non-zero offset ε is necessary for the deterministic version to satisfy the equality constraint. Moreover, the two uncertain problem versions result now in a lower SCP value than the deterministic case – the expected behavior of the robustified solution under uncertainty. As before, a deviation of approximately 0.1% and 1% from the nominal equality constraint is necessary for the uncertain problem with with mean value and with chance constraint robustification, respectively.

The probability density functions of the states T_{evap}, ρ_{cond}, Q_{evap}, Q_{heating}, $T_{\text{hx–fluid,ads2}}$ and $T_{\text{hx–wall,ads2}}$ at different time instances can be observed in Figure 6.27. Again, the plots are shown for the uncertain problem with chance constraint robustification, however, the mean value robustification gives similar plots. Contrary to the periodic version of the problem, the propagated density functions now deviate from the initial normal distribution and the nonlinear effects of the dynamics become visible.

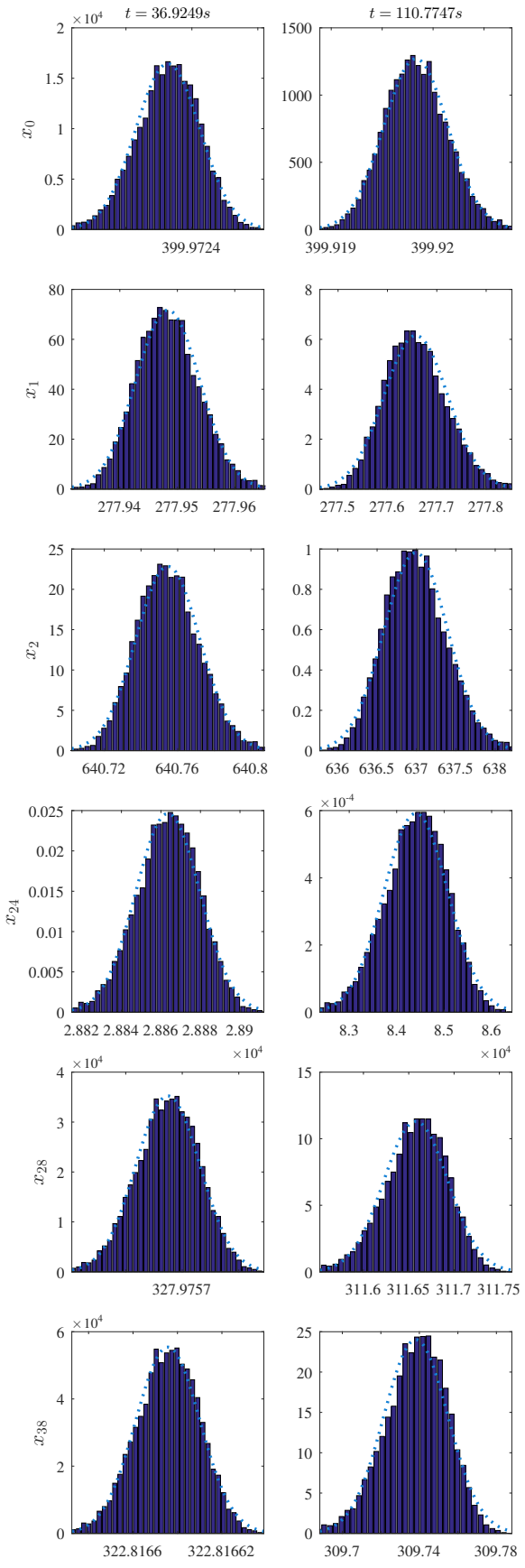

Figure 6.26: Sampled PDF ($N_{\mathrm{MC}} = 10,000$) of adsorption chiller under uncertainty with periodic constraints for selected states (T_{evap}, ρ_{cond}, Q_{evap}, Q_{heating}, $T_{\mathrm{hx-fluid,ads2}}$, $T_{\mathrm{hx-wall,ads2}}$). The initial standard deviation is $\sigma_{D_{\mathrm{ads}}} = 0.075 \cdot \overline{D}_{\mathrm{ads}}$ and a chance contraint robustification was applied. Dotted light curve depicts Gaussian fit with abscissa ranging over $[-3\sigma_{\mathrm{dev}}, 3\sigma_{\mathrm{dev}}]$.

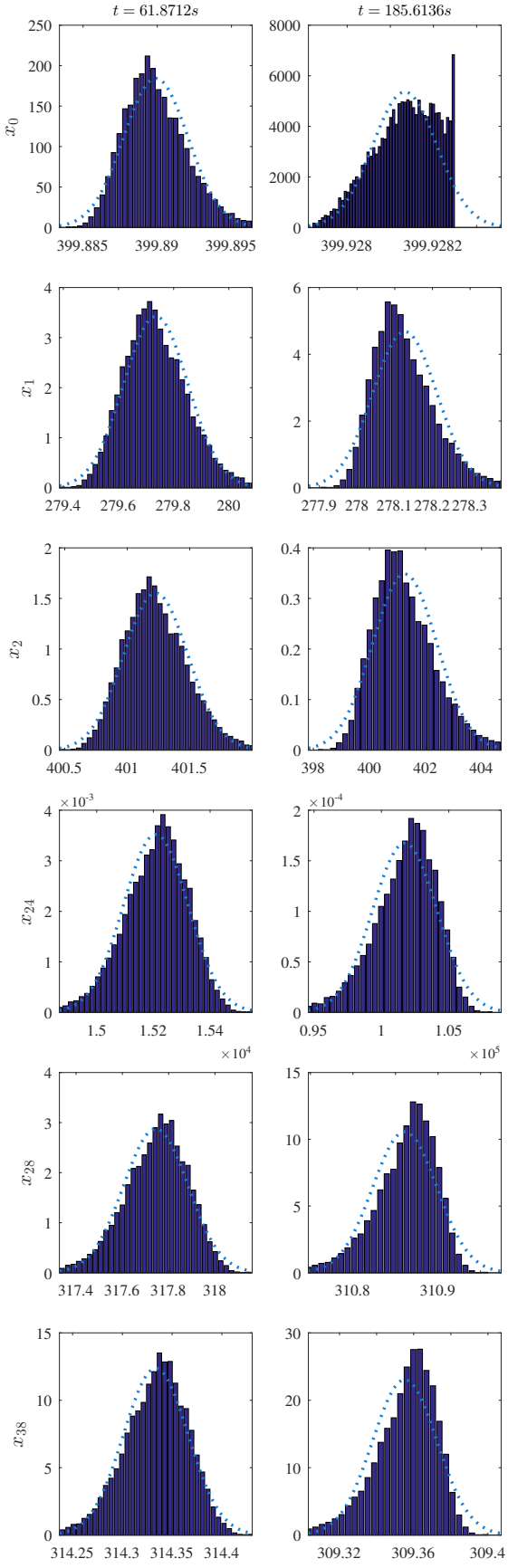

Figure 6.27: Sampled PDF ($N_{\text{MC}} = 10,000$) of adsorption chiller under uncertainty with fixed initial value for selected states (T_{evap}, ρ_{cond}, Q_{evap}, Q_{heating}, $T_{\text{hx–fluid,ads2}}$, $T_{\text{hx–wall,ads2}}$). The initial standard deviation is $\sigma_{D_{\text{ads}}} = 0.15 \cdot \overline{D}_{\text{ads}}$ and a chance contraint robustification was applied. Dotted light curves illustrate Gaussian fit with abscissa ranging over $[-3\sigma_{\text{dev}}, 3\sigma_{\text{dev}}]$. **101**

	SCP [W/kg^{-1}]	t_{cycle}[s]	l_{ads}[mm^2]	l_{evp}	l_{cond}	ε
chance constraint	122.6	185.6	7.50	2.01	4.00	$1.9 \cdot 10^{-2}$
mean value	122.7	180.4	7.22	2.01	4.00	$1.7 \cdot 10^{-3}$
deterministic	125.5	178.4	7.10	2.35	4.64	$9.0 \cdot 10^{-5}$

Table 6.10: Optimal control results for adsorber problem with fixed initial value for chance constraint robustification, mean value robustification and deterministic version. The initial standard deviation is $\sigma_{D_{\text{ads}}} = 0.15 \cdot \overline{D}_{\text{ads}}$ and COP=14%.

Discussion of the results The presented model of an adsorption chiller is a high-dimensional optimal control problem with a complex DAE-ODE process model that is given as a blackbox in form of a dynamic FMU model. Solving it robustly in the deterministic case already proves to be challenging.

Solving the presented optimal control problem under uncertainty is even more demanding and takes up to several hours compared to a few minutes for the solution of the deterministic version. There are several reasons for this discrepancy. The applied resolution of the (periodic) equality constraint results in a complex optimal control problem with an objective function that contains a weighted sum of two terms. This may result in multiple local solutions of the optimization problem. Slight variations in the values for the state variables, which are unavoidable under uncertainty, often lead to infeasibilities that are difficult to resolve due to the blackbox structure. Moreover, due to modeling issues of the FMU dynamic model, changing the realizations of the uncertain parameters in different simulations of the model – an important requirement in the implementation of the applied non-intrusive polynomial chaos method – involves a considerably high computational effort. Consequently, the adsorber model only permits the analysis of a one-dimensional uncertainty.

We find that the effects of the uncertainty on the state trajectories and on the optimal control solution are low to moderate, thus a low polynomial chaos order as well as a low number of discretization points in the resolution of the chance constraints proved to be sufficient to capture the effects of the uncertainty propagation. It is interesting to note that the periodic initial and final state condition further appears to prevent the emergence of the nonlinear effects.

7 Conclusion

In this work, we have developed theory and algorithms for optimal control problems under uncertainty. Special focus was put on the nonlinear propagation of the uncertainty and on a problem-dependent robustification of the solution in form of chance constraints. To this end, we applied the polynomial chaos method to optimal control under uncertainty and solved the resulting surrogate optimal control problem. Our efforts involve the extensive application of the polynomial chaos method to real-world optimal control problems including a challenging new industrial application study under uncertainty illustrating that it is able to capture the nonlinear uncertainty propagation while remaining computationally tractable as long as the number of uncertainties is low to moderate.

From a theoretical point of view, we rigorously studied the properties of the polynomial chaos surrogate optimal control problem with end point constraints in order to prove convergence of the polynomial chaos approximation for increasing orders.
On this basis, we proposed two algorithms which aim for the fast numerical solution of the surrogate problems. The proposed adaptive algorithm identifies the smallest expansion order for each state variable necessary to capture the nonlinear uncertainty propagation with a prescribed accuracy. Due to the smaller problem size as well as the adaptive search procedure, the computational effort is considerably reduced compared to the standard procedure of solving the polynomial chaos surrogate with a fixed, pre-determined order. An additional significant saving of computation time is achieved by developing a fast derivative generation technique that exploits the structure resulting from the spectral projection of the polynomial chaos method.
The two algorithmic contributions are complemented by an extensive numerical case demonstrating the performance gain of both methods.

The robustification of objective and constraint functions against uncertainty variations is another main topic of this thesis. We proposed a new method to reformulate chance constraints within optimal control problems by using the polynomial chaos method to propagate reachable sets of all uncertain states. Our method is well suited for nonlinear and asymmetric uncertainty propagation. The strength of the estimator in guaranteeing a satisfaction level is supported by a proof of convergence and an a-priori error estimate.
A numerical case study illustrates the tradeoff between low cost objective, chance constraint satisfaction and variance minimization, and demonstrates the suitability of the proposed robustification technique for nonlinear optimal control problems under uncertainty.

We hope that the theoretical, algorithmic and numerical results of this thesis contribute to a better understanding of the class of uncertain optimal control problems. Not all of the open questions in this field as well as the new research directions that arose during the work on this thesis have been fully answered. We therefore conclude this thesis with the most important possible directions of further work.

Directions of further research A deeper investigation of the effects of uncertainties on optimal control problems is desirable, concerning in particular questions such as the trade-off between cost optimality and robustification in terms of constraint satisfaction, as well as solution stability and convergence properties. The convergence proof for the polynomial chaos method applied to optimal control problems is a first result of this kind. A possible extension to a larger problem class, such as optimal control problems with path constraints, is subject to further work.

For the fast numerical solution of the optimal control surrogate problem, we think that the adaptive algorithm deserves further attention. For instance, a more refined order selection strategy that selects new basis functions in a non-monotonic way seems to be a promising strategy to capture the nonlinear uncertainty propagation with an even smaller total number of basis functions.

Further research directions for the chance constraint reformulation method include the simultaneous solution of the optimal control surrogate problem and the polynomial subproblem arising in the computation of the reachable set by enlarging the state and/or parameter space. This would also allow the treatment of non-compact sets. A second direction is the determination of near-optimal uncertainty sets in order to reduce the over-approximation of the chance constraints, for example with a two-stage approach, prior knowledge or decomposition of the uncertainty space. This seems to be an interesting problem in itself, in particular as the proposed approach to chance constraint approximation is not restricted to the utilized uncertainty propagation method.

The study of the adsorption chiller under uncertainty, the industrial application problem of this thesis, requires many further improvements and numerical experiments. In particular numerical improvements to decrease the run time for the solution of the uncertain problem are necessary. Moreover, it would be appropriate to consider the problem with a higher dimensional uncertainty. The applied resolution of the periodic equality constraints under uncertainty can possibly be improved. Another task is the consideration of the original multi-objective optimal control problem without fixing one of the two objective function terms COP or SCP. This can be achieved, for instance, by computing the whole Pareto frontier under the influence of the uncertainty.

A Foundations of probability theory

Probability theory deals with the mathematical concepts that help to describe events that occur in a non-deterministic way or with uncertainty. We restrict the following presentation of important definitions and lemmas of probability theory to what we need throughout this thesis. The aim of this appendix is to lay out the foundations to understand the concept of transformations of multidimensional random variables.
For a detailed overview we refer to the textbooks [48, 47].

Probability space

The basic abstract fundament is a probability space comprising the sample space of possible outcomes or realizations, the set of possible events and the assignment of probabilities to the events.

Definition A.1 *A* probability space *is a triple* $(\Omega, \mathcal{F}, \mathrm{P})$ *consisting of*

- *the* sample space $\Omega \neq \emptyset$
- *the* σ-algebra $\mathcal{F} \subseteq 2^{\Omega}$ *consisting of measurable sets such that*
  - $\Omega \in \mathcal{F}$
  - $A \in \mathcal{F} \Rightarrow \Omega / A \in \mathcal{F}$
  - $A_i \in \mathcal{F},\ i = 1, \ldots \Rightarrow \cup_{i=1}^{\infty} A_i \in \mathcal{F}$
- *the* probability measure $\mathrm{P} : \mathcal{F} \to [0,1]$ *with* $\mathrm{P}(\Omega) = 1$
  - P *is countably additive: if* $\{A_i\}_{i=1}^{\infty} \subseteq \mathcal{F}$ *is a countable collection of pairwise disjoint sets, then* $\mathrm{P}(\cup_{i=1}^{\infty} A_i) = \sum_{i=1}^{\infty} A_i$.

Random variables

A random variable is a measurable function whose values can be interpreted as numerical outcomes of a random phenomenon. The definition requires an abstract set-up.

Definition A.2 *A function* $\boldsymbol{X} : \Omega \to \mathbb{R}^d$ *is called* $\mathcal{F}$-measurable *if*

$$X^{-1}(B) = \{\omega \in \Omega \mid \boldsymbol{X}(\omega) \in B\} \in \mathcal{F}$$

for all open sets $B \subseteq \mathbb{R}^d$. *It suffices to consider*

$$\boldsymbol{X}^{-1}([-\infty, b]) = \{\omega \in \Omega \mid \boldsymbol{X}(\omega) \leqslant b\} \in \mathcal{F} \quad \forall b \in \mathbb{R}^d$$

We denote by $\mathcal{B}(\mathbb{R}^d)$ the Borel σ-algebra on $\mathbb{R}^d$ which is defined to be the σ-algebra generated by the open sets, or equivalently, by the closed sets.

Definition A.3 *A real-valued, multivariate* random variable $\boldsymbol{X}$ *is an* $\mathcal{F}$*-measurable function from* $(\Omega, \mathcal{F}, \mathrm{P})$ *to* $(\mathbb{R}^d, \mathcal{B}(\mathbb{R}^d))$. *Every random variable induces a measure on* $(\mathbb{R}^d, \mathcal{B})$, *called* probability law $\mu_{\boldsymbol{X}} : \mathbb{R}^d \to [0,1]$ *and defined by*

$$\mu_{\boldsymbol{X}}(B) := \mathrm{P}(\boldsymbol{X}^{-1}(B))$$

with $B \in \mathcal{B}$. The function

$$F_X : \mathbb{R}^d \to [0,1],\ F_X(\boldsymbol{x}) := \mathrm{P}(\omega \in \Omega \mid \boldsymbol{X}(\omega) \leqslant \boldsymbol{x})$$

is called the cumulative distribution function (CDF) *of $\boldsymbol{X}$.*

Definition A.4 *If $\int_\Omega |\boldsymbol{X}| \,\mathrm{d}\,\mathrm{P}(\omega) < \infty$, then we define the* expectation *of $\boldsymbol{X}$ with respect to* P *as*

$$\mathrm{E}[\boldsymbol{X}] = \int_\Omega \boldsymbol{X}(\omega)\,\mathrm{dP}(\omega) = \int_{\mathbb{R}^d} \boldsymbol{x}\,\mathrm{d}\mu_{\boldsymbol{X}}(\boldsymbol{x}).$$

If $f : \mathcal{B} \to \mathbb{R}$ is Borel-measurable and $\int_\Omega |f(\boldsymbol{X})| \,\mathrm{dP}(\omega) < \infty$, then the expectation *of $f(\boldsymbol{X})$ is similarly defined via*

$$\mathrm{E}[f(\boldsymbol{X})] = \int_\Omega f(\boldsymbol{X}(\omega))\,\mathrm{dP}(\omega) = \int_{\mathbb{R}^d} f(x)\mathrm{d}\mu_{\boldsymbol{X}}(\boldsymbol{x}).$$

If $\mathrm{E}\left[|\boldsymbol{X}|^2\right] < \infty$, we obtain the variance *of $\boldsymbol{X}$ by*

$$\mathrm{Var}[\boldsymbol{X}] = \mathrm{E}\left[(\boldsymbol{X} - \mathrm{E}[\boldsymbol{X}])^2\right] = \mathrm{E}\left[\boldsymbol{X}^2\right] - \mathrm{E}[\boldsymbol{X}]^2.$$

Random variables with finite variance are contained in $L^2(\Omega, \mathcal{F}, \mathrm{P})$, the Hilbert space of (equivalence classes of) real-valued square-integrable random variables on Ω with inner product $\langle \boldsymbol{X}, \boldsymbol{Y} \rangle_{L^2(\mathcal{S})} = \mathrm{E}[XY] = \int_\Omega XY \,\mathrm{dP}$.

Definition A.5 *A random variable $\boldsymbol{X}$ is* continuous *if there exist a non-negative, measurable function $\rho_{\boldsymbol{X}} : \mathbb{R}^d \to [0, \infty)$, called the* probability density function (PDF) *of $\boldsymbol{X}$, such that*

$$F_{\boldsymbol{X}}(\boldsymbol{x}) = \int_{-\infty}^{x_1} \dots \int_{-\infty}^{x_d} \mathrm{d}\mu_{\boldsymbol{X}}(\boldsymbol{x}) = \int_{-\infty}^{x_1} \dots \int_{-\infty}^{x_d} \rho_{\boldsymbol{X}}(\boldsymbol{x})\mathrm{d}\boldsymbol{x} \quad \forall \boldsymbol{x} = (x_1, \dots, x_d) \in \mathbb{R}^d.$$

In this case, the formulas for the moments from the previous definition can be simplified to

$$\mathrm{E}[\boldsymbol{X}] = \int_{\mathbb{R}^d} \boldsymbol{x}\,\rho_{\boldsymbol{X}}(\boldsymbol{x})\mathrm{d}\boldsymbol{x},$$
$$\mathrm{E}[f(\boldsymbol{X})] = \int_{\mathbb{R}^d} f(\boldsymbol{x})\rho_{\boldsymbol{X}}(\boldsymbol{x})\mathrm{d}\boldsymbol{x}, \quad \text{etc.}$$

Transformations of random variables

Any function $\boldsymbol{Y} = \boldsymbol{g}(\boldsymbol{X})$ of a random variable $\boldsymbol{X}$ is also a random variable. Let

$$\mathcal{S} = \{\boldsymbol{x} \in \mathbb{R}^d \mid \rho_{\boldsymbol{X}}(\boldsymbol{x}) > 0\}$$

be the support of the PDF of $\boldsymbol{X}$. The function $\boldsymbol{g} : \mathbb{R}^d \to \mathbb{R}^k$ is assumed to be a continuous function, or any function that preserves measurability. Then, we can infer the CDF of the transformed random variable $\boldsymbol{Y} = \boldsymbol{g}(\boldsymbol{X})$ completely from that of $\boldsymbol{X}$ by

$$F_{\boldsymbol{Y}}(\boldsymbol{y}) = \mathrm{P}(\boldsymbol{Y} \leqslant \boldsymbol{y}) = \mathrm{P}(\boldsymbol{g}(\boldsymbol{X}) \leqslant \boldsymbol{y}) = \mathrm{P}(\{\boldsymbol{x} \in \mathcal{S} \mid \boldsymbol{g}(\boldsymbol{x}) \leqslant \boldsymbol{y}\}) = \int_{\{\boldsymbol{x} \in \mathcal{S} \,|\, \boldsymbol{g}(\boldsymbol{x}) \leqslant \boldsymbol{y}\}} \rho_{\boldsymbol{X}}(\boldsymbol{x})\mathrm{d}\boldsymbol{x}.$$

It may be difficult to identify the set $\{\boldsymbol{x} \in \mathbb{R}^d \mid \boldsymbol{g}(\boldsymbol{x}) \leqslant \boldsymbol{y}\}$ in particular for non-monotone functions. If $\boldsymbol{g}$ is a monotone function, the PDF of $\boldsymbol{Y}$ can be obtained by a simple change-of-variable formula. Let $\left|J_{\boldsymbol{g}}(\cdot)\right|$ and $\left|J_{\boldsymbol{g}^{-1}}(\cdot)\right|$ be the determinants of the Jacobians of $\boldsymbol{g}$ and $\boldsymbol{g}^{-1}$, respectively.

Lemma A.1 *Let $\boldsymbol{X}$ have a continuous PDF $\rho_{\boldsymbol{X}}$, $\boldsymbol{Y} = \boldsymbol{g}(\boldsymbol{X})$ where $\boldsymbol{g}$ is a strictly monotone function with (continuously differentiable) inverse $\boldsymbol{g}^{-1}$ on $\mathcal{S}$. Then*

$$\rho_Y(\boldsymbol{y}) = \rho_X(\boldsymbol{g}^{-1}(\boldsymbol{y}))\left|J_{\boldsymbol{g}}(\boldsymbol{g}^{-1}(\boldsymbol{y}))\right| = \frac{\rho_X(\boldsymbol{g}^{-1}(\boldsymbol{y}))}{\left|J_{\boldsymbol{g}^{-1}}(\boldsymbol{y})\right|}$$

for $\boldsymbol{y} \in \boldsymbol{g}(\mathcal{S})$.

The situation is more complicated if $\boldsymbol{g}$ is non-monotone, in which case we need to consider partitions of $\mathcal{S}$ over which $\boldsymbol{g}$ is monotone.

Lemma A.2 *Let $\{\mathcal{S}_i\}_{i=1}^m$ be a partition of $\mathcal{S}$ such that $\rho_{\boldsymbol{X}}$ is continuous and $\boldsymbol{g}(\boldsymbol{x})$ is monotone with (continuously differentiable) inverse $\boldsymbol{g}_i^{-1}$ on $\mathcal{S}_i$. Then*

$$\rho_Y(\boldsymbol{y}) = \sum_{i=1}^{m} \rho_X(\boldsymbol{g}_i^{-1}(\boldsymbol{y}))\left|J_{\boldsymbol{g}_i^{-1}}(\boldsymbol{y})\right|^{-1} \mathcal{I}(\boldsymbol{g}_i^{-1}(\boldsymbol{y} \in \mathcal{S}_i))$$

where $\mathcal{I}(\cdot)$ is the indicator function.

B Perturbation and stability analysis of mathematical problems

In this appendix, we summarize useful results of perturbation analysis for initial value problems and nonlinear programming problems. For a detailed overview we refer to the textbooks [143, 142].

B.1 Initial value problems

Existence and uniqueness theory

An initial value problem (IVP) is written in the standard form

$$\dot{\boldsymbol{x}}(t) = \boldsymbol{f}(t, \boldsymbol{x}(t)), \quad \boldsymbol{x}(t_0) = \boldsymbol{x}_0 \tag{B.1}$$

with initial values $(t_0, \boldsymbol{x}_0)$. The continuously differentiable solution trajectory $\boldsymbol{x} : [t_0, t_f] \to \mathbb{R}^n$, denoted by $\boldsymbol{x}(\cdot; t_0, \boldsymbol{x}_0)$, satisfies the integral form

$$\boldsymbol{x}(t) = \boldsymbol{x}_0 + \int_{t_0}^{t} \boldsymbol{f}(\tau, \boldsymbol{x}(\tau)) \mathrm{d}\tau.$$

Remark B.1 *For autonomous problems that do not depend explicitly on t, we can assume $t_0 = 0$ because, by time translation, $\boldsymbol{x}(t - t_0)$ is a solution whenever $\boldsymbol{x}(t)$ is a solution.*

For uniqueness of the solution, we require the function $\boldsymbol{f}$ to be Lipschitz continuous.

Definition B.1 *A function $\boldsymbol{f} : D \subset \mathbb{R} \times \mathbb{R}^n \to \mathbb{R}^n$ is* locally Lipschitz continuous *in $\boldsymbol{x} \in D$ if $\forall (t_0, \boldsymbol{x}_0)$ there exist a neighborhood $U \times V$ such that for all $(t, \boldsymbol{y}), (t, \boldsymbol{z}) \in U \times V$ for some appropriate $L < \infty$*

$$||\boldsymbol{f}(t, \boldsymbol{y}) - \boldsymbol{f}(t, \boldsymbol{z})|| \leqslant L \, ||\boldsymbol{y} - \boldsymbol{z}|| \, .$$

The following theorem asserts that a solution exist locally in a neighborhood of the initial values whenever $\boldsymbol{f}$ is continuous, and is unique whenever $\boldsymbol{f}$ is Lipschitz continuous.

Theorem B.1 (Picard-Lindelöf) *Assume $\boldsymbol{f} : D \subset \mathbb{R} \times \mathbb{R}^n \to \mathbb{R}^n$ is* locally Lipschitz continuous. *Then, for each pair of initial values $(t_0, \boldsymbol{x}_0) \in D$, there exist a unique solution $\boldsymbol{x} : U \to \mathbb{R}^n$ of Equation (B.1) in a neighborhood $U := (t_0 - \varepsilon, t_0 + \varepsilon)$ of t_0 for some $\varepsilon > 0$.*

The solution can be extended to the whole of $\mathbb{R} \times \mathbb{R}^n$ if $\boldsymbol{f}$ is globally Lipschitz continuous on $\mathbb{R} \times \mathbb{R}^n$.

Dependence on initial values and parameters

Statements about the continuously differentiable dependence of the solution on the initial values can be made under a regularity assumption on $\boldsymbol{f}$.

Theorem B.2 *Assume $\boldsymbol{f}$ to be m times continuously differentiable in its arguments with $m \geqslant 1$. Then, there exist a neighborhood of $(t_0, \boldsymbol{x}_0)$ such that*

$$\boldsymbol{x}(t; t_0, \boldsymbol{x}_0) \text{ is m-times continuously differentiable in } t_0 \text{ and } \boldsymbol{x}_0.$$

This theorem can be proved with the help of the sensitivity matrix

$$G(t; t_0, \boldsymbol{x}_0) := \frac{\partial \boldsymbol{x}}{\partial \boldsymbol{x}_0}(t; t_0, \boldsymbol{x}_0)$$

and the variational differential equation (VDE)

$$\begin{aligned}
\dot{G}(t; t_0, \boldsymbol{x}_0) &= \frac{\partial}{\partial \boldsymbol{x}} \boldsymbol{f}(t, \boldsymbol{x}(t; t_0, \boldsymbol{x}_0))\, G(t; t_0, \boldsymbol{x}_0) \\
\dot{G}(t_0; t_0, \boldsymbol{x}_0) &= \boldsymbol{I}.
\end{aligned}$$

The VDE is equivalent to the integral form

$$0 = G(t; t_0, \boldsymbol{x}_0) + \boldsymbol{I} - \int_{t_0}^{t} \frac{\partial}{\partial \boldsymbol{x}} \boldsymbol{f}(\tau, \boldsymbol{x}(\tau; t_0, \boldsymbol{x}_0))\, G(\tau; t_0, \boldsymbol{x}_0) \mathrm{d}\tau =: F(G, t).$$

According to the *implicit function theorem*, this equation can be solved for G if and only if $\dfrac{\partial F}{\partial G}$ is regular which follows from the regularity assumption posed on $\boldsymbol{f}$.
We suppose now that the IVP depends on parameters $\boldsymbol{p} \in \mathbb{R}^{n_\mathrm{P}}$, i.e., it reads

$$\dot{\boldsymbol{x}}(t) = \boldsymbol{f}(t, \boldsymbol{x}(t), \boldsymbol{p}),\ \boldsymbol{x}(t_0) = \boldsymbol{x}_0$$

with solution $\boldsymbol{x}(t; t_0, \boldsymbol{x}_0, \boldsymbol{p})$.
Similar to Theorem B.2, we can formulate the following result for the dependence on the parameters.

Theorem B.3 *Assume $\boldsymbol{f} : D \subset \mathbb{R} \times \mathbb{R}^n \times \mathbb{R}^{n_p} \to \mathbb{R}^n$ is m times continuously differentiable in its arguments with $m \geqslant 1$. Then $\boldsymbol{x}(t; t_0, \boldsymbol{x}_0, \boldsymbol{p})$ is m-times continuously differentiable in $\boldsymbol{p}$.*

This result can be proved with the help of the following matrix

$$G^p(t; t_0, \boldsymbol{x}_0, \boldsymbol{p}) := \frac{\partial \boldsymbol{x}}{\partial \boldsymbol{p}}(t; t_0, \boldsymbol{x}_0, \boldsymbol{p})$$

and the VDE

$$\begin{aligned}
\dot{G}^p(t; t_0, \boldsymbol{x}_0, \boldsymbol{p}) &= \frac{\partial}{\partial \boldsymbol{x}} \boldsymbol{f}(t, \boldsymbol{x}(t; t_0, \boldsymbol{x}_0, \boldsymbol{p}), \boldsymbol{p})\, G^p(t; t_0, \boldsymbol{x}_0, \boldsymbol{p}) + \frac{\partial}{\partial \boldsymbol{p}} \boldsymbol{f}(t, \boldsymbol{x}(t; t_0, \boldsymbol{x}_0, \boldsymbol{p}), \boldsymbol{p}) \\
\dot{G}^p(t_0; t_0, \boldsymbol{x}_0, \boldsymbol{p}) &= \boldsymbol{0}.
\end{aligned}$$

Perturbation and stability analysis

Theorem B.4 *Assume $\boldsymbol{f} \in C^0(\bar{D})$ is Lipschitz continuous on $\bar{D} = [a, b] \times \{||\boldsymbol{x} - \boldsymbol{x}_0|| \leqslant K\} \subset D$ with Lipschitz constant $L < \infty$. The solutions of the IVP and of the perturbed IVP*

$$\begin{aligned}
\dot{\boldsymbol{x}}(t) &= \boldsymbol{f}(t, \boldsymbol{x}(t)), \quad \boldsymbol{x}(t_0) = \boldsymbol{x}_0 \\
\dot{\boldsymbol{y}}(t) &= \boldsymbol{f}(t, \boldsymbol{y}(t)) + \delta \boldsymbol{f}(t, \boldsymbol{y}(t)), \quad \boldsymbol{y}(t_0) = \boldsymbol{y}_0 = \boldsymbol{x}_0 + \delta \boldsymbol{x}_0
\end{aligned}$$

exist both on $[t_0, t_f] \subset [a,b]$ *on* $\bar{D}$. *Under the assumption* $||\delta \boldsymbol{x}_0|| \leqslant \varepsilon_1$ *for all* $(t, \boldsymbol{y}(t))$ *with* $||\delta \boldsymbol{f}(t,\boldsymbol{y})|| \leqslant \varepsilon_2$, *the difference* $\delta \boldsymbol{x}(t) = \boldsymbol{y}(t) - \boldsymbol{x}(t)$ *between the two IVP solutions can be bounded by*

$$||\delta \boldsymbol{x}(t)|| \leqslant (\varepsilon_1 + \varepsilon_2(t-t_0))\, e^{L(t-t_0)}.$$

Proof *We have*

$$\delta \boldsymbol{x}(t) = \delta \boldsymbol{x}_0 + \int_{t_0}^{t} \boldsymbol{f}(\tau, \boldsymbol{y}(\tau)) - \boldsymbol{f}(\tau, \boldsymbol{x}(\tau)) + \delta \boldsymbol{f}(\tau, \boldsymbol{y}(\tau)) \mathrm{d}\tau.$$

and therefore, by using the L-Lipschitz-continuity of $\boldsymbol{f}$,

$$\begin{aligned} ||\delta \boldsymbol{x}(t)|| &\leqslant ||\delta \boldsymbol{x}_0|| + \int_{t_0}^{t} ||\boldsymbol{f}(\tau, \boldsymbol{y}(\tau)) - \boldsymbol{f}(\tau, \boldsymbol{x}(\tau))|| + ||\delta \boldsymbol{f}(\tau, \boldsymbol{y}(\tau)||\, \mathrm{d}\tau \\ &\leqslant \varepsilon_1 + L \int_{t_0}^{t} ||\delta \boldsymbol{x}(\tau)||\, \mathrm{d}\tau + \varepsilon_2 (t - t_0). \end{aligned}$$

Applying Gronwall's inequality from Lemma B.5 with $w(t) = ||\delta \boldsymbol{x}(\tau)||$ *and* $b(t) = \varepsilon_1 + \varepsilon_2(t-t_0)$ *satisfies the claim.* □

Lemma B.5 (Gronwall) *Assume* $w(t)$, $b(t)$ *are scalar function, integrable on* $[t_0, t_f]$, $b(t)$ *monotone non-decreasing and* $|b(t)| \leqslant K < \infty$. *Assume for* $0 \leqslant L < \infty$

$$w(t) \leqslant b(t) + \int_{t_0}^{t} L \cdot w(\tau)\, \mathrm{d}\tau, \quad t \in [t_0, t_f].$$

Then

$$w(t) \leqslant b(t) e^{L(t-t_0)}.$$

B.2 Nonlinear programming problems

Introduction

A standard nonlinear programming problem has the form

$$\begin{aligned} \min_{\boldsymbol{x}} \quad & f(\boldsymbol{x}) && \text{(B.2a)} \\ \text{s.t.} \quad & \boldsymbol{g}(\boldsymbol{x}) = \boldsymbol{0} && \text{(B.2b)} \\ & \boldsymbol{h}(\boldsymbol{x}) \leqslant \boldsymbol{0} && \text{(B.2c)} \end{aligned}$$

We assume that the objective function f and the constraints $\boldsymbol{g}$ and $\boldsymbol{h}$ are twice continuously differentiable and that a standard regularity assumption on the active constraints holds.

Definition B.1 *A feasible point* $\boldsymbol{x}$ *is called* regular *if the gradients of the equality constraints* $\boldsymbol{g}$ *and of the inequality constraints* $\boldsymbol{h}$ *active in* $\boldsymbol{x}$ *are linear independent, i.e.,*

$$\operatorname{rank} \begin{pmatrix} \nabla \boldsymbol{g}^T(\boldsymbol{x}) & \boldsymbol{0} \\ \nabla \boldsymbol{h}^T(\boldsymbol{x}) & \operatorname{diag}(\boldsymbol{h}^T(\boldsymbol{x})) \end{pmatrix} = n_g + n_h$$

where $\nabla \boldsymbol{g}^T(\boldsymbol{x})$ *and* $\nabla \boldsymbol{h}^T(\boldsymbol{x})$ *are the Jacobian matrices evaluated at* $\boldsymbol{x}$ *with dimensions* $n_g \times n$ *and* $n_\mathrm{h} \times n$*, respectively.*

Regular points are said to satisfy the *linear independence constraint qualification (LICQ)*. Another constraint qualification, which is generalizable to optimization problems in Banach spaces, is the following.

Definition B.2 *A feasible point* $\boldsymbol{x}$ *satisfies the Mangasarian–Fromovitz constraint qualification (MFCQ) if*

a) $\nabla \boldsymbol{g}^T(\boldsymbol{x})$ *has full column rank*

b) $\exists \boldsymbol{d} \in \mathbb{R}^n$ *with*

$$\nabla \boldsymbol{g}^T(\boldsymbol{x})\boldsymbol{d} = 0,\ \nabla h_i^T(\boldsymbol{x})\boldsymbol{d} < 0 \text{ for } 1 \leqslant i \leqslant n_\mathrm{h} \text{ with } h_i(\boldsymbol{x}) = 0.$$

The necessary optimality conditions are defined using the *Lagrange function*

$$L(\boldsymbol{x}, \boldsymbol{\lambda}, \boldsymbol{\mu}) = f(\boldsymbol{x}) + \boldsymbol{\lambda}^T \boldsymbol{g}(\boldsymbol{x}) + \boldsymbol{\mu}^T \boldsymbol{h}(\boldsymbol{x})$$

with *Lagrange multipliers* $\boldsymbol{\lambda}$ and $\boldsymbol{\mu}$. Further, the notion of the tangent space of the equality constraints and of the active inequality constraints is required.

Definition B.3 *The* tangent space *is defined as*

$$T(\boldsymbol{x}) = \{\boldsymbol{d} \mid \boldsymbol{d}^T \nabla \boldsymbol{g}(\boldsymbol{x}) = 0, \boldsymbol{d}^T \nabla h_i(\boldsymbol{x}) = 0 \text{ for } 1 \leqslant i \leqslant n_\mathrm{h} \text{ with } h_i(\boldsymbol{x}) = 0\}.$$

Theorem B.1 (Necessary optimality conditions, Karush–Kuhn–Tucker (KKT) point) *Assume* $\boldsymbol{x}^\star$ *is a minimum of* (B.2) *and regular. Then, there exist Lagrange multipliers* $\boldsymbol{\lambda} \in \mathbb{R}^{n_g}$ *and* $\boldsymbol{\mu} \in \mathbb{R}^{n_h}$ *satisfying the following system of equations*

1. *stationarity:* $\nabla L(\boldsymbol{x}^\star, \boldsymbol{\lambda}, \boldsymbol{\mu}) = \nabla f(\boldsymbol{x}^\star) + \nabla \boldsymbol{g}(\boldsymbol{x}^\star)\boldsymbol{\lambda} + \nabla \boldsymbol{h}(\boldsymbol{x}^\star)\boldsymbol{\mu} = \boldsymbol{0}$
2. *constraints:* $\boldsymbol{g}(\boldsymbol{x}^\star) = \boldsymbol{0},\ \boldsymbol{h}(\boldsymbol{x}^\star) \leqslant \boldsymbol{0}$
3. *complementarity:* $\boldsymbol{\mu}^T \boldsymbol{h}(\boldsymbol{x}^\star) = \boldsymbol{0},\ \boldsymbol{\mu} \geqslant \boldsymbol{0}$
4. *second-order condition:* $\boldsymbol{d}^T \nabla_{xx} L(\boldsymbol{x}^\star, \boldsymbol{\lambda}, \boldsymbol{\mu})\boldsymbol{d} \geqslant 0$ *for* $\boldsymbol{d} \in T(\boldsymbol{x}^\star)$

If inequality constraints are present, we require strict complementarity for the stability analysis.

Definition B.4 Strict complementarity *holds at a feasible point* $\boldsymbol{x}$ *if, for* $i = 1, \ldots, n_\mathrm{h}$,

$$\mu_i > 0 \Leftrightarrow h_i(\boldsymbol{x}) = 0.$$

Theorem B.2 (Strict local minimum, second-order sufficient condition) *Assume* $(\boldsymbol{x}^\star, \boldsymbol{\lambda}, \boldsymbol{\mu})$ *is a KKT-point, strict complementarity holds and*

$$\boldsymbol{d}^T \nabla_{xx} L(\boldsymbol{x}^\star, \boldsymbol{\lambda}, \boldsymbol{\mu})\boldsymbol{d} > 0 \text{ for } \boldsymbol{d} \in T(\boldsymbol{x}^\star) \backslash \{\boldsymbol{0}\}.$$

Then $\boldsymbol{x}^\star$ *is a strict local minimum.*

Perturbation and stability analysis

A perturbed nonlinear programming problem has the form

$$\min_{\boldsymbol{x}} \quad f(\boldsymbol{x},\tau) \tag{B.3a}$$
$$\text{s.t.} \quad \boldsymbol{g}(\boldsymbol{x},\tau)=\boldsymbol{0} \tag{B.3b}$$
$$\boldsymbol{h}(\boldsymbol{x},\tau)\leqslant\boldsymbol{0} \tag{B.3c}$$

where τ is the perturbation parameter.
We assume that the functions are twice continuously differentiable in their arguments.
In what follows, we summarize the active inequality constraints, for which $h_i(\boldsymbol{x},\tau)=0$, as $\tilde{\boldsymbol{h}}(\boldsymbol{x},\tau)$.

Theorem B.3 (Strict local minimum for the perturbed problem) *Assume that for $\tau=\tau^\star$, there exist a solution $(x^\star,\lambda^\star,\mu^\star)$, i.e., in a neighborhood U of $\tau^\star$ there exist functions*

$$\boldsymbol{x}: U\to\mathbb{R}^n,\ \boldsymbol{\lambda}: U\to\mathbb{R}^{n_\mathrm{g}},\ \boldsymbol{\mu}: U\to\mathbb{R}^{n_\mathrm{h}}$$

with $\boldsymbol{x}(\tau^\star)=\boldsymbol{x}^\star,\ \boldsymbol{\lambda}(\tau^\star)=\boldsymbol{\lambda}^\star,\ \boldsymbol{\mu}(\tau^\star)=\boldsymbol{\mu}^\star$ and $\boldsymbol{x}(\tau)$ is solution of the perturbed problem with Lagrange multipliers $\boldsymbol{\lambda}(\tau)$ and $\boldsymbol{\mu}(\tau)$. Assume that $(x^\star,\lambda^\star,\mu^\star)$ satisfies regularity, strict complementarity and the second-order sufficient condition.
Then, $\boldsymbol{x}(\tau)$ is a strict local minimum and strict complementarity holds for all $\tau\in U$.

Proof *(scratch) Apply the implicit function theorem to*

$$F(\boldsymbol{x},\boldsymbol{\lambda},\boldsymbol{\mu},\tau):=\begin{pmatrix}\nabla f(\boldsymbol{x},\tau)+\nabla\boldsymbol{g}(\boldsymbol{x},\tau)\boldsymbol{\lambda}+\nabla\boldsymbol{h}(\boldsymbol{x},\tau)\boldsymbol{\mu}\\ \boldsymbol{g}(\boldsymbol{x},\tau)\\ \tilde{\boldsymbol{h}}(\boldsymbol{x},\tau)\end{pmatrix}=\boldsymbol{0}.$$

Note that

$$\frac{\partial F}{\partial(\boldsymbol{x},\boldsymbol{\lambda},\boldsymbol{\mu})}(\boldsymbol{x}^\star,\boldsymbol{\lambda}^\star,\boldsymbol{\mu}^\star,\tau^\star)=\begin{pmatrix}\nabla_{xx}L(\boldsymbol{x}^\star,\boldsymbol{\lambda}^\star,\boldsymbol{\mu}^\star,\tau^\star) & \nabla\boldsymbol{g}(\boldsymbol{x}^\star,\tau^\star) & \nabla\boldsymbol{h}(\boldsymbol{x}^\star,\tau^\star)\\ \nabla\boldsymbol{g}^T(\boldsymbol{x}^\star,\tau^\star) & \boldsymbol{0} & \boldsymbol{0}\\ \nabla\tilde{\boldsymbol{h}}^T(\boldsymbol{x}^\star,\tau^\star) & \boldsymbol{0} & \boldsymbol{0}\end{pmatrix}$$

is regular and therefore the functions $\boldsymbol{x}(\tau)$, $\boldsymbol{\lambda}(\tau)$ and $\boldsymbol{\mu}(\tau)$ exist in a neighborhood U of $\tau^\star$.
The neighborhood U can be further restricted such that the set of active inequality indices does not change. It follows immediately that

$$\boldsymbol{d}^T\nabla_{xx}L(\boldsymbol{x},\boldsymbol{\lambda},\boldsymbol{\mu})\boldsymbol{d}>0 \text{ for } \boldsymbol{0}\neq\boldsymbol{d}\in T(\boldsymbol{x}^\star).$$

□

Bibliography

[1] R. Adams and J. Fournier. *Sobolev Spaces*. Pure and Applied Mathematics. Elsevier Science, 2003. ISBN 9780080541297.

[2] K. C. A. Alam, Y. T. Kang, B. B. Saha, A. Akisawa, and T. Kashiwagi. A novel approach to determine optimum switching frequency of a conventional adsorption chiller. *Energy*, 28(10):1021–1037, 2003. doi: 10.1016/S0360-5442(03)00064-1.

[3] J. Albersmeyer. *Adjoint based algorithms and numerical methods for sensitivity generation and optimization of large scale dynamic systems*. Dissertation, *Heidelberg University*, 2010.

[4] J. Albersmeyer and H. G. Bock. Sensitivity generation in an adaptive BDF-method. *Modeling, Simulation and Optimization of Complex Processes: Proceedings of the International Conference on High Performance Scientific Computing, March 6–10, 2006, Hanoi, Vietnam*, pages 15–24. Springer Verlag Berlin Heidelberg New York, 2008.

[5] G. E. Andrews and R. Askey. Classical orthogonal polynomials. Springer Berlin Heidelberg, 1985. ISBN 978-3-540-39743-4. doi: 10.1007/BFb0076530.

[6] M. Anitescu. Spectral finite-element methods for parametric constrained optimization problems. *SIAM J. Numer. Anal.*, 47(3):1739–1759, 2009. doi: 10.1137/060676374.

[7] P. Artzner, F. Delbaen, J.-M. Eber, and D. Heath. Coherent measures of risk. *Mathematical Finance*, 9(3), 1999. doi: 10.1111/1467-9965.00068.

[8] F. Augustin, A. Gilg, M. Paffrath, P. Rentrop, and U. Wever. Polynomial chaos for the approximation of uncertainties: chances and limits. *European J. Appl. Math.*, 19(02): 149–190, 2008.

[9] U. Bau, F. Lanzerath, M. Gräber, H. Schreiber, N. Thielen, and A. Bardow. Adsorption energy systems library - Modeling adsorption based chillers, heat pumps, thermal storages and desiccant systems. In H. Tummescheit and K.-E. Årzén, editors, *Proceedings of the 10th International Modelica Conference*, Volume 96 of *Linköping electronic conference proceedings*, pages 875–883, Linköping, 2014. Modelica Association. ISBN 9789175193809.

[10] U. Bau, P. Hoseinpoori, S. Graf, H. Schreiber, F. Lanzerath, and A. Bardow. Rigorous assessment of adsorber-bed designs using dynamic optimization. In I. W. Eames and M. J. Tierney, editors, *Heat Powered Cycles 2016*. Heat Powered Cycles, 2016. ISBN 978-0-9563329-5-0.

[11] U. Bau, P. Hoseinpoori, S. Graf, H. Schreiber, F. Lanzerath, C. Kirches, and A. Bardow. Dynamic optimisation of adsorber-bed designs ensuring optimal control. *Applied Thermal Engineering*, 125(Supplement C):1565–1576, 2017. doi: https://doi.org/10.1016/j.applthermaleng.2017.07.073.

[12] I. Bauer. *Numerische Verfahren zur Lösung von Anfangswertaufgaben und zur Generierung von ersten und zweiten Ableitungen mit Anwendungen bei Optimierungsaufgaben in Chemie und Verfahrenstechnik*. Dissertation, *Heidelberg University*, 1999.

[13] R. Bellman. The theory of dynamic programming. *Bull. Amer. Math. Soc.*, 60(6):503–515, 1954.

[14] A. Ben-Tal and A. Nemirovski. Robust convex optimization. *Mathematics of Operations Research*, 23(4):769–805, 1998. doi: 10.1287/moor.23.4.769.

[15] A. Ben-Tal and A. Nemirovski. Robust solutions of uncertain linear programs. *Operations Research Letters*, 25(1):1–13, 1999. doi: http://dx.doi.org/10.1016/S0167-6377(99)00016-4.

[16] G. Ben-Yu. *Spectral methods and their applications*. World Scientific, Singapore, 1998.

[17] L. J. Bergh. *Interpolation spaces: an introduction*, Volume 223. Springer Science & Business Media, 1976.

[18] L. Bergner and C. Kirches. The polynomial chaos approach for reachable set propagation with application to chance-constrained nonlinear optimal control under parametric uncertainties. *Optimal Control Applications and Methods*, 2017. doi: 10.1002/oca.2329.

[19] L. Bergner and C. Kirches. Structure-exploiting polynomial chaos for uncertain optimal control problems with sparse derivative generation. *PAMM*, 17(1), *to appear*.

[20] D. P. Bertsekas. *Dynamic programming and optimal control*, Volume 1. ISBN 1-886529-26-4 Athena scientific Belmont, MA, 1995.

[21] S. Bhattacharyya, H. Chapellat, and L. Keel. *Robust Control: The Parametric Approach*. Prentice-Hall information and system sciences series. Prentice Hall PTR, 1995. ISBN 9780137815760.

[22] L. Biegler. Solution of dynamic optimization problems by successive quadratic programming and orthogonal collocation. *Computers & Chemical Engineering*, 8(3):243–247, 1984. doi: 10.1016/0098-1354(84)87012-X.

[23] J. Björnberg and M. Diehl. Approximate robust dynamic programming and robustly stable MPC. *Automatica*, 42(5):777–782, 2006. doi: http://dx.doi.org/10.1016/j.automatica.2005.12.016.

[24] H. G. Bock. Numerical treatment of inverse problems in chemical reaction kinetics. In K. Ebert, P. Deuflhard, and W. Jäger, editors, *Modelling of Chemical Reaction Systems*, Volume 18 of *Springer Series in Chemical Physics*, pages 102–125. Springer, Heidelberg, 1981.

[25] H. G. Bock. Recent advances in parameter identification techniques for ODE. In P. Deuflhard and E. Hairer, editors, *Numerical Treatment of Inverse Problems in Differential and Integral Equations*, pages 95–121. Birkhäuser, Boston, 1983.

[26] H. G. Bock. *Randwertproblemmethoden zur Parameteridentifizierung in Systemen nichtlinearer Differentialgleichungen*, Volume 183 of *Bonner Mathematische Schriften*. *Rheinische Friedrich–Wilhelms–Universität Bonn*, Bonn, 1987.

[27] H. G. Bock and K. Plitt. A Multiple Shooting algorithm for direct solution of optimal control problems. In *Proceedings of the 9th IFAC World Congress, Budapest*, pages 242–247, Budapest, 1984. Pergamon Press.

[28] B. Bonnard, J.-B. Caillau, and E. Trélat. Second order optimality conditions in the smooth case and applications in optimal control. *ESAIM: COCV*, 13(2):207–236, 2007. doi: 10.1051/cocv:2007012.

[29] I. N. Bronstein, J. Hromkovic, B. Luderer, H.-R. Schwarz, J. Blath, A. Schied, S. Dempe, G. Wanka, and S. Gottwald. *Taschenbuch der Mathematik*, Volume 1. Springer-Verlag, 2012.

[30] G. C. Calafiore and M. C. Campi. Uncertain convex programs: randomized solutions and confidence levels. *Mathematical Programming*, 102(1):25–46, 2005. doi: 10.1007/s10107-003-0499-y.

[31] G. C. Calafiore and M. C. Campi. The scenario approach to robust control design. *IEEE Transactions on Automatic Control*, 51(5):742–753, May 2006. doi: 10.1109/TAC.2006.875041.

[32] R. H. Cameron and W. T. Martin. The orthogonal development of non-linear functionals in series of Fourier-Hermite functionals. *Annals of Mathematics*, 48(2):385–392, 1947. doi: 10.2307/1969178.

[33] C. Canuto and A. Quarteroni. Approximation results for orthogonal polynomials in sobolev spaces. *Math. Comp.*, 38(157):67–86, 1982. doi: 10.2307/2007465.

[34] Y. Cao, M. Hussaini, and T. Zang. An efficient monte carlo method for optimal control problems with uncertainty. *Computational Optimization and Applications*, 26(3):219–230, 2003. doi: 10.1023/A:1026079021836.

[35] L. Cesari. *Optimization-theory and applications: problems with ordinary differential equations*. Applications of mathematics. Springer-Verlag, 1983. ISBN 9783540906766.

[36] A. Charnes, W. W. Cooper, and G. H. Symonds. Cost horizons and certainty equivalents: An approach to stochastic programming of heating oil. *Management Science*, 4(3):235–263, 1958.

[37] P. Chen, A. Quarteroni, and G. Rozza. Multilevel and weighted reduced basis method for stochastic optimal control problems constrained by stokes equations. *Numer. Math.*, pages 1–36, 2013. doi: 10.1007/s00211-015-0743-4.

[38] H.-S. Chen and M. A. Stadtherr. Enhancements of the han–powell method for successive quadratic programming. *Computers & Chemical Engineering*, 8(3):229–234, 1984. doi: http://dx.doi.org/10.1016/0098-1354(84)87010-6.

[39] H. T. Chua, K. C. Ng, W. Wang, C. Yap, and X. L. Wang. Transient modeling of a two-bed silica gel–water adsorption chiller. *International Journal of Heat and Mass Transfer*, 47(4):659–669, 2004. doi: 10.1016/j.ijheatmasstransfer.2003.08.010.

[40] M. Diehl. *Real-Time Optimization for Large Scale Nonlinear Processes*. Dissertation, *Heidelberg University*, 2001.

[41] M. Diehl and J. Björnberg. Robust dynamic programming for min-max model predictive control of constrained uncertain systems. *IEEE Transactions on Automatic Control*, 49 (12):2253–2257, Dec 2004. doi: 10.1109/TAC.2004.838489.

[42] M. Diehl, H. G. Bock, and E. Kostina. An approximation technique for robust nonlinear optimization. *Mathematical Programming*, 107(12):213–230, 2006. doi: 10.1007/s1010700506851.

[43] M. Diehl, J. Gerhard, W. Marquardt, and M. Mönnigmann. Numerical solution approaches for robust nonlinear optimal control problems. *Computers & Chemical Engineering*, 32(6):1279–1292, 2008.

[44] J. Doyle. Guaranteed margins for lqg regulators. *IEEE Transactions on Automatic Control*, 23(4):756–757, Aug 1978. doi: 10.1109/TAC.1978.1101812.

[45] T. N. Driscoll T, Hale N. *Chebfun Guide*. Pafnuty Publications, Oxford, UK, 2014. URL http://www.chebfun.org/docs/guide/.

[46] G. E. Dullerud and F. Paganini. *A course in robust control theory: a convex approach*, Volume 36. Springer Science & Business Media, 2013.

[47] R. Durrett. *Probability: theory and examples*. Cambridge University Press, 2010.

[48] E. Lehmann *Elements of large-sample theory*. Springer Science & Business Media, 1999.

[49] M. S. Eldred. Recent advances in non-intrusive polynomial chaos and stochastic collocation methods for uncertainty analysis and design. *AIAA Paper*, 2274(2009):37, 2009. doi: 10.2514/6.2009-2274.

[50] M. S. Eldred, C. Webster, and P. Constantine. Evaluation of nonintrusive approaches for wiener-askey generalized polynomial chaos. In *Proceedings of the 10th AIAA Non-Deterministic Approaches Conference, number AIAA20081892, Schaumburg, IL*, Volume 117, 2008.

[51] O. G. Ernst, A. Mugler, H. Starkloff, and E. Ullmann. On the convergence of generalized polynomial chaos expansions. *ESAIM: Mathematical Modelling and Numerical Analysis*, 46(2):317–339, 2012. doi: 10.1051/m2an/2011045.

[52] L. Fagiano and M. Khammash. Nonlinear stochastic model predictive control via regularized polynomial chaos expansions. In *IEEE 51st IEEE Conference on Decision and Control (CDC), Maui, Hawaii*, pages 142–147, 2012. doi: 10.1109/CDC.2012.6425919.

[53] M. Farina, L. Giulioni, L. Magni, and R. Scattolini. A probabilistic approach to model predictive control. In *IEEE 52nd Annual Conference on Decision and Control (CDC), Maui, Hawaii*, pages 7734–7739, 2013. doi: 10.1109/CDC.2013.6761117.

[54] J. Fisher and R. Bhattacharya. On stochastic LQR design and polynomial chaos. In *Proceedings of American Control Conference, Seattle, Washington*, pages 95–100, 2008. doi: 10.1109/ACC.2008.4586473.

[55] J. Fisher and R. Bhattacharya. Optimal trajectory generation with probabilistic system uncertainty using polynomial chaos. *J. Dyn. Sys., Meas., Control*, 133(1):014501, 2011. doi: 10.1115/1.4002705.

[56] M. Gerritsma, J. B. V. der Steen, P. Vos, and G. E. Karniadakis. Time-dependent generalized polynomial chaos. *J. Comput. Phys.*, 229(22):8333–8363, 2010.

[57] R. G. Ghanem and P. Spanos. *Stochastic finite elements: a spectral approach*, Volume 41. Springer, 1991.

[58] L. E. Ghaoui, F. Oustry, and H. Lebret. Robust solutions to uncertain semidefinite programs. *SIAM Journal on Optimization*, 9(1):33–52, 1998. doi: 10.1137/S1052623496305717.

[59] B. Gollan. On optimal control problems with state constraints. *Journal of Optimization Theory and Applications*, 32(1):75–80, 1980. doi: 10.1007/BF00934843.

[60] G. H. Golub and J. H. Welsch. Calculation of gauss quadrature rules. *Mathematics of computation*, 23(106):221–230, 1969. doi: 10.1090/S0025-5718-69-99647-1.

[61] M. Gräber, K. Kosowski, C. Richter, and W. Tegethoff. Modelling of heat pumps with an object-oriented model library for thermodynamic systems. *Mathematical and Computer Modelling of Dynamical Systems*, 16(3):195–209, 2010. doi: 10.1080/13873954.2010.506799.

[62] M. Gräber, C. Kirches, H. G. Bock, J. P. Schlöder, W. Tegethoff, and J. Köhler. Determining the optimum cyclic operation of adsorption chillers by a direct method for periodic optimal control. *International Journal of Refrigeration*, 34(4):902–913, 2011. doi: http://dx.doi.org/10.1016/j.ijrefrig.2010.12.021.

[63] M. Gräber, C. Kirches, J. P. Schlöder, and W. Tegethoff. Optimal cyclic operation of two-bed adsorption chillers with mass recovery. In *Proceedings of ISHPC 2011, Padua, Italy, April 5–7, 2011*, 2011.

[64] M. Gräber, C. Kirches, D. Scharff, and W. Tegethoff. Using functional mock-up units for nonlinear model predictive control. In *Proceedings of the 9th International MODELICA Conference; Munich; Germany*, number 076, pages 781–790. Linköping University Electronic Press, 2012.

[65] A. Griewank and A. Walther. *Evaluating Derivatives: Principles and Techniques of Algorithmic Differentiation*. SIAM, 2nd Edition, 2008.

[66] L. Grüne and P. E. Kloeden. Pathwise approximation of random ordinary differential equations. *BIT Numerical Mathematics*, 41(4):711–721, 2001. doi: 10.1023/A:1021995918864.

[67] S. Han. A globally convergent method for nonlinear programming. *Journal of Optimization Theory and Applications*, 22:297–310, 1977.

[68] R. Hannemann-Tamás and W. Marquardt. How to verify optimal controls computed by direct shooting methods? – a tutorial. *Journal of Process Control*, 22(2):494–507, 2012. doi: http://dx.doi.org/10.1016/j.jprocont.2011.11.002.

[69] T. Heine, M. Kawohl, and R. King. Robust model predictive control using the unscented transformation. In *2006 IEEE Conference on Computer Aided Control System Design, 2006 IEEE International Conference on Control Applications, 2006 IEEE International Symposium on Intelligent Control*, pages 224–230, 2006. doi: 10.1109/CACSD-CCA-ISIC.2006.4776650.

[70] R. Hettich and K. O. Kortanek. Semi-infinite programming: Theory, methods, and applications. *SIAM Review*, 35(3):380–429, 1993. doi: 10.1137/1035089.

[71] C. Hoffmann, C. Kirches, A. Potschka, S. Sager, L. Wirsching, M. Diehl, D. B. Leineweber, A. Schäfer, H. G. Bock, and J. P. Schlöder. MUSCOD-II user's manual, release 6, 2011. http://www.iwr.uni-heidelberg.de/~agbock/RESEARCH/muscod.php

[72] B. Houska, J. C. Li, and B. Chachuat. Towards rigorous robust optimal control via generalized high-order moment expansion. *Optimal Control Applications and Methods*, 2017. doi: 10.1002/oca.2309.

[73] F. S. Hover and M. S. Triantafyllou. Application of polynomial chaos in stability and control. *Automatica*, 42(5):789–795, 2006. doi: 10.1016/j.automatica.2006.01.010.

[74] K. Ito and K. Kunisch. Sensitivity analysis of solutions to optimization problems in hilbert spaces with applications to optimal control and estimation. *Journal of Differential Equations*, 99(1):1–40, 1992. doi: http://dx.doi.org/10.1016/0022-0396(92)90133-8.

[75] F. J. and B. R. Stability analysis of stochastic systems using polynomial chaos. In *Proceedings of American Control Conference, Seattle, Washington*, pages 4250–4255. IEEE, 2008. doi: 10.1109/ACC.2008.4587161.

[76] A. M. J. A. Paulson, S. Streif. Stability for receding-horizon stochastic model predictive control. In *American Control Conference, Chicago, Illinois*, pages 937–943, 2015. doi: 10.1109/ACC.2015.7170854.

[77] J. Jakeman, M. Eldred, and K. Sargsyan. Enhancing l1-minimization estimates of polynomial chaos expansions using basis selection. *Journal of Computational Physics*, 289:18–34, 2015. doi: http://dx.doi.org/10.1016/j.jcp.2015.02.025.

[78] S. J. Julier and J. K. Uhlmann. A general method for approximating nonlinear transformations of probability distributions. Technical report, Technical report, Robotics Research Group, Department of Engineering Science, University of Oxford, 1996.

[79] R. E. Kalman. A new approach to linear filtering and prediction problems. *Transactions of the ASME–Journal of Basic Engineering*, 82(Series D):35–45, 1960.

[80] K. K. Kim and R. D. Braatz. Generalised polynomial chaos expansion approaches to approximate stochastic model predictive control. *International Journal of Control*, 86(8):1324–1337, 2013. doi: 10.1080/00207179.2013.801082.

[81] K.-K. Kim, D. Shen, Z. Nagy, and R. Braatz. Wiener's polynomial chaos for the analysis and control of nonlinear dynamical systems with probabilistic uncertainties [historical perspectives]. *IEEE Control Systems*, 33(5):58–67, 2013. doi: 10.1109/MCS.2013.2270410.

[82] C. Kirches. *Fast Numerical Methods for Mixed-Integer Nonlinear Model-Predictive Control*. Vieweg, 2011. ISBN 3834815721, 9783834815729. doi: 10.1007/978-3-8348-8202-8.

[83] P. E. Kloeden and E. Platen. A survey of numerical methods for stochastic differential equations. *Stochastic Hydrology and Hydraulics*, 3(3):155–178, 1989. doi: 10.1007/BF01543857.

[84] D. P. Kouri. A multilevel stochastic collocation algorithm for optimization of PDEs with uncertain coefficients. *SIAM/ASA Journal on Uncertainty Quantification*, 2(1):55–81, 2014. doi: 10.1137/130915960.

[85] D. P. Kouri, M. Heinkenschloss, D. Ridzal, and B. G. van Bloemen Waanders. A trust-region algorithm with adaptive stochastic collocation for PDE optimization under uncertainty. *SIAM J. Sci. Comput.*, 35(4):A1847–A1879, 2013. doi: 10.1137/120892362.

[86] A. B. Kurzhanski. *Ellipsoidal Calculus for Estimation and Feedback Control*, pages 229–243. Birkhäuser Boston, Boston, MA, 1997. ISBN 978-1-4612-4120-1. doi: 10.1007/978-1-4612-4120-1_12.

[87] A. B. Kurzhanski and P. Varaiya. On reachability under uncertainty. *SIAM Journal on Control and Optimization*, 41(1):181–216, 2002. doi: 10.1137/S0363012999361093.

[88] F. Lanzerath, U. Bau, J. Seiler, and A. Bardow. Optimal design of adsorption chillers based on a validated dynamic object-oriented model. *Science and Technology for the Built Environment*, 21(3):248–257, 2015. doi: 10.1080/10789669.2014.990337.

[89] O. Le Maître and O. M. Knio. *Spectral methods for uncertainty quantification: with applications to computational fluid dynamics*. Springer Science & Business Media, 2010.

[90] C. Leidereiter, A. Potschka, and H. G. Bock. Dual decomposition for qps in scenario tree nmpc. In *2015 European Control Conference (ECC)*, pages 1608–1613, July 2015. doi: 10.1109/ECC.2015.7330767.

[91] D. Leineweber. *Analyse und Restrukturierung eines Verfahrens zur direkten Lösung von Optimal-Steuerungsproblemen*. Diplomarbeit, *Heidelberg University*, 1995.

[92] D. Leineweber. *Efficient reduced SQP methods for the optimization of chemical processes described by large sparse DAE models*, Volume 613 *Fortschritt-Berichte VDI Reihe 3, Verfahrenstechnik*. VDI Verlag, Düsseldorf, 1999.

[93] D. Leineweber, I. Bauer, A. Schäfer, H. G. Bock, and J. Schlöder. An Efficient Multiple Shooting Based Reduced SQP Strategy for Large-Scale Dynamic Process Optimization (Parts I and II). *Computers & Chemical Engineering*, 27:157–174, 2003.

[94] D. B. Leineweber. The theory of muscod in a nutshell, 2011. *IWR-Preprint 96-19* Heidelberg University, 1996

[95] M. Loeve. *Probability Theory II*. F.W.Gehring P.R.Halmos and C.C.Moore. Springer, 1978. ISBN 9780387902623.

[96] R. H. Lopez and A. A. T. A. Beck. Reliability-based design optimization strategies based on FORM: a review. *Journal of the Brazilian Society of Mechanical Sciences and Engineering*, 34:506–514, 12 2012.

[97] S. Lucia and S. Engell. Robust nonlinear model predictive control of a batch bioreactor using multi-stage stochastic programming. In *2013 European Control Conference (ECC)*, pages 4124–4129, July 2013.

[98] S. Lucia, T. Finkler, D. Basak, and S. Engell. A new robust nmpc scheme and its application to a semi-batch reactor example*. 8th IFAC Symposium on Advanced Control of Chemical Processes. *IFAC Proceedings Volumes*, 45(15):69–74, 2012. doi: http://dx.doi.org/10.3182/20120710-4-SG-2026.00035.

[99] D. Lucor and G. E. Karniadakis. Adaptive generalized polynomial chaos for nonlinear random oscillators. *SIAM J. Sci. Comput.*, 26(2):720–735, 2004. doi: 10.1137/S1064827503427984.

[100] J. Luedtke and S. Ahmed. A sample approximation approach for optimization with probabilistic constraints. *SIAM J. Optim.*, 19(2):674–699, 2008. doi: 10.1137/070702928.

[101] D. Ma and R. Braatz. Worstcase analysis of finitetime control policies. *Control Systems Technology, IEEE Transactions on*, 9(5):766–774, 2001.

[102] C. V. Mai and B. Sudret. Surrogate models for oscillatory systems using sparse polynomial chaos expansions and stochastic time warping. *SIAM/ASA Journal on Uncertainty Quantification*, 5(1):540–571, 2017. doi: 10.1137/16M1083621.

[103] K. Malanowski, C. Büskens, and H. Maurer. Convergence of approximations to nonlinear optimal control problems. *Lecture Notes in Pure and Applied Mathematics*, pages 253–284, 1997.

[104] A. Mesbah and S. Streif. A probabilistic approach to robust optimal experiment design with chance constraints. *IFAC-PapersOnLine*, 48(8):100–105, 2015. doi: http://dx.doi.org/10.1016/j.ifacol.2015.08.164.

[105] A. Mesbah, S. Streif, R. Findeisen, and R. D. Braatz. Active fault diagnosis for nonlinear systems with probabilistic uncertainties. *IFAC Proceedings Volumes*, 47(3):7079–7084, 2014. doi: http://dx.doi.org/10.3182/20140824-6-ZA-1003.01594. 19th IFAC World Congress.

[106] A. Mesbah, S. Streif, R. Findeisen, and R. D. Braatz. Stochastic nonlinear model predictive control with probabilistic constraints. In *American Control Conference, Portland, Oregon*, pages 2413–2419, June 2014. doi: 10.1109/ACC.2014.6858851.

[107] B. L. Miller and H. M. Wagner. Chance constrained programming with joint constraints. *Operations Research*, 13(6):930–945, 1965. doi: 10.1287/opre.13.6.930.

[108] V. M. Monti A, Ponci F. Extending polynomial chaos to include interval analysis. *IEEE Transactions on Instrumentation and Measurement*, 59(1):48–55, 2010. doi: 10.1109/TIM.2009.2025688.

[109] Z. Nagy and R. Braatz. Distributional uncertainty analysis using power series and polynomial chaos expansions. *Journal of Process Control*, 17(3):229–240, 2007. doi: http://dx.doi.org/10.1016/j.jprocont.2006.10.008.

[110] Z. K. Nagy and R. D. Braatz. Open-loop and closed-loop robust optimal control of batch processes using distributional and worst-case analysis. *Journal of Process Control*, 14 (4):411–422, 2004. doi: http://dx.doi.org/10.1016/j.jprocont.2003.07.004.

[111] Z. K. Nagy and R. D. Braatz. Distributional uncertainty analysis using power series and polynomial chaos expansions. *Journal of Process Control*, 17(3):229–240, 2007. doi: 10.1016/j.jprocont.2006.10.008.

[112] A. Nemirovski and A. Shapiro. Convex approximations of chance constrained programs. *SIAM J. Optim.*, 17(4):969–996, 2007. doi: 10.1137/050622328.

[113] S. Oladyshkin and W. Nowak. Data-driven uncertainty quantification using the arbitrary polynomial chaos expansion. *Reliability Engineering & System Safety*, 106:179–190, 2012. doi: http://dx.doi.org/10.1016/j.ress.2012.05.002.

[114] S. Oladyshkin, H. Class, R. Helmig, and W. Nowak. An integrative approach to robust design and probabilistic risk assessment for CO2 storage in geological formations. *Computational Geosciences*, 15(3):565–577, Jun 2011. doi: 10.1007/s10596-011-9224-8.

[115] H. C. Ozen and G. Bal. Dynamical polynomial chaos expansions and long time evolution of differential equations with random forcing. *SIAM/ASA Journal on Uncertainty Quantification*, 4(1):609–635, 2016. doi: 10.1137/15M1019167.

[116] Z. Perkó, L. Gilli, D. Lathouwers, and J. L. Kloosterman. Grid and basis adaptive polynomial chaos techniques for sensitivity and uncertainty analysis. *J. Comput. Phys.*, 260: 54–84, 2014. doi: 10.1016/j.jcp.2013.12.025.

[117] H. J. Pesch and R. Bulirsch. The maximum principle, bellman's equation and caratheodory's work. *Journal of Optimization Theory and Applications* 80 (2):203–229, 1994.

[118] L. Petzold, S. Li, Y. Cao, and R. Serban. Sensitivity analysis of differential-algebraic equations and partial differential equations. *Computers & Chemical Engineering*, 30: 1553–1559, 2006.

[119] C. Phelps, Q. Gong, J. O. Royset, C. Walton, and I. Kaminer. Consistent approximation of a nonlinear optimal control problem with uncertain parameters. *Automatica*, 50(12): 2987–2997, 2014. doi: http://dx.doi.org/10.1016/j.automatica.2014.10.025.

[120] C. Phelps, J. O. Royset, and Q. Gong. Optimal control of uncertain systems using sample average approximations. *SIAM J. Control Optim.*, 54(1):1–29, 2016. doi: 10.1137/140983161.

[121] K. Plitt. *Ein superlinear konvergentes Mehrzielverfahren zur direkten Berechnung beschränkter optimaler Steuerungen*. Diplomarbei, Rheinische Friedrich–Wilhelms–Universität Bonn, 1981.

[122] L. S. Pontryagin, V. G. Boltyanskii, R. V. Gamkrelidze, and E. F. Mishchenko. *The Mathematical Theory of Optimal Processes*. Translated from the Russian by K. N. Trirogoff; edited by L. W. Neustadt. Interscience Publishers John Wiley & Sons, Inc. New York-London, 1962.

[123] A. Potschka. *Handling path constraints in a direct multiple shooting method for optimal control problems*. Diplomarbeit, Universität Heidelberg, 2006. http://apotschka.googlepages.com/APotschka2006.pdf.

[124] A. Potschka, H. G. Bock, and J. Schlöder. A minima tracking variant of semi-infinite programming for the treatment of path constraints within direct solution of optimal control problems. *Optimization Methods and Software*, 24(2):237–252, 2009.

[125] M. Powell. A fast algorithm for nonlinearly constrained optimization calculations. In G. Watson, editor, *Numerical Analysis, Dundee 1977*, Volume 630 of *Lecture Notes in Mathematics*, Berlin, 1978. Springer.

[126] A. Prekopa. On probabilistic constrained programming *Proceedings of the Princeton symposium on mathematical programming*, pages 113–138. Princeton University Press, 1970.

[127] L. Pursell and S. Y. Trimble. Gram-Schmidt orthogonalization by Gauss elimination. *The American Mathematical Monthly*, 98(6):544–549, 1991. http://www.jstor.org/stable/2324877.

[128] R. G. V. Richard F. Hartl, Suresh P. Sethi. A survey of the maximum principles for optimal control problems with state constraints. *SIAM Review*, 37(2):181–218, 1995.

[129] R. T. Rockafellar. Coherent approaches to risk in optimization under uncertainty. *INFORMS*, Chapter 3, pages 38–61, 2007. doi: 10.1287/educ.1073.0032.

[130] J. Ruths and J.-S. Li. Optimal control of inhomogeneous ensembles. *IEEE Transactions on Automatic Control*, 57(8):2021–2032, 2012.

[131] Y. Sakawa and Y. Shindo. Optimal control of container cranes. *Automatica*, 18(3): 257–266, 1982. doi: http://dx.doi.org/10.1016/0005-1098(82)90086-3.

[132] A. Sapienza, S. Santamaria, A. Frazzica, and A. Freni. Influence of the management strategy and operating conditions on the performance of an adsorption chiller. *Energy*, 36(9):5532–5538, 2011. doi: 10.1016/j.energy.2011.07.020.

[133] A. Schäfer. *Efficient reduced Newton-type methods for solution of large-scale structured optimization problems with application to biological and chemical processes*. Dissertation, *Heidelberg University*, 2005. http://archiv.ub.uni-heidelberg.de/volltextserver/volltexte/2005/5264/.

[134] C. Schillings and V. Schulz. On the influence of robustness measures on shape optimization with stochastic uncertainties. *Optimization and Engineering*, 16(2):347–386, Jun 2015. doi: 10.1007/s11081-014-9251-0.

[135] A. Shapiro, D. Dentcheva, and A. Ruszczynski. *Lectures on Stochastic Programming: Modeling and Theory*, 2nd Edition. Society for Industrial and Applied Mathematics, Philadelphia, PA, USA, 2014. ISBN 9781611973426.

[136] J. Shen, T. Tang, and L.-L. Wang. *Spectral Methods: Algorithms, Analysis and Applications*. Springer Publishing Company, Incorporated, 1st Edition, 2011. ISBN 9783540710400. doi: 10.1007/978-3-540-71041-7.

[137] C. C. Smiley M. An algorithm for finding all solutions of a nonlinear system. *J. Comput. Appl. Math.*, 137(2):293–315, 2001. doi: http://dx.doi.org/10.1016/S0377-0427(00)00711-1.

[138] A. Smith, A. Monti, and F. Ponci. Robust controller using polynomial chaos theory. In *Industry Applications Conference, 2006. 41st IAS Annual Meeting. Conference Record of the 2006 IEEE*, Volume 5, pages 2511–2517. IEEE, 2006. doi: 10.1109/IAS.2006.256892.

[139] A. Smith, A. Monti, and F. Ponci. Confidence interval estimation using polynomial chaos theory. In *Advanced Methods for Uncertainty Estimation in Measurement, 2008. AMUEM 2008. IEEE International Workshop on*, pages 12–16, 2008. doi: 10.1109/AMUEM.2008.4589927.

[140] F. Ponci, A. Smith, and A Monti. Bounding the dynamic behavior of an uncertain system via polynomial chaos-based simulation. *Simulation*, 86(1):31–40, 2010. doi: 10.1177/0037549709101942.

[141] S. Smolyak. Quadrature and interpolation formulas for tensor products of certain classes of functions. *Soviet Mathematics, Doklady*, 4:240–243, 1963.

[142] J. Stoer and R. Bulirsch. *Numerische Mathematik 2*. Springer, Berlin Heidelberg New York, 4th edition, 2000. ISBN 3-540-67644-9.

[143] J. Stoer and R. Bulirsch. *Numerische Mathematik 1*. Springer-Verlag, Berlin Heidelberg New York, 10th edition, 2007. ISBN 978-3-540-45390-1

[144] G. Szegő. *Orthogonal Polynomials*. American Mathematical Society. Volume 23, 4th Edition, 1975.

[145] D. Telen, M. Vallerio, L. Cabianca, B. Houska, J. V. Impe, and F. Logist. Approximate robust optimal control of nonlinear dynamic systems under process noise. In *2015 European Control Conference (ECC)*, pages 1581–1586, 2015. doi: 10.1109/ECC.2015.7330763.

[146] G. Terejanu, P. Singla, T. Singh, and S. PD. Approximate interval method for epistemic uncertainty propagation using polynomial chaos and evidence theory. In *American Control Conference*, pages 349–354. IEEE, 2010. doi: 10.1109/ACC.2010.5530816.

[147] M. Tootkaboni, A. Asadpoure, and J. K. Guest. Topology optimization of continuum structures under uncertainty – a polynomial chaos approach. *Computer Methods in Applied Mechanics and Engineering*, 201:263–275, 2012. doi: http://dx.doi.org/10.1016/j.cma.2011.09.009.

[148] X. Wan and G. E. Karniadakis. An adaptive multi-element generalized polynomial chaos method for stochastic differential equations. *J. Comput. Phys.*, 209(2):617–642, 2005. doi: 10.1016/j.jcp.2005.03.023.

[149] R. J.-B. Wets. Challenges in stochastic programming. *Mathematical Programming*, 75 (2):115–135, 1996. doi: 10.1007/BF02592149.

[150] N. Wiener. The homogeneous chaos. *American Journal of Mathematics*, pages 897–936, 1938. doi: 10.2307/2371268.

[151] D. Xiu and G. E. Karniadakis. The Wiener-Askey polynomial chaos for stochastic differential equations. *SIAM J. Sci. Comput.*, 24(2):619–644, 2002. doi: 10.1137/S1064827501387826.

[152] D. Xiu and G. E. Karniadakis. Modeling uncertainty in steady state diffusion problems via generalized polynomial chaos. *Computer Methods in Applied Mechanics and Engineering*, 191(43):4927–4948, 2002. doi: 10.1016/S0045-7825(02)00421-8.

[153] G. Zames. Feedback and optimal sensitivity: Model reference transformations, multiplicative seminorms, and approximate inverses. *IEEE Transactions on Automatic Control*, 26(2):301–320, 1981. doi: 10.1109/TAC.1981.1102603.

[154] K. Zhou, J. Doyle, and K. Glover. *Robust and optimal control*. Prentice-Hall, Inc., Upper Saddle River, NJ, USA, 1996. ISBN 0-13-456567-3.

[155] J. C. Ziems. Adaptive multilevel inexact SQP-methods for PDE-constrained optimization with control constraints. *SIAM J. Optim.*, 23(2):1257–1283, 2013. doi: 10.1137/110848645.

List of Figures

List of Tables

List of Algorithms

List of Acronyms

aPC arbitrary polynomial chaos
AD algorithmic differentiation
BVP boundary value problem
CDF cumulative distribution function
COP coefficient of performance
CVaR conditional value-at-risk
DAE differential algebraic equation
EKF extended Kalman filter
FMI Functional Mock-up Interface
FMU functional mock-up unit
gPC generalized polynomial chaos
IND internal numerical differentiation
IVP initial value problem
KKT Karush–Kuhn–Tucker
LICQ linear independence constraint qualification
MCS Monte Carlo sampling
ME-gPC multi-element generalized polynomial chaos
MFCQ Mangasarian–Fromovitz constraint qualification
NLP nonlinear program
ODE ordinary differential equation
PC polynomial chaos
PDE partial differential equation
PDF probability density function
QMC quasi Monte Carlo
RDE random differential equations
SCP specific cooling power
SQP sequential quadratic programming
SDE stochastic differential equations
UT unscented transform
UKF unscented Kalman filter
VaR value-at-risk
VDE variational differential equation